# FACTORS AFFECTING THE PERFUSION AND DELIVERY OF CURCUMINOIDS AND OTHER MOLECULES TO TELEOST MUSCLE

---

A thesis submitted in

fulfillment of the requirements

for the Degree of

DOCTOR OF PHILOSOPHY IN ZOOLOGY

in the University of Canterbury

by

Gerard J A Janssen

---

University of Canterbury

2008

# Contents

# List of Figures

## Chapter 2



## Chapter 3

## Chapter 4

## Chapter 6



## Chapter 7

## Chapter 8

# List of Tables

## Chapter 2



## Chapter 3



## Chapter 4



## Chapter 5



## Chapter 6

# Thesis Abstract

The primary objectives of this thesis were: to explore potential delivery pathways of supportive molecules to teleost musculature, and combined with perfusion visualisation experiments, to generate a greater understanding of teleost white muscle perfusion. A Chinook salmon (*Oncorhynchus tshawytscha*) perfused isolated tail preparation was assessed as a delivery platform with limited results as perfusion to the white muscle did not replicate that in the live fish. A direct uptake delivery method, where hydrophobic molecules diffuse across the gill lamellae and accumulate in the blood and white muscle, was assessed with the aquatic anaesthetic isoeugenol (AQUI-S$^{TM}$). Snapper (*Pagrus auratus*) exposed to low (4.5±0.3 mg.L$^{-1}$), medium (8.6±0.1 mg.L$^{-1}$) and high (14.0±0.3 mg.L$^{-1}$) isoeugenol concentrations had maximum plasma isoeugenol concentrations of 10.5, 5.8 and 4.9 times (low, medium and high) and white muscle concentrations 9.7, 4.6 and 1.9 times (respectively) the exposure concentration. Direct uptake delivery, compared with the perfused tail preparation, was a relatively non-invasive and non-technical method of delivery that has potential for large scale commercial application. The curcuminoids, which are strong antioxidants derived from the spice turmeric, were also shown to rapidly diffuse into the plasma and musculature of snapper. There were no short term benefits on white muscle metabolic rundown in fish treated with curcumnoids compared to a non-treated control. However, a short term accelerated storage trial suggested that snapper treated with curcuminoids showed reduced lipid peroxidation. The successful delivery of supportive molecules to the white muscle is dependent on perfusion. There is very little research on white muscle perfusion and how it is affected by changing environmental parameters. Cardiac performance and white muscle perfusion and haemoglobin saturation were recorded from anaesthetised snapper during acute progressive hypoxia and hypothermia (and recovery) in real time, using fibre optics. White muscle perfusion, as assessed by haemoglobin concentration, decreased during hypoxia and hypothermia. The intrinsic control of cardiac function and white muscle perfusion in an anaesthetised fish, and the adaptive significance of reduced white muscle perfusion during hypoxia and hypothermia are discussed.

# Chapter 1 Thesis Introduction

The opaque fish fillets stacked on beds of ice or the frozen fish fingers we see in the supermarket are, metabolically speaking, the end of the line. Maintaining fresh fish quality is paramount in the various stages and processes on the pathway from the sea to supermarket. The primary area where large quality gains can be made is by maintaining the inherent energy reserves present in rested teleost muscle, which can only be done through reducing harvesting stress (Sigholt et al 1997, Robb 2001, Bosworth et al. 2007). However, many current industry practices do not promote stress free harvest and until greater emphasis is placed on retaining the inherent fish quality, exhausted fish will continue to be delivered to market. As the starting quality is already compromised, preservation of what little energy remains in the tissue can be achieved through storage methodology and the addition of supportive molecules to improve storage potential. The primary objectives of this thesis were: to explore potential delivery pathways of supportive molecules to teleost musculature, and combined with perfusion visualisation experiments, to generate a greater understanding of teleost white muscle perfusion.

Rested harvested fish that retain their inherent muscle energy reserves, have been shown to maintain fillet quality longer during storage than fish that have been stressed during harvest (Kiessling et al. 2004, Bosworth et al. 2007). Rested harvested catfish (*Ictalurus punctatus*) had lower blood cortisol concentrations, greater white muscle adenosine triphosphate (ATP) reserves, higher white muscle and blood pH values, lower white muscle and blood lactate concentrations and delayed rigor compared to fish harvest with induced stress (Bosworth et al. 2007). During storage, the rested harvest catfish fillets showed less water loss which is associated with an increase in soluble muscle protein due to the more rapid decrease in white muscle pH in the stressed harvested fish (Robb 2001). Kiessling et al. (2004) also showed greater water retention in Atlantic salmon (*Salmo salar*) steaks after 12 months frozen storage in rested harvested fish compared to fish not

rested harvested. Rested harvest and controlled storage prolongs muscle phosphogen and glycogen stores, delaying the inevitable increase in lactate and $H^+$ ions produced from anaerobic metabolism and subsequent tissue autolysis.

Perfusion experiments using *post-mortem* whole fish or isolated tissue preparations have been widely used in fish physiology research (Bolis and Rankin 1978, Perry et al. 1984, Bubien and Meade 1986, Perry et al. 2000). There are physiological (and ethical) benefits of using an isolated perfused tissue preparation, such as avoiding the potential interactions between tissues and organ systems. However, it is these interactions found in the intact live animal that can be most interesting. The aim of the isolated perfused tail preparation experiments in this thesis was to determine and improve blood flow distribution to the white muscle, with the addition of electrical stimuli to mimic muscle contractions, or by adding a vasodilating agent to the perfusate. By so doing we might discover methods of increasing the perfusion delivery potential of supportive media to the white muscle.

Results from the perfusion experiments showed that white muscle perfusion in the isolated tail preparation did not replicate that in the whole live fish. A new method of delivery was investigated which used direct uptake delivery, a method in which hydrophobic molecules diffuse across the gills into the blood, and are then perfused throughout the tissues of the live fish, via the circulatory system. Previous research, especially environmental toxicology research (van der Oost et al. 2002, Belpaire and Goemans 2007), has focused on the negative aspect of direct uptake and has shown that that small toxic hydrophobic molecules readily diffuse across the gills and rapidly accumulate in fish tissue. In this research I investigated positive benefits of direct uptake and its potential to deliver supportive molecules to the white muscle.

Isoeugenol is the active ingredient in the aquatic anesthetic AQUI-S$^{TM}$ and has been shown to readily diffuse into the blood to bioaccumulate in fish musculature

(Kildea et al. 2004, Meinertz et al. 2006). In this thesis, isoeugenol was used as a model molecule to evaluate the potential of the direct uptake delivery pathway. The uptake and recovery of isoeugenol from the plasma and white muscle and the anesthetic effect, at low, medium and high isoeugenol concentrations, was determined.

The direct up-take delivery methodology and progressive isoeugenol accumulation in the white muscle was shown to be very effective. The delivery of other supportive molecules was then investigated. Particular attention was placed on strong natural antioxidants with fluorescent properties, with which uptake could be readily assessed with fluorimetry and digital image analysis.

The spice turmeric contains curcumin and its curcuminoid derivatives (Anand et al. 2007), which are potent antioxidants (Toda et al. 1985, Jayaprakasha et al. 2006). Zhou et al. (2000) showed that turmeric at 40ppm almost completely prevented the formation of aldehydes in fermented cucumber pickle products exposed to oxygen. Cleary and McFeeters (2006) demonstrated that the addition of turmeric in the packout process of pasteurized dill pickles reduced the formation of oxidative off-flavours.

Research into the many medicinal benefits of curcumin and its derivatives has intensified over the last 20 years. Curcumin has been shown to have not only antioxidant activities, but also anti-inflamatory, anti-cancer, anti-bacterial, anti-viral, and anti-fungal activities (Sharma et al. 2005, Aggarwal at al. 2007). Curcumin may offer many other health benefits aside from strong antioxidant properties, and could be considered as a potential generic treatment for multiple ailments (Parker-Pope 2008).

The curcuminoids, eluted from an ethanol based turmeric stock solution, rapidly diffused across the gill and accumulated in the tissue of snapper. The inherent fluorescent properties of curcumin allowed the use of digital image analysis to

evaluate uptake and recovery, which was verified with conventional spectro-fluorimetric analysis.

By utilising direct uptake and the fish's own circulatory system, the successful perfusion and accumulation of an antioxidant into the musculature of a fish was achieved. Conventional antioxidant application is either dietary (Mourente et al. 2000, Chen et al. 2008) or topical (Aubourg et al. 2004, Sanchez-Alonso et al. 2008). The advantages of a diffusion-based application (especially compared with perfusion), are that the methodology is non- technical, non-invasive and there is potential for large-scale application.

The hydrophobic properties of the curcuminoids promote accumulation in lipid rich areas, which are more susceptible to lipid peroxidation and the rapid onset of rancidity during storage. A comparison between curcuminoid perfused and unperfused snapper showed that the curcuminoids offered no benefit in preserving the short term white muscle metabolic rundown. However, an accelerated storage trial showed reduced lipid peroxidation in the lipid rich red muscle in fish perfused with curcuminoids, suggesting the curcuminoids could have beneficial antioxidant effects during frozen storage, which when delivered via direct uptake, could potentially be applied as a pre-harvest treatment.

The delivery of all metabolites and additional supportive molecules to the musculature of fish relies on perfusion and continuing cardiac output. White muscle perfusion in teleosts is not well understood. A few studies with radioactive or fluorescent labeled microspheres have shown a snap-shot of blood flow and perfusion in the white muscle before, during and after exercise (Neumann et al. 1983, Kolok et al. 1993). However, very little is known about how changes in external environmental parameters affect white muscle perfusion. Cameron (1975) showed no significant change in the percentage distribution of blood to any organ or tissue during hypoxia. In this thesis, the use of fibre optodes and knowledge of the oxy-haemoglobin and deoxy-haemoglobin absorbance

spectra allowed real time observation of white muscle perfusion and haemoglobin saturation during progressive hypoxia and recovery, and progressive hypothermia and recovery. These results, combined with recorded cardiac performance allowed an insight into the control of white muscle perfusion in an anaesthetised fish.

## 1.1 References

Aggarwal BB, Sundaram C, Malani N, Ichikawa H (2007) Curcumin: The Indian solid gold. Molecular Targets and Therapeutic Uses of Curcumin in Health and Disease 595: 1-13

Anand P, Kunnumakkara AB, Newman RA, Aggarwal BB (2007) Bioavailability of Curcumin: Problems and Promises. Molecular Pharmaceutics 4: 807-818

Aubourg SP, Perez-Alonso F, Gallardo JM (2004) Studies on rancidity inhibition in frozen horse mackerel (*Trachurus trachurus*) by citric and ascorbic acids. European Journal of Lipid Science and Technology 106: 232-240

Belpaire C, Goemans G (2007) Eels: contaminant cocktails pinpointing environmental contamination. ICES Journal of Marine Science 64: 1423-1436

Bolis L, Rankin JC (1978) Vascular effects of acetylcholine, catecholamines and detergents on isolated perfused gills of pink salmon *Oncorhynchus gorbuscha* coho salmon, *O. kisutch* and chum salmon, *O. keta*. Journal of Fish Biology 13: 543-547

Bosworth BG, Small BC, Gregory D, Kim J, Black SE, Jerrett AR (2007) Effects of rested-harvest using the anesthetic AQUI-S™ on channel catfish, *Ictalurus punctatus*, physiology and fillet quality. Aquaculture 262: 302-318

Bubien JK, Meade TL (1986) Electrophysiological abnormalities produced by ammonium in isolated perfused brook trout, *Salvelinus fontinalis*, hearts. Journal of Fish Biology 28: 47-53

Cameron JN (1975) Blood flow distribution as indicated by tracer microspheres in resting and hypoxic arctic grayling (*Thymallus arcticus*). Comparative Biochemistry and Physiology 52A: 441-444

Chen YC, Nguyen J, Semmens K, Beamer S, Jaczynski J (2008) Effects of dietary alpha-tocopheryl acetate on lipid oxidation and alpha-tocopherol content of novel omega-3-enhanced farmed rainbow trout (*Oncorhynchus mykiss*) fillets. Food Science and Technology 41: 244-253

Cleary K, McFeeters RF (2006) Effects of oxygen and turmeric on the formation of oxidative aldehydes in fresh-pack dill pickles. Journal of Agricultural and Food Chemistry 54: 3421-3427

Jayaprakasha GK, Jaganmohan Rao I, Sakariah KK (2006) Antioxidant activities of curcumin, demethoxycurcumin and bisemethoxycurcumin. Food Chemistry 98: 720-724

Kildea MA, Allan GL, Kearney RE (2004) Accumulation and clearence of the anaesthetics clove oil and AQUI-S$^{TM}$ from the edible tissue of silver perch (*Bidyanus bidyanus*). Aquaculture 232: 265-277

Kiessling AK, Espe M, Rouohonen K, Morkore T (2004) Texture, gaping and colour of flesh and frozen Atlantic salmon flesh as affected by pre-slaughter iso-eugenol or CO2 anaesthesia. Aquaculture 236: 645-657.

Kolok AS, Spooner RM, Farrall AP (1993) The effect of exercise on the cardiac output and blood flow distribution of the largescale sucker *Catostomus macrocheilus*. Journal of Experimental Biology 183: 301-321

Meinertz JR, Greseth SL, Schreier TM, Bernardy JA, Gingerich WH (2006) Isoeuganol concentrations in Rainbow trout (*Salmo gairdneri*) skin-on fillet tissue after exposure to AQUI-S$^{TM}$ at different temperatures, durations and concentrations. Aquaculture 254: 347-354

Mourente G, Diaz-Salvago E, Tocher DR, Bell JG (2000) Effects of dietary polyunsaturated fatty acid/vitamin E (PUFA/tocopherol ratio on antioxidant defence mechanisms of juvenile gilthead sea bream (*Sparus aurata L.*, Osteichthyes, Sparidae). Fish Physiology and Biochemistry 23: 337-351

Neumann P, Holeton GF, Heisler N (1983) Cardiac output and regional blood flow in gills and muscles after exhaustive exercise in rainbow trout (*Salmo gairdneri*). Journal of Experimental Biology 105: 1-14

Parker-Pope T (2008) The eleven best foods you aren't eating. New York Times, June 30

Perry SF, Davie PS, Daxboeck C, Ellis AG, Smith DG (1984) Perfusion methods for the study of gill physiology. In Hoar WS, Randall DJ eds, Fish Physiology, Vol. XB. Academic Press, New York, pp 325-388

Perry SF, Montpetit C J, Borowska M (2000) The effects of acute hypoxia on chemically or neuronally induced catecholamine secretion in rainbow trout (*Oncorhynchus mykiss*) in situ and in vivo. Journal of Experimental Biology 203: 1487-1495

Robb DHF (2001) The relationship between killing methods and quality. In Kestin S C, WPD Ed, Farmed Fish Quality. Fishing News Books, Ch 20 pp220-233

Sanchez-Alonso I, Borderias AJ (2008) Technological effect of red grape antioxidant dietary fibre added to minced fish muscle. International Journal of Food Science and Technology 43: 1009-1018

Sharma RA, Gescher AJ, Steward WP (2005) Curcumin: The story so far. European Journal of Cancer 41: 1955-1968

Sigholt T, Erikson U, Rustard T, Johansen S, Nordtvedt TS, Seland A (1997) Handling stress and storage temperature affect meat quality of farmed-raised Atlantic salmon (*Salmo Salar*). Journal of Food Science 62: 898-905

Toda S, Miyase T, Arichi H, Tanizawa H, Takino Y (1985) Natural anti-oxidants III. Antioxidative components isolated from rhizome *Curcuma longa* L. Chemical and Pharmaceutical Bulletin 33: 1725-1728

van der Oost R, Beyer J, Vermeulen NPE (2002) Fish bioaccumulation and biomarkers in environmental risk assessment: a review. Environmental Toxicology and Pharmacology 13: 57-149

Zhou A, McFeeters RF, Fleming HP (2000) Inhibition of formation of oxidative volatile components in fermented cucumbers by ascorbic acid and turmeric. Journal of Agricultural and Food Chemistry 48: 4910-4912

# Chapter 2 Blood flow distribution to the red and white muscle in the perfused Chinook salmon (*Oncorhynchus tshawytscha*) tail

## 2.1 Abstract

The blood flow distribution (BFD) to the red and white muscle of an isolated Chinook salmon (*Oncorhynchus tshawytscha*) perfused tail preparation was determined using fluorescent microspheres. Perfusion was assessed as a method of delivering supportive media to the white muscle of teleost fish. The perfused isolated tail preparation showed reduced perfusion to the white muscle compared with that in the live fish, with a red muscle:white muscle BFD ratio of 5.8±1.8, compared with 1.8±0.5 in the live Chinook salmon. Adding a vasodilating agent (sodium nitroprusside) to the perfusate or stimulating the tail electrically improved perfusion to the red muscle but not the white muscle. Both treatments also decreased venous outflow, suggesting that vessel permeability was affected. Tail perfusions have been and still are a useful experimental preparation in physiological research, not least for ethical reasons, but the preparation needs further refinement before it can mimic the perfusion parameters in the live fish.

## 2.2 Introduction

The aims of the Chinook salmon isolated tail perfusion experiments are: to determine and improve blood flow distribution to the white muscle in the perfused tail preparation, and to assess artificial perfusion as a method of delivering supportive molecules to teleost musculature.

The separation of teleost myotomal muscle into distinct zones is ideal for research on individual fibre types. White, pink and red muscle fibres differ physically, metabolically and functionally. Red muscle (RM) is located in a thin wedge running under the lateral line from the behind the head to the caudal fin, and the remaining bulk of the myotome is comprised of white muscle (WM) (Bone 1978, Johnston 1981). WM consists of large diameter fast twitch glycolytic fibres, whereas RM consists of smaller diameter slow twitch oxidative fibres. Pink (intermediate) muscle fibres have intermediate properties, both anatomically and physiologically (Johnston 1981). The diameters of rainbow trout red and white muscle fibres were 20-25μ and 35-55μ respectively (Johnston et al. 1975) and RM is more vascularised than WM. Davie et al. (1986) found that the number of capillaries per muscle fibre in rainbow trout RM was 2.28±0.07 compared with 0.64±0.06 in WM, but ratios vary between species (Egginton 1992). The product of smaller muscle fibres, with a higher surface to volume ratio, and greater capillary density allows RM to rapidly exchange substrates and metabolites, enabling it to function aerobically without exhaustion. By contrast WM, with a lower capillary density and larger fibre diameter, functions anaerobically and is rapidly fatigued. RM is used when low to medium activity is required (slow swimming and positioning in the water column). WM however, is used when a high level of activity is required (prey capture and predator avoidance) (Johnston 1981).

Perfusion as an experimental method has been, and still is applied in many fields of scientific research, from the transplantation of mammalian tissues (Southard

and Belzer 1995, Wagh et al. 2000), to the study of vasculature physiology in teleosts (Bolis and Rankin 1978, Bubien and Meade 1986, Perry et al. 2000). By perfusing isolated tissues following euthanasia the potential interactions with other organ systems are reduced, and use of a conscious animal is avoided. The composition of the perfusate used is important; polyvinylpyrrolidone (PVP) and bovine serum albumin (BSA) are often added as colloid osmotic fillers to reduce the severity of oedema. The delivery of supportive molecules via perfusion allows flexibility as the composition of the perfusate can be modified easily.

Regional blood flow distribution (BFD) to the red and white muscle has been determined in a number of teleost species: Arctic grayling (Cameron 1975), rainbow trout (Neumann et al. 1983, Barron et al. 1987), large-scale sucker (Kolok et al. 1993), and channel catfish (Schultz et al. 1999). The majority of BFD research has been undertaken on dorsal aorta (DA) cannulated live fish. Little is known of the BFD in the perfused tail, a preparation that has been used to assess vascular flow and resistance (Wood and Shelton 1975, Davie 1981, Canty and Farrell 1985). This study compares the regional blood flow to the red and white muscle in live Chinook salmon fitted with a DA cannula, and in the perfused, isolated tail preparation. The effects of adding sodium nitroprusside (SNP) (a nitric oxide (NO) releasing agent) to the perfusate, and of electrical stimulation of the muscle are assessed. NO has been shown to dilate the vasculature in fish (McGeer and Eddy 1996, Olson et al. 1997). Neumann et al. (1983) and Kolok et al. (1993) demonstrated that the BFD in the teleost changes after exercise. By electrically stimulating the tail post-mortem we aimed to simulate exercise (Egginton and Hudlická 2000, Behnke et al. 2001).

Radioactively-labelled microspheres (MS) have been widely used in physiology to quantify regional blood flow distribution and cardiac output of teleost preparations (Cameron 1975, Neumann et al. 1983, Barron et al. 1987, Schultz et al. 1999). More recently there has been a move towards the use of fluorescent MS, which has been shown to be as accurate as using radioactive MS (Kolok et al. 1993, Van

Oosterhout et al. 1995, Deveci and Egginton 1999, Mulder et al. 2001). Fluorescent MS work on the same principle as radioactive MS. They are injected into the circulation system and become entrapped in small vessels. The number of MS trapped in each tissue can be assessed using fluorescence detection.

## 2.3 Methods

### 2.3.1 Experimental animals

Chinook salmon (*Oncorhynchus tshawytscha*) were kindly provided by Isaac Salmon Farm, McLeans Island, Christchurch, who also allowed us the use of their site hatchery as a location to store fish. Fish were removed from the raceways and transported to the hatchery where they were held at a maximum density of 6 in circular tanks (1.6$m^3$, 13.0±2.0$^oC$). Fish were unfed for 48 hours prior to experimentation. The experimental protocol was approved by the University of Canterbury's Animal Ethics Committee.

### 2.3.2 Blood flow distribution in the perfused tail

#### 2.3.2.1 Chinook salmon tail perfusion

Chinook salmon were anaesthetised with 20 $mg.L^{-1}$ AQUI-S$^{TM}$ until they were unconscious and could be handled without struggling (approximately 45 min). The fish was removed, and killed by iki jime (inserting a metal spike into the brain destroying the brain) and 1ml heparinised saline was injected into the dorsal aorta (DA). Dorso-ventral incisions all the way to the vertebrae were made from the dorsal, ventral and lateral surfaces in two locations, posterior to the dorsal fin and 15mm anterior of this. The tissue between the incisions was removed leaving the tail attached by a connecting column containing vertebrae, nerve cord, caudal artery (CA) and caudal vein (CV). The connecting column was severed at the anterior end, the tail weighed, and the CA and CV were cannulated (1.0mm ID, 1.5mm OD). Two cable ties were tightened around the 'stump' to hold the cannulae in place and create a seal. The tail was placed upright in air in a temperature controlled unit at 4-5$^oC$. Aerated saline, stored in the temperature controlled unit, was pumped (Gilson Minipulse 3, France) at 3$ml.min^{-1}.100g^{-1}$ through the tail. Perfusion pressure was recorded (ADInstruments, Dunedin, with Chart 4.0 software). Venous outflow was recorded with a force transducer (MLT

0210/D, ADInstruments) triggered by each drop of saline dripping out of the caudal vein cannula. All transducers were contained within the temperature controlled chamber (4-5$^{o}$C).

#### 2.3.2.2 Saline

The saline used was a modified Rees-Simpson saline (Clements and Rees, 1998), balanced to pH 7.8, osmolarity 299±2.0 mOsmol.L$^{-1}$ (Wescor 5100C Vapour Pressure Osmometer). The composition of the saline was; 8.00g.L$^{-1}$ NaCl, 0.157g.L$^{-1}$KCl, 0.203g.L$^{-1}$ $MgCl_2.6H_2O$, 0.191g.L$^{-1}$ $CaCl_2.2H_2O$, 1.802g.L$^{-1}$ $C_6H_{12}O_6$, 0.213g.L$^{-1}$ BES, 0.051g.L$^{-1}$ $Na^+$-glutamate, 0.059g.L$^{-1}$ L-glutamate, 0.003g.L$^{-1}$ $Na^+$-asparate, 0.010g.L$^{-1}$ DL-carnitine, 30.000g.L$^{-1}$ Polyvinylpyrrolidone (PVP) (MW 40 000), 20.000g.L$^{-1}$ Bovine serum albumin fraction V, low endotoxin (BSA). Chemicals were obtained from Sigma Chemical Company, St. Louis., apart from BSA fraction V, low endotoxin, which was purchased from Invitrogen (Auckland, NZ).

#### 2.3.2.1 Muscle samples

White D block muscle samples (the white muscle D block is the first and largest white muscle group dorsal to the vertebra) and corresponding RM samples were taken at 6 standardised locations in the tail (anterior to the anal fin, anterior to the adipose fin and anterior to the caudal fin on both left and right sides). Blood flow distribution to the red and white muscle was determined by the distribution of 15µm diameter fluorescent MS trapped in each tissue. Colours of MS used were; orange (Ex 534 nm, Em 554 nm), yellow/green (Ex 495 nm, Em 505 nm), red (Ex 580 nm, Em 605 nm) and crimson (Ex 625 nm, Em 645 nm). Muscle samples were weighed, placed in test tubes with 10ml digestion fluid (2M ethanolic KOH and 0.5% Tween 80) and were incubated in the dark at 37$^{o}$C for 48 hours. The sample was centrifuged (Eppendorf 3200) for 10 min at 3400rpm and the supernatant removed. The pellet was resuspended by adding 10ml of 0.25% Tween 80 in distilled water and vortexing for 3 min. The sample was then

centrifuged and the supernatant removed. The pellet was then resuspended in distilled water before centrifugation and removal of the supernatant. 3ml of solvent (2-ethoxyethyl acetate) was added to the pellet, which was resuspended before being incubated at 37$^{o}$C for 3 hours. The samples were centrifuged and 150µL of supernatant was pipetted into a fluorescent well plate to be read in the Cary Eclipse Fluorimeter (Varian Instruments, Australia). MS distribution was expressed per gram tissue mass (MS.g$^{-1}$), and as a red muscle/white muscle ratio (RM:WM).

### 2.3.3 Experimental treatments

Tails were perfused with modified Rees-Simpson saline for 60 min. At 30 min (pre-treatment) and 50 min (5min before the end of the treatment, referred to as post-treatment), different coloured MS were injected into the CA cannula. The quantity of MS injected was approximately 100 000 per 100g tail. A sleeve was pulled over the cannula after each injection to prevent leakage from the injection site. The treatment duration was 20 min (from 35 min to 55 min)

#### 2.3.3.1 Live fish (LIVE)

The methodology used to obtained dorsal aortic pressures and BFD in the white and red muscle can be found in Janssen, (2003).

#### 2.3.3.2 Control tail (CNTRL)

No additional treatment.

#### 2.3.3.3 Sodium Nitroprusside tail (SNP)

Tail perfusion switched at 35 min to Rees-Simpson saline containing SNP ($10^{-5}$M).

#### 2.3.3.4 Neural stimulated tail (NSTIM)

Tails were stimulated at elapsed time from 35 min to 55 min. Stimulation was 2mA for 1ms at a frequency of 1Hz (Danish Myotechnology current stimulator,

CS200). The first electrode was a small alligator clip attached to the fork of the tail. The second electrode was a stainless steel needle inserted horizontally along the nerve cord from the anterior cut surface

## 2.4 Results

### 2.4.1 Blood flow distribution in the perfused tail

Data from the LIVE fish treatment were derived from Janssen (2003), a MSc thesis that preceded this PhD research. The actual MS.$g^{-1}$ values are not presented, however the calculated total MS recovered from the tail in each treatment is very similar to the approximated number of MS injected.

**Table 2.1 Salmon white muscle cut surface pH, body and tail weight from a live fish (LIVE) and perfused tails; control (CNTRL), sodium nitroprusside added (SNP) and electrically stimulated (NSTIM).**

| | White muscle cut surface pH | Fish (g) | Tail (g) | (%) |
|---|---|---|---|---|
| LIVE (5) | n/a | 1248±135 | n/a | |
| CNTRL (6) | 7.64±0.01 | 965±55 | 268±19 | (27.7±0.4) |
| SNP (4) | 7.57±0.03 | 1012±11 | 274±12 | (27.1±0.9) |
| NSTIM (5) | 7.64±0.02 | 941±44 | 256±10 | (27.3±0.3) |

The initial muscle cut surface pH for all treatments was ~ 7.6 indicating that the animals were at a highly rested state for experimentation (Table 2.1) (Jerrett et al., 1996). In preliminary experiments weight change was measured by placing the tail on a balance and determined that the saline used and flow rates delivered did not cause a weight gain or loss, suggesting that oedema did not develop. Oedema has proved to be a problem with perfused preparations in the past (Perry and Farrell, 1989).

Figure 2.1 shows the pre and post treatment MS injection BFD RM:WM ratios. The pre treatment BFD ratios were as follows; LIVE 1.8±0.5, CONTROL 5.8±1.8, SNP 6.8±1.9, NSTIM 4.2±0.6 (Figure. 2.1). The BFD RM:WM ratio determined from the pre treatment MS injection was significantly greater in all of the perfused tail treatments than in the LIVE fish pre treatment BFD RM:WM ratio. In all perfused tail treatments there was an increase in the BFD RM:WM ratio between

the pre and post treatment MS injections, but the increase was only significant (unpaired, two-tailed Student's t-test, $P<0.05$) in the NSTIM treatment.

Figure 2.2 shows the BFD as percentage $MS.g^{-1}$ from the pre and post treatment MS injections in both the red and white muscle. The percentage $MS.g^{-1}$ distribution in the red muscle from the LIVE fish pre treatment MS injection was significantly (unpaired, two-tailed Student's t-test, $P<0.05$) lower than the pre treatment MS injection in the perfused tail treatments. However the inverse was found in the white muscle, the percentage $MS.g^{-1}$ distribution in the white muscle from the LIVE fish pre treatment MS injection was significantly greater than all of the perfused tail treatments pre treatment MS injections (unpaired, two-tailed Student's t-test, $P<0.05$).

In all perfused tail treatments the percentage $MS.g^{-1}$ distribution increased in the red muscle post treatment, but the increase was only significant in the NSTIM treatment (Figure 2.2). In all perfused tail treatments the percentage $MS.g^{-1}$ distribution decreased in the white muscle, and was again only significant in the NSTIM treatment. There was no significant difference in the red or white muscle pre or post treatment MS injection percentage $MS.g^{-1}$ distribution between the CONTROL treatment and the other perfused tail treatments.

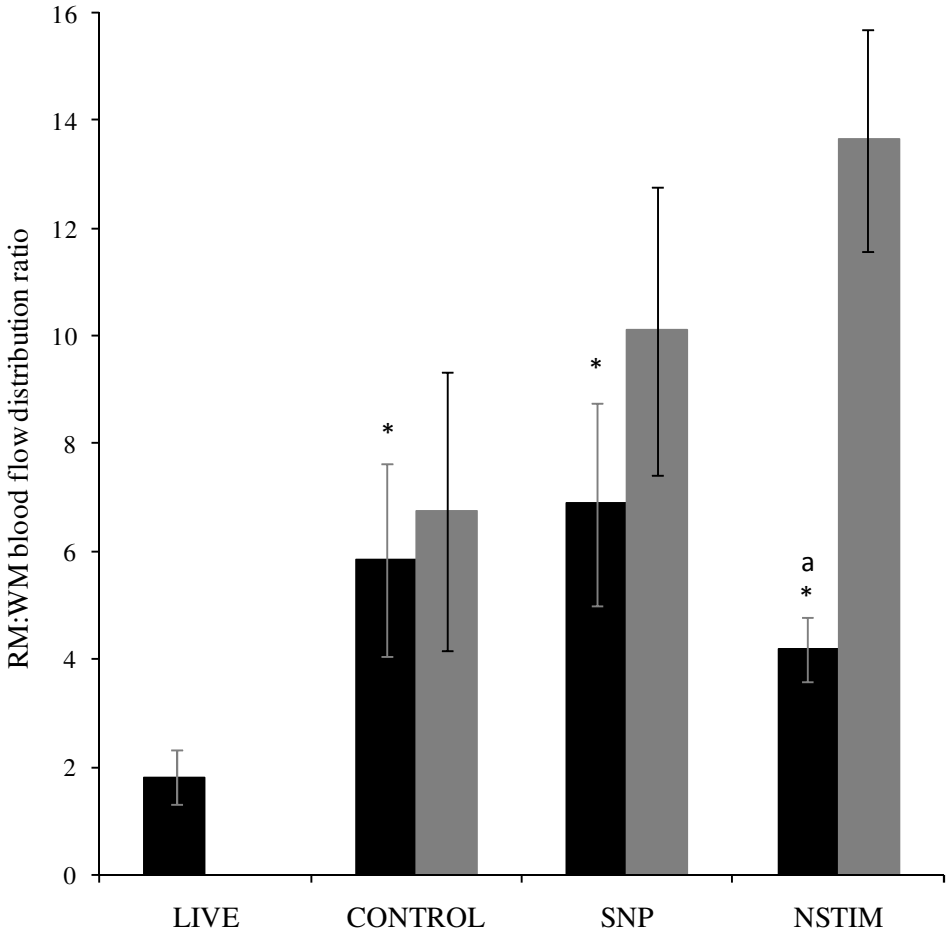


**Figure 2.1 RM:WM blood flow distribution ratio pre treatment (black), and post treatment (grey).** * indicates significant difference from the LIVE pre treatment, a indicates significant difference between the pre and post treatment ratios within a treatment. Significance determined by an unpaired two tailed Students t-test, $P<0.05$. Values are means ± sem. LIVE (N=5), CNTRL (N=6), SNP (N=4) NSTIM (N=5).

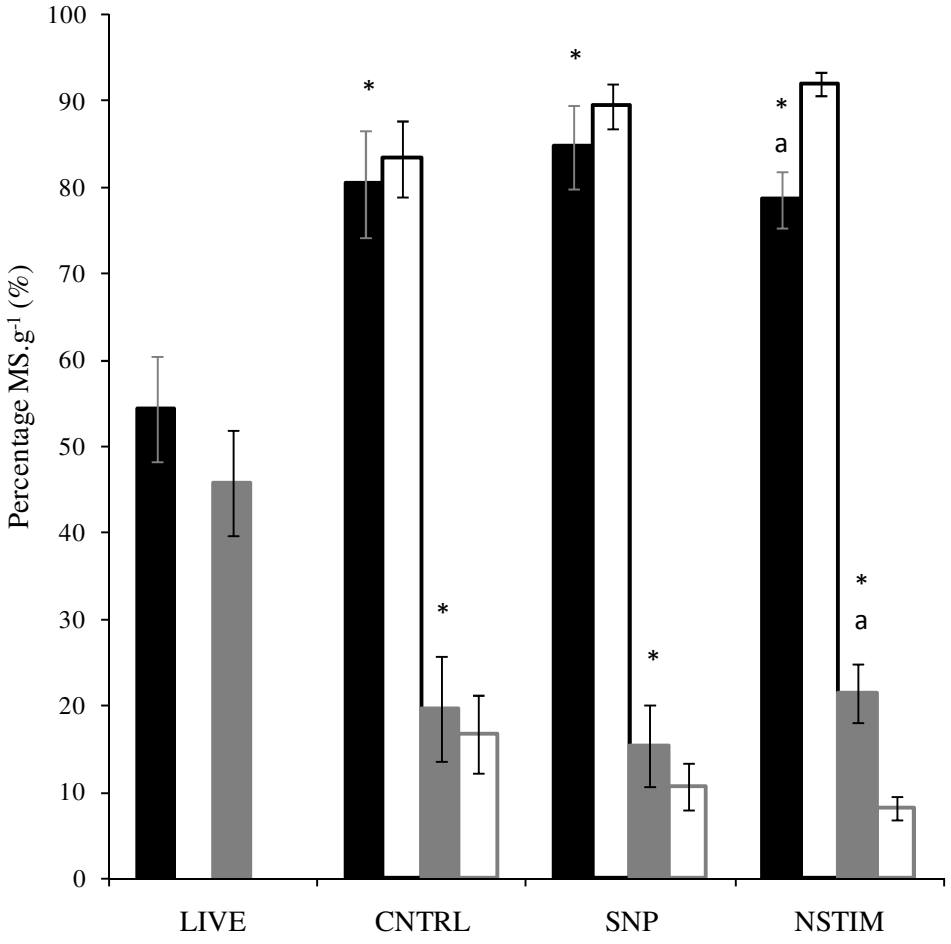


**Figure 2.2 Percentage of recovered MS.g$^{-1}$ in red muscle (black) and white muscle (grey) from pre treatment (solid) and post treatment (clear) MS injection.** * denotes a significant difference from the LIVE pre treatment within muscle type. a denotes a significant difference within treatment and muscle type between pre and post MS injection. Significant difference was determined with an unpaired two-tailed Student's t-test, $P<0.05$. Values are means ± sem. LIVE (N=5), CNTRL (N=6), SNP (N=4).

The resting dorsal aortic pressure (DAP) of the LIVE salmon prior to injection of fluorescent MS was 50.8±0.8 cm water (Table 2.2).

**Table 2.2 Perfusion pressure in the Chinook salmon tail.** The first MS pressure value in the LIVE treatment is the dorsal aortic pressure (DAP). Initial perfusion pressure was measured as the mean pressure over the first 15 min. Perfusion pressures when the first and second MS were injected at 30 min and 50 min, respectively. The average pressure is taken over the duration of the experiment. Values are mean ± sem.

| | Initial ($cm H_2O$) | First MS ($cm H_2O$) | Second MS ($cm H_2O$) | Average ($cm H_2O$) |
|---|---|---|---|---|
| LIVE (5) | n/a | 50.8±0.8 | n/a | n/a |
| CNTRL (6) | 29.16±0.05 | 28.48±1.02 | 29.57±1.1 | 29.90±0.38 |
| SNP (4) | 31.45±0.46 | 30.18±0.88 | 29.78±1.05 | 30.87±0.26 |
| NSTIM (5) | 31.49±0.76 | 31.13±1.63 | 31.04±2.15 | 30.86±0.5 |

Figures 2.3.A and B show changes in perfusion pressure as a percentage of the initial perfusion pressure (average over the first 15 min), allowing relative comparison between treatments. Actual perfusion pressures at the start, MS injections and an average are described in Table 2.2. A two-tailed unpaired Student's t-test was used to determine significant difference between the treatments at a given time value and a Tukey's multiple comparison test was used within treatments to determine significant difference from the 5 min time value.

The perfusion pressure in all the CNTRL tail increased significantly (two-tailed, un-paired Student's t-test, $P<0.05$) with each MS injection. The perfusion pressure increased from 97.6±1.3% initial perfusion pressure at 30 min to 102.3±1.2% initial perfusion pressure at 35 min and from 101.3±1.3% initial perfusion pressure at 50 min to 115.5±2.7% initial perfusion pressure at 55 min (Figure.2.3.A).

Perfusion pressure increased significantly (two-tailed, un-paired Student's t-test, $P<0.05$) with each MS injection in the SNP tail. Pressure decreased when the

saline containing SNP was perfused through the tail, but the decrease was not significantly different from the 5 min perfusion pressure value. The perfusion pressure was significantly lower in the SNP tail than in the CNTRL tail at 50 and 60 min (Figure 2.3.A).

There was no increase in perfusion pressure with the pre and post MS injections in the neurally stimulated tail (NSTIM). However when the tail was stimulated (35 min), the perfusion pressure initially decreased (significantly, two-tailed, unpaired Student's t-test, $P<0.05$) to 89.71±4.88% initial pressure by 40 min, before increasing to 98.21±6.70% initial pressure at 50 min, a level similar to the CNTRL treatment (101.35±3.14% initial pressure) (Figure 2.3.B). Pressure in the NSTIM treatment was significantly lower than the CNTRL treatment between 40-45 min and 55-60 min (Figure. 2.3.B).

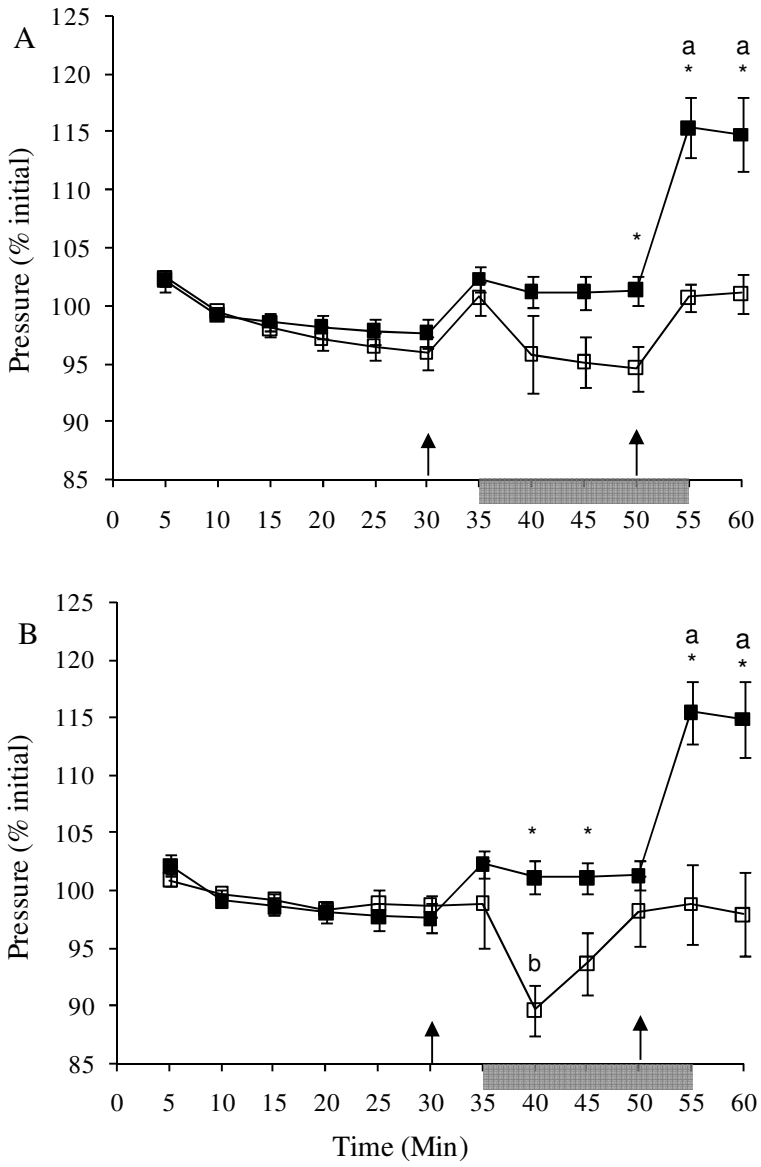


**Figure 2.3 Change in perfusion pressure (percentage change from initial 15 min average) during the tail perfusion experiments.** A) CNTRL (black) and SNP (clear), B) CNTRL (black) and NSTIM (clear). * indicates significant difference (unpaired two tailed Students t-test, P<0.05) between CNTRL and treatment. a denotes a significant difference (Tukey's Multiple Comparison Test, P<0.05) from the 5 min CNTRL value and b denotes a significant difference (Tukey's Multiple Comparison Test, P<0.05) from the 5 min treatment value. Values are mean ± sem, CNTRL (N=6), SNP (N=4) NSTIM (N=5). Arrows indicate MS injections, shading indicates treatment duration.

Table 2.3 shows the perfusion outflow from each tail preparation, 3 ml.min.$^{-1}$100g$^{-1}$ was perfused through the tail, and in each treatment the actual measured outflow was slightly less than the perfused inflow.

**Table 2.3 Perfusion outflow in the Chinook salmon tail.** Initial outflow is taken as the mean outflow over of the first 15 min. The first and second MS were injected at 30 min and 50 min, respectively. Values are mean ± sem.

| | Initial (ml.min$^{-1}$100g$^{-1}$) | First MS (ml.min$^{-1}$100g$^{-1}$) | Second MS (ml.min$^{-1}$100g$^{-1}$) | Average (ml.min$^{-1}$100g$^{-1}$) |
|---|---|---|---|---|
| CNTRL (6) | 2.89±0.05 | 2.80±0.1 | 2.80±0.11 | 2.82±0.03 |
| SNP (4) | 2.78±0.03 | 2.72±0.05 | 2.63±0.02 | 2.69±0.01 |
| NSTIM (5) | 2.95±0.03 | 2.83±0.08 | 2.56±0.09 | 2.77±.0.03 |

Perfusion outflow (ml.min$^{-1}$.100g$^{-1}$) via the venous cannula is presented as a percentage of the initial outflow (average of the first 15 min) (Figures 2.4.A and B). In all treatments, perfusion outflow from the venous cannula decreased over the 60 min perfusion period. A two-tailed unpaired Student's t-test was used to determine significant difference between the treatments at a given time value and a Tukey's multiple comparison test was used within treatments to determine significant difference from the 5 min time value.

The outflow in the CNTRL tail decreased over the duration of the 60 min perfusion, but there was no significant difference at any time value with the initial 5 min value (Figure 2.4.A). There was no increase or decrease in outflow attributed to the pre or post treatment MS injection in any of the treatments.

The outflow in the SNP tail also decreased gradually over time. It showed a slightly greater rate than the CNTRL but was not significantly different. The outflow in the SNP tail was significantly different to the initial outflow from 45 min-60 min (Figure 2.4.A).

The perfusion outflow in the NSTIM tail decreased significantly from 98.9±3.8% at 35 min to 89.7±2.1% at 40 min when stimulated neurally. The perfusion outflow from 40-60 min was significantly lower than the initial NSTIM out-flow and corresponding CNTRL value (Figure 2.4.B).

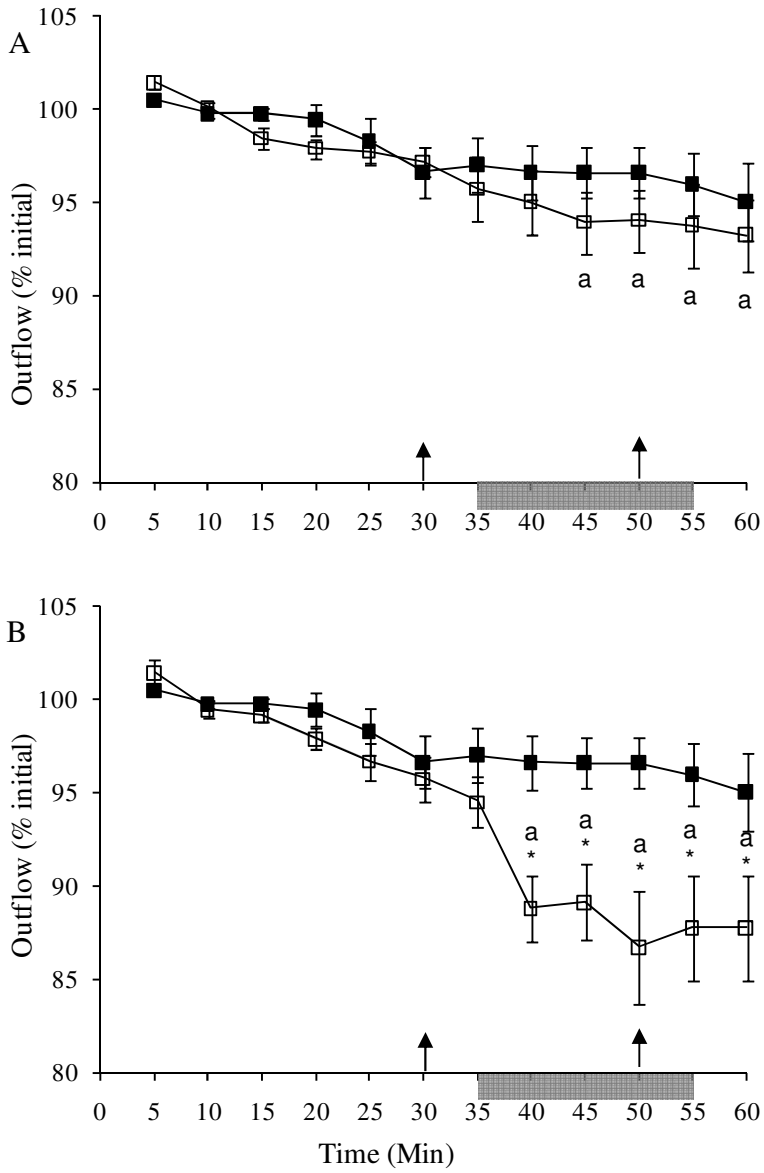


**Figure 2.4 Change in perfusion outflow (percentage change from initial 15 min average).** A) CNTRL (black) and SNP (clear), B) CNTRL (black) and NSTIM (clear). * indicates significant difference (unpaired two tailed Students t-test, $P<0.05$) between CNTRL and treatment. a denotes a significant difference (Tukey's Multiple Comparison Test, $P<0.05$) from 5 min value and in the treatment. Values are means ± sem, CNTRL (N=6), SNP (N=4) NSTIM (N=5). Arrows indicate MS injections, shading indicates treatment duration.

## 2.5 Discussion

The resting DAP of the live Chinook salmon was 50.8±0.8 $cmH_20$ (Table 2.2), slightly higher than the value recorded by Hill and Forster (2004) and Rothwell et al. (2005), with fish of similar body mass (46.0±1.9 $cmH_20$ and 41.1±3.4 $cmH_20$, respectively). Our recorded DAP lies in the range of those recorded by Kiceniuk and Jones (1977) in resting and exercised rainbow trout (*Salmo gairdneri*), demonstrating that our DAP was within the physiological range.

Oedema is the build-up of interstitial fluid due to an imbalance between the colloid osmotic pressure of the perfusate and the vascular hydrostatic pressure and has been a persistent problem with perfused preparations. However, most researchers now use PVP and BSA in the perfusate as colloid osmotic fillers to reduce the severity of oedema (Perry and Farrell 1989). Oedema is often measured by a weight gain in the perfused tissue. Previous work by the author (unpublished) showed that with rested harvested salmon tissue (tail), and the saline used in the current treatments, the weight gain was only 1.8±1.3% over 22 hours perfusion. As the preparations in this series of tail perfusions were only perfused for 60 min, oedema was deemed to be negligible.

The BFD RM:WM ratio in the live Chinook salmon tail was 1.8±0.5 (Figure 2.1). Neumann et al. (1983) recorded a ratio of 2.25 in the rainbow trout (*S. gairdneri*). Our ratio is also lower than the capillary density (CD) ratio of 3.5 recorded by Davie et al. (1986) in the rainbow trout. Other published values vary from a RM:WM BFD of 1.37 in the channel catfish (*Ictalurus punctatus*, Schultz et al. 1999) to 10 in Artic grayling (*Thymallus arcticus*, Cameron 1975).

Capillary densities in RM and WM fibres of teleost fish also vary considerably between species, and are also affected by developmental and seasonal changes (Egginton 1992). In striped bass (*Morone saxatilis*) the CD ratio (RM:WM) was 7 in cold-adapted fish, and 11 in warm-acclimated fish (Egginton and Sidell 1989).

In sub-adult freshwater eels the value was 6 and in adult conger eels (*Conger conger*) it was close to 30 (Egginton et al. 1988). Greater capillary density in the red muscle should be reflected in the BFD ratio. Our data suggest that either farmed Chinook salmon has a relatively well developed WM blood supply, or that the RM blood supply is poorly developed.

The salmon used in our experiments were all farmed fish. Farmed fish are often referred to as "lazy fish" as they live in a predator-free, food abundant environment, compared with wild populations which have to avoid predators and catch food. Farmed fish may not use their WM as much as wild fish, and are often seen "cruising" round the tank at speeds that would only require the recruitment of the red muscle. They may only recruit the white muscle when they accelerate to catch pellets at feeding times or in times of stress (crowding, harvest etc). Dunmal et al. (2003) found no significant difference in cardiac performance between wild and farmed Atlantic salmon (*Salmo salar*). However, cardiac abnormalities have been noted in some cultured fish (Gamperl and Farrell 2004) and aerobic performance correlates with cardiac morphology (Claireaux et al. 2005). It is also possible to argue that farmed fish in constantly flowing water without a refuge may be aerobically trained. Davie et al. (1986) described a maximum increase in rainbow trout capillary density per muscle fibre in red and white muscle of 27% and 95%, after aerobic training at 1.0 $bls^{-1}$ for 200 days.

The perfused tail preparation did not reproduce the BFD in the live animal. A mean BFD RM:WM ratio of 5.8±1.8in the tail preparation, indicated a relatively greater perfusion of the RM than the WM compared with the live fish (Figure 2.1). This is reiterated with a greater percentage of the $MS.g^{-1}$ distributed in the red muscle (Figure 2.2).

The perfusion pressure increased acutely with each MS injection indicating an increase in vascular resistance (Figure 2.3). The overall increase in perfusion pressure was approximately ~5-15% over the 60 min perfusion, except for the

NSTIM tail (Figure 2.3B). These acute increases in perfusion pressure can be attributed to the microspheres wedging within and blocking the small arterioles. However, as the RM:WM BFD values from the first and second MS injection in the CNTRL tail (Figure 2.1) were similar, we can assume that any blockages were uniformly distributed.

The tail perfusion pressures were lower than that seen in the DAP in the live fish (Table 2.2). The perfusion flow was set to $3ml.min^{-1}100g^{-1}$ tail which was shown in previous work (unpublished) by the author to produce almost negligible oedema. However a low perfusion pressure may have biased the blood flow distribution as it may have directed it towards the more vascularised, and potentially vasodilated red muscle.

Rothwell et al. (2005) showed an increase in heart rate but decrease in dorsal aortic pressure (DAP) during anaesthesia with AQUI-S$^{TM}$ in Chinook salmon. The decrease in DAP may be attributed to the vasorelaxing properties of isoeugenol, since blood flow may be redirected to highly vascularised (and vasodilated) tissues.

There were no significant changes in the $MS.g^{-1}$ distribution between the pre and post treatment MS injections, in either the red or white muscle (Figure 2.2). The addition of SNP to the tail reduced the perfusion pressure (Figure. 2.3A). Because the inflow was constant, the reduction in pressure can be attributed to the dilating effect of NO on the tail vasculature. NO has been shown to dilate a variety of vessels in teleost fish (McGeer and Eddy 1996, Mustafa et al. 1997, Schwerte et al. 1999, Jennings et al. 2004) and the relative sensitivity of different vascular beds, indicated above, deserves further attention. If the dimensions of the vascular beds differ between tissues, the choice of size of the MS (15µm diameter in our case) might also affect the apparent distribution. The vasodilating effect of NO on the tail vasculature may have been limited by an already reduced vascular tonus due to the vasodilating effects of isoeugenol (Rothwell et al. 2005).

Electrical stimulation was used to mimic the effects of exercise, which has been shown to increase perfusion to the tail musculature of fish. Kolok et al. (1993) demonstrated in the largescale sucker (*Catostomus macrocheilus*) that perfusion increased significantly in the RM during exercise and there was little effect on perfusion of the WM. However, Neumann et al. (1983) showed that blood flow increased to both the RM (230%) and WM (490%) in the rainbow trout following exercise induced by electric shock, the effect being greater for the WM than the RM. Stimulation of our tail preparation via the nerve cord increased perfusion to the RM more than to theWM, shown by an increase in the RM:WM (Figure 2.1). There was also a significant increase (RM) and decrease (WM) in the $MS.g^{-1}$ distribution between the pre and post treatment MS injections (Figure 2.2). The NSTIM treatment showed an initial decrease in perfusion pressure when stimulation started (Figure 2.3), which at constant inflow indicates a fall in vascular resistance attributed to vasodilation or capillary recruitment during "exercise".

Outflow in the CNTRL and SNP treatments were very similar, as the outflow slowly decreased over the duration of the perfusion, regardless of the treatment applied (Figure 2.4). This decrease may be due to increased "leaks" from the cut face of the tail, accentuated by increased perfusion pressure (Figure 2.3) The acute decrease in outflow in the NSTIM tail (Figure 2.4B) is more difficult to explain. Since perfusion pressures fell it is unlikely that filtration increased, which suggests that either the vascular beds became more permeable (Olson 1998) and some oedema might have occurred, or that the stimulation opened up more "leaks" in the cut face of the tail preparation, which would reduce both pressure and "observed" outflow.

There have been improvements in the performance of isolated, perfused tissues and organs and they clearly have a role in physiological research, both by eliminating potential interactions with other organ systems and by virtue of their

lower ethical cost, but the reproducible BFD is not the same as in the live animal. Our methods allowed long term perfusion without the development of tissue oedema. Even with the addition of bovine serum albumin, with the attendant possibilities of introducing unknown bioactive agents, we may not be maintaining the vascular endothelium in its physiological state.

Although our sample sizes were low, it is clear that the perfused isolated tail preparation needs further refinement before it can mimic the perfusion parameters in the live fish and be successfully used as pathway to deliver beneficial molecules to the white muscle. A less invasive method which uses the whole live fish is recommended.

## 2.6 References

Barron MG, Tarr BD, Hayton WL (1987) Temperature-dependence of cardiac output and regional blood flow in rainbow trout, *Salmo gairdneri* Richardson. Journal of Fish Biology 31: 735-744

Behnke BJ, Kindig CA, Musch TI, Koga S, Poole DC, (2001) Dynamics of microvascular oxygen pressure across the rest-exercise transition in rat skeletal muscle. Respiration Physiology 126: 53-63

Bolis L, Rankin JC (1978) Vascular effects of acetylcholine, catecholamines and detergents on isolated perfused gills of pink salmon *Oncorhynchus gorbuscha* coho salmon, *O. kisutch* and chum salmon, *O. keta*. Journal of Fish Biology 13: 543-547

Bone Q (1978) Locomotor muscle. In Hoar WS, Randall DJ, eds. Fish Physiology, Vol. VII. Academic Press, London, pp 361-424

Bubien JK, Meade TL (1986) Electrophysiological abnormalities produced by ammonium in isolated perfused brook trout, *Salvelinus fontinalis*, hearts. Journal of Fish Biology 28: 47-53

Cameron JN (1975) Blood flow distribution as indicated by tracer microspheres in resting and hypoxic arctic grayling (*Thymallus arcticus*). Comparative Biochemistry and Physiology 52A: 441-444

Canty AA, Farrell AP (1985) Intrinsic regulation in an isolated tail preparation of the ocean pout (*Macrozoarces americanus*). Canadian Journal of Zoology 63: 2013-2020

Claireaux G, McKenzie DJ, Gange AG, Chatelier A, Aubin J, Farrell AP (2005) Linking swimming performance, cardiac pumping ability and cardiac anatomy in rainbow trout. Journal of experimental Biology 208: 1775-1784

Clements KD, Rees D (1998) Preservation of inherent contractility in isolated gut segments from herbivorous and carnivorous marine fish. Journal of Comparative Physiology B 168: 61-72

Davie PS (1981) Vascular resistance responses of an eel tail preparation: alpha constriction and beta dilation. Journal of Experimental Biology 90: 65-84

Davie PS, Wells RMG, Tetens V (1986) Effects of sustained swimming on rainbow trout muscle structure, blood oxygen transport, and lactate dehydrogenase isozymes: evidence for increased aerobic capacity of white muscle. Journal of Experimental Zoology 237: 159-171

Deveci D, Egginton S (1999) Development of the fluorescent microsphere technique for quantifying regional blood flow in small mammals. Experimental Physiology 84: 615-630

Dunmall KM, Schreer JF (2003) A comparison of the swimming and cardiac performance of farmed and wild Atlantic salmon, *Salmo salar*, before and after gamete stripping. Aquaculture 220: 869-882

Egginton S (1992) Adaptability of the anatomical capillary supply to skeletal muscle of fishes. Journal of Zoology, London 226: 691-698

Egginton S, Hudlická O (2000) Selective long-term electrical stimulation of fast glycolytic fibres increases capillary supply but not oxidative enzyme activity in rat skeletal muscles. Experimental Physiology 85: 567-574

Egginton S, Sidell BD (1989) Thermal acclimation induces adaptive changes in subcellular structure of fish skeletal muscle. American Journal of Physiology 256: R1-R9

Egginton S, Turek Z, Hoofd LJC (1988) Differing patterns of capillary distribution in fish and mammalian skeletal muscle. Respiration Physiology 74: 383-396.

Gamperl AK, Farrell AP (2004) Cardiac plasticity in fishes: environmental influences and intraspecific differences. Journal of Experimental Biology 207: 2539-2550

Hill JV, Forster ME (2004) Cardiovascular responses of Chinook salmon (*Oncorhynchus tshawytscha*) during rapid anaesthetic induction and recovery. Comparative Biochemistry and Physiology C-Pharmacology Toxicology & Endocrinology 137:167-177

Janssen GJ (2003) Factors affecting the in-vitro performance of tissue from Chinook salmon. MSc thesis, University of Canterbury Christchurch

Jennings BL, Broughton BRS, Donald JA (2004) Nitric oxide control of the dorsal aorta and the intestinal vein of the Australian short-finned eel *Anguilla australis*. Journal of experimental Biology 207:1295-1303

Jerrett AR, Stevens J, Holland AJ (1996) Tensile properties of white muscle in rested and exhausted chinook salmon (*Oncorhynchus tshawytscha*). Journal of Food Science 61: 527-53

Johnston IA, Ward PS, Goldspink G (1975) Studies on the swimming musculature of the rainbow trout. Journal of Fish Biology 7: 451-458

Johnston IA (1981) Structure and function of fish muscles. Symposia of the Zoological Society of London 48: 71-113

Johnson TP, Johnston IA (1981) Temperature adaptation and the contractile properties of live muscle fibres from teleost fish. Journal of Comparative Physiology B 161: 27-36

Kiceniuk JW, Jones DR, (1977) Oxygen transport system in trout (*Salmo gairdneri*) during exercise. Journal of experimental Biology 69: 247-261

Kolok AS, Spooner RM, Farrell AP (1993) The effect of exercise on the cardiac output and blood flow distribution of the largescale sucker *Catostomus macrocheilus*. Journal of Experimental Biology 183: 301-321

McGeer JC, Eddy FB (1996) Effects of sodium nitroprusside on blood circulation and acid - base and ionic balance in rainbow trout: Indications for nitric oxide induced vasodilation. Canadian Journal of Zoology-Revue Canadienne De Zoologie 74: 1211-1219

Mulder ALM, Van Goor CA, Giussani DA, Blanco CE (2001) Alpha-adrenergic contribution to the cardiovascular response to acute hypoxemia in the chick embryo. American Journal of Physiology 281: R2004-R2010

Mustafa T, Agnisola C, Hansen JK (1997) Evidence for NO-dependent vasodilation in the trout (*Oncorhynchus mykiss*) coronary system. Journal of Comparative Physiology B 167: 98-104

Neumann P, Holeton GF, Heisler N (1983) Cardiac output and regional blood flow in gills and muscles after exhaustive exercise in rainbow trout (*Salmo gairdneri*). Journal of Experimental Biology 105: 1-14

Olson KR, Conklin DJ, Farrell AP, Keen JE, Takei Y, Weaver L, Smith M.P, Zhang YT (1997). Effects of natriuretic peptides and nitroprusside on venous function in trout. American Journal of Physiology 273: R527-R539

Olson KR (1998) The Cardiovascular System. In Evans DH ed, The Physiology of Fishes. CRC Press, Baton Rouge, pp 129-154

Perry SF, Farrell AP (1989) Perfused preparations in comparative respiratory physiology. In Bridges CR, Butler PJ eds, Techniques in Comparative Respiratory Physiology: an Experimental Approach. Cambridge University Press, Cambridge, pp 223-257

Perry SF, Montpetit CJ, Borowska M (2000) The effects of acute hypoxia on chemically or neuronally induced catecholamine secretion in rainbow trout (*Oncorhynchus mykiss*) in situ and in vivo. Journal of Experimental Biology 203: 1487-1495

Rothwell SE, Black SE, Jerrett AR, Forster ME (2005) Cardiovascular changes and catecholamine release following anaesthesia in Chinook salmon (*Oncorhynchus tshawytscha*) and snapper (*Pagrus auratus*). Comparative Biochemistry and Physiology - Part A: Molecular & Integrative Physiology 140: 289-298

Schwerte T, Holmgren S, Pelster B (1999) Vasodilation of swimbladder vessels in the European eel (*Anguilla anguilla*) induced by vasoactive intestinal polypeptide, nitric oxide, adenosine and protons. Journal of Experimental Biology 202:1005-1013

Schultz IR, Barron MG, Newman MC, Vick AM (1999) Blood flow and distribution and tissue allometry in channel catfish. Journal of Fish Biology 54: 1275-1286

Southhard JH, Belzer FO (1995) Organ preservation. Annual Review of Medicine 46: 235-247

Van Oosterhout MFM, Willigers HMM, Reneman RS, Prinzen FW (1995) Fluorescent microspheres to measure organ perfusion: validation of a simplified processing technique. American Journal of Physiology 269: H725-H733

Wagh M, Pantazi G, Romeo R, Hurley JV, Morrison WA, Knight KR (2000) Cold storage of rat skeletal muscle free flaps and pre-ischemic perfusion with modified UW solution. Microsurgery 20: 343-349

Wood CM, Shelton G (1975) Physical and adrenergic factors affecting systemic and vascular resistance in the rainbow trout: A comparison with branchial vascular resistance. Journal of Experimental Biology 63: 505-523

# Chapter 3 Uptake and recovery of isoeugenol from the plasma and white muscle of juvenile snapper (*Pagrus auratus*)

## 3.1 Abstract

Isoeugenol, the active ingredient found in the aquatic anaesthetic AQUI-S$^{TM}$, is known to pass across the gills of aquatic organisms and into the tissues of teleosts crustaceans and molluscs. In this research, methodology that utilises the fluorescent properties isoeugenol was developed and used to quantify the uptake and bioaccumulation of isoeugenol at low (4.5±0.3 mg.L$^{-1}$), medium (8.6±0.1 mg.L$^{-1}$), and high (14.0±0.3 mg.L$^{-1}$) exposure concentrations. In all three exposure concentrations, the accumulated isoeugenol concentration in the plasma and white muscle was greater than the ambient water concentration within 10 min, and continued to increase or maintain concentration for the duration of the exposure. Maximum isoeugenol plasma concentration reached 4.9 (69.3±5.3 mg.L$^{-1}$), 5.8 (50.2±5.8 mg.L$^{-1}$) and 10.5 (47.3±4.7 mg.L$^{-1}$) times ambient exposure concentration in the high, medium and low exposure treatments, respectively. Maximum isoeugenol white muscle concentration reached 1.9 (26.8±2.6 mg.L$^{-1}$), 4.6 (39.5±4.4 mg.L$^{-1}$) and 9.7 (43.8±3.2 mg.L$^{-1}$) times ambient exposure concentrations in the high, medium and low exposure treatments, respectively. The greatest differential between plasma and white muscle isoeugenol concentration occurred in the high exposure treatment. The rate and depth of anesthesia was greatest in the high exposure treatment. However, in the low exposure treatment the snapper only reached deep sedation, even though plasma and white muscle isoeugenol concentrations reached levels found in the medium and high exposure fish which reached deep anesthesia. This result poses several questions about the mode of action of AQUI-S$^{TM}$ and the role of hypoxia as either cause and/or effect of deep anaesthesia. The potential for other beneficial molecules to use the same direct uptake pathway as isoeugenol is discussed.

## 3.2 Introduction

In chapter 2 we saw that it is possible to perfuse supportive media to the white muscle of Chinook salmon in an isolated tail preparation, however compared with the whole live fish, the blood distribution to the white muscle in the perfused tail preparation is limited. Another method to deliver supportive molecules to the white muscle is direct uptake via the gills. This method, like the perfused tail preparation, still utilises the fish's circulatory system as a delivery pathway but relies on the diffusion of molecules from the water across the gills and into the blood.

Isoeugenol, the active ingredient in the aquatic anaesthetic AQUI-S$^{TM}$ diffuses across the gills and bioaccumulates in the fillet. Research elsewhere has calculated total residual isoeugenol concentrations in the fillet and clearance rates (Kildea et al. 2004, Meinertz et al. 2006). However, there has been little work on the uptake rates of isoeugenol into the plasma and white muscle with varying exposure concentration. In this application we measure the uptake, distribution and anaesthetic effects of isoeugenol, and assess the direct uptake delivery method for the potential delivery of other supportive molecules into the musculature.

In fish, the primary function of the gills is respiration but they also play an important role in osmotic regulation (Evans et al. 2005). Fish gills are very efficient at removing oxygen from the surrounding water as they have a large surface area and a counter-current blood flow. Water passes over the gills either passively (ram ventilation) or actively (opercular ventilation). Without constant renewal of oxygenated water over the gills, the oxygen in a stagnant layer adjacent to the gills would soon be depleted (Gilmour 1998). Blood is pumped through the gill lamellae in a counter-current direction to the flow of oxygenated water which greatly increases the efficiency of oxygen uptake. Lamella wall thickness (diffusion distance) varies with species, and activity. For example the lamella wall thickness in a highly active pelagic species may be less than 1µm, compared

with greater than 10 µm in a slow benthic species (Hughes 1970, Steen 1971). A layer of mucus secreted by goblet cells protects the lamellae, this can vary in thickness due to environmental and physical factors and can influence the delivery of molecules to the gills (Shephard 1993).

There is an osmotic gradient between the internal cellular environment of many marine teleosts (250-500 $mOsmol.kg^{-1}$) and the hyperosmotic sea water environment they live in (1000 $mOsmol.L^{-1}$) (Evans 1998). This osmotic gradient is constantly challenged and water is continuously drawn from the fish. To maintain this osmotic gradient, marine fish have to actively drink sea water (Keys 1933). Water and sodium chloride (NaCl) are absorbed in the intestine and excess NaCl in the blood is excreted through the gills. At the gills, $Cl^-$ is actively transported across the cell membrane into a chloride secreting cell before exiting passively through an apical channel. $Na^+$ passively exits down an electrochemical gradient between the chloride cell and an accessory cell (Pritchard 2003).

Previously we have described how the gills are an effective point of entry for a diffusion delivery system. Oxygen, however, is not the only molecule that readily diffuses across the gill lamellae and into the blood. Small hydrophobic molecules can easily diffuse into the blood, many of which bioaccumulate in fish tissues and are only slowly eliminated because of their high affinity for lipid. Bioaccumulation is the increased chemical concentration in an organism, compared with that in the external environment, whereas bioconcentration is the uptake of a chemical from the water through a respiratory surface (Mackay and Fraser 2000). There has been a lot of research on bioconcentration and bioaccumulation, especially with an increased awareness of potentially hazardous molecules (organic and inorganic) polluting the aquatic environment. Bioaccumulated pollutants can move up trophic levels, even accumulating in humans (Colborn et al. 1996) The bioconcentration and bioaccumulation of chemicals in organisms can be used as an environmental monitoring tool (van de Oost et al. 2002, Belpaire and Goeman 2007).

Thousands of chemicals have the potential to bioconcentrate and accumulate in the tissues of fish. Bioconcentration experiments on live fish or perfused gill preparations have only tested a small number of them. There have, however, been many models constructed to predict a chemical's bioconcentration factor (BCF), an estimation of the chemical's ability to accumulate in an aquatic animal (Barron 1990). Barber (2003) describes the two commonly made assumptions made when modelling bioconcentration as, 1) chemical uptake via the gills is the major site of uptake and 2) movement across the gill is by passive diffusion, not active transport. Hayton and Barron (1990) suggest that there are four components to transport of chemicals from the water, across the gills and into the blood; 1) ventilation rate, 2) aqueous diffusion layer, 3) lipid membrane, 4) blood flow rate. Models for predicting bioconcentration based on the above criteria become very complex (Erickson and McKim 1990, Mackay and Fraser 2000, Barber 2003, Dearden and Shinnawei 2004, Weisbrod et al. 2007). Other important parameters when predicting BCF values are the chemical family and species, known hydrophilic properties (especially the octanol-water partition coefficient), molecular size, neutrality, temperature (Sijm 1993) and the gill mucus layer (Shephard 1993).

The active ingredient in AQUI-S$^{TM}$ is food grade isoeugenol (12% cis isomer and 88% trans isomer). Isoeugenol is a naturally occurring compound and is often used as a flavouring additive and/or a storage agent as it has strong antioxidant properties (Rajakumar and Rao 1993, Priyadarsini et al. 1998, Atsumi et al. 2005).

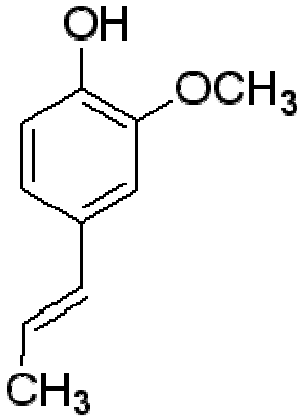


Isoeugenol (2-Methoxy-4-propenylphenol, $C_{10}H_{12}O_2$)

Isoeugenol is a small hydrophobic molecule with a molecular weight of 164.2. It is readily diffused across the gill membrane and into the blood of aquatic organisms. In AQUI-S$^{TM}$ isoeugenol is solubilised by a detergent (Polysorbate) creating a fine suspension of small micelles in the water column. It is effective at very low concentrations and can be used for mild sedation (5 mg.L$^{-1}$) to heavy anaesthesia (20 mg.L$^{-1}$). Stehly and Gingerich (1999) tested the efficacy and toxicity of AQUI-S$^{TM}$ on six species of US aquacultured fish and found that in all the species it performed very well against practiced efficacy and toxicity criteria. The efficacy and toxicity criteria were based on those described by Gilderhus and Marking (1987), which included: (1) induction of anaesthesia in 3 min or less allowing handling of fish; (2) full recovery (swimming) in 10 min or less; and (3) no mortalities after 15 min at an effective concentration.

AQUI-S$^{TM}$ is routinely used in aquaculture to reduce stress during handling, transporting, grading, tagging, and harvesting in order to produce a premium product. During a harvest, fish are exposed to several stressors: crowding, hypoxia, and physical damage. Fish that have been sedated with AQUI-S$^{TM}$ prior to handling show reduced plasma cortisol levels, a commonly used stress indicator. Small (2004) exposed channel catfish (*Icatlurus punctatus*) to three stressors; confinement, high concentrations of unionized ammonia and acute oxygen depletion. Compared with un-sedated fish, plasma cortisol levels in fish

anaesthetised with isoeugenol were 60% lower during confinement, 74% lower in hypoxic conditions, and were not significantly different in the elevated ammonia treatment. Iverson et al. (2002) demonstrated that the stress of moving fish from tank to tank significantly elevated plasma cortisol levels. The plasma cortisol levels in fish transferred into a tank containing AQUI-S$^{TM}$ were not elevated above baseline values. Kiessling et al. (2004) determined that in Atlantic salmon (*Salmo salar*), harvesting with AQUI-S$^{TM}$ resulted in firmer and paler fillets with a higher flesh pH and reduced liquid loss compared with fish harvested with conventional $CO_2$. Jerrett et al. (1996) showed that after 40 hours storage at 2$^{o}$C Chinook salmon white muscle from fish that were rested harvested with AQUI-S$^{TM}$ had 2.7 times the tensile strength than fish that had been exhausted. Fish that have been rested harvested with AQUI-S$^{TM}$ had a longer pre-rigor period and a less intense rigor.

Because AQUI-S$^{TM}$ has been used in the aquaculture industry there have been studies focused on the total uptake and residual clearance of isoeugenol from fish tissue (Kildea et al. 2004, Meinertz et al. 2006). The two current recovery methods of isoeugenol involve High-Performance Liquid Chromatography (HPLC) (Meinertz et al. 2006), and Gas Chromatography/Mass Spectrometry (GC/SM) (Kildea et al. 2003). By using the fluorescent properties of isoeugenol a novel method to determine the isoeugenol concentration in fish plasma and tissue was developed.

Isoeugenol is excited at 266 nm and emits at 340 nm which is very similar to that of the fluorescent spectra of some fluorescent proteins. Many proteins may contain one or more of the three known fluorescent aromatic amino acids; tryptophan, tryrosine and phenylalanine. Fluorescent protein residues are complex, with several variables that determine the fluorescent excitation, emission and quantum yield. These include protein residue combinations, conformational changes, excitation state, substrate binding, de-naturation, acidity, quenching, and solvent effects. In aqueous solution (pH 7), phenylalanine emits at ~282 nm, tryrosine at

~303 nm and tryptophan at ~350 nm (Lakowicz 1999). Tryptophan has an emission very close to that of isoeugenol and would interfere with additional fluorescence to an emission scan of plasma or white muscle sample containing isoeugenol. A simple methodology was developed to precipitate proteins out of the plasma and white muscle sample, leaving the isoeugenol.

## 3.3 Methods

### 3.3.1 Experimental fish

Initially yellow-eyed mullet was chosen as the experimental species, but as snapper became readily available through the Crop & Food Research aquaculture breeding programme a switch was made. The change to snapper was also influenced by their uniformity and known history.

#### 3.3.1.1 Snapper

The juvenile snapper used in the isoeugenol uptake and recovery series of experiments were reared from eggs collected from brood stock in November 2004. The larvae were fed rotifers until day 23 and enriched artemia until day 57. After day 57 they were weaned on to a diet of frozen snapper eggs, crumb (NRD, proton) and alginate (wet fish based fish food made on site with added vitamins and minerals). The juvenile snapper were raised in 4500L tanks at 10kg.m$^3$ density with a water flow of ~50L.min$^{-1}$. The seawater was pumped from the end of the wharf at Crop & Food Research, 300 Wakefield Quay, Port Nelson, using a 3-KW Lowara centrifugal pump (ITT Industries, Italy). Raw seawater was first filtered through a series of high rate sand filters (Sta-Rite system 3, S8570, Sta-Rite Pool/Spa Group, USA). Since 2007 raw seawater has been filtered through an ARKAL filtration system (ARKAL, Israel), consisting of a Spin-Klin battery and three ARKAL gravity filters (AGF). When required, the experimental fish were anaesthetised with 20 mg.L$^{-1}$ AQUI-S$^{TM}$ before being shifted to a 1000 L experimental holding tank with a water flow of 20 L.min$^{-1}$. Snapper were held in the holding tank at a maximum density of 50 fish per 1000 L. The fish were fasted for 48 hours prior to experimentation. When required, fish were quickly and humanely killed by iki-jime.

#### 3.3.1.2 Yellow eyed mullet

Yellow-eyed mullet were caught in a baited bag net off the Crop & Food wharf (Crop & Food Research Ltd, 300 Wakefield Quay, Nelson). They were anaesthetised and transported to a 4000L tank where they were left to recover. The mullet sampled in this research had been in captivity for over a year and were fed a diet of wet fish alginate and fish pellets (Reliance).

### 3.3.2 Experimental setup and trials

#### 3.3.2.1 Snapper

Juvenile snapper were exposed to three different isoeugenol concentrations 4.5±0.3 mg.$L^{-1}$ (low), 8.6±0.1 mg.$L^{-1}$ (med), and 14.0±0.3 mg.$L^{-1}$ (high), (8.3±0.2 mg.$L^{-1}$, 15.9±0.3 mg.$L^{-1}$ and 25.9±0.6 mg.$L^{-1}$ AQUI-S$^{TM}$, respectively). Seawater samples were taken from the treatment tank to accurately assess the isoeugenol concentration 5 min after the AQUI-S$^{TM}$ was added. Fish were sampled every 10 min for 80 min. After 60 min in the anesthetic the remaining un-sampled anaesthetised fish were netted and placed in a tank containing fresh seawater to recover. Fish were not sampled after 80 min as the effects of the anaesthetic had worn off and they became difficult to catch without inducing stress. Two fish were sampled at a time, and assessed for anaesthetic stage before being killed by iki jime. Approximately 200uL of blood was sampled from the fish via a ventral heart puncture using a heparinised 25gauge needle and 1.0cc syringe. The blood sample was put on ice until both fish had been sampled. Fish length, weight and muscle cut surface pH were recorded. The right hand fillet was removed and approximately 1g of white muscle was dissected from the D muscle block from a location 10mm posterior to the pectoral fin. The tissue was immediately freeze clamped under liquid nitrogen, wrapped in tinfoil and stored at -80$^{o}$C until analysis.

#### 3.3.2.2 Mullet

Rested yellow-eyed mullet were anaesthetised with 17.3±1.0 mg.$L^{-1}$ isoeugenol (32.0±1.0 mg.$L^{-1}$ AQUI-S$^{TM}$). Fish were sampled every 10 min for 80 min. After 60 min in the anesthetic the remaining anaesthetised fish were netted and put into a tank with fresh seawater to recover. Fish were not sampled after 80 min as the effects of the anesthetic had worn off and they became difficult to catch without inducing stress. Sampling procedure was the same as the snapper (Section 3.3.2.1).

### 3.3.3 Isoeugenol recovery

#### 3.3.3.1 Plasma

Blood samples were centrifuged (MSE Micro Centaur) at 10000 rpm for 5 min. 50uL of the supernatant (plasma) was pipetted out and added to 450uL (1:10) of reagent grade ethanol before being vortexed (IKA Labortechnik, MSI Minishaker) for 30 sec. The ethanol plasma samples were stored on ice for 15 min before being vortexed again for 30 sec and centrifuged at 10000 rpm for 10 min. The supernatant was collected and stored on ice until analysis.

#### 3.3.3.2 Muscle sample

The white muscle samples were analysed within two weeks of freezing. Samples were ground under liquid nitrogen using a mortar and pestle. 900uL regent grade ethanol was added to an accurately weighed (0.1g) sample of muscle powder and was homogenised using the Ultra-Turrax (IKA Labortechnik T8). The sample was vortexed for 30 sec then stored on ice for 15 min before being vortexed again for 30 sec. The sample was then centrifuged at 10000 rpm for 10 min. The supernatant was collected and stored on ice until analysis.

#### 3.3.3.3 Fluorimetric isoeugenol analysis

A stock solution of 1000 mg.$L^{-1}$ AQUI-S$^{TM}$ was made up with regent grade ethanol (540 mg.$L^{-1}$ isoeugenol). The stock solution was further diluted to 50 mg.$L^{-1}$ AQUI-S$^{TM}$ (27 mg.$L^{-1}$ isoeugenol). Standards (using the 50 mg.$L^{-1}$ AQUI-S$^{TM}$) and samples were analysed with a Cary Eclipse Fluorimeter (Varian Instruments, Australia). 50uL of sample (seawater, plasma or white muscle extract) was pipetted into 2950uL of reagent grade ethanol in a 3ml disposable cuvette (Marco Fluorimetric KTL-1961). The sample was excited at 266 nm and the emission read at 340 nm. The emission and excitation slit widths were set at 5 nm, the excitation filter was set to auto, the emission filter was open, the photomultiplier voltage was set to 700V and the average time for reading was 1 sec. Triplicate samples were run and an average intensity recorded.

### 3.3.3.4 Isoeugenol standards

**Table 3.1 Isoeugenol standards and the required volumes of 50 mg.L$^{-1}$ AQUI-S$^{TM}$ stock solution and reagent grade ethanol.**

| Isoeugenol Standard (mg.L$^{-1}$) | 50 mg.L$^{-1}$ AQUI-S$^{TM}$ (µL) | Ethanol (µL) |
|---|---|---|
| 0.000 | 0 | 3000 |
| 0.054 | 6 | 2994 |
| 0.108 | 12 | 2998 |
| 0.162 | 18 | 2982 |
| 0.216 | 24 | 2976 |
| 0.270 | 30 | 2970 |

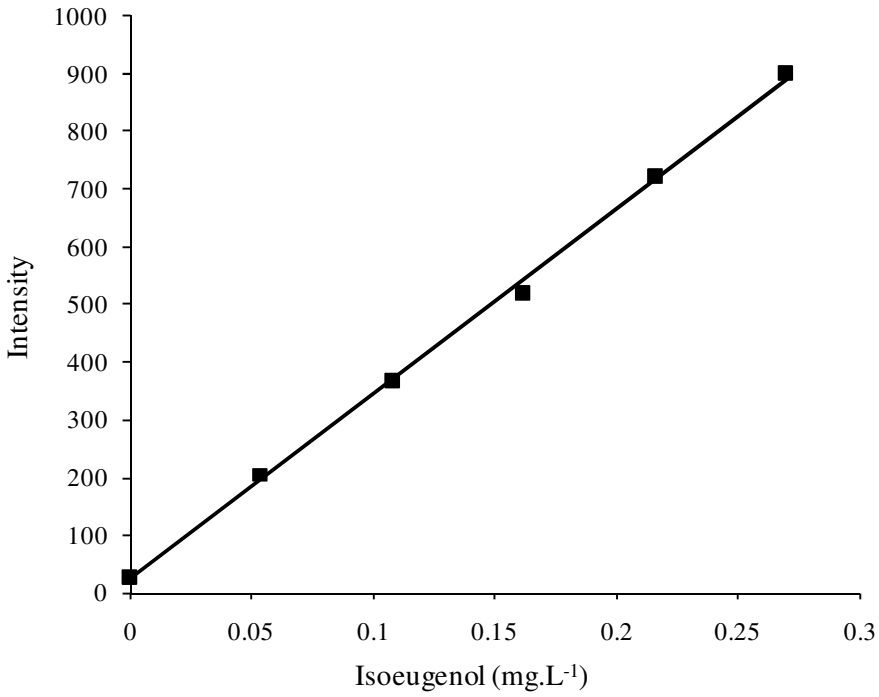


**Figure 3.1 Example of an isoeugenol standard curve.** $r^2 = 0.99$.

#### 3.3.3.5 Anaesthetic staging guide

The depth of anaesthesia was determined for each sampled fish. As each fish was removed from the tank it was ranked on a continuum from 1-5 using the anaesthetic staging guide (Table 3.2, Crop & Food Research Ltd).

**Table 3.2 Anaesthetic staging guide**

| | | |
|---|---|---|
| **Stage 1** | **Light sedation** | • Addition of anaesthetic<br>• Loss of reaction to external stimulation – wave hand over tank and no startle reaction |
| **Stage 2** | **Deep sedation** | • Partial loss of equilibrium<br>• Fish may be swimming on side<br>• No avoidance of obstacles |
| **Stage 3** | **Partial anaesthesia** | • Total loss of equilibrium<br>• No reaction to being held against tank for 3 seconds |
| **Stage 4** | **Light anaesthesia** | • No reaction to caudal peduncle squeeze<br>• Fish still operculating |
| **Stage 5** | **Deep anaesthesia** | • Medullary collapse<br>• Death |

## 3.4 Results

### 3.4.1 Isoeugenol recovery methodology

Isoeugenol was successfully extracted with ethanol and quantified fluorimetrically from teleost plasma and white muscle. Isoeugenol is excited at 266 nm (and 301 nm) and emits at 340 nm (and 663 nm) (Figure 3.2). Figure 3.3 illustrates how the fluorescent proteins in a plasma sample without isoeugenol (scan 4) interfere with a scan of 0.4 $mg.L^{-1}$ isoeugenol in ethanol (scan 3). Scan 6 shows the accumulative effect of the plasma fluorescent proteins and 0.4 $mg.L^{-1}$ isoeugenol. Scan 5 demonstrates the effectiveness of the 1:10 ethanol extraction of the plasma proteins as a plasma sample (without iso-eugenol) emission scan is reduced to a similar base line to that of distilled water (scan 1) and ethanol (scan 2). Scan 7 shows the removal of the proteins from a plasma sample containing 0.4 $mg.L^{-1}$ isoeugenol by 1:10 dilution in ethanol, successfully retaining the 0.4 $mg.L^{-1}$ isoeugenol.

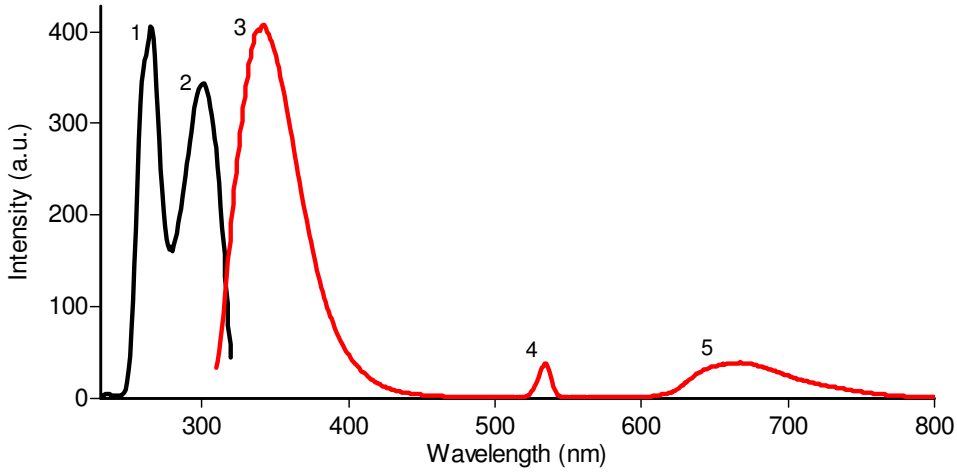


**Figure 3.2 Fluorescent excitation and emission scan of AQUI-S™.** Excitation (1, 266 nm and 2, 301 nm) and emission (3, 340 nm and 5, 663 nm). Second order back scattering (4, 532 nm - two times excitation wavelength).

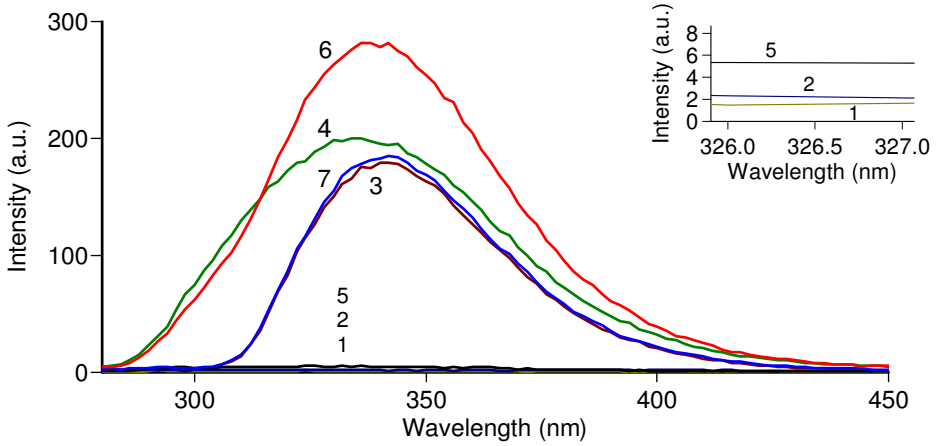


**Figure 3.3 Fluorescent emission scans (Ex, 266 nm).** 1) Distilled water, 2) ethanol, 3) 0.4 mg.L$^{-1}$ isoeugenol in ethanol, 4) plasma in distilled water, 5) 1:10 plasma and ethanol, 6) plasma and 0.4 mg.L$^{-1}$ isoeugenol, 7) 1:10 plasma, ethanol and 0.4 mg.L$^{-1}$ isoeugenol. Insert shows low intensity lines.

### 3.4.2 Experimental trials

Table 3.3 shows the snapper trial seawater AQUI-S$^{TM}$ and equivalent isoeugenol concentrations of the low, medium and high exposure treatments as well as the ambient water temperature, fish weight, length, calculated condition factor and sample size.

**Table 3.3 Experimental parameters for the snapper isoeugenol exposure trial.**

| | Treatment | | |
|---|---|---|---|
| | Low | Medium | High |
| AQUI-S$^{TM}$ (mg.L$^{-1}$) | 8.3±0.2 | 15.9±0.3 | 25.9±0.6 |
| Isoeugenol (mg.L$^{-1}$) | 4.5±0.3 | 8.6±0.1 | 14.0±0.3 |
| Temperature ($^{o}$C) | 16.6±0.3 | 13.5±0.3 | 16.4±0.5 |
| Fish weight (g) | 24.9±0.7 | 20.5±0.5 | 24.0±0.7 |
| Length (mm) | 107.0±0.8 | 100.7±0.7 | 108±0.9 |
| N | 8 | 8 | 8 |
| Condition index (w/l$^3$) | 2.0±0.1 | 1.97±0.1 | 1.86±0.1 |

Table 3.4 shows the yellow-eyed mullet trial AQUI-S$^{TM}$ and equivalent isoeugenol concentrations of the low and high exposure treatments as well as the ambient water temperature, fish weight, length, calculated condition factor and sample size.

**Table 3.4 Experimental parameters for the yellow-eyed mullet isoeugenol exposure trial.**

| | Treatment |
|---|---|
| AQUI-S$^{TM}$ (mg.L$^{-1}$) | 32.0±1.0 |
| Isoeugenol (mg.L$^{-1}$) | 17.3±1.0 |
| Temperature ($^{o}$C) | 20±0.07 |
| Fish weight (g) | 375±10 |
| Length (mm) | 306±2 |
| N | 8 |
| Condition index (w/l$^{3}$) | 1.28±0.02 |

Isoeugenol rapidly diffused from the water, across the gills, and into the plasma of snapper (Figure 3.4). In all three isoeugenol treatments, 4.5±0.3 mg.L$^{-1}$ (low), 8.6±0.1 mg.L$^{-1}$ (medium), and 14.0±0.3 mg.L$^{-1}$ (high) the isoeugenol concentration in the plasma was greater than the concentration in the ambient water within 10 min exposure (low 21.8±4.8 mg.L$^{-1}$, medium 19.2±2.2 mg.L$^{-1}$, high 41.3±2.6 mg.L$^{-1}$). A linear regression from 10 min to 60 min (after the rapid increase in the initial 10 min, shows that the uptake rate of isoeugenol was similar in all three treatments; low 0.64 mg.L$^{-1}$min$^{-1}$ ($r^2$ = 0.86), medium 0.56 mg.L$^{-1}$min$^{-1}$ ($r^2$ = 0.94) and high 0.60 mg.L$^{-1}$min$^{-1}$ ($r^2$ = 0.88). Overall there was little difference in the plasma isoeugenol concentration in snapper exposed to the low and medium exposure treatments, but plasma isoeugenol concentrations in the high exposure treatment were significantly ($P<0.05$) greater than the low and medium treatments over all of the sample times except 50 min and 80 min. In the high exposure treatment the plasma concentration almost reached a saturation plateau at ~65 mg.L$^{-1}$ after 40 min. The maximum plasma isoeugenol concentration in the high exposure treatment was 69.3±5.3 mg.L$^{-1}$ after 60 min, 4.9 times ambient. The medium and low exposure treatments did not reach an obvious saturation plateau. The medium exposure treatment had a maximum plasma isoeugenol concentration of 50.2±5.8 mg.L$^{-1}$ after 60 min, 5.8 times

ambient. Plasma isoeugenol in the low exposure treatment was 47.3±4.7 $mg.L^{-1}$ after 60 min, 10.5 times ambient.

During the 20 min (time 60-80 min) recovery in fresh seawater the plasma isoeugenol concentration in all treatments decreased. Clearance rate during the recovery was similar in the high and medium exposure treatment and slower in the low exposure treatment. Linear regression from 60 min to 80 min shows the clearance rates in the low, medium and high exposure treatments to be -0.59 $mg.L^{-1}.min^{-1}$ ($r^2 = 0.94$), -1.38 $mg.L^{-1}.min^{-1}$ ($r^2 = 0.91$) , and -1.39 $mg.L^{-1}.min^{-1}$ ($r^2 = 0.99$), respectively.

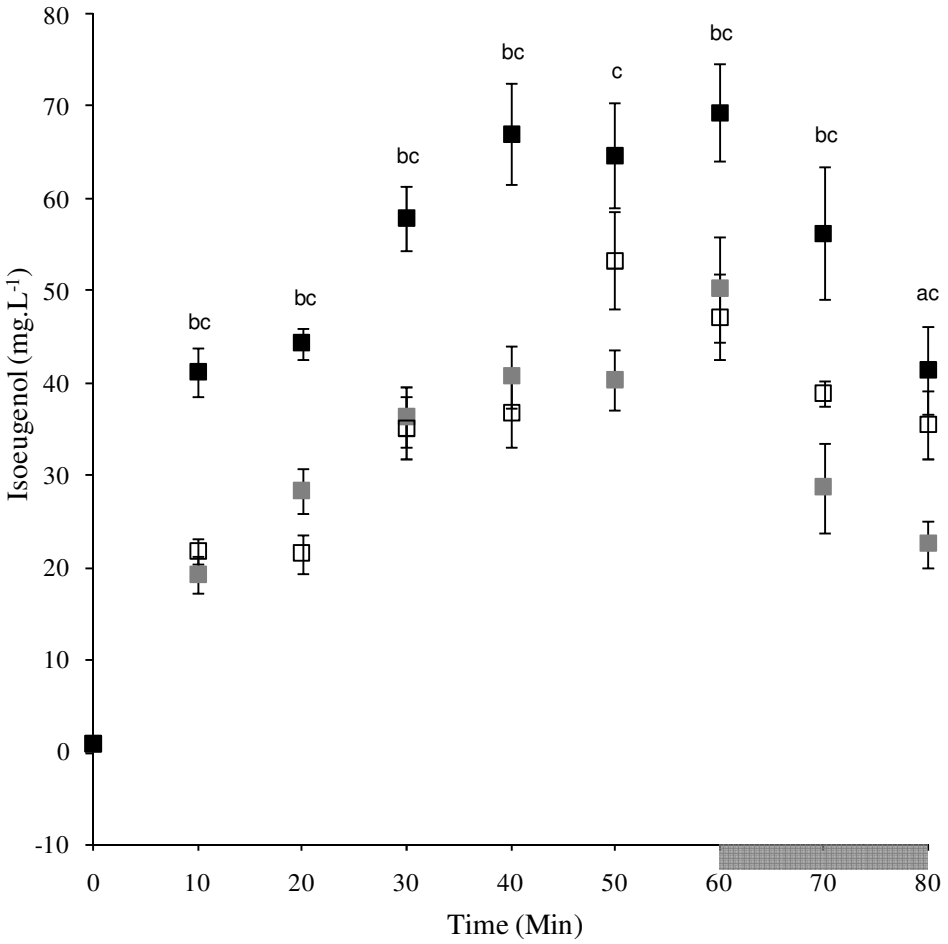


**Figure 3.4 Snapper plasma isoeugenol concentration during exposure to 4.5±0.3 mg.L$^{-1}$ (clear), 8.6±0.1 mg.L$^{-1}$ (grey), and 14.0±0.3 mg.L$^{-1}$ (black) isoeugenol.** Fish were exposed for 60 min before being recovered in fresh seawater for 20 min (60-80 min). a denotes a significant difference (unpaired two-tailed Student's t-test, $P<0.05$) between 4.5±0.3 mg.L$^{-1}$ and 14.0±0.3 mg.L$^{-1}$ treatments, b between 4.5±0.3 mg.L$^{-1}$ and 8.6±0.1 mg.L$^{-1}$ treatments, and c between 8.6±0.1 mg.L$^{-1}$ and 14.0±0.3 mg.L$^{-1}$ treatments. Values are mean±sem. (N=8).

Figure 3.5 shows the bioaccumulation of isoeugenol in the white muscle. As with the accumulation in the plasma, the isoeugenol concentration in the white muscle was greater than the exposure concentration after 10 min. Isoeugenol concentration in the muscle increased over the 60 min exposure. The apparent decrease at 60 min in the high exposure treatment was not significantly different from the 40 or 60 min values (unpaired two-tailed Student's t-test $P<0.05$) and probably reflects individual variation. The rate of isoeugenol uptake in the white muscle decreased with increasing exposure concentration. Linear regression, from 10 min to 60 min (10 to 50 min in the high exposure treatment), shows that the uptake rates of isoeugenol for each exposure concentration were: low, 0.46 $mg.L^{-1}min^{-1}$ ($r^2 = 0.80$), medium, 0.39 $mg.L^{-1}min^{-1}$ ($r^2 = 0.53$) and high, 0.27 $mg.L^{-1}min^{-1}$ ($r^2 = 0.89$).

The maximum white muscle isoeugenol concentration in the high exposure treatment was 26.8±2.6 $mg.L^{-1}$ after 50 min, 1.9 times greater than ambient. The medium exposure treatment was 39.5±4.4 $mg.L^{-1}$ after 60 min, 4.6 times greater than ambient, and the maximum isoeugenol concentration in the low exposure treatment was 43.8±3.2 $mg.L^{-1}$ after 50 min, 9.7 times greater than ambient.

During the 20 min recovery in fresh seawater the white muscle isoeugenol concentration in all treatments decreased. The clearance rate was deduced from a linear regression from time 60-80 min. In the high exposure treatment the clearance was positive due to low concentration found in the white muscle at time 60 min, a clearance rate from an extrapolated 60 min value has been calculated. The white muscle clearance rates in the low, medium and high (from an extrapolated 60 min value) exposure treatments were -0.64 $mg.L^{-1}.min^{-1}$ ($r^2 = 0.72$), -0.69 $mg.L^{-1}.min^{-1}$ ($r^2 = 0.91$), and -0.26 $mg.L^{-1}.min^{-1}$ ($r^2 = 0.99$), respectively.

Figure 3.6 compares the plasma and white muscle isoeugenol concentrations in each exposure concentration. With increasing exposure concentration, the

differential between the isoeugenol accumulation in the plasma and white muscle increased. There was no significant difference (unpaired Students t-test, two tailed, $P<0.05$) between the plasma and white muscle concentrations in the low exposure treatment. There were significant differences between plasma and white muscle isoeugenol concentrations in the medium exposure treatment at 10, 30 and 50 min. There were significant differences between plasma and white muscle isoeugenol concentrations at all sample times except 0 min in the high exposure treatment. In all treatments the maximum isoeugenol concentration that accumulated in the white muscle was less than in the plasma.

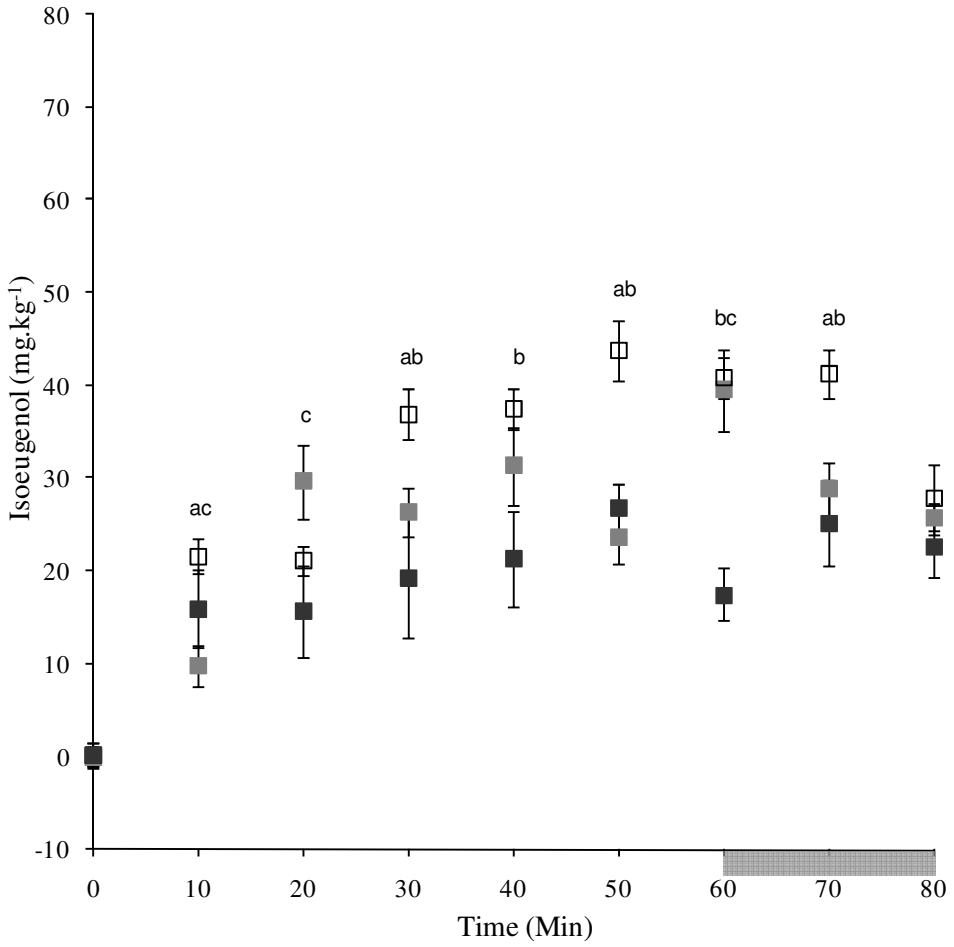


**Figure 3.5 Snapper white muscle isoeugenol concentration during exposure to 4.5±0.3 mg.L$^{-1}$ (clear), 8.6±0.1 mg.L$^{-1}$ (grey), and 14.0±0.3 mg.L$^{-1}$ (black) isoeugenol.** Fish were exposed for 60 min before being recovered in fresh seawater for 20 min (60 min-80 min). Values are mean±sem. a denotes significant difference (unpaired two-tailed Student's t-test, $P<0.05$) between 4.5±0.3 mg.L$^{-1}$ and 14.0±0.3 mg.L$^{-1}$ treatments, b between 4.5±0.3 mg.L$^{-1}$ and 8.6±0.1 mg.L$^{-1}$ treatments, 8.6±0.1 mg.L$^{-1}$ and c between 8.6±0.1 mg.L$^{-1}$ and 14.0±0.3 mg.L$^{-1}$ treatments. (N=8, except 80 min 14.0±0.3 mg.L$^{-1}$ N=7).

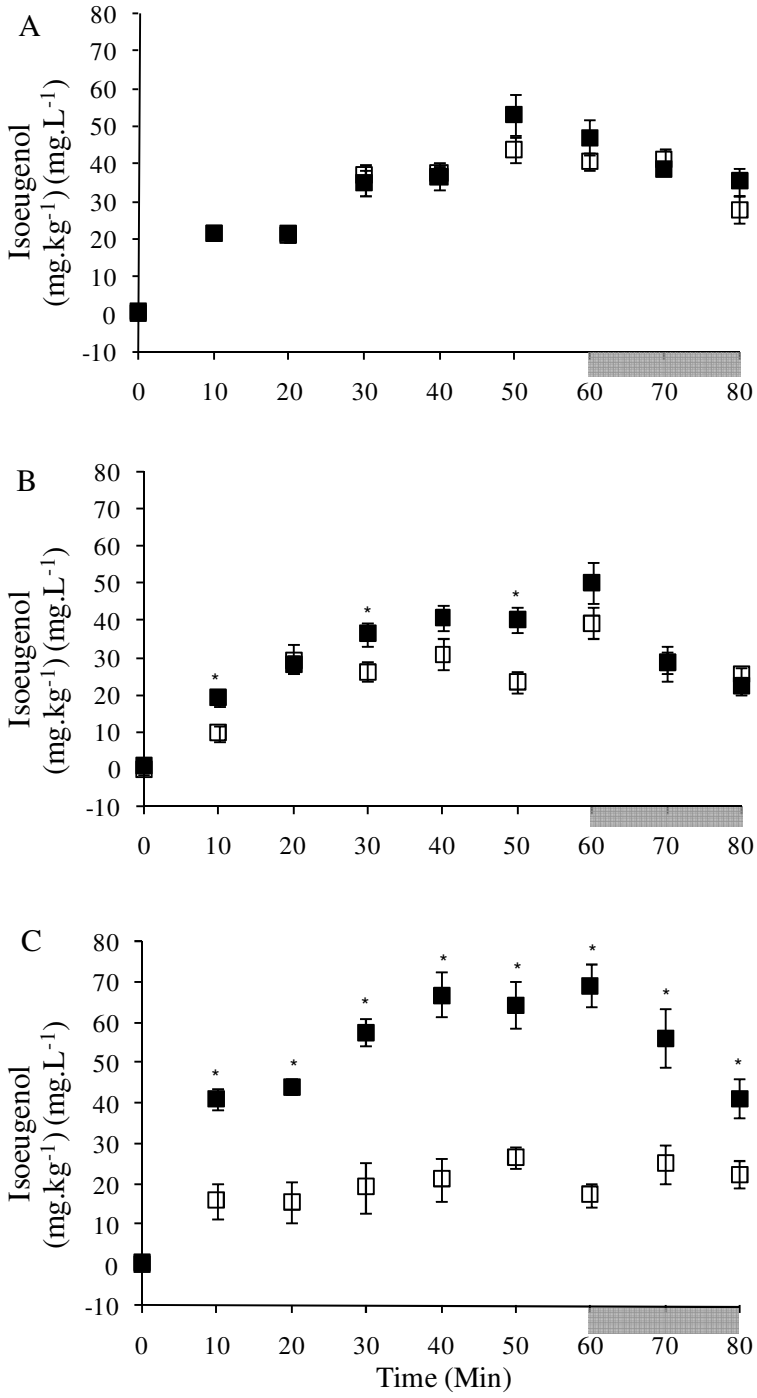


**Figure 3.6 Isoeugenol concentration in the plasma (black) and white muscle (clear) of snapper exposed to A) 4.5±0.3 mg.L$^{-1}$, B) 8.6±0.1 mg.L$^{-1}$, and C) 14.0±0.3 mg.L$^{-1}$ isoeugenol for 60 min.** Fish were recovered in fresh seawater for 20 min (60-80 min). Values are mean±sem. (N=8). Significance difference between plasma and white muscle was determined with an unpaired two-tailed Student's t-test (P<0.05).

Figure 3.7 illustrates that the higher the exposure concentration the faster the rate and the greater the depth of anesthesia. Snapper exposed to 4.5±0.3 $mg.L^{-1}$ isoeugenol had a mean anesthetic stage of 1.9±0.1 within 10 min and maintained a level of anesthesia slightly above stage 2 for the duration of the exposure. Snapper exposed to 8.6±0.1 $mg.L^{-1}$ isoeugenol reached a mean stage of 2.7±0.1 within 10 min before increasing to a mean stage of 4.8±0.1after 60 min exposure. Snapper exposed to 14.0±0.3 $mg.L^{-1}$ reached a mean stage 3.9±0.2 within 10 min and mean stage 4.9±0.1 within 30 min before maintaining stage 5 for the duration of the exposure. Recovery rates were very rapid for the medium and high exposure levels, with the fish recovering to a mean stage of 2.4±0.1 and 2.8±0.2, respectively, after 10 min in fresh seawater. Snapper recovering from the low exposure were still at mean stage 2.0±0.1 after 10 min recovery. All treatments showed a fall in the mean stage of anesthesia of 0.4 stage units from 70 to 80 min.

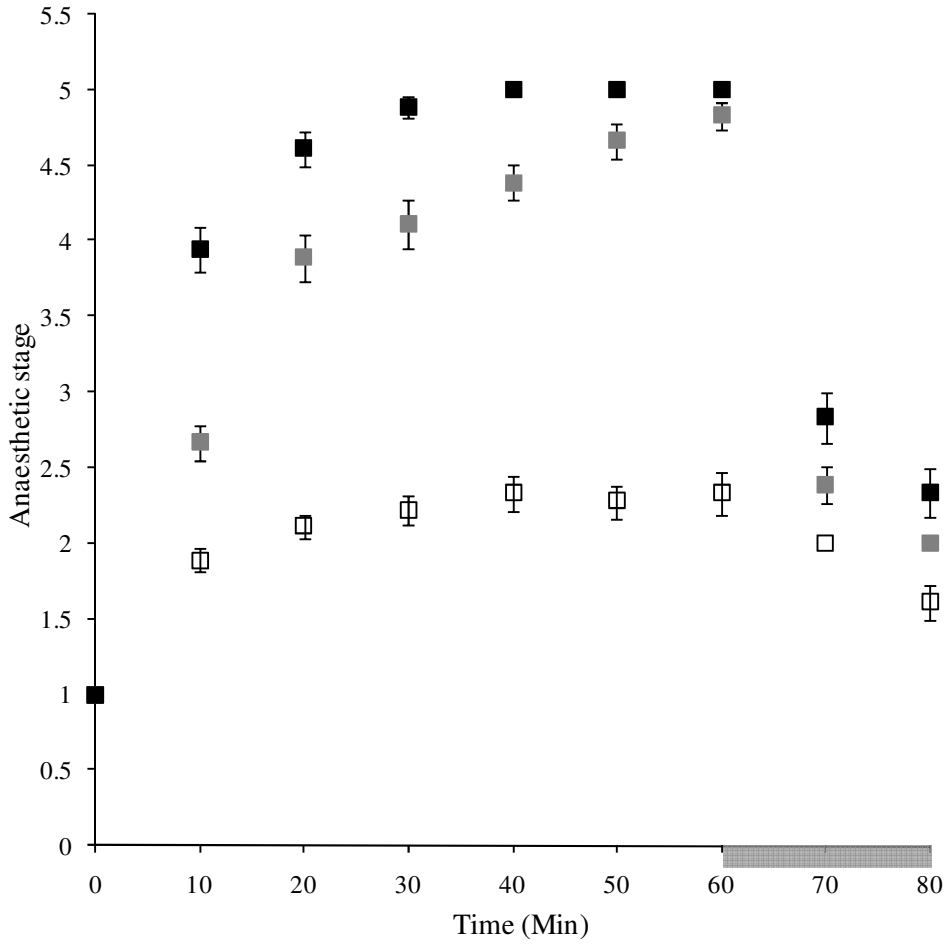


**Figure 3.7 Anaesthetic stage of snapper during exposure to 4.5±0.3 mg.L$^{-1}$ (clear), 8.6±0.1 mg.L$^{-1}$ (grey), and 14.0±0.3 mg.L$^{-1}$ (black) isoeugenol.** Fish were exposed for 60 min before being recovered in fresh seawater for 20 min (60-80 min). Values are mean±sem, (N=8). The 3 treatments are all significantly different (unpaired Student's t-test, two-tailed, $P<0.05$) at each time interval, except between treatments 8.6±0.1 mg.L$^{-1}$ and 14.0±0.3 mg.L$^{-1}$ at 60 min and 80 min.

Figure 3.8 shows the plasma (A) and white muscle (B) isoeugenol concentration plotted against anaesthetic stage. There are two distinct patterns in the plasma isoeugenol concentration and the anaesthetic stage. Fish exposed to 4.5±0.3 mg.$L^{-1}$ achieved similar plasma isoeugenol concentration to those exposed to 8.6±0.1 mg.$L^{-1}$ but remained at a level of anaesthesia below stage 2.5, whereas those exposed to 8.6±0.1 mg.$L^{-1}$ attained anaesthetic stage 4-4.5. Fish exposed to 14.0±0.3 mg.$L^{-1}$ isoeugenol also attained anesthetic stag 4-5 with similar plasma concentrations to those exposed to 4.5±0.3 mg.$L^{-1}$ before attaining stage 5 with elevated plasma concentrations.

Figure 3.8.B shows the white muscle isoeugenol concentration and anaesthetic stage between the low and medium and high exposure concentrations. Snapper exposed to 4.5±0.3 mg.$L^{-1}$ only attained a low level of anaesthesia but accumulated the highest white muscle isoeugenol concentrations, compared with fish exposed to 8.6±0.1 mg.$L^{-1}$ and 14.0±0.3 mg.$L^{-1}$ isoeugenol. Fish exposed to 14.0±0.3 mg.$L^{-1}$ had the greatest depth of anesthesia but the lowest white muscle isoeugenol concentration.

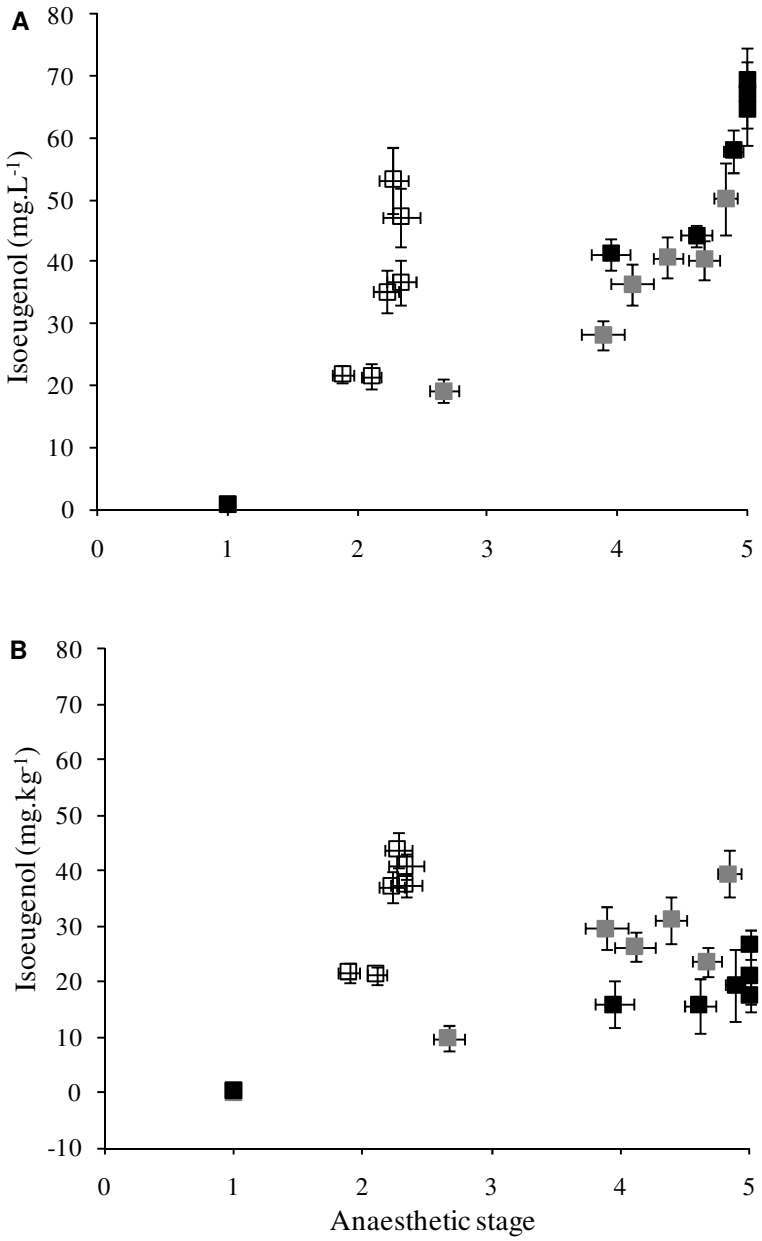


**Figure 3.8 Isoeugenol concentration in the A) plasma and B) white muscle plotted against anaesthetic stage from snapper exposed to 4.5±0.3 mg.L$^{-1}$ (clear), 8.6±0.1 mg.L$^{-1}$ (grey), and 14.0±0.3 mg.L$^{-1}$ (black) isoeugenol for 60 min.** Values are mean±sem, (N=8).

White muscle cut surface pH is a measure often used as an indicator of fatigue in fish muscle. Figure 3.9 shows snapper that were exposed to 4.5±0.3 $mg.L^{-1}$ isoeugenol had lower white muscle pH values at all sampling points (exception of 60 min) than fish exposed to 8.6±0.1 $mg.L^{-1}$ and 14.0±0.3 $mg.L^{-1}$ isoeugenol. Maximum cut surface pH was measured in the 8.6±0.1 $mg.L^{-1}$ and 14.0±0.3 $mg.L^{-1}$ isoeugenol exposure at 30 and 40 min, respectively. There was a decrease in the white muscle pH in fish exposed to 8.6±0.1 $mg.L^{-1}$ and 14.0±0.3 $mg.L^{-1}$ isoeugenol during 40-60 min. Figure 3.10 illustrates the relationship between white muscle cut surface pH and anaesthetic stage, showing that the deeper the fish is anaesthetised (the greater the anaesthetic stage), the higher the white muscle cut surface pH. It also shows that fish sampled from stage 3 onwards had a cut surface pH above 7.5, indicating they had reached a level of anaesthesia deep enough to be rested harvested without struggling, decreasing the white muscle cut surface pH.

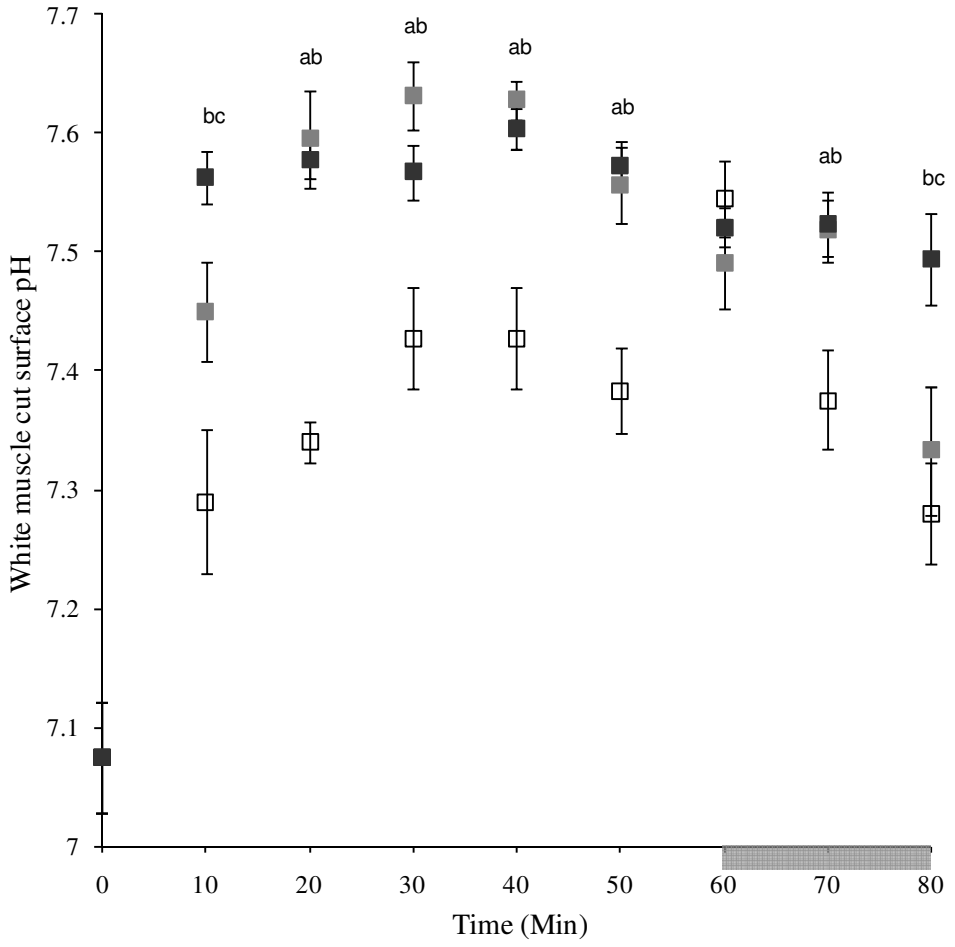


**Figure 3.9 White muscle cut muscle pH of snapper during exposure to 4.5±0.3 mg.L$^{-1}$ (clear), 8.6±0.1 mg.L$^{-1}$ (grey), and 14.0±0.3 mg.L$^{-1}$ (black) isoeugenol.** Fish were exposed for 60 min before being recovered in fresh seawater for 20 min (60-80 min). a denotes a significant difference (unpaired two-tailed Student's t-test, $P<0.05$) between 4.5±0.3 mg.L$^{-1}$ and 14.0±0.3 mg.L$^{-1}$ treatments, b between 4.5±0.3 mg.L$^{-1}$ and 8.6±0.1 mg.L$^{-1}$ treatments, 8.6±0.1 mg.L$^{-1}$ and c between 8.6±0.1 mg.L$^{-1}$ and 14.0±0.3 mg.L$^{-1}$ treatments. Values are mean±sem, (N=8)

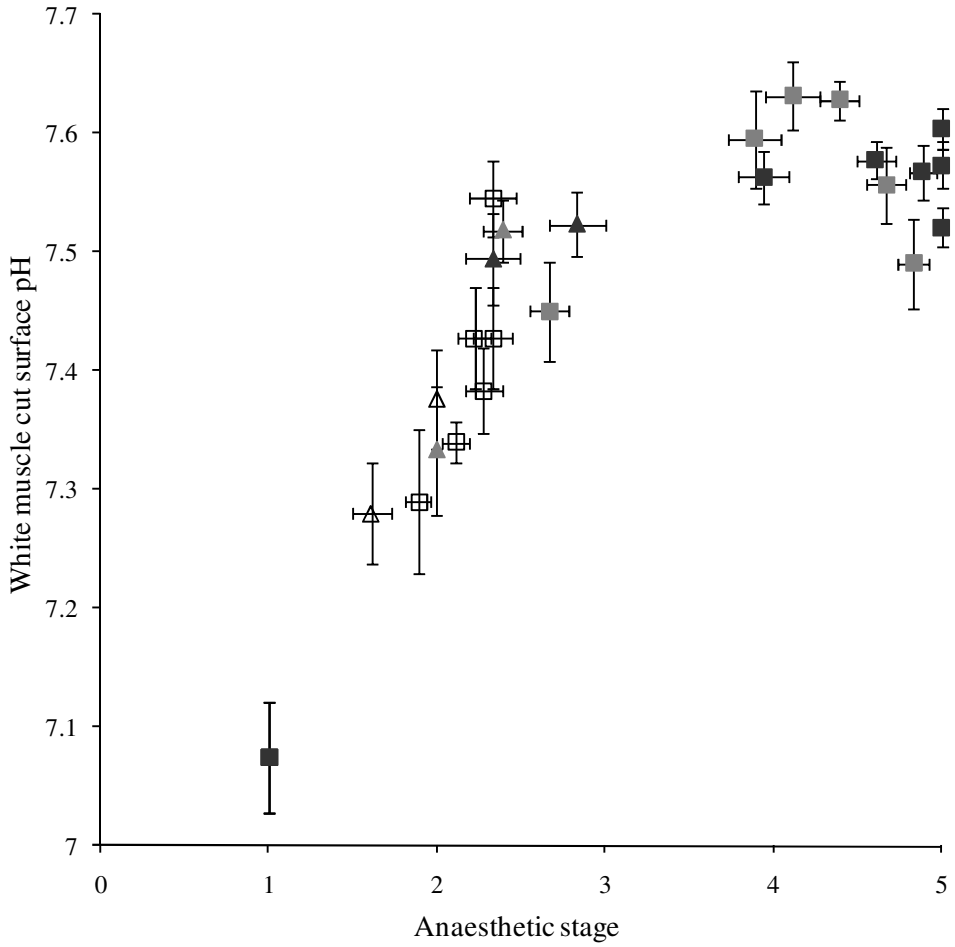


**Figure 3.10 White muscle cut surface pH with anaesthetic stage of snapper during exposure to 4.5±0.3 mg.L$^{-1}$ (clear), 8.6±0.1 mg.L$^{-1}$ (grey), and 14.0±0.3 mg.L$^{-1}$ (black) isoeugenol.** Fish were exposed for 60 min before being recovered in fresh seawater for 20 min (60-80 min). Recovery values (70 min and 80 min) from each series are plotted-with triangular data points. Values are mean±sem, (N=8).

The uptake of isoeugenol into the plasma in yellow-eyed mullet exposed to 17.3±1.0 $mg.L^{-1}$ isoeugenol was rapid (Figure 3.11). Within 10 min exposure, the plasma concentration was 45.7±3.8 $mg.L^{-1}$ (2.6 times the exposure concentration). The uptake rate from time 10-60 min was 0.6 $mg.L^{-1}.min^{-1}$ ($R^2$ = 0.93) and reached a maximum concentration at 60 min of 80.1±9.7 $mg.L^{-1}$, 4.6 times the exposure concentration. Clearance was also rapid, with the plasma concentration lowering to 46.4±3.7 $mg.L^{-1}$ within 10 min recovery in fresh seawater.

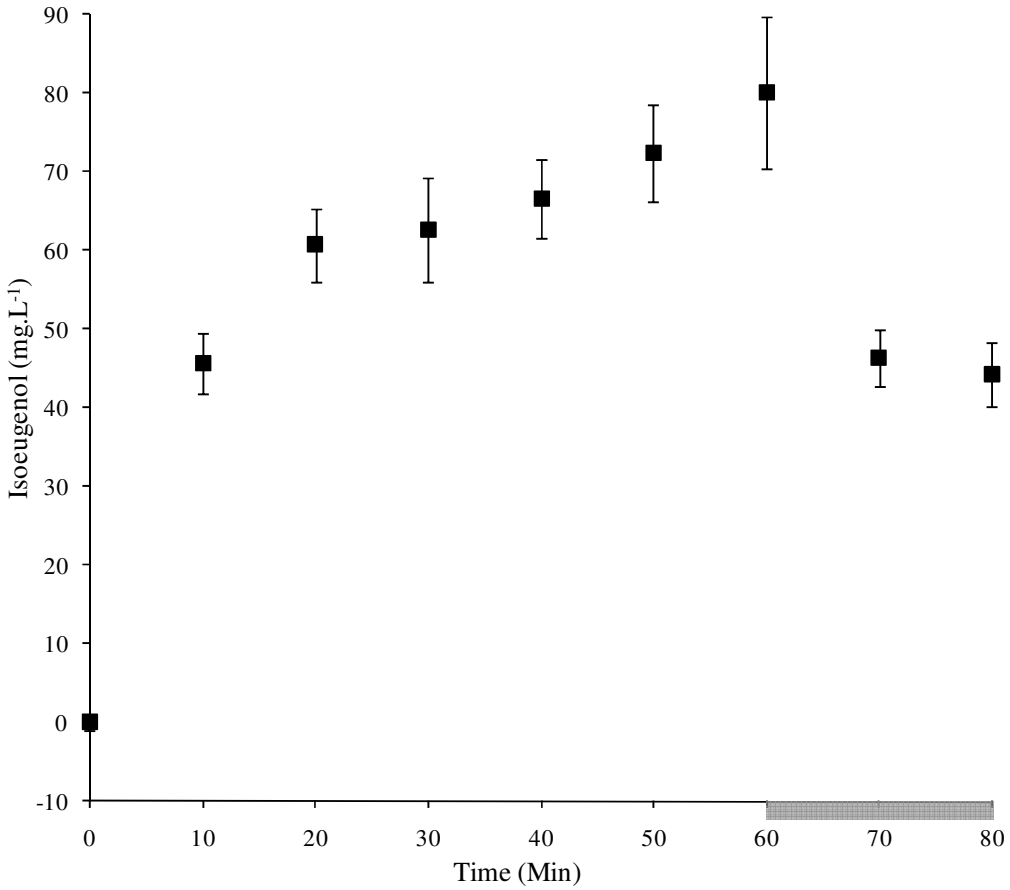


**Figure 3.11 Isoeugenol concentration (mg.L$^{-1}$) in mullet plasma during exposure to 17.3±1.0 mg.L$^{-1}$ isoeugenol.** Fish were exposed for 60 min before being recovered in fresh seawater for 20 min (60-80 min), Values are mean±sem, N=8.

## 3.5 Discussion

Many hydrophobic molecules bioaccumulate in fish tissue from low exposure concentrations, due to their high affinity to lipid. Many are broken down and/or are excreted, but some build up and maintain higher than ambient concentrations in the tissues. Bioaccumulation of chemicals can have both positive and negative consequences. Bioaccumulation of hazardous chemicals may not only be unhealthy for the fish but also for higher trophic level organisms, including humans that consume the contaminated tissue. However, there is potential to bioaccumulate beneficial substances, such as antibiotic, anti-inflammatory and antioxidant molecules in the muscle of fish, assuming the molecules have appropriate physical properties, which include low molecular weight and a high lipid partition coefficient.

Isoeugenol rapidly diffuses across the gills and into the blood and white muscle of fish (Figure 3.6). Passive diffusion is based on a molecule being driven down a concentration gradient. Initially isoeugenol diffuses from high external concentration in the ambient water to low concentration in the blood. However, this does not fully explain the bioconcentration and bioaccumulation of isoeugenol that we see in this research and the research of others. Within 10 min the isoeugenol concentration in the plasma and white muscle exceeds that of the water (Figure 3.4). Our current hypothesis on the bioconcentration of isoeugenol is as follows, AQUI-S$^{TM}$ correctly applied to the water forms isoeugenol micelles which, when in contact adsorb onto the gill lamellae, forming a layer of concentrated isoeugenol (greatly increasing the effective isoeugenol concentration on the gill surface to concentration far greater than that in the ambient water). The diffusion gradient is therefore maintained and isoeugenol continues to diffuse into the blood, in turn elevating the plasma concentration to levels many times greater than the ambient water exposure concentration.

In the low, medium and high isoeugenol exposure treatments the concentration in the snapper plasma (Figure 3.4) and white muscle (Figure 3.5) exceeded that of the ambient water within 10 min exposure. Snapper exposed to 14.0±0.3 $mg.L^{-1}$ isoeugenol had a plasma concentration of 41.3±2.6 $mg.L^{-1}$ and white muscle concentration of 16.0±4.2 $mg.L^{-1}$ after 10 min. Yellow-eyed mullet exposed to 17.3±1.0 $mg.L^{-1}$ isoeugenol had a plasma concentration of 45.7±3.8 $mg.L^{-1}$ isoeugenol after 10 min. Meinertz et al. (2006) found that rainbow trout (*Salmo gairdneri*) anaesthetised with 34 mg.L-1 AQUI-S$^{TM}$ (18.4 $mg.L^{-1}$ isoeugenol) at 12$^{o}$C had a skin-on fillet tissue isoeugenol concentration of 40.1 $mg.kg^{-1}$ after 10 min. This is greater than we found in snapper and yellow-eyed mullet white muscle, but Meinertz et al. (2006) sampled a skin on fillet which includes the skin and the red and white muscle. The skin and red muscle has greater vascularisation than the white muscle, which may lead to greater isoeugenol accumulation. The area between the skin and the red and white muscle of many fish is an area of high lipid concentration, so isoeugenol would accumulate rapidly in this area and may have brought about the elevated skin-on fillet concentrations noted by Meinertz et al. (2006).

Kildea et al. (2004) found that silver perch (*Bidyanus bidyanus*) accumulated ~23 $mg.kg^{-1}$ isoeugenol in the muscle after exposure to 15 $mg.L^{-1}$ AQUI-S$^{TM}$ (8.1 $mg.L^{-1}$ isoeugenol) at 13$^{o}$C for 60 min. This is a lower concentration than we found in the snapper exposed to a similar concentration (8.6±0.1 $mg.L^{-1}$ isoeugenol) for 60 min of 39.5±3.0 $mg.L^{-1}$ isoeugenol. This may be a species-specific difference.

Snapper exposed to the highest isoeugenol treatment had the greatest accumulation of isoeugenol in the plasma within the first 10 min (Figure 3.4). Beyond the initial 10 min rapid rise, the uptake rates in the three exposure treatments were similar; low, 0.64 $mg.L^{-1}.min^{-1}$ ($r^2 = 0.86$); medium, 0.56 $mg.L^{-1}min^{-1}$ ($r^2 = 0.94$); and high, 0.60 $mg.L^{-1}.min^{-1}$ ($r^2 = 0.88$). Mullet exposed to 17.3±1.0 $mg.L^{-1}$ isoeugenol also showed a very rapid rise in plasma isoeugenol

concentration in the initial 10 min before slowing to a similar uptake rate shown in the snapper (0.6 $mg.L^{-1}.min^{-1}$) (Figure 3.11). These uptake data support our isoeugenol uptake hypothesis which enables bioconcentration and bioaccumulation of isoeugenol. The adsorbtion of isoeugenol onto the gill lamellae increases the immediate isoeugenol concentration and continues to drive isoeugenol across the gills into the blood at a constant rate (~0.6 $mg.L^{-1}.min^{-1}$) to levels many times that of the ambient water concentration. This may also help explain the differences in the initial 10 min plasma isoeugenol concentration between the low medium and high exposure concentrations. A greater exposure concentration may increase the speed at which the adsorbed layer of isoeugenol on the gill lamellae forms, thus increasing the amount of isoeugenol passed into the blood within the initial 10 min. However, contrary to this theory, the initial 10 min plasma isoeugenol concentrations in the low and medium exposure treatments were similar (Figure 3.4). Uptake may be similar at lower concentrations until an exposure concentration threshold is reached somewhere between 8.6±0.1 $mg.L^{-1}$ and 14.0±0.3 $mg.L^{-1}$ isoeugenol. However the similarities between the low and medium exposure concentrations may be better explained as temperature effects.

The medium isoeugenol exposure concentration was administered at ~3$^{o}$C lower than that in the low and high exposure trials (Table 3.3). In our trials all fish were exposed to isoeugenol at the seasonal ambient temperature.

The influence of temperature on the uptake of hydrophobic molecules has been documented (Sijm et al. 1993, Bahadur et al. 1997, Smith and McLachlan 2006). Sijm et al. (1993) showed that the uptake rate of several hydrophobic chemicals across a perfused gill preparation decreased with at low ambient temperatures. .Lower temperatures affect epithelium membrane structure and permeability, potentially reducing diffusion (Sijm et al., 1993).

The uptake of isoeugenol may not be exclusively via the gills. There has been significant research into bioaccumulation via dietary uptake of hydrophobic

molecules (Qiao et al. 2000, Nichols et al. 2004). Isoeugenol may be absorbed across the membranes of the gastro-intestinal tract from seawater swallowed by fish during anaesthesia. However, the duration of a routine exposure during general fish husbandry may not be long enough for dietary uptake to have any significant effects.

Body size and gill mucus can also influence diffusion of chemicals across the gill lamellae. Sijm et al. (1995) showed that allometry affects the uptake rate of hydrophobic chemicals in fish. Smaller fish have higher uptake rates as they have greater ventilation rates (due to the energy demand of a higher metabolic rate), and larger relative gill surface area. However, the similar plasma uptake rates shown by snapper exposed to 14.0±0.3 $mg.L^{-1}$ isoeugenol (Figure 3.4) and the much larger yellow-eyed mullet exposed to 17.3±1.0 $mg.L^{-1}$ isoeugenol suggest that size my not limit isoeugenol uptake.

Most fish have a protective layer of mucus covering their gills. Shephard (1993) suggests that most molecules will not be significantly excluded by mucus, except those that interact with the mucus. However, the mucus layer does increase the diffusion distance. Often surfactants are administered with drugs to 'wash' mucus from the gills resulting in greater drug uptake. AQUI-S$^{TM}$ is a mixture of isoeugenol and polysorbate. The polysorbate not only enables the isoeugenol molecules to be dispersed in fine micelles in the water column but also may assist the delivery of the isoeugenol by removing the mucus layer, thus reducing the diffusion distances.

Although we see the highest plasma accumulative concentration in snapper exposed to the high isoeugenol concentration, the opposite correlation seems to occur in the white muscle. The greater the isoeugenol exposure concentration, the lower the white muscle isoeugenol accumulation (Figure 3.5). As the isoeugenol exposure concentration increases, we also see that the differential between the plasma and white muscle accumulation concentration increases (Figure 3.6).

Rothwell et al. (2005) showed an increase in heart rate but decrease in dorsal aortic pressure (DAP) during anaesthesia with AQUI-S$^{TM}$ in Chinook salmon. The decrease in DAP may be attributed to the vasorelaxing properties of isoeugenol, since blood flow may be redirected to highly vascularised (and vasodilated) tissues. A reduced DAP and redirected blood flow could lead to capillary de-recruitment in the white muscle, reducing the perfusion of the white muscle and the potential isoeugenol accumulation. This may explain the decrease in white muscle isoeugenol accumulation with increasing isoeugenol exposure concentration.

Residual chemical concentration in the white muscle is an important factor in a commercial application; our data suggest that if the objective is low residual isoeugenol concentrations in the muscle, then anaesthetising fish with higher exposure concentrations is beneficial. However, caution should always be taken when anaesthetising fish at high concentrations as the margin of error is increased.

There have been several studies on the use of AQUI-S$^{TM}$ during fish handling and harvesting (Stehly and Gingerich 1999, Iverson et al. 2002, Bosworth et al. 2006). However, the physiological mode of action of isoeugenol is not well understood. Current research has suggested it has smooth muscle relaxant properties (Lin et al. 1999, Hill et al. 2003).

From the anaesthetic staging experiment we saw that the anaesthetic stage of the snapper was related to the isoeugenol exposure concentration, the greater the exposure concentration the greater the rate and depth of anaesthesia (Figure 3.7). However, the concentration of isoeugenol in the plasma did not always correlate with the depth of anaesthesia. The highest isoeugenol exposure concentration resulted in the greatest accumulation of isoeugenol in the plasma and the fastest rate and depth of anaesthesia. However, the snapper anaesthetised with low and medium isoeugenol concentrations accumulated similar concentrations of isoeugenol in the plasma during the 60 min exposure (Figure 3.4), but attained

different depths of anaesthesia (Figure 3.8.A). The fish in the low exposure treatment never reached anaesthetic stage 2.5, whereas those in the medium exposure treatment fish reached anaesthetic stage 4-5 (Figure 3.8.A).

These two distinct relationships involving the depth of anaesthesia and isoeugenol concentration found in the in the plasma were also prevalent in isoeugenol concentrations in the white muscle, but the relationship is inverse (Figure 3.8.B). The fish exposed to low isoeugenol concentrations, which never reached anaesthetic stage 2.5, attained the greatest white muscle isoeugenol concentrations. By contrast, fish exposed to the highest isoeugenol concentrations, which reached anaesthetic stage 5, accumulated the lowest white muscle isoeugenol concentrations. This unpredicted anaesthetic uptake and anaesthesia behaviour relationship requires further research as it poses more questions than it answers on the mode of action of isoeugenol as an anaesthetic.

Observations of ventilation rate, mobility, depth of anaesthesia, white muscle cut surface pH and recovery rates suggest that hypoxia during anaesthesia may play a role in achieving deep anaesthesia. However, we also have to consider that hypoxia may just be an effect of deep anaesthesia (stage 4-5) and not a contributing factor.

During anaesthesia, fish slowly lose responsiveness to the external environment and their mobility and ventilation rate decreases. Ventilation rate was not monitored during anaesthesia in this experiment. However, personal experience of anaesthetising fish with AQUI-S$^{TM}$ and the criteria that the anaesthetic staging guide (Section 3.3.3.5) is based on, show a decreasing ventilation rate with increasing anaesthesia, to the point of cessation during very deep anaesthesia. A reduced ventilation rate decreases the refreshed oxygenated water flow over the gill lamellae, increasing the duration which stagnant water is in contact with the gills. The combination of reduced ventilation rate, reduced mobility and a layer of adsorbed isoeugenol on the gill surface may create a localised hypoxic

environment. The decrease in the cut surface white muscle pH after 40 min exposure (Figure 3.9) may have been due to increased lactate production associated with hypoxia mediated anaerobic metabolism. Fish in the high and medium isoeugenol exposed concentration at 40 min were in anaesthetic stage 4-5 (Figure 3.7), so they showed no signs of struggling while being restrained before being killed. Any increase in anaerobic metabolism and subsequent decrease in white muscle pH after 40 min exposure was induced by environmental hypoxia and not muscular activity. All the factors caused by hypoxia discussed thus far could support either hypothesis; that hypoxia is the cause or the effect of deep anaesthesia. The rapid recovery from deep anaesthesia, however, lends support to the hypothesis that hypoxia may induce deep anaesthesia in snapper anaesthetised with AQUI-S$^{TM}$.

Recovery from the high and medium exposure concentrations was rapid, decreasing from stage ~5 to stage 2-3 anaesthesia within 10 min recovery in fresh seawater. Fish exposed to the low isoeugenol concentration only recovered from stage ~2.3 to stage ~2 in the initial 10 min recovery. All three exposure concentrations decreased by ~0.4 of a stage during 10-20 min recovery (Figure 3.7). During recovery in fresh seawater isoeugenol may be rapidly washed off the gill lamellae. The low exposure fish never reached stage 2.5 anaesthesia and were able to maintain ventilation and movement (albeit without co-ordination) around the tank (anaesthetic staging guide, Section 3.3.3.5), maintaining oxygen uptake and avoiding hypoxia.

The clearance of isoeugenol from the plasma and white muscle of snapper was concentration dependent, the greater the accumulated concentration the more rapid the initial clearance (Figure 3.4 and Figure 3.5). The non-linear clearance was also demonstrated by the mullet during recovery (Figure 3.11). A non-linear clearance rate of isoeugenol from the plasma (and potentially the nervous tissue) may also explain the rapid recovery from anaesthesia from fish from stage 4-5 anaesthesia (with high plasma isoeugenol concentrations). Kiessling et al. (2009) also

demonstrated a non-linear clearance of plasma isoeugenol in cannulated Atlantic Salmon (*Salmo salar*) after administration of AQUI-S$^{TM}$.

Hypoxia, however, may still only partly explain the deep anaesthesia effects of isoeugenol. The primary neurological mechanisms of isoeugenol are still not well understood and in depth research is required in this area. The question still remains as to why a fish anaesthetised at a low isoeugenol exposure concentration, which shows elevated plasma concentrations similar to those at a medium isoeugenol exposure concentration, and whose white muscle isoeugenol concentration exceeds that of fish exposed to high isoeugenol concentrations, still does not reach the depth of anaesthesia demonstrated by the medium and high isoeugenol concentration exposed fish. An explanation to why the fish anaesthetised at the low isoeugenol concentration never reached beyond stage 2.5 anaesthesia may be that the layer of adsorbed isoeugenol micelles on the gill lamellae was not thick enough to reduce oxygen uptake sufficient to cause hypoxia-induced deep anaesthesia. The adsorbed layer of micelles was, however, concentrated enough to maintain a gradient driving isoeugenol into the blood, elevating plasma and white muscle isoeugenol concentrations without the full anaesthetic effect induced by hypoxia. Research into at the effects of AQUI-S$^{TM}$ on oxygen diffusion efficiency across a perfused gill preparation may further clarify what role hypoxia plays in anaesthesia.

In summary, this study of the direct uptake delivery of isoeugenol via the gills, into the blood and perfused into the musculature using the fish's own circulatory system shows that this is a relatively non-invasive, non-intensive and simple method of potentially delivering supportive molecules, such as antioxidants, into live fish prior to harvest and storage.

## 3.6 References

Atsumi T, Fujisawa S, Tonosaki K (2005) A comparative study of the antioxidant/prooxidant activities of eugenol and iso-eugenol with various concentrations and oxidation conditions. Toxicology in Vitro 19: 1025-1033

Bahadur NP, Shiu WY, Boocock DGB, Mackay D (1997) Temperature dependence of octanol-water partition coefficient for selected chlorobenzenes. Journal of Chemical and Engineering Data 42: 685-688

Barber MC (2003) A review and comparison of models for predicting dynamic chemical bioconcentration in fish. Environmental Toxicology and Chemistry 22: 1963-1992

Barron MG (1990) Bioconcentration. Environmental Science and Technology 24: 1612-1618

Belpaire C, Goemans G (2007) Eels: contaminant cocktails pinpointing environmental contamination. ICES Journal of Marine Science 64: 1423-1436

Bosworth BG, Small BC, Gregory D, Kim J, Black SE, Jerrett AR (2006) Effects of rested-harvest using the anaesthetic AQUI-S$^{TM}$ on channel catfish, *Ictalurus punctatus*, physiology and fillet quality. Aquaculture 262: 302-318

Colborn T, Dumanoski D, Myers JP (1996) Our stolen future. Are we threatening our fertility, intelligence, and survival? A scientific story. London, Abacus, 306 pp

Dearden JC, Shinnawei NM (2004) Improved prediction of fish bioconcentration factor of hydrophobic chemicals. SAR and QSAR in Environmental Research 15: 449-455

Erickson RJ, McKim JM (1990) A model for exchange of organic chemicals at fish gills: flow and diffusion limitations. Aquatic Toxicology 18: 175-198

Evans DH, Piermarini PM, Choe KP (2005) The multifunctional fish gill: dominant site of gas exchange, osmoregulation, acid-base regulation, and excretion of nitrogenous waste. Physiological Reviews 85: 97-177

Evans DH (1998) In Karnaky K J eds. The physiology of fishes, Ed 2. CRC Press LLC, USA, pp 157-158

Gilderhus PA, Marking LL (1987) Comparative efficacy of 16 anesthetic chemicals on rainbow trout. North American Journal of Fisheries Management 7: 288-292

Gilmour KM (1998) Gas exchange. In Evans DH, eds, The Physiology of Fishes, CRC Press, Baton Rouge, pp 101-127

Hayton WL, Barron MG (1990) Rate limiting barriers to xenobiotic uptake by the fish gill. Environmental Toxicology and Chemistry 9: 151-158

Hill JV, Davison W, Forster ME (2003) The effects of fish anaesthetics (MS222, metomidate and AQUI-S) on heart ventricle, the cardiac and branchial vessels from Chinook salmon (*Oncorhynchus tshawytscha*). Fish Physiology and Biochemistry 27: 19-29

Hughes GM (1970) A comparative approach to fish respiration. Experientia 26: 113-224

Iversen M, Finstad B, McKinley RS, Eliassen RA (2002) The efficacy of metomidate, clove oil, Aqui-s$^{TM}$ and Benzoak$^{(R)}$ as anaesthetics in Atlantic salmon (*Salmo salar L.*) smolts and their potential stress reducing capacity. Aquaculture 221: 549-566

Jerrett AR, Stevens J, Holland AJ (1996) Tensile properties of white muscle in rested and exhausted chinook salmon (*Oncorhynchus tshawtscha*). Journal of Food Science 61: 527-532

Keys AB (1933) The mechanism of adaptation to varying salinities in the common eel and the general problem of osmotic regulation in fishes. Procedings of the Royal Society of London, Series B 112: 184-199

Kiessling AK, Espe M, Rouohonen K, Morkore T (2004) Texture, gaping and colour of flesh and frozen Atlantic salmon flesh as affected by pre-slaughter iso-eugenol or CO2 anaesthesia. Aquaculture 236: 645-657

Kiessling A, Johansson D, Zahl IH, Samuelsen OB (2009) Pharmacokinetics, plasma cortisol and effectiveness of benzocaine, MS-222 and isoeugenol measured in individual dorsal aorta-cannulated Atlantic salmon (*Salmo salar*) following bath administration. Aquaculture 286: 301-308

Kildea MA, Allan GL, Kearney RE (2004) Accumulation and clearance of the anaesthetics clove oil and AQUI-S$^{TM}$ from the edible tissue of silver perch (*Bidyanus bidyanus*). Aquaculture 232: 265-277

Lakowicz JR (1999) Principles of Fluorescence Spectroscopy. Kluwer Academic / Plenum Publishers, New York, pp 445-450

Lin YT, Wu BN, Horng CF, Huang YC, Hong SJ, Lo YC, Cheng CJ, Chen IJ (1999) Iso-eugenol: A Selective $\beta_1$-Adrenergic Antagonist with Tracheal and

Vascular Smooth Muscle Relaxant Properties. Japan Journal of Pharmacology 80: 127-136

Mackay D, Fraser A (2000) Bioaccumulation of persistent organic chemicals: mechanisms and models. Environmental Pollution 110: 375-391

Meinertz JR, Greseth SL, Schreier TM, Bernardy JA, Gingerich WH (2006) Isoeuganol concentrations in Rainbow trout (*Oncorhynchus mykiss*) skin-on fillet tissue after exposure to AQUI-S$^{TM}$ at different temperatures, durations and concentrations. Aquaculture 254: 347-354

Nichols JW, Fitzsimmons PN, Whiteman FW (2004) A Physiologically Based Toxicokinetic Model for Dietary Uptake of Hydrophobic Organic Compounds by Fish. Toxicological Sciences 77; 219-229

Pritchard JB (2003) The gill and homeostasis: transport under stress. American Journal of Physiology-Regulatory, Integrative and Comparative Physiology 285: R1269-R1271

Priyadarsini KI, Guha SN, Rao MNA (1998) Physio-chemical properties and antioxidant activities of methoxy phenols. Free Radical Biology and Medicine 24: 933-941

Qiao P, Gobas FAPC, Farrell AP (2000) Relative contributions of aqueous and dietary uptake of hydrophobic chemicals to the body burden in juvenille rainbow trout. Archives of Environmental Contamination and Toxicology 39: 369-377

Rajakumar DV, Rao MNA (1993) Dehydrozingerone and iso-eugenol as inhibitors of lipid-peroxidation and as free-radical scavengers. Biochemical Pharmacology 46: 2067-2072

Rothwell SE, Black SE, Jerrett AR, Forster ME (2005) Cardiovascular changes and catecholamine release following anaesthesia in Chinook salmon (*Oncorhynchus tshawytscha*) and snapper (*Pagrus auratus*). Comparative Biochemistry and Physiology - Part A: Molecular & Integrative Physiology 140: 289-298

Shephard KL (1993) Mucus on the epidermis of fish and its influence on drug delivery. Advanced Drug Delivery Reviews 11: 403-417.

Sijm DTHM, Part P, Opperhuizen A (1993) The influence of temperature on the uptake rate constants of hydrophobic compounds determined by the isolated perfused gills of rainbow trout (*Oncorhynchus mykiss*). Aquatic Toxicology 25: 1-14

Sijm DTHM, Verberne ME, De Jonge WJ, Part P, Opperhuizen A (1995) Allometry in the Uptake of Hydrophobic Chemicals Determined in Vivo and in Isolated Perfused Gills. Toxicology and Applied Pharmacology 131: 130-135

Small BC (2004) Effect of isoeuganol sedation on plasma cortisol, glucose and lactate dynamics in channel catfish *Ictalurus punctatus* exposed to three stressors. Aquaculture 238: 469-481

Smith KEC, McLachlan MS (2006) Concentrations and partitioning of polychlorinated biphenyls in the surface waters of the southern Baltic Sea - Seasonal effects. Environmental Toxicology and Chemistry 25: 2569-2575

Steen JB (1971) Comparative Physiology of Respiratory Mechanisms. London, Academic Press, London pp 182

Stehly GR, Gingerich WH (1999) Evaluation of AQUI-S (efficacy and minimum toxic concentration) as a fish anesthetic/sedative for public aquaculture in the United States. Aquaculture Research 30: 365-372

US FDA database of approved Animal Drug Products, abstract 200-226, http://dil.vetmed.vt.edu/Display/NadaBrowse.cfm?NadaString=200-226).

van der Oost R, Beyer J, Vermeulen NPE (2002) Fish bioaccumulation and biomarkers in environmental risk assessment: a review. Environmental Toxicology and Pharmacology 13: 57-149

Weisbrod AV, Burkhard LP, Arnot J, Mekenyan O, Howard PH, Russom C, Boethling R, Sakuratani Y, Traas T, Bridges T, Lutz C, Bonnell M, Woodburn K, Parkerton T (2007) Workgroup report: Review of fish bioaccumulation databases used to identify persistent, bioaccumulative, toxic substances. Environmental Health Perspectives 155: 255-261

# Chapter 4 Uptake and recovery of curcuminoids from the plasma and white muscle of juvenile snapper (*Pagrus auratus*)

## 4.1 Abstract

Recently, there has been a concerted research effort into the medicinal benefits of the curcuminoids, the active ingredients found in the spice turmeric. However, uptake of dietary and intraperitoneal (i.p.) administrated curcuminoids in animals is low. In this research I demonstrate the rapid uptake and accumulation of curcuminoids in the plasma, via direct uptake across the gills, and the subsequent accumulation in the white and red muscle of anaesthetised snapper (*Pagrus auratus).* The uptake and recovery of the curcuminoids in the plasma, and white and red muscle from low, medium and high exposure concentrations of turmeric stock solution was quantified with fluorescent digital image analysis and further verified with conventional fluorimetry. Uptake in all concentration treatments was rapid, with plasma curcuminoid concentrations reaching near maximum within 10 min exposure. With all treatment concentrations, uptake was greatest in the plasma, then red muscle and lowest in the white muscle, suggesting that blood flow and tissue perfusion limited distribution. However, uptake of the curcuminoids in the musculature increased over the duration of the exposure. The potential benefits of the curcuminoids as potent natural occurring antioxidants, coupled with a minimally invasive and highly efficient direct uptake delivery pathway (potentially for any gilled organism), is discussed.

## 4.2 Introduction

In the previous chapter we saw that the uptake of AQUI-S$^{TM}$ at the gills and the subsequent delivery to the white muscle via the circulation system is potentially a very efficient and non-invasive method of delivering molecules to the white muscle. After pilot studies involving many different molecules (predominantly naturally occurring antioxidants), turmeric stock solution (primarily curcumin and curcuminoid derivatives) was found to successfully bioconcentrate in the plasma and bioaccumulate in the tissues of snapper. The uptake of curcuminoids from the aquatic environment via the gills and the subsequent delivery to the white muscle in teleosts has not been studied before. In this chapter we look at the uptake and recovery of curcuminoids at low, medium and high exposure concentrations. Curcuminoids have fluorimetric properties, which with digital image analysis, can be used to quantify their uptake and recovery from fish.

The spice turmeric is derived from the plant *Curcuma longa*, native to South Asia. The plant's rhizomes are dried and ground to make the spice. The principal ingredient in turmeric are the curcuminoids, know as curcumin, and two naturally occurring derivatives, bisdemethoxycurcumin and demethoxycurcumin (Anand et al. 2007). For centuries turmeric has not only been used in cooking, as a food preservative and dye, but also as a medicinal aid in Chinese and Indian medicine practices. Since the early 1990s there have been many reviews and a few thousand journal articles published on the diverse medicinal properties of curcumin. The primary focus of this thesis is on perfusion and delivery of supportive molecules to the white muscle, rather than the actual benefits or mode of action of the molecules. I will only briefly discuss the beneficial biological effects that curcumin has been shown to have, but for a more comprehensive synopsis I recommend reviews by Sharma et al. (2005), Maheshwari et al. (2006), Aggarwal et al. (2007) and Anand et al. (2007).

Curcumin was traditionally known for its anti-inflammatory effects. Research has shown that curcumin down regulates various proinflammatory cytokines and chemokines (Hidaka et al. 2002, Okunieff et al. 2006). Curcumin has been shown to enhance the immune system by modulating the growth and cellular response of various immune system cells such as T cells, B-cells, macrophages, neutrophils, NK cells and dendritic cells (Jagetia and Aggarwal 2007).

There have been many studies over the recent years demonstrating that curcumin targets several steps in the biochemical pathways of cancer transformation, proliferation and invasion (Shishodia et al. 2007). In-vitro studies have shown that curcumin possesses anti-cancer activity in a variety of cell lines including breast, cervical, gastric, colon, hepatic, leukaemia, oral epithelial, ovarian, pancreatic and prostrate (Johnson and Mukhtar 2007). Initially the curcumin anti-cancer research was undertaken on animals. Rao et al. (1995) showed that dietary uptake of curcumin significantly inhibited the incidence of azoxymethane induced colon adenocarcinomas in rats. We now see several clinical trials in progress looking at the safety and tolerability of curcumin in human colo-rectal cancer patients, with promising results (Johnson and Mukhtar 2007).

Antioxidants are important in not only the preservation of food products but for the prevention of cellular oxidation and free radical damage in living tissue. Curcumin has been shown to have excellent antioxidant properties, similar to those of vitamins E and C (Toda et al. 1985). More recently, Jayaprakasha et al. (2006) demonstrated the in vitro antioxidant activity of three curcuminoids, curcumin and its two naturally occurring derivatives, bisdemethoxycurcumin and demethoxycurcumin. Their results suggested that curcumin was the most potent of the three, but the other two curcuminoids should also be considered as they may have different modes of antioxidant behaviour.

Curcumin has been beneficial in tissue preservation and transplantation research. Chen et al. (2006) added curcumin to Euro-Collins solution, phosphate buffer

saline and University of Wisconsin solution and found that it enhanced tissue preservation time and maintained organ quality. Shoskes (1998) showed that curcumin could reduce ischemia-reperfusion injury and inflammation sequelae in rats.

Curcumin is a polyphenolic compound (1,7-bis(4-hydroxy-3-methoxyphenyl)-1,6-heptadiene-3,5-dione) and is fairly inert. Toxicology studies on animals (Shankar and Shanta 1980), and humans (Soni and Kuttan 1992) have shown it to be non-toxic. The bioavailability of curcumin in humans is poor. Ammon and Wahl (1991) showed that curcumin was far less active in their studies on anti-inflammatory effects from oral administration than when it was administered via an intraperitoneal (i.p.) injection. It was suggested that this was because of poor absorption. Anand et al. (2007) reinforced this theory when they showed that even at a high safe dietary dose of 12 $mg.day^{-1}$ uptake into the plasma and tissue was low.

Curcumin can be used as a specific treatment or as a generic therapy to treat multiple ailments. Many beneficial biological properties of curcumin have been described and more may be discovered.

In this research, turmeric powder was used to make the curcuminoid stock solution for the uptake experiments. As stated earlier, curcumin is the main active ingredient in turmeric (2-5%) (Aggarwal et al. 2007). However, it is acknowledged that there are many other molecules in turmeric that would also be present in the turmeric stock solution. The reason that cooking grade turmeric powder was used to make the stock solution and not pure curcumin was cost.

# 4.3 Methods

## 4.3.1 Experimental fish

### 4.3.1.1 Snapper

The same cohort of snapper was used and treated the same as in the AQUI-S$^{TM}$ uptake and recovery experiments (Chapter 3.3.1.1).

## 4.3.2 Experimental methodology and trials

### 4.3.2.1 Turmeric stock solution

Turmeric stock solution was made by saturating reagent grade ethanol with turmeric. 50g of turmeric powder was added to 250ml of ethanol and shaken every 10 min for 1 h before being left over night for the grainy particulate root matter to settle out. The following day the yellow turmeric saturated ethanol was decanted. Fluorimetric analysis of the turmeric stock solution and a stock solution made from curcumin (Sigma C7727 94%) showed them to be very similar. Therefore we can conclude that the major component of the ethanol extraction was curcumin. No other fluorescent peaks were detected.

### 4.3.2.2 Snapper

Juvenile snapper were exposed to three different concentrations of turmeric stock solution; 0.63 ml.L$^{-1}$, 1.25 ml.L$^{-1}$, and 1.88 ml.L$^{-1}$. The water baths also contained 10 mg.L$^{-1}$ AQUI-S$^{TM}$. Fish were sampled every 10 min for 80 min (60 min in the turmeric bath and 20 min in the fresh seawater recovery tank). After 60 min in the turmeric water bath the remaining anaesthetised fish were netted and placed in a tank containing fresh seawater to recover. Fish were not sampled after 80 min as the anesthetic effect of the isoeugenol had worn off and they became difficult to catch without inducing stress. Two fish were sampled at a time and killed by iki jime. Approximately 200uL of blood was sampled from the fish via a ventral

heart puncture using a heparinised 25 gauge needle and 1.0cc syringe. The blood samples were stored on ice until analysis.

## 4.3.3 Turmeric (curcumin) recovery

### 4.3.3.1 Fluorimetric analysis

Blood samples were treated the same way as in chapter 3.3.3.1 (with the exception of 30µl of plasma which was removed after the first centrifuge run to be imaged). 100µl of the plasma supernatant was pipetted into a 3ml fluorimetric cuvette and 2900µl of reagent grade ethanol was added. The samples were analysed with a Cary Eclipse Fluorimeter (Varian Instruments, Australia). The sample was excited at 445 nm and the emission intensity recorded at 530 nm. The recorded emission intensity was not stardised against curcumin or turmeric stock standards but left as a raw intensity value. The emission and excitation slit widths were set at 5 nm, the excitation filter was set to auto, the emission filter was open, the photomultiplier voltage was set to 750V and the average time for reading was 1 second.

### 4.3.3.2 Digital image analysis

A lighting rig containing six, 1 Watt LED clusters was assembled to ensure even lighting. Each LED cluster consisted of three ~460 nm LED's. The LED clusters were bolted at even intervals around a ring of 300mm PVC pipe. The camera (Canon Powershot G5) and filter holder fitted in the centre between the LED clusters. After testing various commercial filters, the most effective was a filter comprised of three pieces of 3mm Amber 202 acrylic sheet. The assembled digital imagery rig is shown in Figure 4.1.

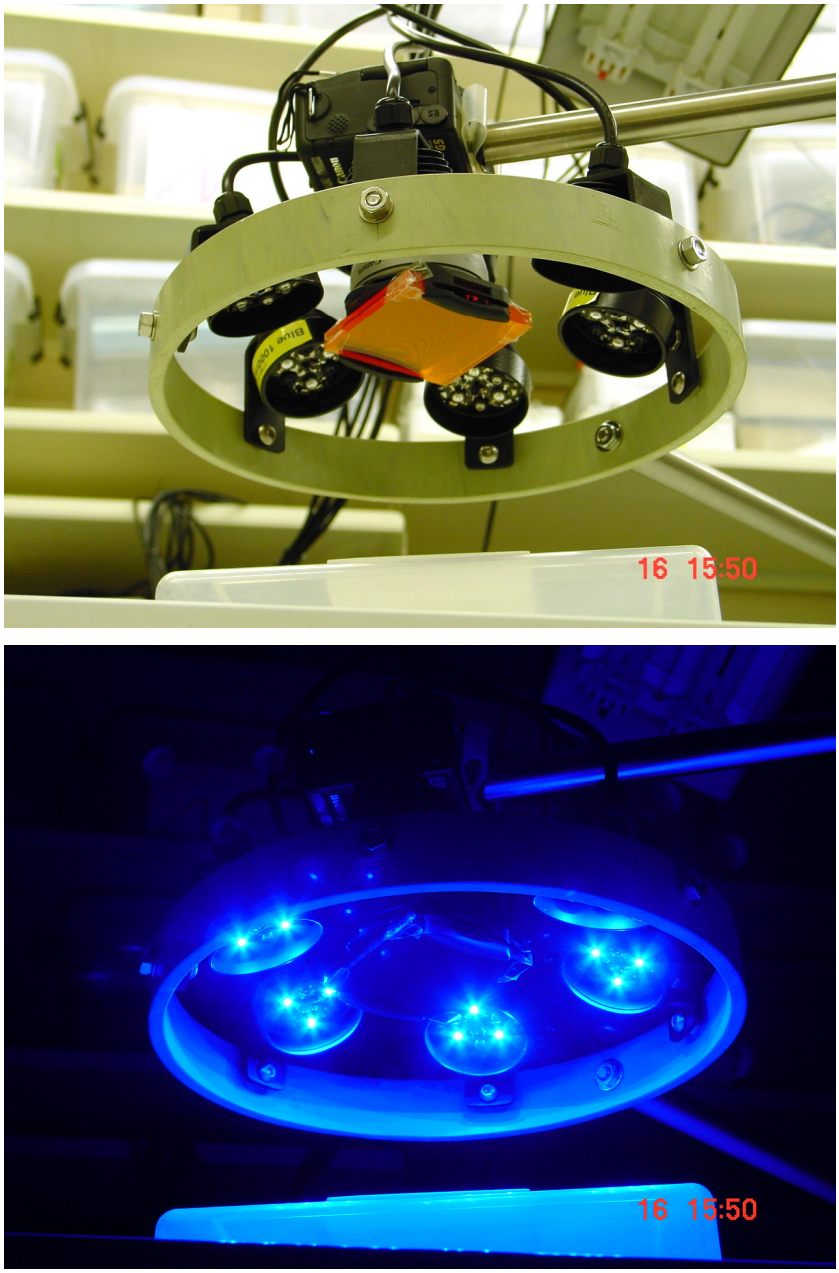


**Figure 4.1 Off and on photos of the digital imagery rig used to acquire images of the snapper muscle and plasma after exposure in the turmeric water bath.**

30ul of plasma was pipetted into a small well (Ø5mm, depth1.5mm) that had been milled in a white Teflon plate. An image of the plasma was taken and the Teflon plate cleaned. The snapper were cut transversely at the anus and again 10mm anterior to the anus. The 10mm thick "steak" was placed posterior down on the white Teflon plate and an image acquired.

Digital image analysis was done using Image Pro (Version 5). The image was converted from Red, Green, Blue (RGB) colour space colour to the Hue, Saturation, Intensity (HSI) colour space. The intensities of the plasma, the left and right white muscle D block and the red muscle wedge were measured.

## 4.4 Results

### 4.4.1 Digital and Fluorimetric analysis of curcuminoids

Figure 4.2 compares the emission scans (excited at 445 nm) of the turmeric stock solution, pure curcumin in ethanol, and the plasma from a fish exposed to the turmeric solution. The turmeric stock solution emission (2) has an identical emission peak (530 nm) to that of a protein free plasma sample from a fish exposed to the turmeric stock solution (1). The emission peak from 94% pure curcumin (Sigma C7727) (3) dissolved in ethanol is at 540 nm. Emission scan 4, which runs along the baseline, is from a plasma sample from a fish that was not exposed to turmeric stock solution.

The presence of turmeric (curcumin) in the plasma and muscle in juvenile snapper was visible under white light and even more so when illuminated with blue light and viewed through an amber filter. The use of digital imagery to measure the intensity of the turmeric coloration was successful. Turmeric was also able to be extracted from plasma by ethanol and its intensity recorded. Figure 4.3 compares images of the head, plasma and muscle from a snapper with and without exposure to the turmeric stock solution. We can see the bright yellow colour characteristic of turmeric and observe that it has perfused both the red and white muscle. There is slight fluorescent yellow intensity in the gut region on the muscle sample image from the non-treated fish. Analysis of the vitamin supplement fed to the fish found vitamin $B_2$ to be fluorimetrically excited at ~450 nm and emit at ~525 nm, which is very similar to that of curcumin.

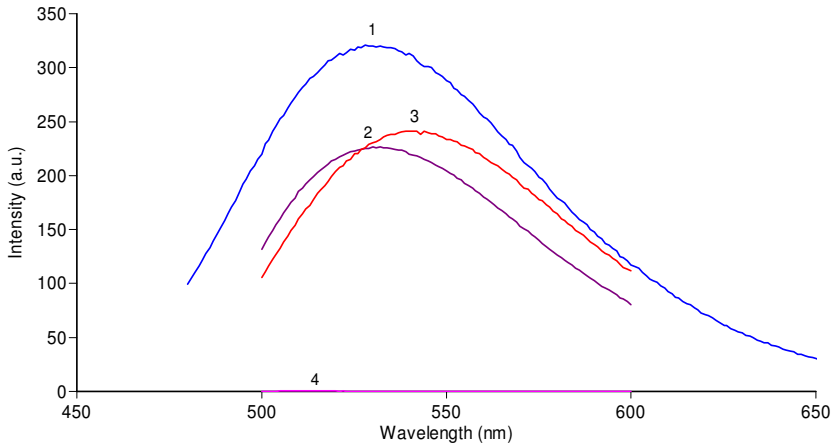


**Figure 4.2 Fluorescent emission scans (excited at 445 nm) of turmeric in a plasma sample (1), turmeric dissolved in ethanol (2), curcumin dissolved in ethanol (3), and plasma from a fish not exposed to the turmeric stock solution (4).**

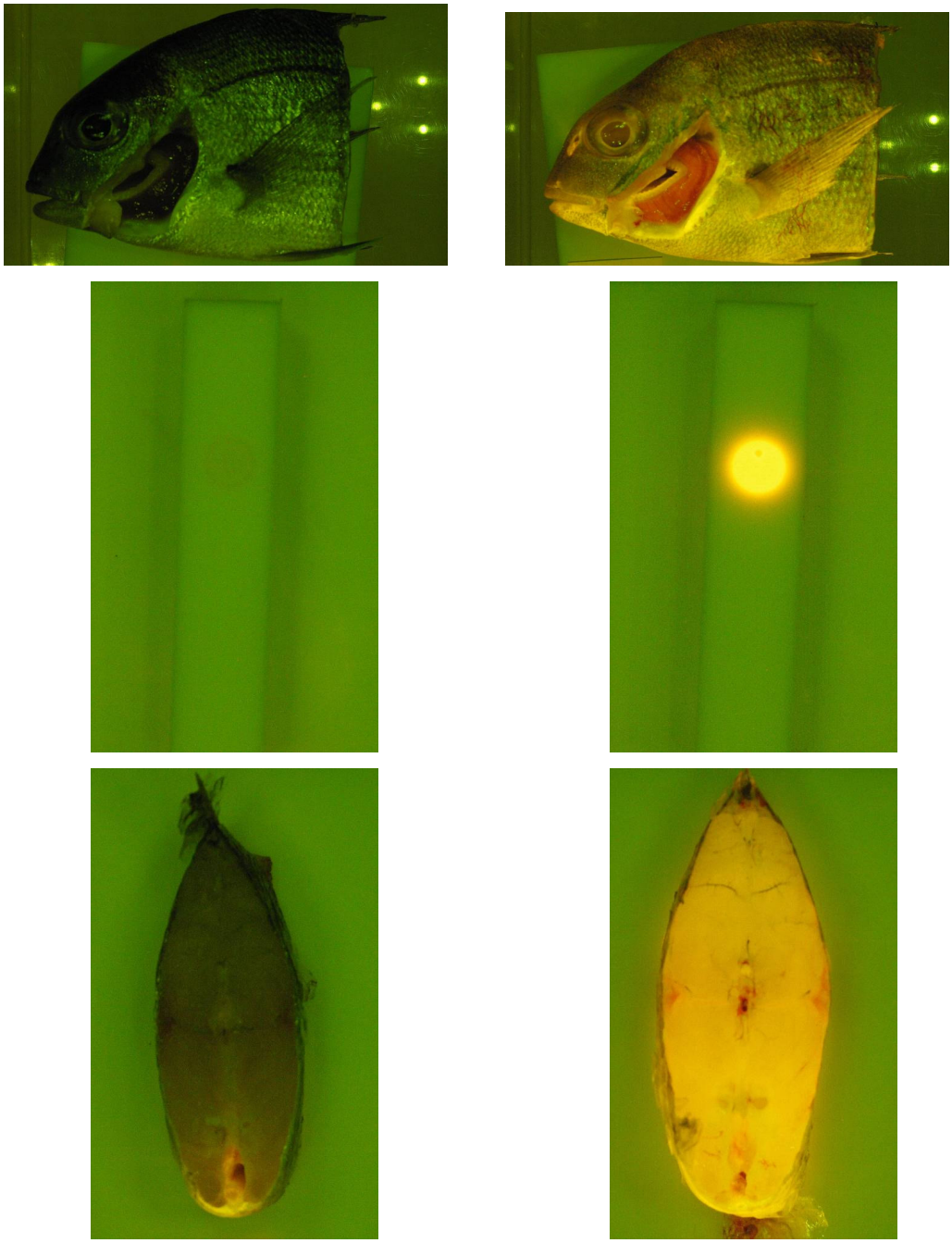

**Figure 4.3 Photographs of the head (top), the plasma (middle) and muscle steak (bottom) of an untreated snapper (left) and a snapper exposed to a water bath containing turmeric stock solution (right).** Images were taken under blue light (~460 nm) through an amber filter, Canon Powershot G5; iso 200, 1/10s F3.2).

## 4.4.2 Experimental trials

**Table 4.1 Experimental parameters for the turmeric exposure trial.**

| | Treatment | | |
|---|---|---|---|
| | Low | Medium | High |
| Turmeric stock ($ml.L^{-1}$) | 0.63 | 1.25 | 1.88 |
| Temperature ($^oC$) | 17.9±0.2 | 17.7±0.2 | 16.3±0.2 |
| Fish weight (g) | 81.6±2.1 | 67.6±1.5 | 86.9±2.3 |
| Length (mm) | 153.5±1.3 | 144.4±1.0 | 157.9±1.4 |
| N | 8 | 8 | 8 |
| Condition index ($w/l^3$) | 2.21±0.01 | 2.21±0.01 | 2.17±0.01 |

The intensity measured from the digital images from the plasma and the white and red muscle from the low, medium and high turmeric exposure treatments are shown in Figure 4.4.A-C. At all exposure concentrations the colour intensity was significantly greatest in the plasma compared with the red and white muscle. The measured colour intensity within each treatment was lowest in the white muscle.

The highest exposure treatment resulted in the greatest measured colour intensity in the plasma (Figure 4.5), which was significantly different from the medium exposure treatment at 60, 70 and 80 min. The measured colour intensity in the low exposure treatment was significantly lower than that in the high and medium exposure treatments at all time values except 0 min. In all three concentration treatments the measured colour intensity in the plasma samples reached a saturation plateau within 10 min. The medium and high exposure concentrations maintained an intensity level of 90-100 units, whereas the low exposure concentration treatment reached saturation at ~70-80 units before a slight decrease in intensity from 40 min to 60 min (Figure 4.5). After 10 min recovery the measured colour intensity of the plasma in the low, medium and high exposure treatments had decreased to 50%, 77% and 80% (respectively), from the 60 min

intensity value. The measured colour intensity had further reduced after 20 min recovery (80 min) to 33% (low), 58% (medium), and 62% (high) of the 60 min intensity value.

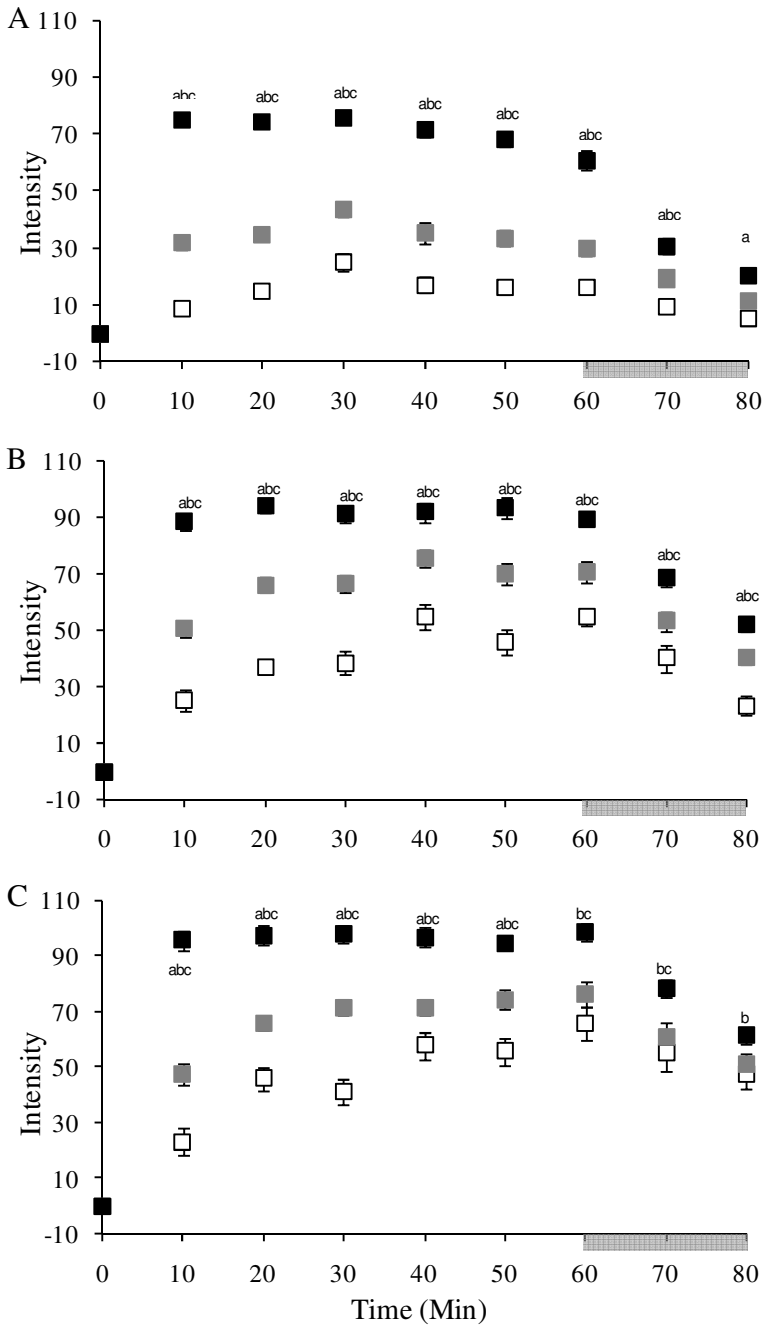


**Figure 4.4 Digital image colour intensity of the plasma (black), red muscle (grey) and white muscle (clear) of snapper exposed to A) 0.63 ml.L$^{-1}$, B) 1.25 ml.L$^{-1}$ , and C) 1.88 ml.L$^{-1}$ turmeric stock solution for 60 min.** Fish were recovered in fresh seawater for 20 min (60-80 min). Values are mean±sem. (N=8). a denotes a significant difference (unpaired two-tailed Student's t-test, P<0.05) between 0.63 ml.L$^{-1}$ and 1.25 ml.L$^{-1}$ treatments, b between 0.63 ml.L$^{-1}$ and 1.88 ml.L$^{-1}$ treatments, and c between 1.25 ml.L$^{-1}$ and 1.88 ml.L$^{-1}$ treatments.

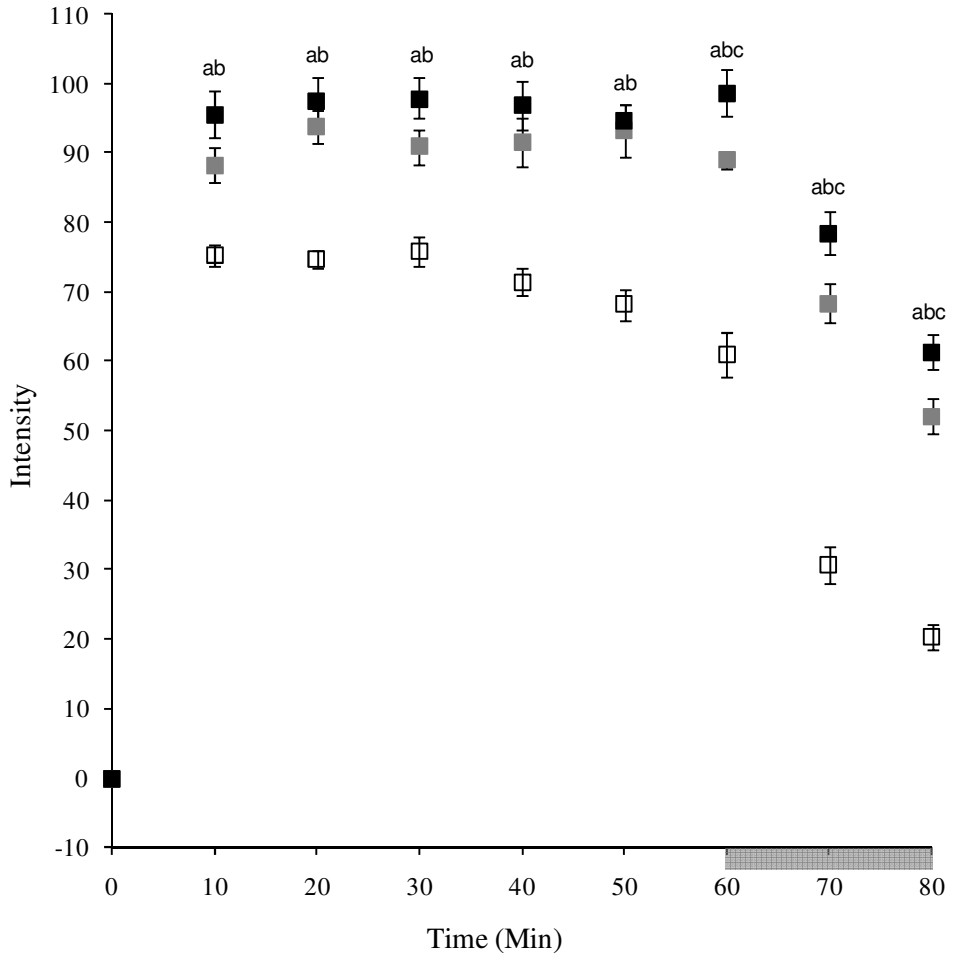


**Figure 4.5 Plasma colour intensity measured by digital image analysis of snapper exposed for 60 min in water baths containing 10 mg.L$^{-1}$ AQUI-S$^{TM}$ and 0.63 ml.L$^{-1}$ (clear), 1.25 ml.L$^{-1}$ (grey), and 1.88 ml.L$^{-1}$ (black) turmeric stock solution.** Fish were recovered in fresh seawater for 20 min (60-80 min). Values are mean±sem. (N=8). a denotes a significant difference (unpaired two-tailed Student's t-test, $P<0.05$) between 0.63 ml.L$^{-1}$ and 1.25 ml.L$^{-1}$ treatments, b between 0.63 ml.L$^{-1}$ and 1.88 ml.L$^{-1}$ treatments, and c between 1.25 ml.L$^{-1}$ and 1.88 ml.L$^{-1}$ treatments.

The uptake of turmeric in the white muscle (Figure 4.6) was not as rapid as that in the plasma (Figure 4.5). At the low turmeric exposure concentration the measured colour intensity of the white muscle reached a maximum after 30 min (25.3±3.2 intensity units) before maintaining saturation at ~15-20 intensity units. The measured intensity in the white muscle in the low turmeric exposure treatment was significantly different (P=0.05) from the medium and high exposure treatments at all time values. In comparison, the high turmeric exposure concentration continued to increase in intensity for the duration of the exposure reaching 66.0±5.9 intensity units at 60 min. The measured colour intensity in the medium exposure treatment reached a plateau of around 45-55 intensity units after 40 min. After 10 min recovery the measured colour intensity of the white muscle in the low, medium and high exposure treatments had decreased to 58%, 74% and 84% (respectively) of the 60 min intensity value. The measured colour intensity had further reduced after 20 min recovery (80 min) to 32% (low), 43% (medium), and 72% (high) of the 60 min intensity value.

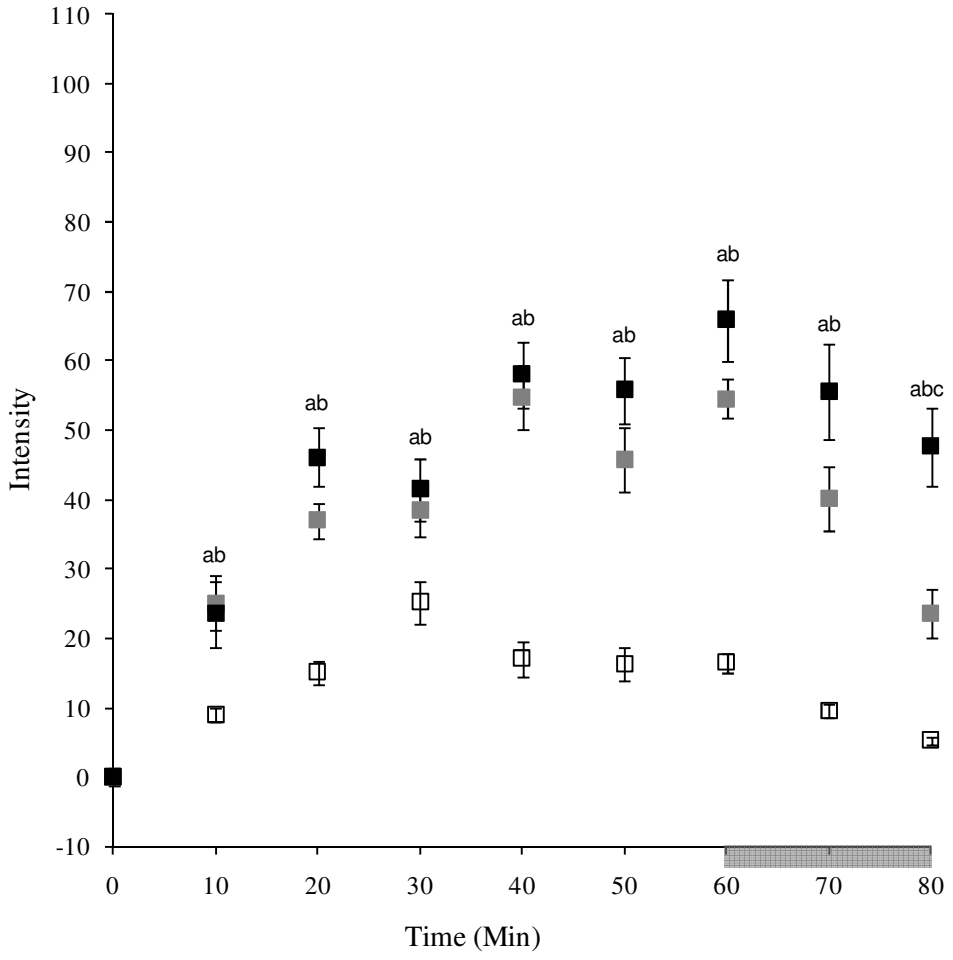


**Figure 4.6 White muscle colour intensity measured by digital image analysis of snapper exposed for 60 min in water baths containing 10 mg.L$^{-1}$ AQUI-S$^{TM}$ and 0.63 ml.L$^{-1}$ (clear), 1.25 ml.L$^{-1}$ (grey), and 1.88 ml.L$^{-1}$ (black) turmeric stock solution.** Fish were recovered in fresh seawater for 20 min (60-80 min). Values are mean±sem. (N=8). a denotes a significant difference (unpaired two-tailed Student's t-test, P<0.05) between 0.63 ml.L$^{-1}$ and 1.25 ml.L$^{-1}$ treatments, b between 0.63 ml.L$^{-1}$ and 1.88 ml.L$^{-1}$ treatments, and c between 1.25 ml.L$^{-1}$ and 1.88 ml.L$^{-1}$ treatments.

The uptake of turmeric in the red muscle was greater than the white muscle in all three exposure treatments, as shown in Figure 4.4. Figure 4.7 compares the uptake in the red muscle between treatments. There was a rapid elevation in the measured colour intensity within the initial 10 min in all the exposure treatments. The low turmeric exposure concentration reached 32.3±3.4 intensity units after 10 min, before peaking at 30 min 43.7±2.6 intensity units) and finally stabilising at ~30-35 intensity units. This pattern of uptake in the low turmeric exposure treatment was very similar to that in the white muscle (Figure 4.6), with the exception of a more pronounced rapid initial 10 min uptake. Both the medium and high turmeric exposure concentration treatments exhibited a rapid uptake in the initial 10 min, to 50.5±2.8 intensity units and 47.6±4.0 intensity units respectively. The medium exposure treatment reached a maximum saturation at 40 min of 75±3.6 intensity units. The high exposure treatment reached a maximum saturation plateau, after 60 min exposure, of 76.6±4.4 intensity units. After 10 min recovery the intensity of the red muscle in the low, medium and high exposure treatments had decreased to 35%, 38% and 52% (respectively) of the 60 min intensity value. The measured colour intensity had further reduced after 20 min recovery (80 min) to 19% (low), 21% (medium), and 27% (high) of the 60 min intensity value.

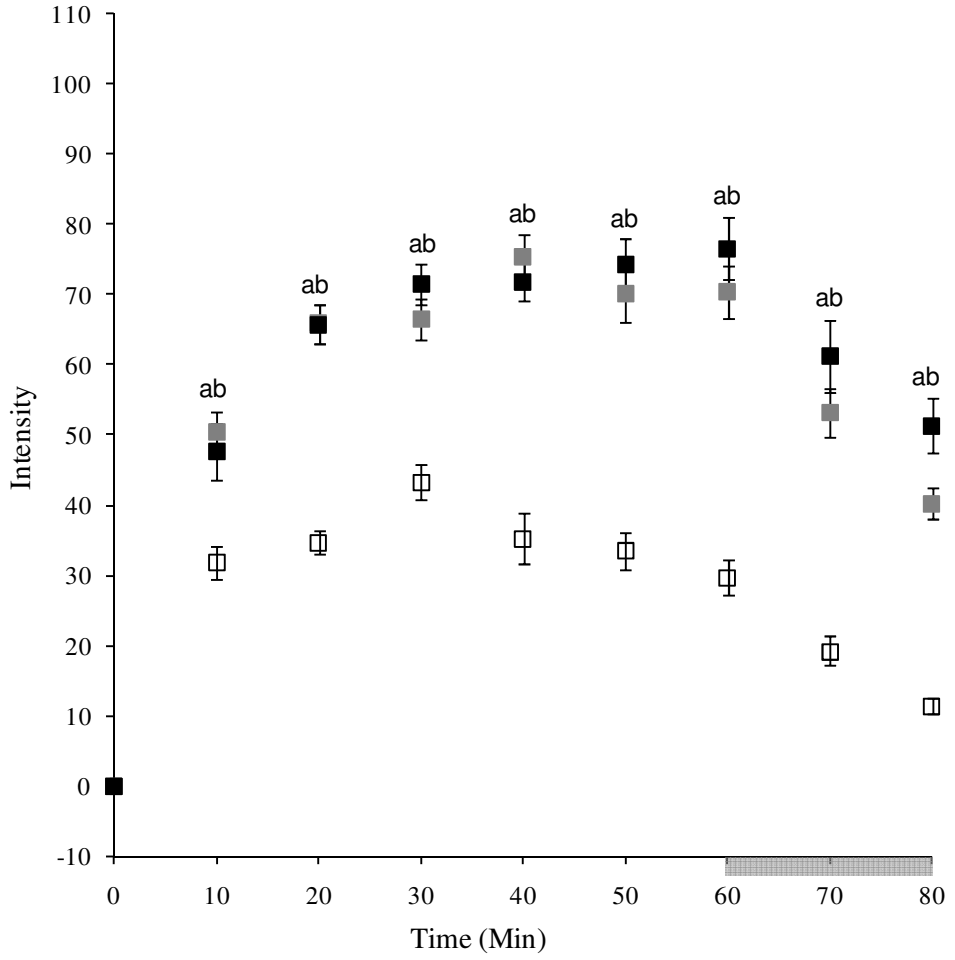


**Figure 4.7 Red muscle colour intensity measured by digital image analysis of snapper exposed for 60 min in water baths containing 10 mg.L$^{-1}$ AQUI-S$^{TM}$ and 0.63 ml.L$^{-1}$ (clear), 1.25 ml.L$^{-1}$ (grey), and 1.88 ml.L$^{-1}$ (black) turmeric stock solution.** Fish were recovered in fresh seawater for 20 min (60-80 min). Values are mean±sem. (N=8). a denotes a significant difference (unpaired two-tailed Student's t-test, $P<0.05$) between 0.63 ml.L$^{-1}$ and 1.25 ml.L$^{-1}$ treatments, b between 0.63 ml.L$^{-1}$ and 1.88 ml.L$^{-1}$ treatments, and c between 1.25 ml.L$^{-1}$ and 1.88 ml.L$^{-1}$ treatments.

Figure 4.8 shows the plasma uptake of turmeric determined by fluorimetric analysis. It shows similarities to Figure 4.5, which was derived from the digital image analysis of plasma. The data from the digital analysis of the plasma images correlated significantly ($r^2$ = 0.94; P= 0.0001) with the fluorimetric analysis of the plasma samples (Figure 4.9). In each treatment there was a rapid rise in saturation within the first 10 min with the low turmeric exposure treatment significantly lower (135±15 intensity units) than the medium and high exposure concentrations (258±42 intensity units and 320±47 intensity units, respectively). The low exposure concentration reached peak plasma saturation at time 30 min (167±47) before slowly decreasing in intensity (90±9 intensity units at 60 min). The medium and high exposure concentrations reached a saturation plateau after 20 min (medium exposure treatment ~250-275 intensity units, high exposure treatment ~350-375 intensity units). After 10 min recovery the measured colour intensity of the plasma in the low, medium and high exposure treatments had decreased to 58%, 74% and 84% (respectively) of the 60 min intensity value. The measured colour intensity had further reduced after 20 min recovery (80 min) to 32% (low), 43% (medium), and 72% (high) of the 60 min intensity value.

Figure 4.10 compares the red muscle to white muscle (RM:WM) colour intensity ratio from each turmeric exposure concentration. After 10 min exposure, the RM:WM ratio was 1.51±0.07 in the 0.63 $ml.L^{-1}$ treatment, 1.44±0.07 in the 1.25 $ml.L^{-1}$ treatment and 1.61±0.2 in the 1.88 $ml.L^{-1}$ treatment. The RM:WM ratios for all exposure treatments decreased over the duration of the exposure.

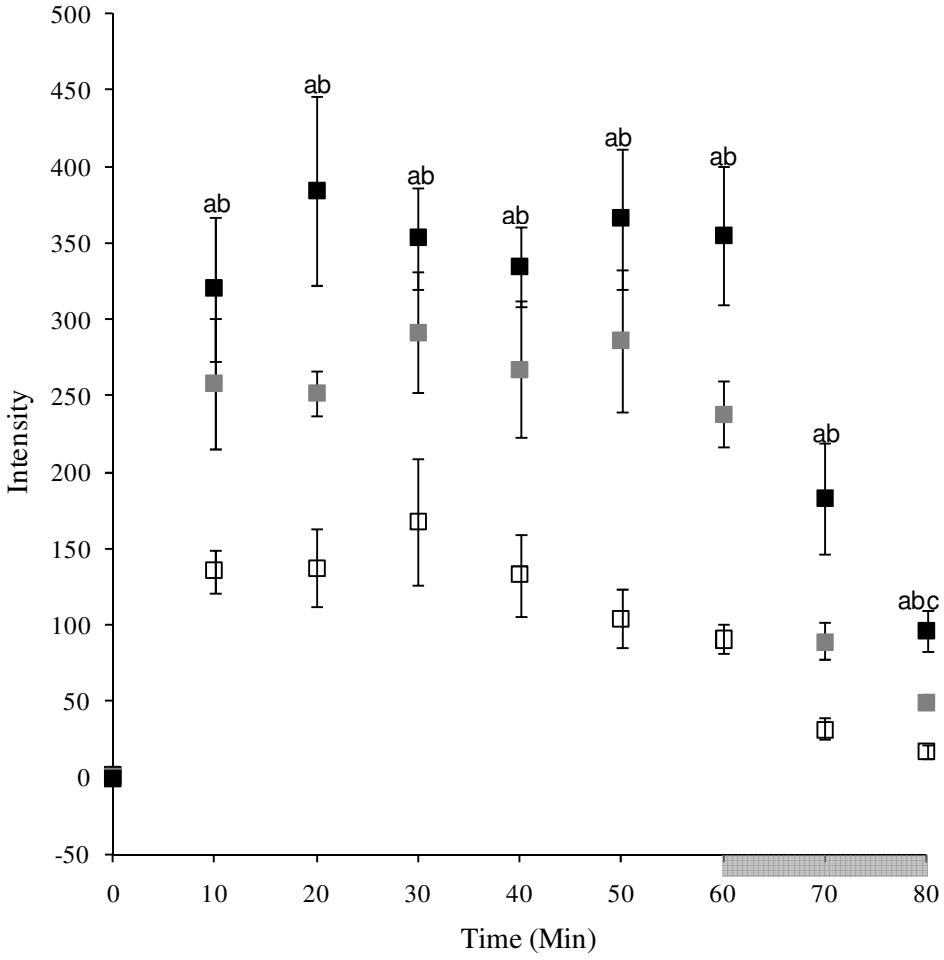


**Figure 4.8 Plasma intensity measured by fluorimetric analysis of snapper exposed for 60 min in water baths containing 10 mg.L$^{-1}$ AQUI-S$^{TM}$ and 0.63 ml.L$^{-1}$ (clear), 1.25 ml.L$^{-1}$ (grey), and 1.88 ml.L$^{-1}$ (black) turmeric stock solution.** Fish were recovered in fresh seawater for 20 min (60-80 min). Values are mean±sem. (N=8). a denotes a significant difference (unpaired two-tailed Student's t-test, $P<0.05$) between 0.63 ml.L$^{-1}$ and 1.25 ml.L$^{-1}$ treatments, b between 0.63 ml.L$^{-1}$ and 1.88 ml.L$^{-1}$ treatments, and c between 1.25 ml.L$^{-1}$ and 1.88 ml.L$^{-1}$ treatments.

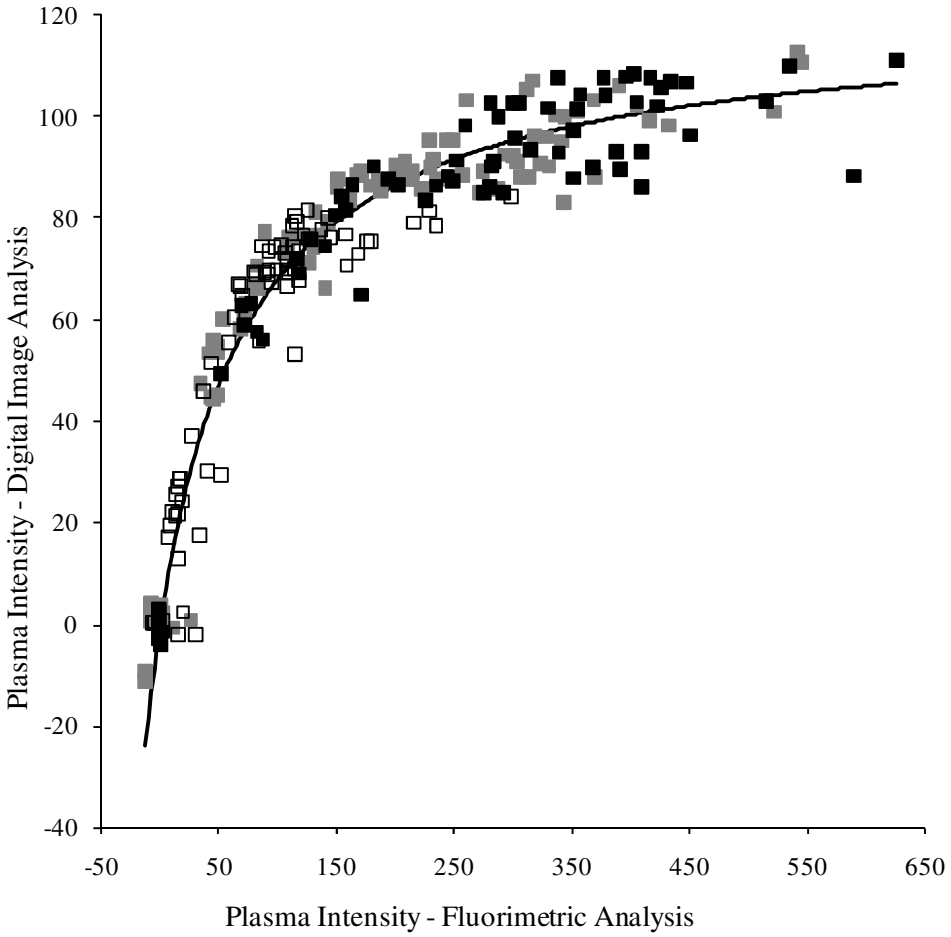


**Figure 4.9 Plasma intensity measured by fluorimetric analysis and digital image analysis of snapper exposed for 60 min in water baths containing 10 mg.L$^{-1}$ AQUI-S$^{TM}$ and 0.63 ml.L$^{-1}$(clear), 1.25 ml.L$^{-1}$ (grey), and 1.88 ml.L$^{-1}$ (black) turmeric stock solution.** The hyperbolic regression line of best fit ($r^2$= 0.94) is taken from all data points.

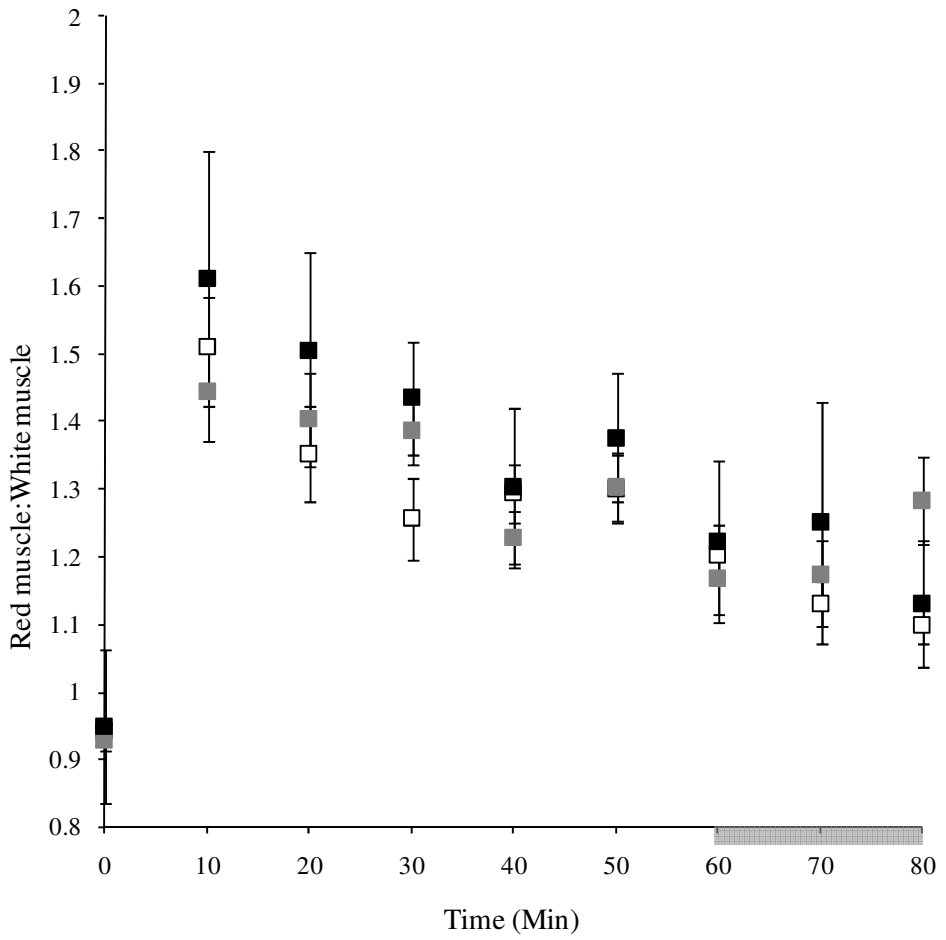


**Figure 4.10 Red muscle:white muscle ratio (RM:WM) of the measured colour intensity from the digital image analysis of snapper exposed to 0.63 ml.L$^{-1}$ (clear), 1.25 ml.L$^{-1}$ (grey), and 1.88 ml.L$^{-1}$ (black) turmeric stock solution for 60 min.** Fish were recovered in fresh seawater for 20 min (60-80 min). Values are mean±sem. (N=8).

## 4.5 Discussion

The bright yellow colour characteristic of turmeric is derived from the curcuminoids; curcumin, demethoxycurcumin and bisdemethoxycurcumin. The aroma of turmeric is due to the volatile oils present, particularly turmerone, ar-turmerone, zingiberene and curlone (Jayaprakasha et al. 2006). All the constituents that make up turmeric could potentially have eluted out into the ethanol based "turmeric stock solution" used in the exposure trials. Braga et al. (2003) tested various extraction methods and showed that ethanol extraction is a satisfactory method to extract the curcuminoids from turmeric. A fluorimetric emission scan of 94% curcumin (Sigma) in ethanol showed an emission peak at 540 nm, whereas the turmeric stock solution showed an emission peak at 530 nm, identical to the emission scan from a plasma sample from a fish exposed to the turmeric stock solution (Figure 4.2). The 10 nm shift in emission peak may be attributed to the other curcuminoids present in the turmeric stock solution (Bong 2000). Wang et al. (2006) showed the fluorimetric emission of curcumin to be closer to ~530nm.

The photographic images of the plasma and muscle from fish exposed and unexposed to the turmeric stock solution visually show that curcuminoids accumulated in the plasma and musculature snapper (Figure 4.3). The fluorescent staining in the gut and gut cavity in the unexposed fish is due to the vitamin supplements added to the wet fish alginate diet that the fish are fed, in particular $B_2$ vitamins, which were shown to be excited and emit at similar wavelengths to that of curcumin.

The yellow colour intensity of the plasma and white and red muscle was measured with digital image software. The measured image plasma intensity was compared with fluorimetric analysis of the plasma (Figure 4.9), which correlated significantly (Regression ANOVA). The measured intensity from the image and fluorimetric analysis is only indicative of the relative curcuminoid concentration

in the plasma and muscle, as actual curcuminoid concentrations were not measured.

Curcuminoids rapidly diffused across the gill lamellae and saturated the blood within 10 min exposure at each exposure concentration. This was shown with both the digital image analysis (Figure 4.5) and the fluorimetric analysis (Figure 4.8). Uptake to the red muscle was faster and greater than to the white muscle (Figure 4.4). The differences in the initial 10 min rate of uptake and the overall uptake to the red and white muscle can be explained by the physiological differences between the muscle types. The red muscle is more vascularised than the white muscle and has smaller muscle fibres. Johnston et al. (1975) showed that the diameters of rainbow trout red (*Salmo gairdneri*) and white muscle fibres were 20-25μ and 35-55μ, respectively. Greater vascularisation and smaller muscle fibres equate to reduced diffusion distances (Egginton et al. 1988). The smaller the diffusion distances, the faster the muscle can potentially uptake molecules. The overall uptake in the red muscle was greater than the white muscle for all three exposure concentrations. The initial 10 min uptake rate was also faster in the red muscle than the white muscle (Figures 4.6, 4.7).

Greater vascularisation and therefore greater perfusion to the red muscle is reiterated with the 10 min RM:WM intensity ratio shown in Figure 4.10. The RM:WM ratio in all of the exposure concentrations was ~1.4-1.6, which is similar to BFD values recorded in other fish species mentioned previously (Chapter 2). The use of turmeric as a fluorescent marker would be a cheap and effective method to determine tissue blood flow distribution in fish without the blockage problems associated with injected microspheres. The RM:WM curcuminoid ratio decreased with the duration of the exposure (Figure 4.10). This is because the less perfused white muscle slowly becomes more coloured as the curcuminoid concentration increases, catching up with the nearly (or already) saturated red muscle. Longer exposure duration may have seen the RM:WM ratio equilibrate.

Curcumin is primarily metabolised in the liver to form glucuronide or sulphate conjugates (Pan et al.1999, Ireson et al. 2001, Hoehle et al. 2006, Pfeiffer et al. 2007). Pan et al. (1999) demonstrated that 99% of the curcumin found in the plasma of rats after an intraperitoneal injection was metabolised glucuronides, particularly tetrahydrocurcumin (THC) and hexahydrocurcumin (HHC). Hoehle et al. (2006) suggest that the metabolites of the curcuminoids are more chemically stable than the parent curcuminoids and are potentially more active than curcumin. There have been conflicting studies of whether the curcumin metabolites are as active as curcumin itself. Portes et al. (2007) demonstrated that the antioxidant properties of several THCs were more efficient than their curcuminoid analogues, whereas Ireson et al. (2001) suggested that the hepatic metabolism of curcumin pharmacologically deactivates it as a chemopreventative agent.

During the recovery period (time 60-80 min) the intensity of the colour in the plasma (Figure 4.5) and white (Figure 4.6) and red (Figure 4.7) muscle decreases, indicating a decrease in curcuminoid concentration. In all the exposure concentrations, the plasma intensity decreased the greatest amount during recovery (time 60-70 min), then the red muscle and the white muscle the least. Again we can attribute the rate of recovery in the red and white muscle to the vascularisation and diffusion differences between the two muscle types. However, this is assuming the curcuminoids are being transported out of the muscle and not metabolised in situ as we were not able to visualise metabolites with our fluorescent analysis. Perkins et al. (2002) in a chemopreventative study on rats showed that once curcumin had reached maximal tissue concentrations (after i.p. injection), the concentrations in those tissues had decreased to 20-30% of the peak values within 4 hours, much slower than in the snapper white and red muscle. Comparing the respiratory uptake of curcumin in a fish with i.p injection in mammals is difficult and there is no other documented research at present on the dietary, i.p or direct uptake of curcuminoids in fish.

AQUI-S$^{TM}$ was present in the water baths containing the turmeric stock solution. It was used to keep the fish sedated and able to be handled without inducing added stress. The polysorbate contained in AQUI-S$^{TM}$ may have aided the diffusion of the curcuminoids across the gills by washing the mucus layer off the gill lamellae, as discussed in Chapter 4. Ethanol was used as a carrier solvent for the curcuminoids, and it might have affected gill uptake. In this study the maximum ethanol concentration used was 0.188%, well below the ranges (and experimental duration) tested by Crawshaw et al. (2006) and Gerlai et al. (2006). Crawshaw et al. (2006) tested the effects of ethanol on temperature regulation in goldfish exposed for 8 h in a thermal gradient. Their evidence indicated that exposure to 0.4%-1.1% ethanol decreased the regulated body temperature. However, Gerlai et al. (2006) showed that acute exposure of 1% ethanol had no deleterious effects on zebra fish.

As stated in the introduction, there has been a lot of research over recent years looking at the potential benefits of curcuminoids over a wide range of medicinal fields. However one of the pressing hurdles has been the low bio-availability of curcumin from oral and i.p. administration in mammals, with most of the curcumin and curcumin metabolites being excreted in faecal and urine waste. This research has shown that curcuminoids are rapidly diffused across teleost gills and into the blood and are transported into the white and red muscle. Potentially, the direct uptake of curcuminoids may be possible in a wide range of gilled organisms. However, research into quantifying the actual tissue concentrations of curcumin and curcumin metabolites is required, as well as whether or not curcuminoids provide any beneficial effects in post-harvest rested fish tissue.

## 4.6 References

Aggarwal BB, Sundaram C, Malani N, Ichikawa H (2007) Curcumin: The Indian solid gold. Molecular Targets and Therapeutic Uses of Curcumin in Health and Disease 595: 1-13

Ammon HPT, Wahl MA (1991) Pharmacology of Curcuma-longa. Plant Medica 57: 1-7

Anand P, Kunnumakkara AB, Newman RA, Aggarwal BB (2007) Bioavailability of Curcumin: Problems and Promises. Molecular Pharmaceutics 4: 807-818

Bong PH (2000) Spectral and photophysical behaviors of curcumin and curcuminoids. Bulletin of the Korean Chemical Society 21: 81-86

Braga MEM, Leal PF, Carvalho JE, Meireles MAA (2003) Comparison of yield, composition, and antioxidant activity of turmeric (Curcuma longa L.) extracts obtained using various techniques. Journal of Agricultural and Food Chemistry 51: 6604-6611

Chen CG, Johnston TD, Wu GH, Ranjan D (2006) Curcumin has potent liver preservation properties in an isolated perfusion model. Transplantation 82: 931-937

Crawshaw LI, Wallace HL, O'Connor CS, Yoda T, Crabbe JC (2006) Tolerance and withdrawal in goldfish exposed to ethanol. Physiology & Behaviour 87: 460-468

Egginton S, Turek Z, Hoofd LJC (1988) Differing patterns of capillary distribution in fish and mammalian skeletal muscle. Respiratory Physiology 74: 383-396

Gerlai R, Lee V, Blaser R (2006) Effects of acute and chronic ethanol exposure on the behavior of adult zebrafish (*Danio rerio*). Pharmacology Biochemistry and Behaviour 85: 752-761

Hidaka H, Ishiko T, Furuhashi T, Kamohara H, Suzuki S, Miyazaki M, Ikeda O, Mita S, Setoguchi T, Ogawa M (2002) Curcumin inhibits interleukin 8 production and enhances interleukin 8 receptor expression on the cell surface - Impact on human pancreatic carcinoma cell growth by autocrine regulation. Cancer 95: 1206-1214

Hoehle SI, Pfeiffer E, Solyom AM, Metzler M (2006) Metabolism of curcuminoids in tissue slices and subcellular fractions from rat liver. Journal of Agricultural and Food Chemistry 54: 756-764

Ireson C, Orr S, Jones DJL, Verschoyle R, Lim CK, Luo JL, Howells L, Plummer S, Jukes R, Williams M, Steward WP, Gescher A (2001) Characterization of metabolites of the chemopreventive agent curcumin in human and rat hepatocytes and in the rat in vivo, and evaluation of their ability to inhibit phorbol ester-induced prostaglandin E-2 production. Cancer Research 61: 1058-1064

Jagetia GC, Aggarwal BB (2007) "Spicing Up" of the Immume System by Curcumin. Journal of Clinical Immunology 27: 19-35

Jayaprakasha GK, Jaganmohan Rao I, Sakariah KK (2006) Antioxidant activities of curcumin, demethoxycurcumin and bisemethoxycurcumin. Food Chemistry 98: 720-724

Johnson JJ, Mukhtar H (2007) Curcumin for chemoprevention of colon cancer. Cancer Letters 255: 170-181

Johnston IA, Ward PS, Goldspink G (1975) Studies on the swimming musculature of the rainbow trout. Journal of Fish Biology 7: 451-458

Maheshwari RK, Singh AK, Gaddipati J, Srimal RC (2006) Multiple biological activities of curcumin: A short review. Life Sciences 78: 2081-2087

Okunieff P, Xu JH, Hu DP, Liu, WM, Zhang LR, Morrow G, Pentland A, Ryan JL, Ding I (2006) Curcumin protects against radiation-induced acute and chronic cutaneous toxicity in mice and decreases mRNA expression of inflammatory and fibrogenic cytokines. International Journal of Radiation Oncology Biology Physics 65: 890-898

Pan MH, Huang TM, Lin JK (1999) Biotransformation of curcumin through reduction and glucurondation in mice. Drug Metabolism and Disposition 27 486-494

Perkins S, Verschoyle RD, Hill K, Parveen I, Threadgill MD, Sharma RA, Williams ML, Steward WP, Gescher AJ (2002) Chemopreventive efficacy and pharmacokinetics of curcumin in the Min/+ mouse, a model of familial adenomatous polyposis. Cancer Epidemiology Biomarkers & Prevention 11: 535-540

Pfeiffer E, Hoehle SI, Walch SG, Riess A, Solyom AM, Metzler M (2007) Curcuminoids form reactive glucuronides in vitro. Journal of Agricultural and Food Chemistry 55: 538-544

Portes E, Gardrat C, Castellan A (2007) A comparative study on the antioxidant properties of tetrahydrocurcuminoids and curcuminoids. Tetrahedron 63: 9092-9099

Rao CV, Rivenson A, Simi B, Reddy BS, (1995) Chemoprevention of colon carcinogenesis by dietary curcumin, a naturally-occuring plant phenolic compound. Cancer Research 55: 259-266

Shankar TNB, Shanta NV, HP, Ramesh HP, Murthy IAS, Murthy VS (1980) Toxicity studies on turmeric Curcuma longa: acute toxicity studies in rats, guinea pigs and monkeys. Indian Journal of Physiological Pharmacology 18: 73-75

Sharma RA, Gescher AJ, Steward WP (2005) Curcumin: The story so far. European Journal of Cancer 41: 1955-1968

Shishodia S, Chaturvedi MM, Aggarwal BB (2007) Role of curcumin in cancer therapy. Current Problems in Cancer 31: 243-305

Shoskes DA (1998) Effect of bioflavonoids quercetin and curcumin on ischemic renal injury - A new class of renoprotective agents. Transplantation 66: 147-152

Soni KB, Kuttan R (1992) Effect of oral curcumin administration on serum peroxides and cholesterol levels in human volunteers. Indian Journal of Physiological Pharmacology 36: 273-275

Toda S, Miyase T, Arichi H, Tanizawa H, Takino Y (1985) Natural antioxidants III. Antioxidative components isolated from rhizome *Curcuma longa L.* Chemical and Pharmaceutical Bulletin 33: 1725-1728

Wang F, Wu X, Wang F, Liu S, Jia Z, Yang J (2006) The sensitive fluorimetric method for the determination of curcumin using the enhancement of mixed micelle. Journal of Fluorescence 16: 53-59

# Chapter 5 The effects of curcuminoids on the short term post mortem metabolism of white muscle in juvenile snapper (*Pagrus auratus*)

## 5.1 Abstract

Anesthetised snapper were exposed to a seawater bath containing curcuminoids, eluted from an ethanolic turmeric solution, for 60 min prior to harvest. Treated and non treated fish (control) were stored whole at half acclimation temperature ($8^{o}$C) for 36 h. There was no difference in the short term metabolic rundown, assessed by white muscle cut surface pH and adenosine triphosphate (ATP) rundown and white muscle lactate accumulation, between the turmeric fish treated fish and the control fish. Using digital image analysis, the characteristic yellow staining of the turmeric accumulated in the plasma and white muscle was shown to be depleted within 8 h and within 12 h in the red muscle, suggesting that curcuminoids were metabolised *in situ* into metabolites undetectable at the set excitation and emission wavelengths used. A longer term storage trial is recommended to assess the antioxidant potential of the curcuminoids.

## 5.2 Introduction

We have shown that curcumin and its derivative curcuminoids found in the spice turmeric rapidly diffuse across the gill, accumulating in the plasma and white and red muscle of snapper. As discussed in the previous chapter, curcumin and the curcuminoids have been widely researched and have been shown to have many beneficial properties, including strong antioxidant activity. Toda et al. (1985) showed curcumin to have similar antioxidant properties to that of vitamin E and C. It is possible that the curcuminoids bioaccumulated in the tissue may have post harvest beneficial effects during storage.

There have been many research trials focusing on the use of natural additives, especially naturally occurring antioxidants, to improve the preservation of fish tissue in storage. The two most common ways of adding a natural preservative to fish tissue are: as a dietary supplement prior to the fish being harvested, or as a topical application to the fillet or mince post mortem. Of the many different naturally occurring antioxidants that have been tested, vitamin E and tea polyphenols are two that have been widely researched for use in the preservation of fish tissue. α-tocopheryl acetate (a stable ester of vitamin E) is a strong natural antioxidant and has been shown to reduce lipid peroxidation in many species of fish after dietary supplementation (Tocher et al. 2002, Huang and Huang 2004, Zhang et al. 2007). Green tea polyphenols (TP) have been shown to have potent antibacterial and antioxidant properties. A TP dip treatment has been used on several species of fish and has been successful in reducing lipid peroxidation and extending fillet shelf life (Banergee 2006, Alghazeer et al. 2008, Fan et al. 2008).

The research trials on fish storage and preservation with naturally occurring antioxidants have been focused on reducing lipid oxidation during long term storage. Little is known on the effects of antioxidants in reducing the rate of metabolic rundown and improving the short term viability of fish tissue. In this

chapter we focus on the potential of the curcuminoids to improve the short term metabolic viability of post mortem white muscle.

Delivery of an antioxidant to fish tissue by using direct uptake, via the gills, and the fish's own circulatory system to deliver the antioxidant to the tissue has many advantages over dietary supplementation and post mortem topical application. As we have discussed previously (Chapter 4), dietary uptake of curcumin in mammals is poor. Direct uptake into the living animal ensures the antioxidant is perfused throughout the fillet and not just applied to the surface, as with topical application. It also offers the potential of a one-off treatment prior to harvest, rather than as series of dietary supplements. For example, Sohn et al. (2007) bled and perfused kingfish with 6-hydroxy-2,5,7,8-tetramethylchroman-2-carboxylic acid (Trolox®). They found that the perfused fish had delayed lipid oxidation in the post mortem tissue compared with just bled and un-bled fish.

# 5.3 Methods

## 5.3.1 Experimental fish

### 5.3.1.1 Snapper

The same cohort of snapper was used, and treated in a similar way prior to the experimental trial, as in the previous experiments.

## 5.3.2 Experimental methodology and trails

### 5.3.2.1 Non-turmeric snapper

40 snapper were held in a 1000L tank at 16$^{o}$C and were fasted for 2 days prior to experimentation. 15 mg.L$^{-1}$ AQUI-S$^{TM}$ was added to the sea water. The anesthetised fish were removed and killed by iki jime after 60 min. Fish were stored at 8$^{o}$C (half acclimation temperature) for the duration of the post harvest trial (36 h). 5 fish were sampled at times 0 h, 2 h, 4 h, 8 h, 12 h, 18 h, 24 h and 36 h. The length and weight of each fish was recorded and a condition index calculated. Blood was sampled by ventral heart puncture with a 1 ml syringe and a 25 gauge hypodermic needle. This was only possible over the first 12 hours. The blood was centrifuged for 5 min at 10 000 rpm (MSE Micro Centaur) and the plasma removed. The plasma was imaged using the digital image rig (Section 4.3.3.2). The fish was cut transversely at the anus and a white muscle D-block cut surface pH was recorded. A 10 mm muscle steak was removed from anterior to the anus and imaged. Approximately 1 g of D-block white muscle was removed from the muscle steak, freeze clamped under liquid nitrogen and stored at -80$^{o}$C until subsequent analysis for lactate and adenosine triphosphate (ATP) concentrations.

#### 5.3.2.2 Turmeric snapper

The experimental protocol for the turmeric treated snapper is the same as for non-turmeric snapper (Section 5.3.2.2), with the exception of 1.25 ml.$L^{-1}$ turmeric stock solution (Section 4.3.2.1) added to the seawater 5 min after the 15 mg.$L^{-1}$ AQUI-S$^{TM}$. The fish were exposed to the turmeric stock solution for 55 min.

#### 5.3.2.3 White muscle extraction

The frozen white muscle sample was placed in a mortar filled with liquid nitrogen and broken into smaller pieces with the pestle. ~0.1g of tissue was accurately weighed and the remaining tissue discarded. 0.5 ml of 0.6 M perchloric acid was added to the sample and ground to a powder under liquid nitrogen. The liquid nitrogen was allowed to evaporate and the powder transferred to a 1.5ml Eppendorf tube. The sample was homogenised for 30 seconds using an Ultra Turrax (IKA Labortechnik T8), followed by centrifugation for 5 min at 10 000 rpm. The supernatant was retained and used for the analysis of lactate and ATP.

#### 5.3.2.4 Lactate methodology

White muscle sample lactate was determined with a lactate meter (Accusport) set on plasma mode. Lactate standards were made using L-(+) Lactic acid 30% aqueous solution (Sigma) in 0.1M perchloric acid, neutralised with KOH. 20 µL of standard or sample was pipetted onto the lactate meter strip.

#### 3.3.2.5 ATP methodology

White muscle sample ATP concentrations were determined using an ATP Bioluminescence Assay Kit CLS 2 (Roche).

## 5.4 Results

### 5.4.1 Experimental trial

**Table 5.1 Experimental parameters for the turmeric exposure trial.**

| | Treatment | |
|---|---|---|
| | Control | Turmeric |
| Turmeric stock (ml) | 0 | 50 |
| Fish weight (g) | 80.3±2.1 | 68.3±1.6 |
| Length (mm) | 151±1.0 | 142±1.0 |
| N | 5 | 5 |
| Condition index ($w/l^3$) | 2.30±0.08 | 2.36±0.03 |

The turmeric colouration was visible in the plasma and white and red muscle of the turmeric exposed snapper. The plasma intensity was significantly higher in the turmeric exposed fish compared to the non-turmeric exposed fish at time 0 h, 2 h and 4 h (unpaired two-tailed Student's t-test, $P<0.05$). Within 8-12 hours storage the intensity of the turmeric colouration in the turmeric exposed fish in the plasma and white and red muscle decreased to a similar intensity to the unexposed fish (Figures 5.1, 5.2 and 5.3).

The white muscle intensity of the turmeric exposed fish at time 0 h (after 60 min exposure) was 50±2 intensity units and was significantly higher than that of the unexposed fish at times 0 h, 2 h and 4 h. From 8 h storage, the white muscle intensities in both the turmeric exposed and unexposed were very similar (Figure 5.2). Both turmeric treated and control fish showed a slight increase in reflectance from 12 h.

The red muscle intensity of the turmeric exposed fish at 0 h (after 60 min exposure) was 67±3 intensity units, significantly higher than that of the unexposed fish at 0-8 hours. From 12 h the red muscle intensities in both the turmeric

exposed and unexposed were very similar. The red muscle intensity in the unexposed fish increased from 0 h to ~5 intensity units peaking at 24 h at ~8 intensity units. The turmeric exposed fish white muscle showed a similar trend to that of the unexposed from 12 h (Figure 5.3).

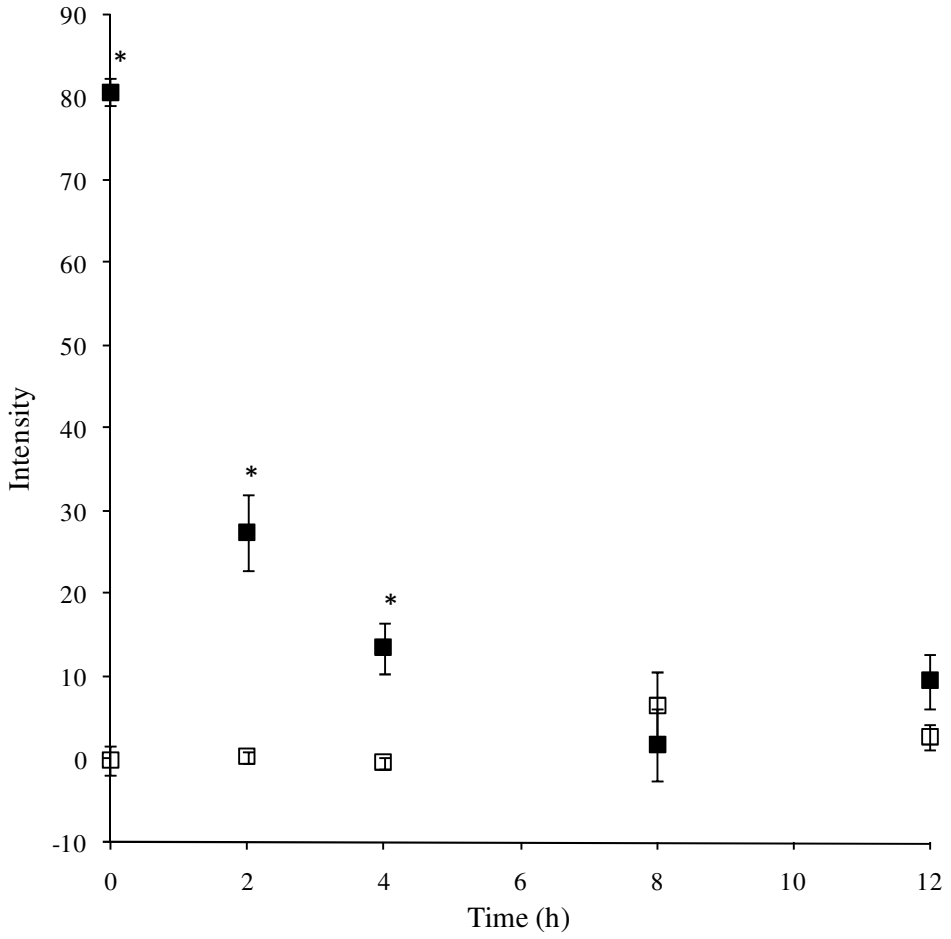


**Figure 5.1 Plasma colour intensity measured by digital image analysis from post-mortem snapper after a pre-mortem 60 min exposure to 15 mg.L$^{-1}$ AQUI-S™ with (black) and without (clear) 1.25 ml.L$^{-1}$ turmeric stock solution.** (N=5). Values are mean±sem. * denotes a significant difference between treatments (unpaired two-tailed Student's t-test, P<0.05).

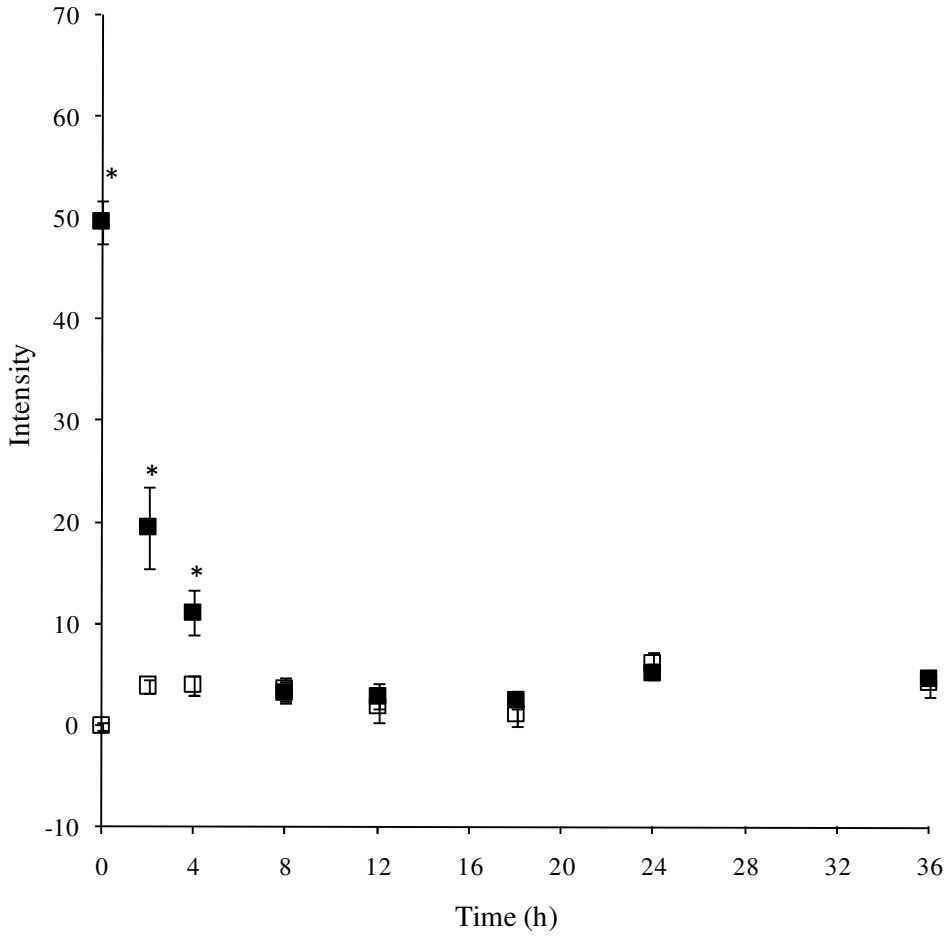


**Figure 5.2 White muscle D-block colour intensity measured by digital image analysis from post-mortem snapper after a pre-mortem 60 min exposure to 15 mg.L$^{-1}$ AQUI-S$^{TM}$ with (black) and without (clear) 1.25 ml.L$^{-1}$ turmeric stock solution.** (N=5). Values are mean±sem. * denotes a significant difference between treatments (unpaired two-tailed Student's t-test, $P<0.05$).

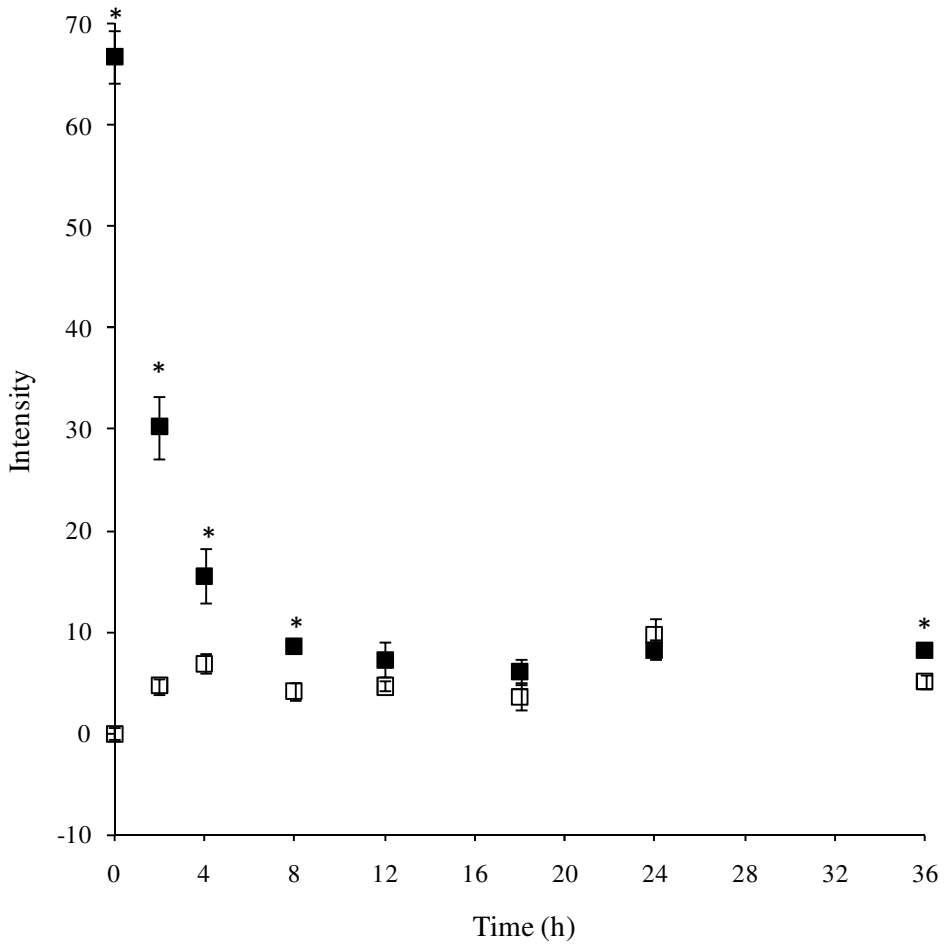


**Figure 5.3 Red muscle D-block colour intensity measured by digital image analysis from post-mortem snapper after a pre-mortem 60 min exposure to 15 mg.L$^{-1}$ AQUI-S$^{TM}$ with (black) and without (clear) 1.25 ml.L$^{-1}$ turmeric stock solution.** (N=5). Values are mean±sem. * denotes a significant difference between treatments (unpaired two-tailed Student's t-test, $P<0.05$).

Figure 5.4 shows the white muscle cut surface pH over time from both the turmeric exposed and unexposed treatments. Initial cut surface ph was ~7.8 for both the turmeric exposed and unexposed fish. The decrease in pH was similar in both treatments except at 12 h where the turmeric exposed treatment had a significantly higher flesh pH (7.33±0.02) than the unexposed treatment (7.23±.03). The pH decreased to ~6.6 in both treatments.

The initial white muscle lactate concentration in both the turmeric exposed and unexposed treatments was ~15µmol.g$^{-1}$ (Figure 5.5). Lactate increased over the duration of the storage reaching a plateau at 24 h at ~83µmol.g$^{-1}$, which was similar in both treatments. At time 12 h the lactate in the turmeric exposed treatment (40.5±0.8 µmol.g$^{-1}$) was significantly higher than that in the unexposed treatment (34.4±1.8 µmol.g$^{-1}$), (Figure 5.5), which is surprising given that cut surface pH was higher in the turmeric treated fish at this time.

There was no significant difference in the white muscle ATP concentration between treatments at any sample time (Figure 5.6). Initial ATP concentrations were ~8-8.5 µmol.g$^{-1}$ and decreased to ~0 µmol.g$^{-1}$ by the 36 h sampling point. ATP was maintained at a level of 6-8 µmol.g$^{-1}$ for ~12 hours before decreasing rapidly over the following 12 h to reach a concentration of ~1 µmol.g$^{-1}$ at 24 h.

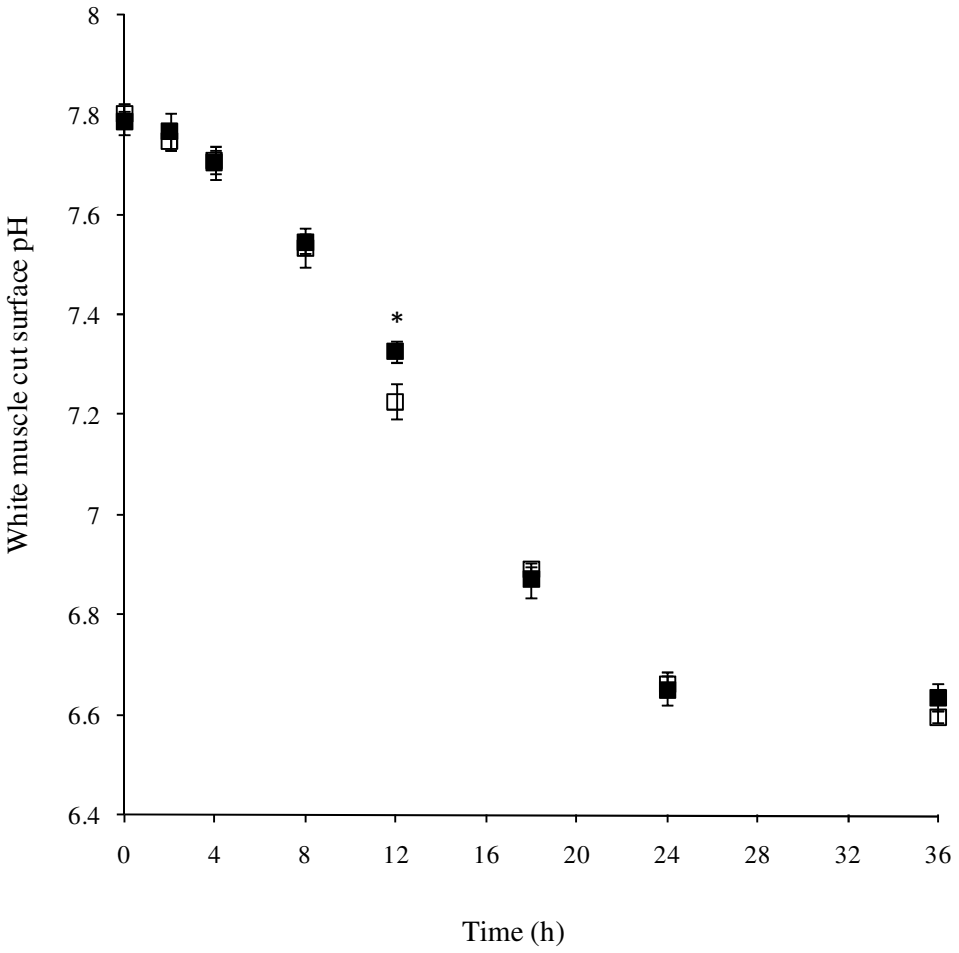


**Figure 5.4 White muscle cut surface pH from post-mortem snapper after a pre-mortem 60 min exposure to 15 mg.L$^{-1}$ AQUI-S$^{TM}$ with (black) and without (clear) 1.25 ml.L$^{-1}$ turmeric stock solution.** (N=5). Values are mean±sem. * denotes a significant difference between treatments (unpaired two-tailed Student's t-test, P<0.05).

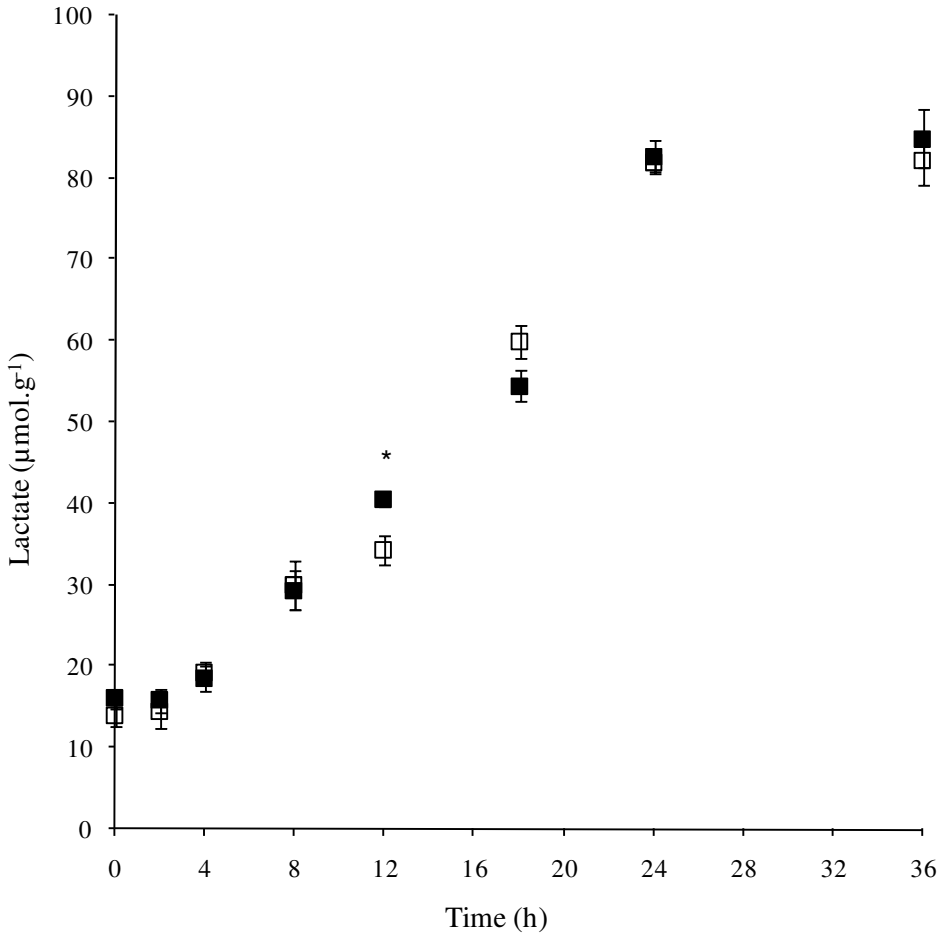


**Figure 5.5 Lactate concentration (µmol.g$^{-1}$) from post-mortem snapper white muscle after a pre-mortem 60 min exposure to 15 mg.L$^{-1}$ AQUI-S$^{TM}$ with (black) and without (clear) 1.25 ml.L$^{-1}$ turmeric stock solution.** (N=5). Values are mean±sem. * denotes a significant difference between treatments (unpaired two-tailed Student's t-test, P<0.05).

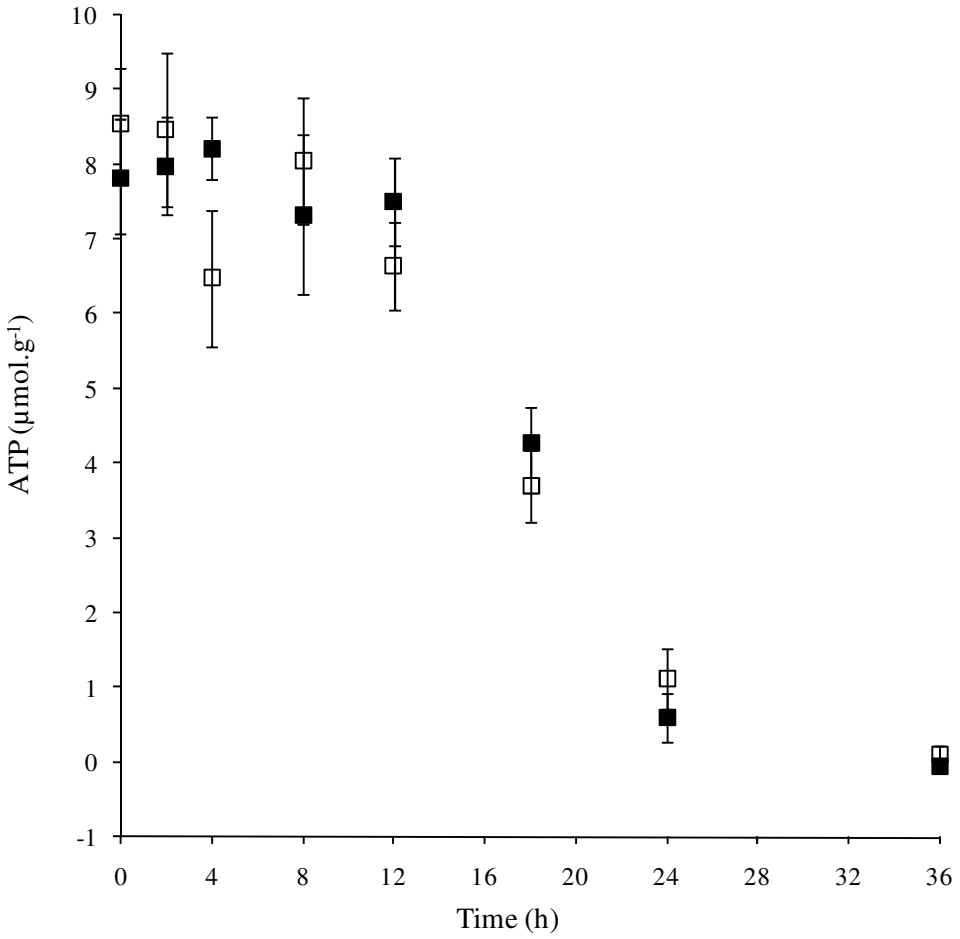


**Figure 5.6 ATP concentration (µmol.g$^{-1}$) from post-mortem snapper white muscle after a pre-mortem 60 min exposure to 15 mg.L$^{-1}$ AQUI-S$^{TM}$ with (black) and without (clear) 1.25 ml.L$^{-1}$ turmeric stock solution.** (N=5). Values are mean±sem.

White muscle cut surface pH is inversely correlated to lactate concentration (linear regression, $P<0.001$) (Figure 5.7) The lower the white muscle cut surface pH, the greater the white muscle lactate concentration.

There is also a significant positive relationship (linear regression, $P<0.001$) between white muscle cut surface pH and white muscle ATP concentration (Figure 5.8) The greater the white muscle cut surface pH, the greater the white muscle ATP concentration.

Figure 5.9 shows the significant linear regression ($P<0.001$) between white muscle ATP and lactate concentration. The greater the ATP concentration, the lower the lactate concentration.

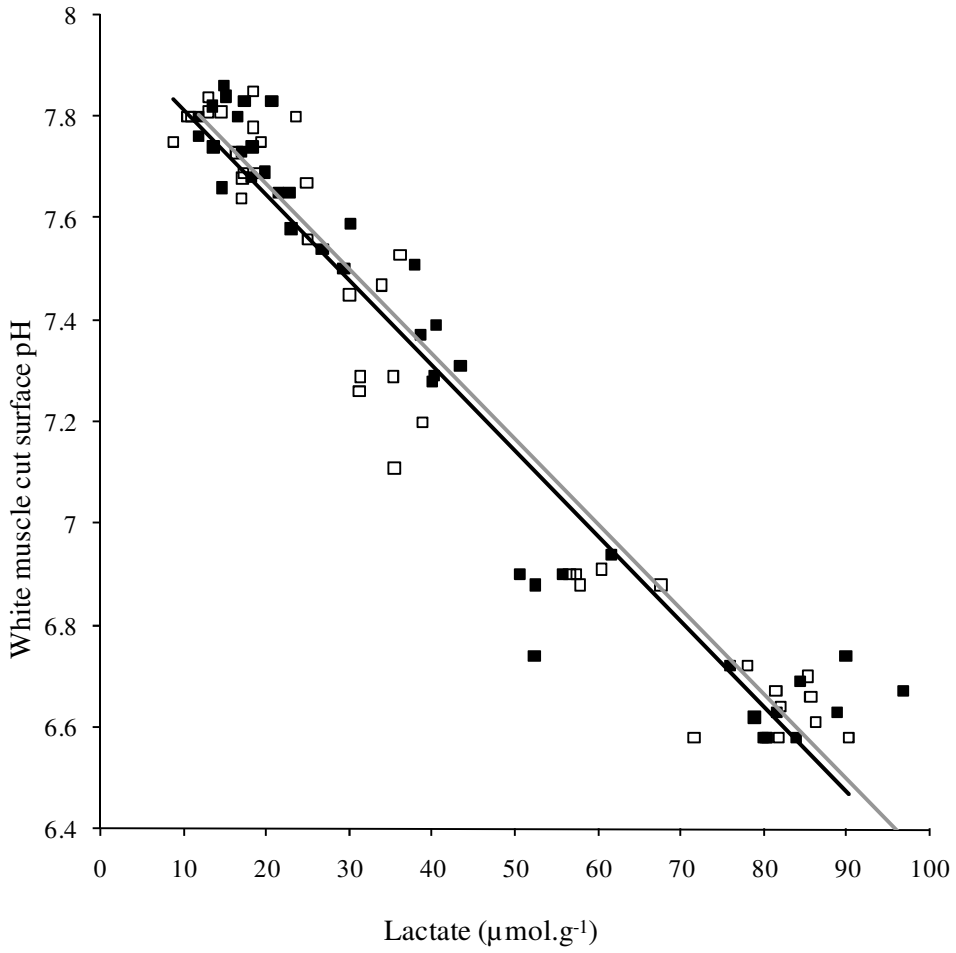


**Figure 5.7 Lactate concentration (µmol.g$^{-1}$) and white muscle cut surface pH from post-mortem snapper white muscle after a pre-mortem 60 min exposure to 15 mg.L$^{-1}$ AQUI-S$^{TM}$ with (black) and without (clear) 1.25 ml.L$^{-1}$ turmeric stock solution.** Linear best fit trendline and $r^2$ values are without turmeric (black, 0.95) and with turmeric (grey, 0.94). (N=5).

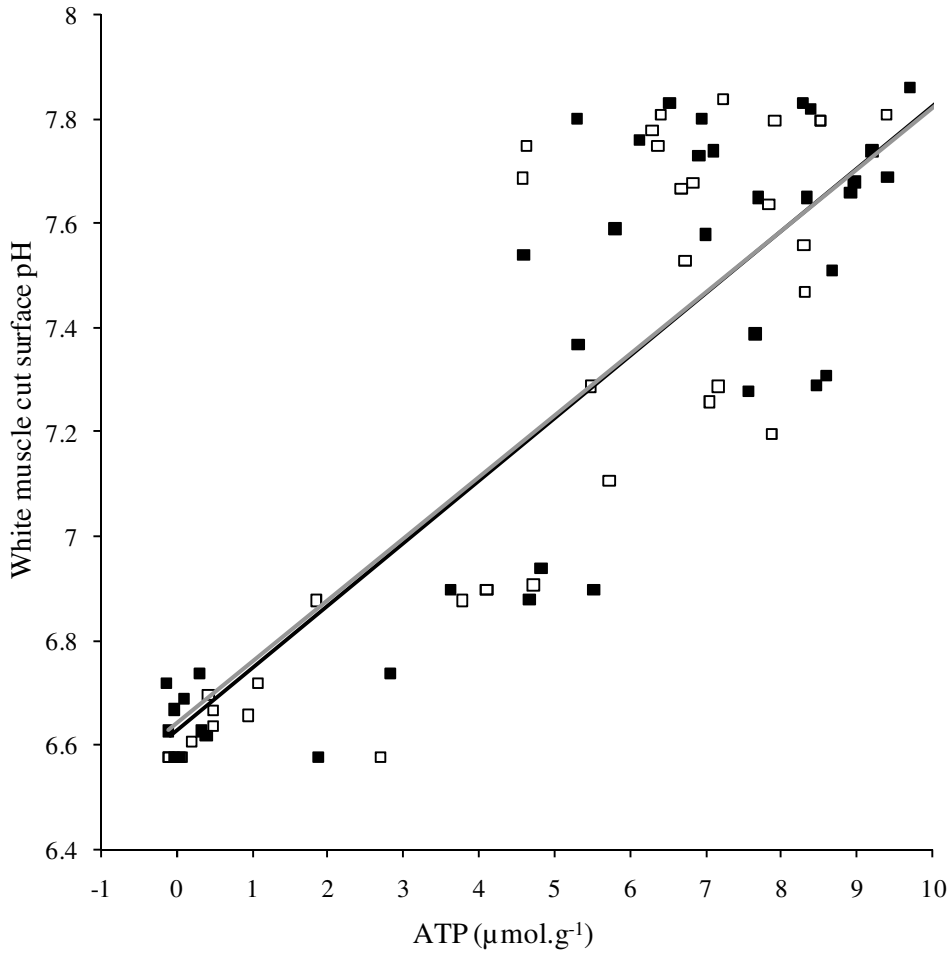


**Figure 5.8 ATP concentration (µmol.g$^{-1}$) and cut surface pH from post-mortem snapper white muscle after a pre-mortem 60 min exposure to 15 mg.L$^{-1}$ AQUI-S™ with (black) and without (clear) 1.25 ml.L$^{-1}$ turmeric stock solution.** (N=5). Linear best fit trendline and $r^2$ values are without (black, 0.73), and with turmeric (grey, 0.75).

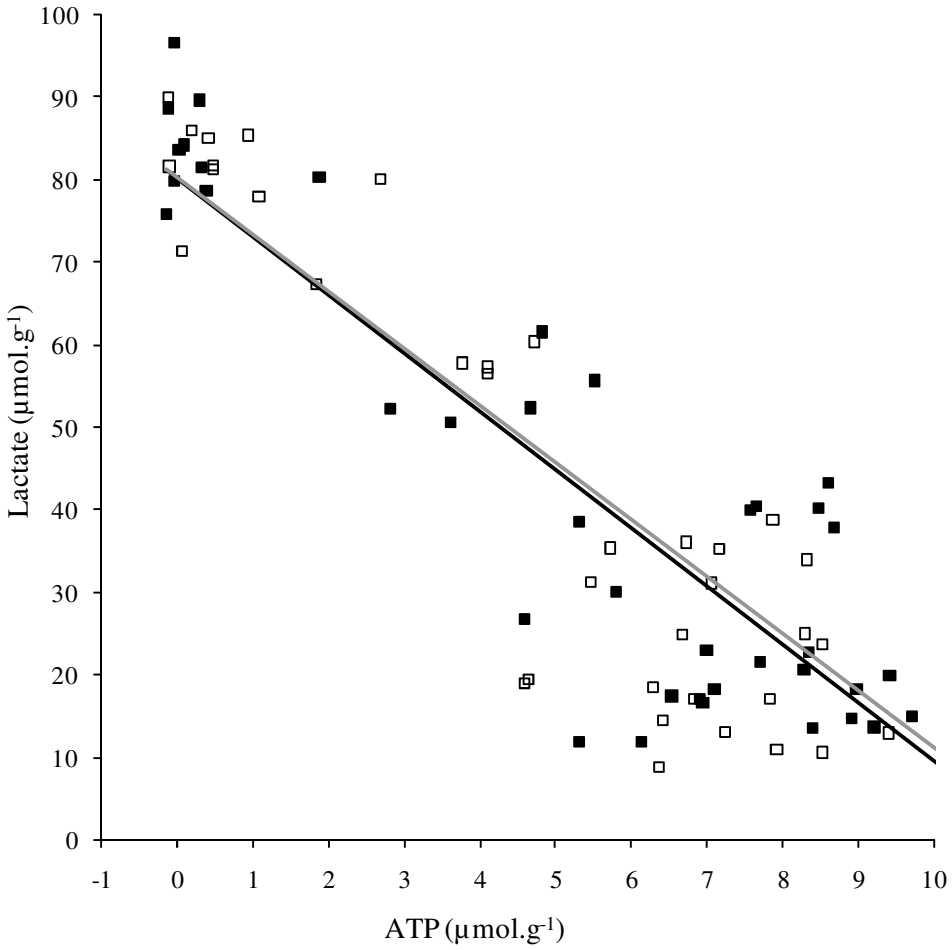


**Figure 5.9 ATP and lactate concentration (µmol.g$^{-1}$) from post-mortem snapper white muscle after a pre-mortem 60 min exposure to 15 mg.L$^{-1}$ AQUI-S$^{TM}$ with (black) and without (clear) 1.25 ml.L$^{-1}$ turmeric stock solution.** Linear best fit trendline and $r^2$ values are without (black, 0.77) and with turmeric (grey, 0.77). (N=5).

## 5.5 Discussion

There was no difference in the white muscle short term metabolic rundown between the turmeric exposed and unexposed snapper. The measured cut surface pH (Figure 5.4) and ATP (Figure 5.6) run down, and lactate accumulation (Figure 5.5) were very similar in both treatments. Muscle cut surface pH, lactate and ATP concentrations are three parameters that can be used to assess the metabolic rundown of fish tissue during short-term storage. Cut surface pH correlates very well with both ATP (Figure 5.7) and lactate (Figure 5.8) concentration, demonstrating its utility to predict the viability and metabolic status of the muscle (Jerrett et al. 1996, Nakayama et al. 1996, Jerrett et al. 2000). However, it is still possible that turmeric will have beneficial long term storage potential due to the strong antioxidant activities of curcumin and the curcuminoids (Pulla Reddy and Lokesha 1994, Masuda et al. 2001, Deng et al. 2006). As discussed in a previous chapter, turmeric has been shown to reduce oxidation during storage in pickle products. As enzymes are proteins, protein oxidation might be expected to have a greater effect on metabolic rundown.

The colour intensity of the plasma (Figure 5.1), white (Figure 5.2) and red (Figure 5.3) muscle in the turmeric exposed fish decreased to values similar to that of the unexposed fish within ~8 hours. The decrease in colour intensity suggests that the curcuminoids are either being bio-transformed or metabolised in situ into molecules that we were not able to detect with our set excitation and emission wavelengths (or the molecules are non-fluorescent), or are being transported out of the muscle and plasma into other tissues such as the liver, where they are metabolised (refer to chapter 4.5).

It was possible to draw blood samples at up to 12 h post-killing, which suggests limited circulation might be maintained. The teleost heart from a fish killed with rested harvesting can continue to beat for a long period of time, circulating blood through the tissues. It is possible that curcumin from the white muscle could have

been transported to other tissues (such as the liver) within the first 12 h. A more likely explanation for the disappearance of the colour is that the curcuminoids were metabolised, in situ, into metabolites that were undetected at our excitation and emission wavelengths.

The red and white muscle in both the turmeric exposed and unexposed fish showed a small increase in the measured colour intensity from 18 h to 24 h storage (Figure 5.2 and 5.3). This corresponds with the decrease in cut surface pH and ATP and an increase in lactate. As fish tissue breaks down it becomes less translucent and more opaque which may have had an effect on the measured colour intensity. The red muscle from the exposed fish at time 36 h had a measured colour intensity significantly greater than that of the unexposed fish. This difference may be sampling coincidence due to low sample size, but it is possible it could be due to reduced lipid oxidation in the lipid rich red muscle. Further work involving storage trials is required to determine this.

The contradictory result at 12 h post-harvest storage where the turmeric exposed fish had a significantly higher white muscle lactate (Figure 5.5) concentration but significantly lower white muscle cut surface pH (Figure 5.4) is inexplicable, except to suggest that it was an anomalous result or a statistical artefact.

The resting ATP and lactate concentrations in rested snapper white muscles were 8.5±0.8µmol.g$^{-1}$ ( Figure 5.6) and 13.9±1.2µmol.g$^{-1}$ (Figure 5.5) respectively, which are similar to previously published teleost white muscle ATP measurements of around 5-8µmol.g$^{-1}$ (Hochachka 1985). Black et al. (2002) measured resting snapper white muscle ATP at 9.3±1.4µmol.g$^{-1}$ and resting lactate at 16.5±2.4µmol.g$^{-1}$. Black et al. (2002) showed snapper white muscle lactate levels after storage in hyperoxic, normobaric conditions of ~70µmol.g$^{-1}$after 36 h and ~80µmol.g$^{-1}$ after 75 h at 10$^{o}$C (half acclimated). In our storage trial the lactate concentration in the white muscle was 82.0±1.5 after 24 h at 8$^{o}$C. The delay to maximum white muscle lactate in the work by Black et al. (2002) can be attributed

to the hyperoxic conditions the fillets were stored in, which would have promoted aerobic oxidative phosphorylation instead of anaerobic glycolysis, retarding the formation of lactate.

Curcuminoids did not have a positive (or negative) effect on the metabolic rundown of snapper muscle, but they may still prove beneficial in reducing lipid peroxidation in a long-term storage trial. The use of AQUI-S$^{TM}$ in the trial may have influenced the null result between the treated and non-treated fish as it has been shown to be a potent antioxidant (Rajakumar and Rao1993, Priyadarsini 1998, Ito et al. 2005).

## 5.6 References

Alghazeer R, Saeed S, Howell NK (2008) Aldehyde formation in frozen mackerel (*Scomber scombrus*) in the presence and absence of instant green tea. Food Chemistry 108: 801-810

Banerjee S (2006) Inhibition of mackerel (*Scomber scombrus*) muscle lipoxygenase by green tea polyphenols. Food Research International 39: 486-491

Black SE (2002) Extension of the pre-rigor period in ischemic white muscle from yellow-eye mullet (*Aldrichetta forsteri*) and New Zealand snapper (*Pagrus auratus*) as affected by hyperbaric oxygen treatment. Food Chemistry and Toxicology 69: 297-302

Deng S, Chen W, Zhou B, Yang L, Lui Z (2006) Protective effects of curcumin and its analogues against free radical-induced oxidative haemolysis of human red blood cells. Food Chemistry 98: 112-119

Fan WJ, Chi YL, Zhang S (2008) The use of a tea polyphenol dip to extend the shelf life of silver carp (*Hypophthalmicthys molitrix*) during storage in ice. Food Chemistry 108: 148-153

Hochachka PW (1985) Fuels and pathways as designed systems for support of muscle work. Journal of Experimental Biology 115: 149-164

Huang CH, Huang SL, (2004) Effect of dietary vitamin E on growth, tissue lipid peroxidation, and liver glutathione level of juvenile hybrid tilapia, *Oreochromis niloticus x O. aureus*, fed oxidized oil. Aquaculture 237: 381-389

Ito M, Murakami K, Yoshino M (2005) Antioxidant action of eugenol compounds: role of metal ion in the inhibition of lipid peroxidation. Food and Chemical Toxicology 43: 461-466

Jerrett AR, Law RA, Holland AJ, Cleaver SE, Ford SC (2000) Optimum post-mortem chilled storage temperature for summer and winter acclimated, rested, chinook salmon (*Oncorhynchus tshawytscha*) white muscle. Journal of Food Science 65: 750-755

Jerrett AR, Stevens J, Holland AJ (1996) Tensile properties of white muscle in rested and exhausted chinook salmon (*Oncorhynchus tshawtscha*). Journal of Food Science 61 527-532

Masuda T, Maekawa T, Hidaka K, Bando H, Takeda Y, Yamaguchi H (2001) Chemical studies on antioxidant mechanism of curcumin: Analysis of oxidative coupling products from curcumin and linoleate. Journal of Agricultural and Food Chemistry 49: 2539-2547

Nakayama T, Toyoda T, Ooi A (1996) Delay in rigor mortis of red sea-bream by spinal cord destruction. Fisheries Science 62: 478-482

Priyadarsini KI, Guha SN, Rao MNA (1998) Physio-chemical properties and antioxidant activities of methoxy phenols. Free Radical Biology and Medicine 24: 933-941

Pulla Reddy AC, Lokesh BR (1994) Effect of dietary turmeric (*Curcuma longa*) on iron-induced lipid peroxidation in the rat liver. Food and Chemical Toxicology 32: 279-283

Rajakumar DV, Rao MNA (1993) Dehydrozingerone and iso-eugenol as inhibitors of lipid-peroxidation and as free radical scavengers. Biochemical Pharmacology 46: 2067-2072

Sohn JH, Ushio H, Ishida N, Yamashita M, Terayama M, Ohshima T (2007) Effect of bleeding treatment and perfusion of yellowtail on lipid oxidation in post-mortem muscle. Food Chemistry 104: 962-970

Tocher DR, Mourente G, Van der Eecken A, Evjemo JO, Diaz E, Bell JG, Geurden I, Lavens P, Olsen Y (2002) Effects of dietary vitamin E on antioxidant defence mechanisms of juvenile turbot (*Scophthalmus maximus L.*), halibut (*Hippoglossus hippoglossus L.*) and sea bream (*Sparus aurata L.*). Aquaculture Nutrition 8: 195-207

Toda S, Miyase T, Arichi H, Tanizawa H, Takino Y (1985) Natural antioxidants III. Antioxidative copmonents isolated from rhizome *Curcuma longa L.* Chemical and Pharmaceutical Bulletin 33: 1725-1728

Zhang XD, Wu TX, Cai LS, Zhu YF (2007) Effects of alpha-tocopheryl acetate supplementation in preslaugter diet on antioxidant enzyme activities and fillet quality of commercial-size *Sparus macrcepalus*. Journal of Zhejiang University-Science B 8: 680-685

# Chapter 6 The effect of curcuminoids on lipid peroxidation in red and white muscle of juvenile snapper (*Pagrus auratus*) during an accelerated storage trial

## 6.1 Abstract

Snapper (*Pagrus auratus*) exposed to a turmeric treatment before harvest, and fish without exposure to a turmeric treatment (control fish), were stored at 14.2±0.4$^{o}$C for 4 days. Very little difference in lipid peroxidation was found in the white and red muscle over 4 days in the control and turmeric treated fish. However, the TBARS concentration in the turmeric treated red muscle at day 4 TBARS was significantly lower than in the control red muscle (Student's t-test). The potential benefits of turmeric as an antioxidant and the limitations of accelerated storage trials are discussed and a long-term frozen storage trial to assess the antioxidant properties of turmeric is recommended.

## 6.2 Introduction

As described in Chapter 5, we saw no difference in the short term metabolic rundown of white muscle between fish exposed to curcuminoids and those not exposed. In this chapter we investigate the antioxidant potential of curcuminoids by assessing their ability to reduce lipid peroxidation in red and white muscle during an accelerated storage trial.

Accelerated storage trials involve storing tissue samples at an elevated temperature to increase the rate of rancidity. They are often used to simulate long term frozen storage trials with the benefit of producing results in days instead of months and are often used in pilot studies to investigate whether a long-term frozen storage trial is warranted. However, caution has to be taken in comparing accelerated storage trails with long term frozen storage trials as the elevated temperature increases tissue autolytic spoilage and also accelerates the bacterial spoilage processes.

Tissue rancidity was assessed by the thiobarbituric acid reactive substances (TBARS) concentration in the white and red muscle. Tissue TBARS concentration is commonly used as an indicator of lipid peroxidation (Oakes and Van der Kraak 2003, Ross and Smith 2006, Rawdkuen 2008, Tuckey 2008). However, some literature suggests that TBARS concentration does not always correlate with sensory analysis (Hoyland and Taylor 1991).

AQUI-S$^{TM}$ has been the aquatic anaesthetic used successfully throughout this thesis to provide rested unstressed experimental fish. However, iso-eugenol is a strong antioxidant, in this part of the study the aquatic anaesthetic tricaine methanesulfonate (MS222) was used instead of AQUI-S$^{TM}$.

# 6.3 Methods

## 6.3.1 Experimental fish

### 6.3.1.1 Snapper

The same cohort of snapper was used, and treated in a similar way prior to the experimental trial, as in the previous experiments.

## 6.3.2 Experimental methodology and trial

### 6.3.2.1 Control snapper

30 snapper were held in a 1000L tank at 18.2$^{o}$C for 2 days unfed prior to experimentation. 15 mg.L$^{-1}$ MS222 was added to the sea water. The sedated fish were removed and killed by iki jime after 60 min. Fish were stored at 14.2±0.4$^{o}$C for the duration of the accelerated storage trial. 6 fish were sampled at days 0, 1, 2, 3 and 4. The length and weight of each fish was recorded and a condition index calculated.

### 6.3.2.2 Turmeric snapper

The experimental protocol for the turmeric treated snapper is the same as the non-turmeric snapper (section 6.3.2.2), with the exception of the addition of 1.25 ml.L$^{-1}$ turmeric stock solution (section 4.3.2.1) to the seawater 5 min after the MS222 was added

### 6.3.2.3 White and red muscle extraction

The right hand fillet was removed and approximately 1 g of white muscle was dissected from the D muscle block from a location about 10 mm posterior to the pectoral fin. The tissue was immediately freeze clamped under liquid nitrogen, wrapped in aluminium foil and stored at -80$^{o}$C until analysis. Red muscle was also removed at the same distance along the fish, and was processed and stored in the same way.

#### 6.3.2.4 TBARS analysis

The TBARS assay was performed by Nick Tuckey (School of Biological Sciences, Canterbury University, New Zealand), using methods that can be found in his PhD thesis (Tuckey 2008) and in Tuckey et al. (2009).

# 6.4 Results

## 6.4.1 Experimental trials

The ambient water temperature was 18.2°C and the storage temperature was 14.2±0.5°C. The turmeric treated fish were all visually assessed for turmeric uptake and all showed the characteristic yellow coloration.

**Table 6.1 Experimental parameters for the turmeric exposed snapper accelerated storage trial.** Data are mean±sem.

| | Treatment | |
|---|---|---|
| | Control | Turmeric |
| Fish weight (g) | 96±2 | 92±2 |
| Length (mm) | 160±1 | 159±1.0 |
| N | 30 | 30 |
| Condition index ($w/l^3$) | 2.35±0.02 | 2.29±0.02 |
| White muscle pH | 7.51±0.04 | 7.59±0.03 |

The TBARS concentration in the control white muscle at day 0 was significantly greater than the turmeric treatment (unpaired two-tailed Student's t-test, $P<0.05$). There was no significant change in TBARS concentration in control and turmeric treated white muscle over the 4 day duration of the storage trial (ANOVA) (Figure 6.1).

Figure 6.2 shows the TBARS concentration in the red muscle. An ANOVA within both the control and turmeric treatments was not significant. The TBARS concentration in the control red muscle (39.9±1.4 $nmol.g^{-1}$) at day 4 was significantly greater than the turmeric treatment (29.6±3.9 $nmol.g^{-1}$) (unpaired two-tailed Student's t-test, $P<0.05$). For the control treatment there was a non-significant trend of increasing TBARS concentrations in the red muscle from day 0 to day 4 (31.2±2.3 $nmol.g^{-1}$ and 39.9±1.4 $nmol.g^{-1}$ respectively), whereas the

TBARS concentration in the red muscle in the turmeric treatment remained at a similar concentration (day 0, 31.5±3.1 nmol.$g^{-1}$ and day 4, 29.9±3.6 nmol.$g^{-1}$).

There was approximately 3 times the TBARS concentration in the red muscle (Figure 6.1) than in the white muscle (Figure 6.1).

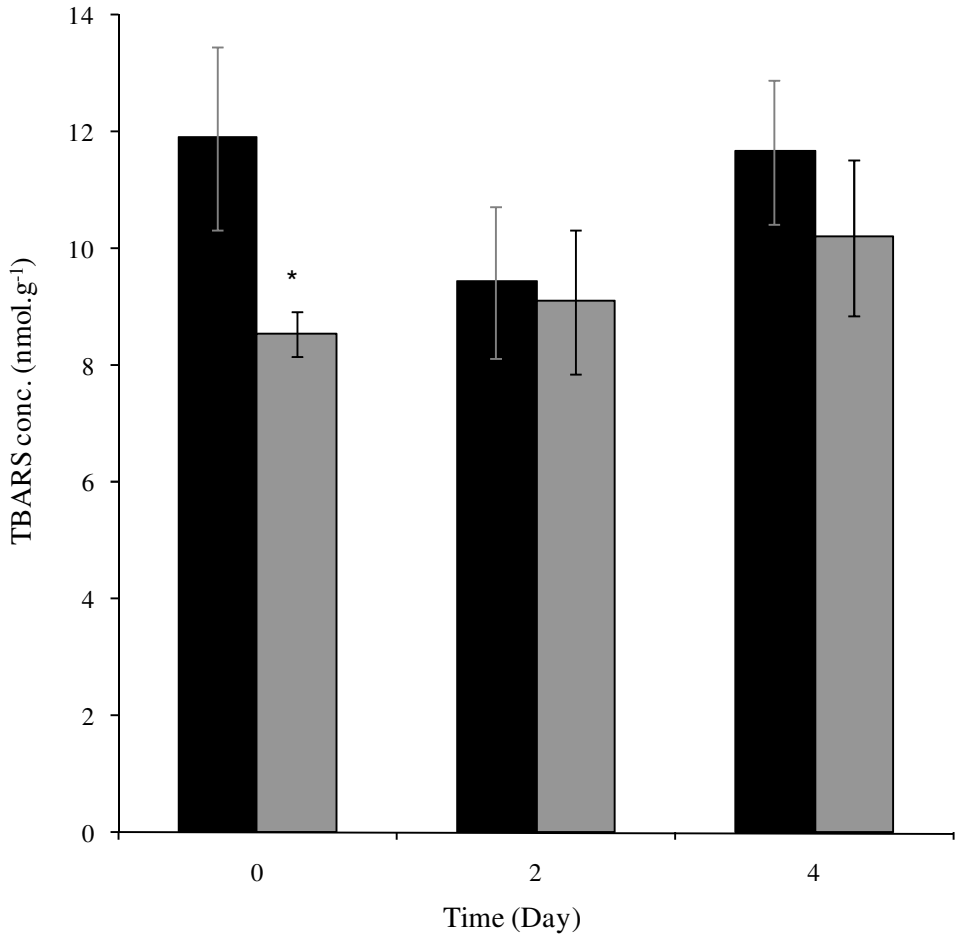


**Figure 6.1 Snapper white muscle TBARS concentration in the control (black) and turmeric treated (grey) fish.** * denotes a significant difference between treatments within days (unpaired two-tailed Student's t-test, $P<0.05$). Values are mean±sem. N=6.

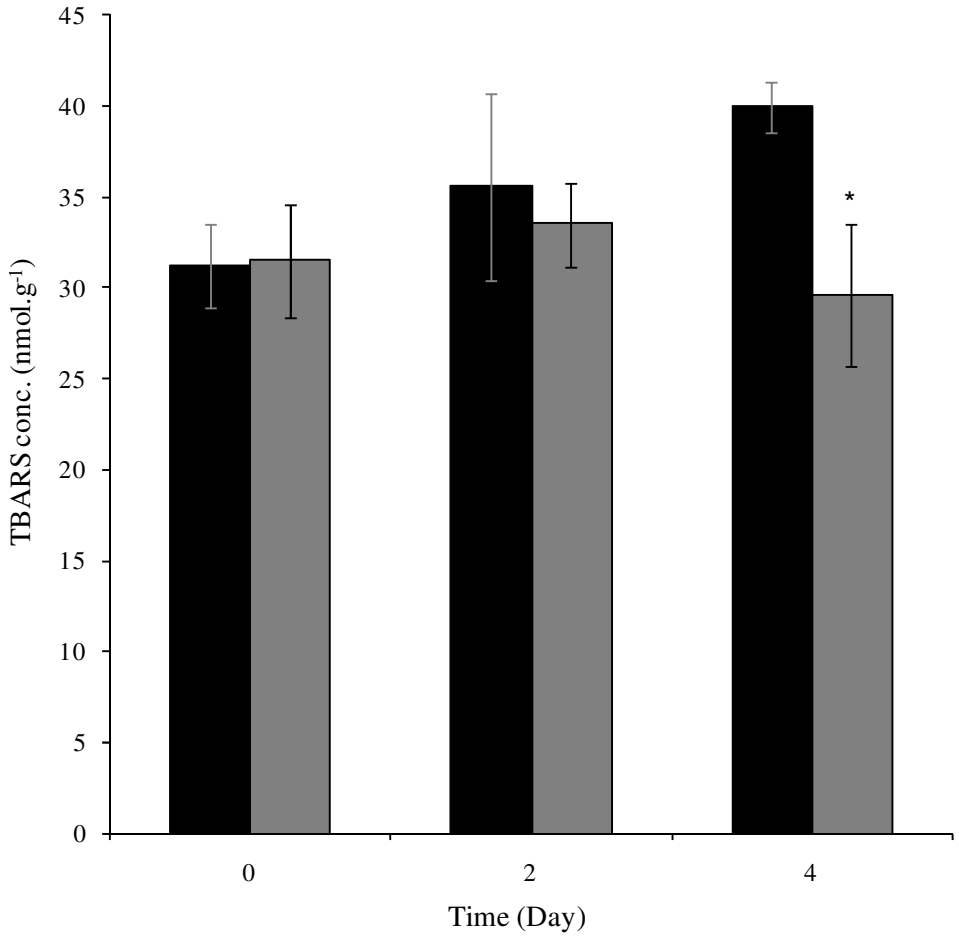


**Figure 6.2 Snapper red muscle TBARS concentration in the control (black) and turmeric treated (grey) fish.** * denotes a significant difference between treatments within days (unpaired two-tailed Student's t-test, $P<0.05$) Values are mean±sem. N=6.

## 6.5 Discussion

The accelerated storage trial showed that the delivery of curcuminoids to the fish prior to harvest may reduce lipid peroxidation in the red muscle (Figure 6.2). The TBARS results showed very little peroxidation in the white muscle (Figure 6.1) compared with the red muscle, which is probably due to the noticeably higher lipid content in the red muscle.

Proximate analysis of the fatty acid/lipid composition of fish tissue has been widely performed, with particular interest in commercial species. Vlieg (1985) showed that New Zealand snapper skinned fillets have an oil content of 1.6g.100g$^{-1}$ tissue, which is similar to the value of 1.9% wet weight described by Hughes et al. (1980). Snapper skinned fillets have a low lipid content compared with other New Zealand fish species such as tarakihi (*Cheilodactylus macropterus,* 3.9%), trevally (*Caranx georgianus,* 2.6%), and moki (*Latridopsis ciliaris,* 4.3%) (Hughes et al. 1980).

Although differences were slight, we noted that after day 4 the TBARS concentration in the red muscle control treatment was significantly higher than that in the turmeric treated red muscle, which suggests that antioxidant properties of the curcuminoids are reducing lipid peroxidation in the red muscle (Figure 6.2).

There was little TBARS formation in the white muscle over the trial period (Figure 6.1). The control white muscle showed significantly higher TBARS concentration than the curcuminoid treated white muscle at day 0, which is difficult to explain.

Tuckey (2008) showed initial TBARS concentration in salmon white muscle at around 20 nmol.g$^{-1}$ (twice that of our snapper values), and around 65 nmol.g$^{-1}$ in rancid tissue stored at a similar temperature to the snapper muscle. Storing salmon tissue at lower temperatures resulted in greater accumulated TBARS

concentrations (up to 120 nmol.g$^{-1}$). Initial salmon red muscle TBARS concentration was around 25-30 nmol.g$^{-1}$, (similar to our snapper values). It is difficult to draw comparisons with TBARS concentration between species with different muscle lipid composition, for the reasons mentioned previously.

The temperature of the storage trial may also play in important role in the TBARS concentrations observed. TBARS are not completely stable and break down in a reaction that, like most biological reactions, is temperature dependent. TBARS breakdown would be less of a problem in lipid rich tissue as production would be greater than breakdown. However, in lipid poor tissue (such as snapper white muscle) we may see TBARS production at a rate close to TBARS break down, resulting in little to no detectable TBARS formation. To reduce TBARS breakdown rates and allow TBARS to accumulate, a cooler storage temperature is required, as shown in the previous example from Tuckey (2008).

Accelerated storage trials at elevated temperatures offer an ideal environment for bacterial growth. Bacterial spoilage causing putrification may be more prolific than muscle autolysis spoilage. High bacteria loading may cause anaerobic conditions within the tissue as little oxygen is left to diffuse in and potentially causes oxidative damage. During a frozen storage trial, bacterial growth and oxygen consumption is low and we may see greater oxidative damage due to increased oxygen concentrations in the tissue. Physical sample size may also play an important role in storage trials. Whole fish were used, whereas fillets with a greater surface area and removal of the skin boundary layer would allow greater oxygen diffusion into the tissue.

We have shown that the curcuminoids can perfuse the white and red muscle of snapper very successfully (Chapter 4). We saw no difference in short term metabolic run down in fish treated with curcuminoids (Chapter 5). Our results are inconclusive as to the potential of the curcuminoids as an lipid antioxidant due to the limits of an accelerated trial, a long-term frozen storage trial is required to

clarify the antioxidant benefits of the curcuminoids. Curcumin has been shown to prevent hepatocyte lipid peroxidation in the climbing pearch (*Anabas testudineus*) (Manju et al. 2008).

By utilising uptake directly via the gills and delivery to the tissues by the fish's own circulatory system we potentially have an effective delivery method for supportive molecules (anti-biotics, anti-inflamatory, anti-oxidant etc.) in large scale aquaculture applications. Also required is a greater understanding of the perfusion parameters in the live fish in order to maximise delivery of supportive molecules.

## 6.6 References

Hoyland DV, Taylor AJ (1991) A review of the methodology of the 2-thiorbarbituric acid test. Food Chemistry 40: 271-291

Hughes JT, Czochanska Z, Pickston L, Hove EL (1980) The nutritional composition of some New Zealand marine fish and shellfish. New Zealand Journal of Science 23: 43-51

Manju M, Sherin TG, Rajeesha KN, Sreejith P, Rajasekharan KN, Oommen OV (2008) Curcumin and its derivatives prevent hepatocyte lipid peroxidation in Anabas testudineus. Journal of Fish Biology 73: 1701-1713

Oakes KD, Van der Kraak GJ (2003) Utility of the TBARS assay in detecting oxidative stress in white sucker (*Catostomus commersoni*) populations exposed to pulp mill effluent. Aquatic Toxicology 63: 447-463

Rawdkuen S, Jongjareonrak A, Benjakul S, Chaijan M (2008) Discoloration and lipid deterioration of farmed giant catfish (*Pangasianodon gigas*) muscle during refrigerated storage. Journal of Food Science 73: C179-C184

Ross CF, Smith DM (2006) Use of volatiles as indicators of lipid oxidation in muscle foods. Comprehensive Reviews in Food Science and Food Safety 5: 18-25

Tuckey NPL (2008) Technologies for tissue preservation: The role of endogenous and exogenous antioxidants in preserving tissue function in Chinook salmon, *Oncorhynchus tshawytscha*. PhD Thesis. University of Canterbury, Christchurch

Tuckey NPL, Forster ME, Gieseg SP (2009) Lipid oxidation is inhibited by idoeugenol exposure in Chinook salmon (*Oncorhynchus tshawytscha*) fillets during storage at 15C. Journal of Food Science *in press*.

Vlieg P (1985) Proximate analysis of commercial New Zealand fish species - 3. New Zealand Journal of Technology 1: 181-185

# Chapter 7 The effects of progressive hypoxia and re-oxygenation on cardiac function and white muscle perfusion in the anaesthetised snapper (*Pagrus auratus*)

## 7.1 Abstract

The effects of progressive hypoxia and re-oxygenation on cardiac function and white muscle perfusion and haemoglobin saturation were investigated in anaesthetised snapper (*Pagrus auratus*). White muscle perfusion and haemoglobin saturation were recorded in real time using fibre optic methodology and a knowledge of the haemoglobin absorption spectra. Snapper exhibited a mild hypoxic bradycardia response when the water bath dissolved oxygen (DO) concentration decreased below 6.1±0.1 $mg.L^{-1}$. However, deep bradycardia was evoked when the water bath DO concentration decreased below 1.5±0.1 $mg.L^{-1}$. Cardiac function also decreased rapidly beyond 1.5±0.1 $mg.L^{-1}$ DO with noticeable arrhythmias suggesting hypoxia had direct and severe effects on the cardiac myocytes. Perfusion to the white muscle decreased below 3.3±0.1 $mg.L^{-1}$ DO concentration. Haemoglobin saturation in the white muscle decreased below 2.4±0.1 $mg.L^{-1}$ DO concentration. During re-oxygenation, heart rate and white muscle perfusion increased from 1.9±0.1 $mg.L^{-1}$ DO concentration, whereas haemoglobin saturation increased from 2.9±0.1 $mg.L^{-1}$ DO concentration. A feed-forward mechanism controlling perfusion in the white muscle is suggested rather than localised receptor control, as white muscle perfusion changed prior to any change in white muscle haemoglobin saturation. Cardiac function was closely correlated with white muscle perfusion, but it is suggested that the primary factor determining white muscle perfusion in the anaesthetised snapper during hypoxia and re-oxygenation is changes in arterial pressure (not measured in this research), and its effects on capillary recruitment and de-recruitment. The control of cardiac function and white muscle perfusion in an anaesthetised preparation, and the

adaptive significance of reduced white muscle perfusion during hypoxia, are discussed.

## 7.2 Introduction

A greater understanding of perfusion in the white muscle of fish is needed in order to better predict and optimise the delivery of oxygen and other molecules. There is no published research to date that shows changing patterns of perfusion to the white muscle during hypoxia in real time. In this chapter we used fibre optics and an understanding of the haemoglobin absorption spectra to investigate perfusion and haemoglobin saturation simultaneously in white muscle, and also record an electrocardiogram (ECG) as an indicator of cardiac function during hypoxia.

Fish have evolved physiological survival mechanisms to tolerate exposure to hypoxia, although prolonged, deep exposure will inevitably result in death. Some species when exposed to hypoxic conditions will, if possible, move to areas with greater dissolved oxygen (Burleson et al. 2001), move to cooler temperatures to reduce their metabolic rate (Schurmann et al. 1991), or physiologically depress their metabolic rate over a period of hypoxia pre-conditioning (Nilsson and Renshaw 2004). If fish are unable to avoid hypoxia or depress their metabolic rate, they can maintain oxygen uptake by increasing gill ventilation rates (Smith and Jones 1981).

Hypoxia-induced bradycardia in teleosts is a reduction in heart rate in response to a decrease in oxygen concentration. Conversely, mammals exhibit tachycardia under hypoxia. Farrell (2007) reviews the several supposed, direct benefits from hypoxia-induced bradycardia, including an increase in stroke volume which compensates for the reduced heart rate and maintains cardiac output. Bradycardia also increases the blood dwell time in the lumen of the heart, combined with the increased stroke volume that stretches the myocardium (thinning the cardiac muscle walls), which might reduce oxygen diffusion distances and assist the uptake of what little oxygen is available into the cardiac myocytes. A slower blood flow through the branchial circulation also benefits gas transfer, maximising the uptake of what oxygen is available (Randall and Smith 1967, Fritsche 1990).

As stated, cardiac output can be maintained during hypoxia because the observed reduction in heart rate is offset by an increasing stroke volume (Randall 1982). However, Stecyk and Farrell (2002) found that during prolonged severe hypoxia the common carp (*Cyprinus carpio*), an anoxia tolerant species, showed significant bradycardia with a reduced cardiac output which was independent of acclimation temperature.

Most vascular beds show vasodilation in response to hypoxia (Russell et al. 2008) and the vasodilation of cerebral arteries (Pearce 1995) should maintain oxygen supply to the brain. There is some literature describing the blood flow distribution to the various tissues during exercise (Neumann et al. 1983, Kolok et al. 1993), but very little on blood flow redistribution during hypoxia. Cameron (1975) showed no significant difference in the blood flow distribution to any tissues in the Arctic grayling (*Thymallus arcticus*) during exposure to hypoxia for 60 min.

Haemoglobin saturation (Farrell and Clutterham 2003, McKenzie et al. 2004) and white muscle perfusion can be measured in living animals with fibre optics. White muscle is illuminated with a blue and green LED light source via a fibre optic cable. Another fibre optic cable, inserted approximately 5mm deeper than the illuminating optode, records the intensity of blue green light that is transmitted through a ~5mm sample of white muscle. The blue and green LED light source is used as it corresponds with several key wavelengths on the haemoglobin absorption spectra (Figure 7.1).

At wavelength 530 nm the molar extinction coefficient of oxy-haemoglobin and deoxy-haemoglobin is the same, which means that both haemoglobin states will absorb light at wavelength 530 nm at the same rate (Figure 7.1). A change in the recorded light intensity at 530 nm is due to the overall amount of haemoglobin (either oxy-haemoglobin or deoxy-haemoglobin) in the white muscle sample between the light optode and the recording optode. If white muscle perfusion

increases, resulting in a greater haemoglobin concentration in the white muscle sample, we will expect to see a reduction in the light transmitted, shown as a decrease in the recorded light intensity at 530 nm. However, if perfusion decreases, reducing the overall amount of haemoglobin delivered to the white muscle sample, we will expect to see an increase in the amount of light transmitted.

At wavelength 466 nm, the molar extinction co-efficient of oxy-haemoglobin is greater than that of deoxy-haemoglobin. Oxy-haemoglobin absorbs more 466 nm light than deoxy-haemoglobin (Figure 7.1). If perfusion and the overall haemoglobin concentration in the white muscle sample remains constant then a change in the recorded intensity of light transmitted at wavelength 466 nm is due to a change in the oxygen saturation of haemoglobin. A decrease in haemoglobin saturation (oxy-haemoglobin to deoxy-haemoglobin, a down shift in the molar extinction coefficient at 466 nm), would result in an increase in the intensity of 466 nm light transmitted through the white muscle sample. Conversely an increase in haemoglobin saturation would result in a decrease in 466 nm light transmitted through the white muscle sample.

At wavelength 516 nm the molar extinction of oxy-haemoglobin is less than that of deoxy-haemoglobin. Oxy-haemoglobin absorbs less 516 nm light than deoxy-haemoglobin (Figure 7.1). The same theory applies to wavelength 516 nm as to 466 nm, but the relationship is inverted. A decrease in haemoglobin saturation would result in a decrease in 516 nm light transmitted through the white muscle sample, shown as a decrease in the recorded 516 nm light intensity, and vice versa.

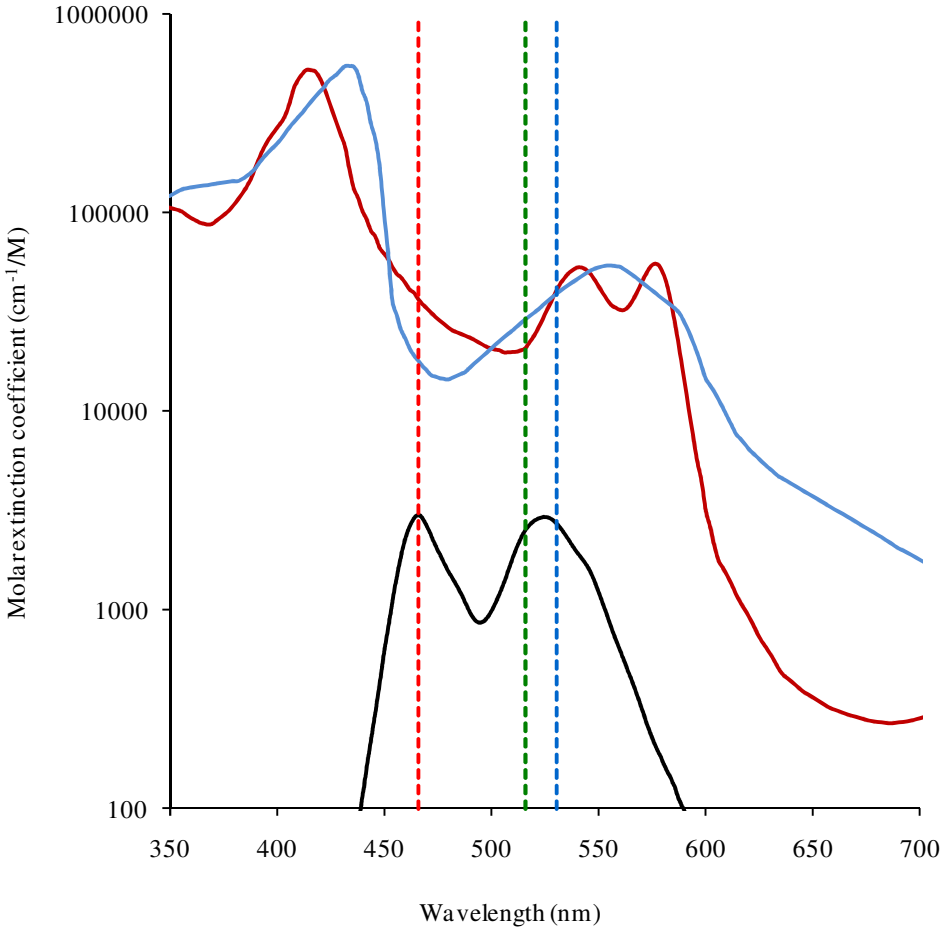


**Figure 7.1 Absorption spectra for oxy-haemoglobin (solid red) and deoxy-haemoglobin (solid blue).** Below the haemoglobin absorption spectra is the blue and green LED profile (solid black) and the recorded wavelengths; 466 nm (dashed red), 516 nm (dashed green) and 530 nm (dashed blue – the isobestic point). Figure sourced from Prahl (1999).

# 7.3 Methods

## 7.3.1 Experimental fish

### 7.3.1.1 Snapper

The same cohort of snapper was used and treated the same as in the AQUI-S$^{TM}$ uptake and recovery experiments (Section 3.3.1.1). The experimental protocol was approved by the University of Canterbury's Animal Ethics Committee.

## 7.3.2 Experimental methodology

### 7.3.2.1 Water bath and ECG

Snapper in a 1000L tank were anaesthetised with 20 mg.L$^{-1}$ AQUI-S$^{TM}$. After ~30 min one fish was removed for experimentation and the remaining fish transferred to a fresh seawater tank to recover. The experimental fish was placed, dorsal surface up in a cradle in a water bath (Grant Instruments, GR150 20L, Cambridge, England) filled with 17 L of seawater containing 15 mg.L$^{-1}$ AQUI-S$^{TM}$ at the holding tank's ambient temperature. Compressed air was used to oxygenate the water bath. A nipple made from rubber hose was inserted into the mouth of the fish and was connected to a small submersible aquarium pump (SCCE, Micra 50, Italy) which ventilated the snapper at 1.25 L.min$^{-1}$ Another small submersible aquarium pump was used to circulate water around the water bath and across a dissolved oxygen (DO) meter (Oxy Guard® Handy Polaris, Denmark). Two stainless steel needle electrodes were inserted through the skin of the ventral surface and run into the fish muscle on either side of the heart. A reference electrode was placed in the fish cradle. The ECG was recorded with Power Lab and Chart software (ADInstruments Castle Hill, NSW, Australia) via a Bio Amp (ADInstruments).

#### 7.3.2.2 Fibre optic methodology

A blue (468 nm peak) and a green (514 nm peak) LED were rigged inside a small plastic box with a fibre optic cable coupler. A 100µm fibre optic cable was coupled to the blue and green LED source. Another 100µm fibre optic cable was connected to a fibre optic spectrometer (S2000, Ocean Optics, Florida, USA). The distal ends of each optic fibre were stripped down to reveal approximately 75mm of the 100µm silica core. The blue green optode and recording optode were arranged side by side and fixed so the recording optode was approximately 5mm below the blue green optode. Using a 21 gauge needle, a small incision was made in the skin of the dorsal surface of the fish approximately 5mm back and 2mm lateral to the dorsal fin. The optodes were inserted vertically approximately 20mm through the incision into the fish into the white muscle D block. The intensity of the signal transmitted light from the blue and green LED was recorded using OmniDriver Spectroscopy software (Ocean Optics). The transmitted light intensities at wavelengths 466 nm, 516 nm and 530 nm were recorded and logged every 5 seconds for the duration of the experiments.

#### 7.3.2.3 Hypoxia methodology

When the ECG, heart rate and white muscle perfusion and haemoglobin saturation baselines in the anaesthetised fish had stabilised for a minimum period of 30 min, the dissolved oxygen (DO) was reduced by bubbling nitrogen at 4 $L.min^{-1}$ in to the water for 60 min. After 60 min the water was aerated to re-oxygenate the water bath to pre-hypoxia saturation values. For statistical analysis the data were subjected to repeated measures ANOVA, using Bonferroni's multiple comparison test at 5 min intervals to determine significant changes ($P < 0.05$) from the initial values.

## 7.4 Results

### 7.4.1 Progressive hypoxia and recovery

The mean fish weight was was 117±3g (N=7) and the ambient water bath temperature 10.0±0.3$^{o}$C.

The intensity of light recorded by the recording optode was dependent on the distance between the light emiting optode and the recording optode. The positioning of the optodes in each fish was very similar, but due to the procedure of blind optode placement, the positioning could never be identical. A slight decrease or increase in the distances between the optode tips caused an increase or decrease in the recorded baseline light intensity. To remove the starting variability between the raw data traces, a baseline mean from 15 min resting prior to experimentation was calculated and the subsequent recorded intensities expressed as a percentage change from this resting value.

Figure 7.2 shows the disolved oxygen content of the water bath and the snapper heart rate and QRS amplitude (as a percentage change from resting) during hypoxia and reoxygenation. The DO concentration in the water bath, with an anaethetised 'resting' snapper was 8.6±0.1 mg.L$^{-1}$. The DO concentration in the water bath reduced to 4.5±0.1 mg.L$^{-1}$ (50% saturation) within 8 min of the $N_2$ being vented into the bath, and reduced further to 2.2±0.1 mg.L$^{-1}$ (25% saturation) within 18 min before reaching a low of 0.7±0.1 mg.L$^{-1}$ (7.5% saturation) after 60 min hypoxia (63 min).

The anaesthetised snapper resting heart rate prior to hypoxia was 39.6±1.0 BPM (Figure 7.3 ). During the hypoxic period the heart rate showed a staged bradycardia event (Figure 7.3). The heart rate remained stable until the DO reached 6.1±0.1 mg.L$^{-1}$ (8 min, 5 min hypoxia), where it began to decrease slowly until it reached 37.7±1.0 BPM (1.5±0.1 mg.L$^{-1}$ DO (28 min, 25 min hypoxia).

Below 1.5±0.1 mg.$L^{-1}$ DO concentration the heart rate decreased at a much faster rate, reaching 31.8±1.8 BPM at 1.0±0.1 mg.$L^{-1}$ DO (38 min, 35 min hypoxia). The heart rate then remained constant at ~31-32 BPM until the water bath DO reached 0.8 mg.$L^{-1}$DO (48min, 45 min hypoxia). Below 0.8 mg.$L^{-1}$DO the heart rate then decreased to its lowest recording of 26.5±1.5 BPM at DO concentration 1.9±0.1 mg.$L^{-1}$ (67 min, 4 min re-oxygenation) before increasing to pre-hypoxia values at 6.8±0.1 mg.$L^{-1}$ DO (30 min, 27 min re-oxygenation). As the DO concentration continued to increase towards initial oxygen saturation values the heart rate decreased to 37-38 BPM (from 8.3±0.1 mg.$L^{-1}$ DO, 121 min, 58 min re-oxygenation) before increasing to resting values once more at 8.6±0.1 mg.$L^{-1}$ (151 min, 88 min re-oxygenation). During hypoxia and re-oxygenation the heart rate was significantly lower (Repeated measures ANOVA and Bonferroni's Multiple Comparison Test, $P<0.05$) than initial resting values from 1.0±0.1 to 3.7±0.1 mg.$L^{-1}$ DO (36 min, 33 min hypoxia to 72 min, 10 min re-oxygenation).

As the water bath DO concentration decreased, the QRS amplitude initially increased by ~9% of its resting amplitude by 4.9±0.1 mg.$L^{-1}$ (21 min, 18 min hypoxia) (Figure 7.2). The QRS amplitude then decreased to below 50% of its resting amplitude by 0.7±0.1 mg.$L^{-1}$ (51 min, 48 min hypoxia). During deep hypoxia the QRS amplitude showed a non-significant (un-paired, two-tailed Student's t-test, $P<0.05$) rise to 43% of its resting amplitude (0.7±0.1 mg.$L^{-1}$, 58 min, 55 min hypoxia), before decreasing again to below 50% of its resting amplitude at 1.4±0.1 mg.$L^{-1}$ (65 min, 2 min re-oxygenation). During re-oxygenation the QRS amplitude increased to ~11% below resting at DO concentration at 7.0±0.1 mg.$L^{-1}$ (63 min, 10 min re-oxygenation). The QRS amplitude then decreased (non-significant) to ~20-21% below resting amplitude at DO concentration 7.5±0.1 mg.$L^{-1}$ (99 min, 36 min re-oxygenation), before increasing over the duration of the experiment to ~3% below resting amplitude. During hypoxia and re-oxygenation the percentage QRS amplitude was significantly lower (Repeated measures ANOVA and Bonferroni's Multiple Comparison Test, $P<0.05$) than initial values from 0.9±0.1 mg.$L^{-1}$ to 2.5±0.1

$mg.L^{-1}$ DO (42 min, 39 min hypoxia to 68 min, 5 min re-oxygenation).

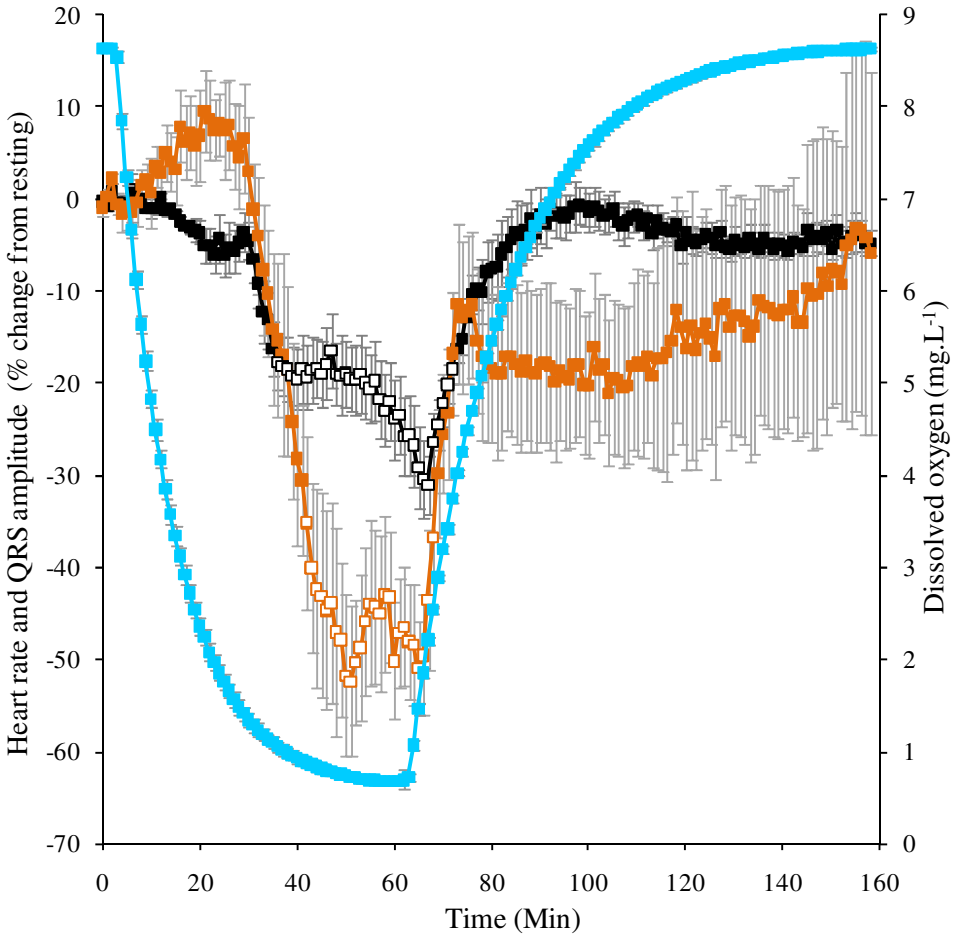


**Figure 7.2 Ambient water bath dissolved oxygen content (light blue) and percentage change in snapper heart rate (black) and QRS amplitude (orange) during hypoxia and re-oxygenation.** Open symbols indicate a significant difference from starting values (Repeated measures ANOVA and Bonferroni's Multiple Comparison Test, $P<0.01$). Values are mean±sem, N=7.

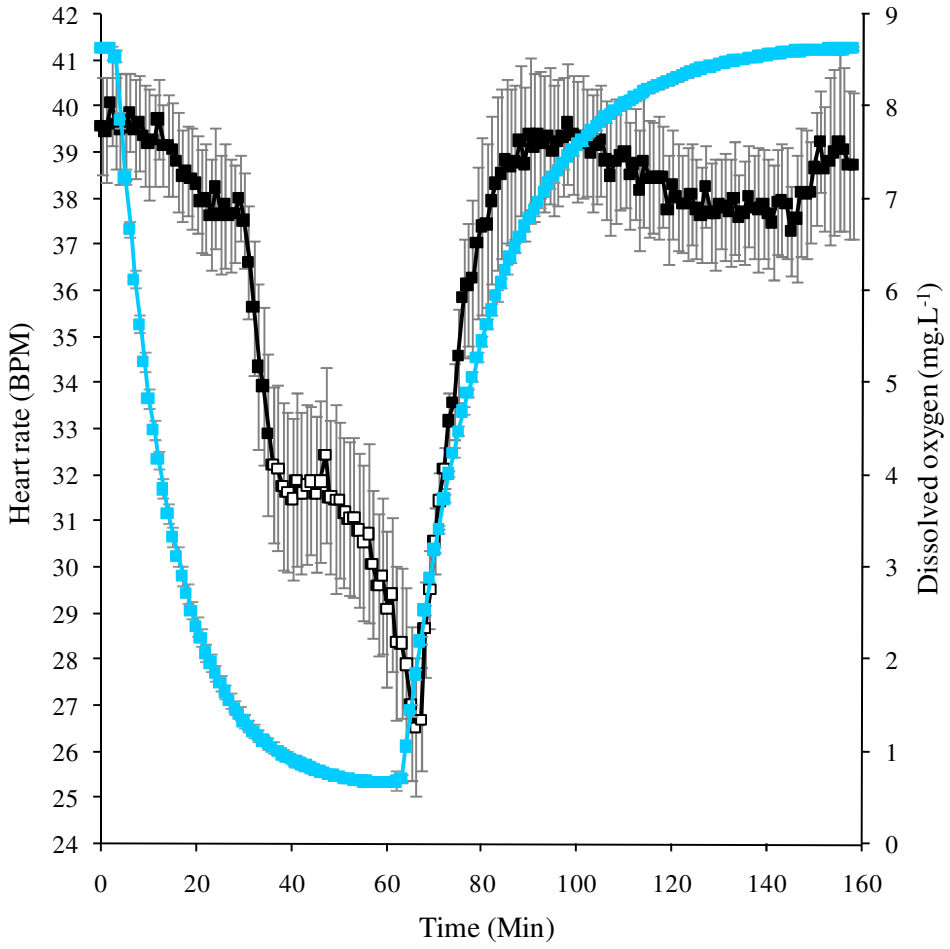


**Figure 7.3 Ambient water bath dissolved oxygen content (light blue) and snapper heart rate (BPM) (black).** Open symbols indicate a significant difference from starting values (Repeated measures ANOVA and Bonferroni's Multiple Comparison Test, $P<0.01$). Values are mean±sem, N=7.

The effects of hypoxia on snapper heart rate and QRS amplitude have already been discussed above, but Figure 7.4 A and Figure 7.4.B show more clearly the relationship between heart rate and QRS amplitude against DO concentration during hypoxia and re-oxygenation.

There was a slow decrease in heart rate until the DO concentration in the water bath reached 1.5±0.1 $mg.L^{-1}$. Once the water bath DO decreased beyond 1.5±0.1 $mg.L^{-1}$ the heart rate decreased at a much faster rate (Figure 7.4.A). During re-oxygenation the heart rate initially decreased before recovering to pre-hypoxia values. There is a hysteresis between hypoxia and re-oxygenation; at any given DO concentration (below 6.0±0.1 $mg.L^{-1}$) heart rate is greater during progressive hypoxia than re-oxygenation.

The QRS amplitude increased gradually until the water bath reached 1.4±0.1 $mg.L^{-1}$, similar to the DO at which the heart rate demonstrated strong bradycardia. Below 1.4±0.1 $mg.L^{-1}$ DO the QRS amplitude decreased at a much faster rate (Figure 7.4.B). During re-oxygenation the QRS amplitude initially decreased before recovering to 11% below its resting amplitude. The QRS amplitude during hypoxia and re-oxygenation exhibits a similar hysteresis to that of the heart rate; the QRS amplitude is greater during hypoxia than re-oxygenation at any given water bath DO concentration.

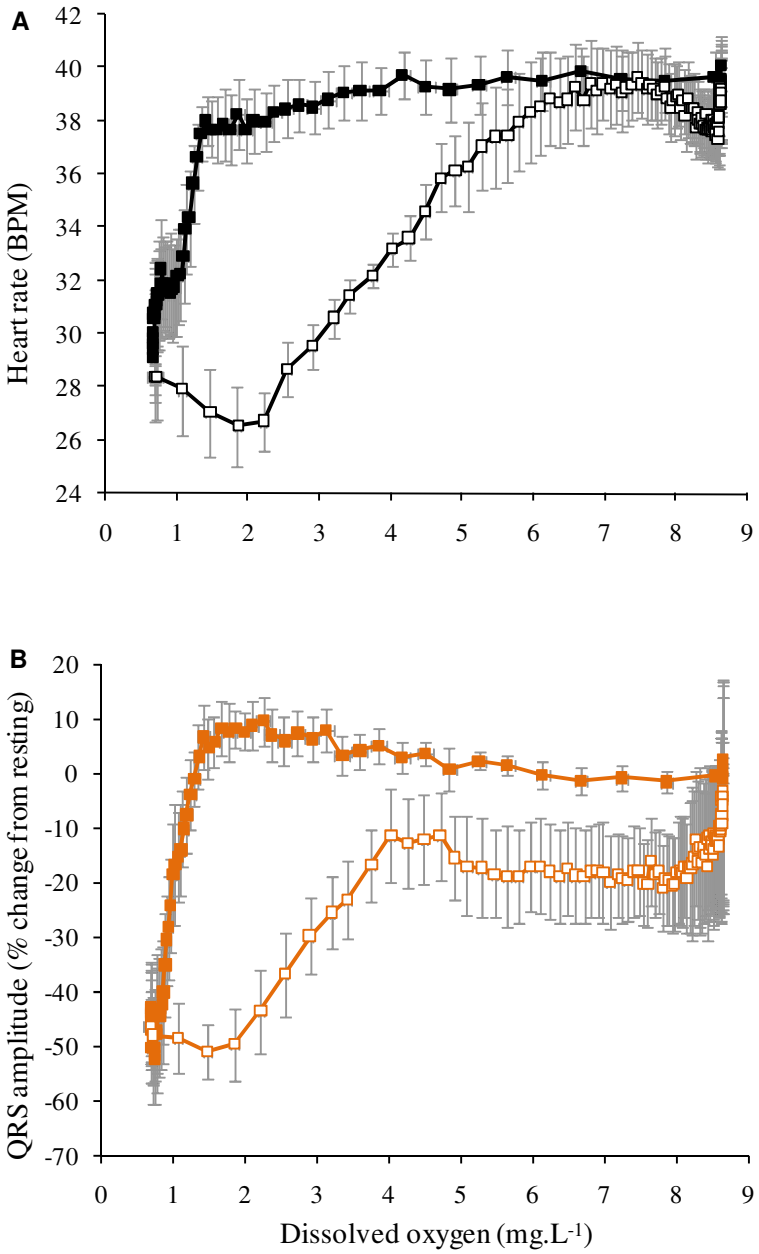


**Figure 7.4 Ambient dissolved oxygen plotted with A) heart rate and B) QRS amplitude during hypoxia (solid) and re-oxygenation (clear).** Values are mean±sem, N=7.

White muscle perfusion and haemoglobin saturation decreased during hypoxia and increased during re-oxygenation. The measured intensity of light at wavelength 530 nm (Figure 7.5) describes the state of perfusion in the sampled white muscle as light at 530 nm is absorbed by both oxy-haemoglobin and deoxy-haemoglobin at the same amount (same molar extinction co-efficient). An increase in the light intensity at 530 nm indicates a decrease in mean haemoglobin concentration (perfusion), as more light can pass through the interrogated tissue sample. Conversely, a decrease in light intensity at 530 nm indicates an increase in combined haemoglobin (perfusion) as less light can pass through the tissue sample.

The measured light intensity at wavelengths 466 nm and 516 nm reflects the oxygen saturation of haemoglobin (Figure 7.5), but the measured intensity at these wavelengths also has a perfusion factor included as all wavelengths on the haemoglobin absorption spectra will increase and decrease if total haemoglobin decreases or increases (perfusion).

Oxy-haemoglobin has a greater molar extinction co-efficient than that of deoxy-haemoglobin, which means that oxy-haemoglobin will absorb more light at 466 nm than deoxy-haemoglobin. If perfusion were static, an increase in the light intensity at 466 nm would indicate a decrease in oxy-haemoglobin, and vice versa. The same principle applies to wavelength 516 nm, at which deoxy-haemoglobin has a greater molar extinction co-efficient than oxy-haemoglobin. If perfusion was unchanged, an increase in light intensity at 516 nm would indicate a decrease in deoxy-haemoglobin.

The light intensity measured at 530nm was not significantly different from initial resting values at any time (Repeated measures ANOVA and Bonferroni's Multiple Comparison Test, $P<0.05$). However, statistical analysis with an unpaired one-

tailed Student's t-test showed significant difference from resting values from 28 to 68 min (inclusive).

Perfusion remained at resting values in the snapper white muscle until the water bath reached 3.3±0.1 $mg.L^{-1}$ DO concentration (15min, 12 min hypoxia) (Figure 7.5). Below 3.3±0.1 $mg.L^{-1}$ DO, perfusion decreased (indicated by an increasing 530 nm light intensity). Perfusion stabilised at 1.0±0.1 $mg.L^{-1}$ DO (38 min, 35 min hypoxia) as the light intensity at 530 nm remaining constant at 4-4.5% above resting intensity. Perfusion decreased again when the water bath reached 0.7±0.1 $mg.L^{-1}$ DO (54 min, 51 min hypoxia), the intensity at 530 nm increasing to 5-6% above resting intensity. Perfusion remained at a constant decreased state until the water bath was re-oxygenated and had reached 1.9±0.1 $mg.L^{-1}$ (66 min, 3 min re-oxygenation). Perfusion in the white muscle then increased as the water bath continued to re-oxygenate, indicated by the intensity at 530 nm decreasing to the initial resting value at 6.4±0.1 $mg.L^{-1}$ DO (26 min, 23 min re-oxygenation), before continuing to decrease and stabilise at -1 to -1.5% below resting 530 nm light intensity at 7.8±0.1 $mg.L^{-1}$ DO (45 min, 42 min re-oxygenation), suggesting greater perfusion than before hypoxia exposure.

Figure 7.5 also shows the light intensity of wavelengths 566 nm and 516 nm (representing haemoglobin saturation); however, as discussed previously, they have an inherent perfusion element. To remove the perfusion element from the saturation element, the raw data recorded intensity at 466 nm and 516 nm were divided by the corresponding 530 nm light intensity which gave a ratio value relative to perfusion. Figure 7.6 shows the light intensity ratio from wavelength 466 nm and 516 nm.

The 466 nm/530 nm and 516 nm/530 nm resting ratios were approximately 1.4 and 0.9, respectively (Figure7.6). The 466 nm/530 nm ratio was significantly different from initial resting values (Repeated measures ANOVA and Bonferroni's Multiple Comparison Test, $P<0.05$) between 32 min and 76 min. The 516 nm/530

nm ratio was significantly different from initial resting values between 32 min and 78 min (Repeated measures ANOVA and Bonferroni's Multiple Comparison Test, $P<0.05$).

Haemoglobin saturation remained at resting values until the water bath reached 2.4±0.1 $mg.L^{-1}$ DO (20 min, 17 min hypoxia) (Figure 7.6). Below 2.4±0.1 $mg.L^{-1}$ DO, saturation decreased, shown by an increase in the 466 nm/530 nm ratio (decreasing oxy-haemoglobin) and a decrease in the 516 nm/530 nm ratio (increasing deoxy-haemoglobin). At 0.8±0.1 $mg.L^{-1}$DO (45 min hypoxia) haemoglobin saturation was constant, shown by stabilised 466 nm/530 nm and 516 nm/530 nm ratios of 1.51-1.53 and 0.84-0.85, respectively. During re-oxygenation the haemoglobin saturation increased from 2.9±0.1 $mg.L^{-1}$ DO (69 min, 6 min re-oxygenation), shown by a decrease in the 466 nm/530 nm ratio and an increase in the 516/530 ratio. Saturation in the white muscle returned to its pre-hypoxia resting values at 7.2±0.1 $mg.L^{-1}$ DO (95 min, 32 min re-oxygenation), where it remained for the duration of the experiment.

Figure 7.7.A demonstrates more clearly the relationship between the DO concentration in the water bath and white muscle perfusion (530 nm light intensity) during hypoxia and re-oxygenation

The relationship between haemoglobin saturation (light intensity measured at wavelength 466 nm and 516 nm) has already been discussed, but Figure 7.7.B clearly denonstrates not only the relationship between the disolved oxygen content in the water bath and the recorded 466 nm and 516 nm light intensities (perfusion adjusted), but also the expected inverse relationship between light intensities measured at 466 nm and 516 nm, which was shown to be significant (ANOVA regressions, $P<0.001$) in Figure 7.8.

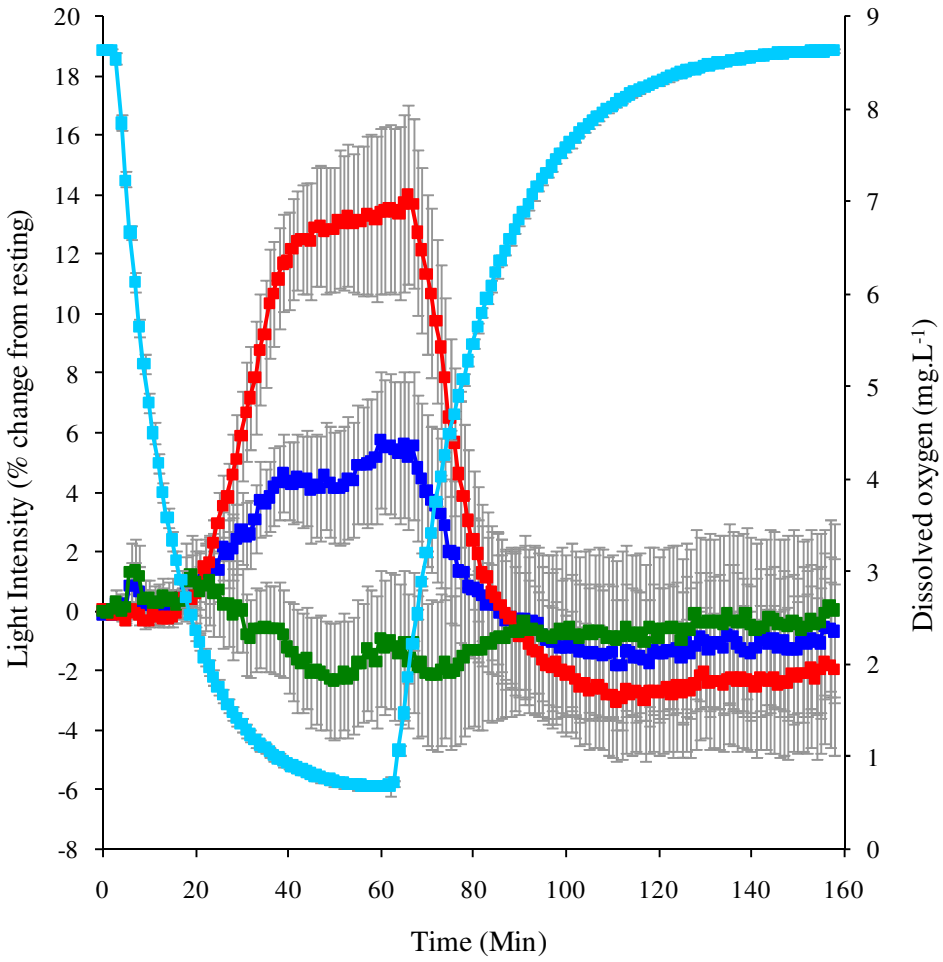


**Figure 7.5 Ambient water bath dissolved oxygen content (light blue) and light intensity from wavelengths 530 nm (dark blue), 466 nm (red), and 516 nm (green) recorded from the white muscle during progressive hypoxia and re-oxygenation.** An increase in intensity at 530 nm, 466 nm and 516 nm wavelengths indicate a decrease in total haemoglobin concentration (perfusion), a decrease in the oxy-haemoglobin concentration and a decrease in deoxy-haemoglobin concentration, respectively, and vice versa. No significant difference were determined in the 530 nm data (Repeated measures ANOVA and Bonferroni's Multiple Comparison Test, $P<0.05$). Significant difference was not calculated in the 466 nm and 516 nm data. Values are mean±sem, N=7.

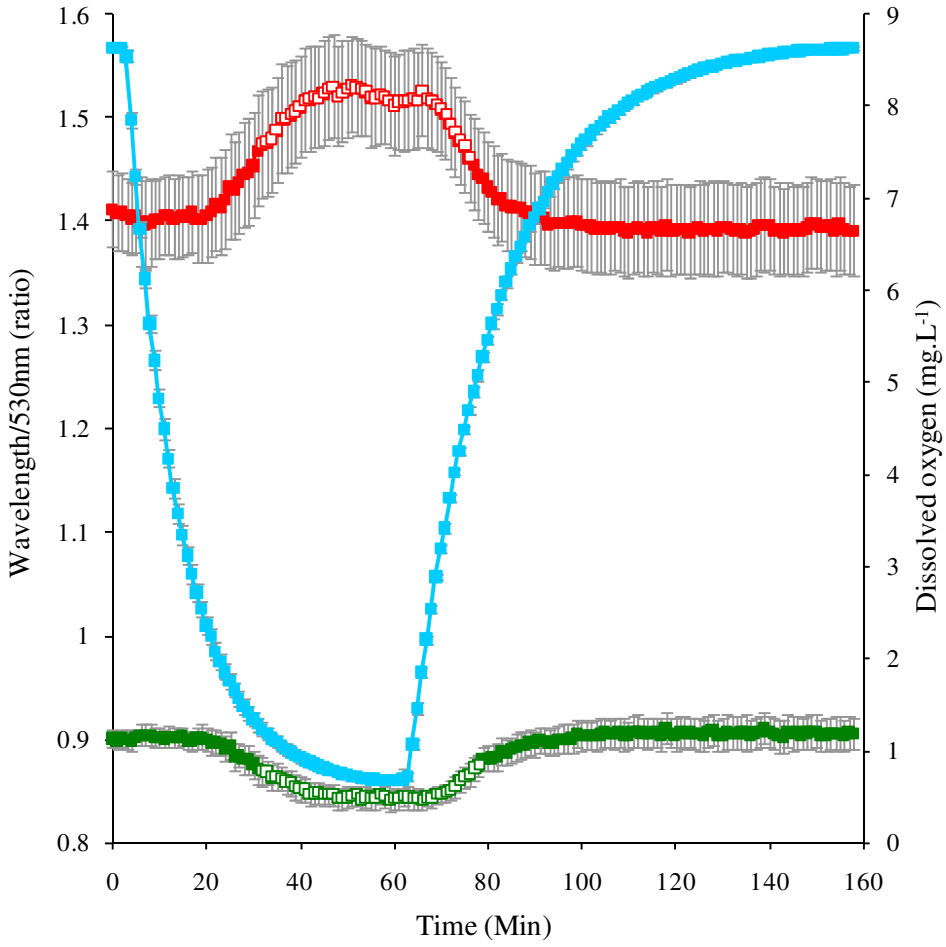


**Figure 7.6 Ambient water bath dissolved oxygen content (light blue) and ratios from wavelengths 466 nm/530 nm (red) and 516 nm/530 nm (green) during progressive hypoxia and re-oxygenation.** An increase in the 466 nm /530 nm and 516 nm/530 nm ratio indicate a decrease in the oxy-haemoglobin concentration and a decrease in the deoxy-haemoglobin concentration, respectively, and vice versa. Open symbols indicate a significant difference from starting values (Repeated measures ANOVA and Bonferroni's Multiple Comparison Test, $P<0.001$).Values are mean±sem, N=7.

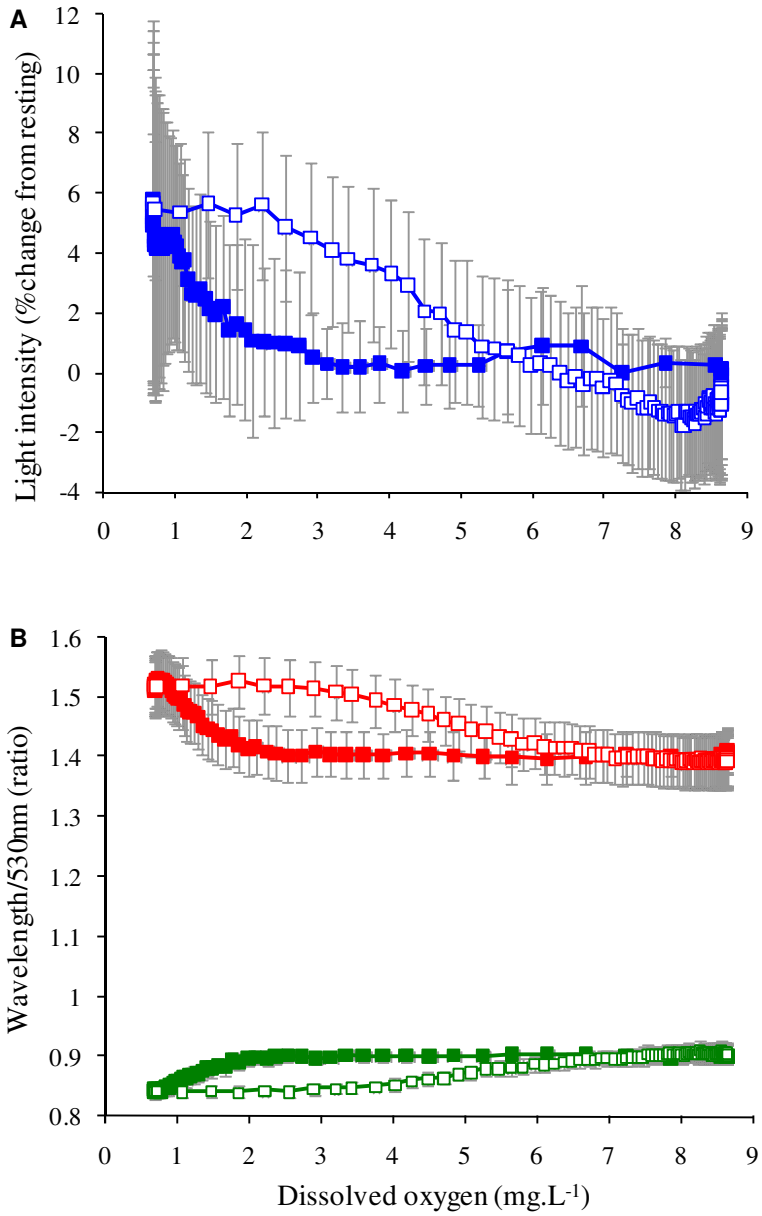


**Figure 7.7 A) Recorded change in light intensity from wavelength 530 nm and B) ratios from wavelength 466 nm/530 nm (red) and 516 nm/530 nm (green) against ambient water dissolved oxygen content during hypoxia (solid) and re-oxygenation (clear).** Values are mean±sem, N=7.

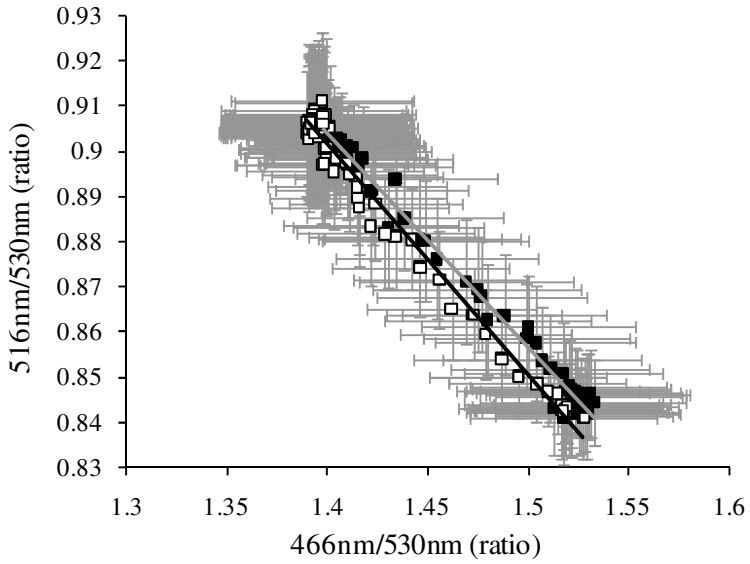


**Figure 7.8 Haemoglobin saturation as measured from 466 nm/530 nm (oxy-haemoglobin) and 516 nm/530 nm (deoxy-haemoglobin) wavelengths during hypoxia (solid) and re-oxygenation (clear).** $r^2$ values for linear trendlines are; hypoxia (grey) 0.96, and re-oxygenation (black) 0.98. Values are mean±sem, N=7.

I have already described both heart rate (Figure 7.3) and white muscle perfusion (Figure 7.5) over time during progressive hypoxia and re-oxygenation. Figure 7.9.B shows a significant linear (ANOVA regressions $P<0.001$) relationship, over much of the range between perfusion (light intensity at 530 nm) and heart rate. During bradycardia, perfusion decreased proportionately (demonstrated by the 530 nm light intensity increasing) (Figure 7.9.B). During re-oxygenation the heart rate and perfusion increased (530 nm light intensity decreased), although perfusion increased relative to heart rate at the end of recovery.

During deep hypoxia cardiac arrhythmias were observed in all 7 experimental fish. However, the degree of the arrhythmias was variable. One fish showed many missed heart beats and the occasional variable interbeat interval (Figure 7.10.A), some fish showed many instances of variable interbeat interval (Figure 7.10.B), and some only few (7.10.C). A regular cardiac rhythm was restored during re-oxygenation.

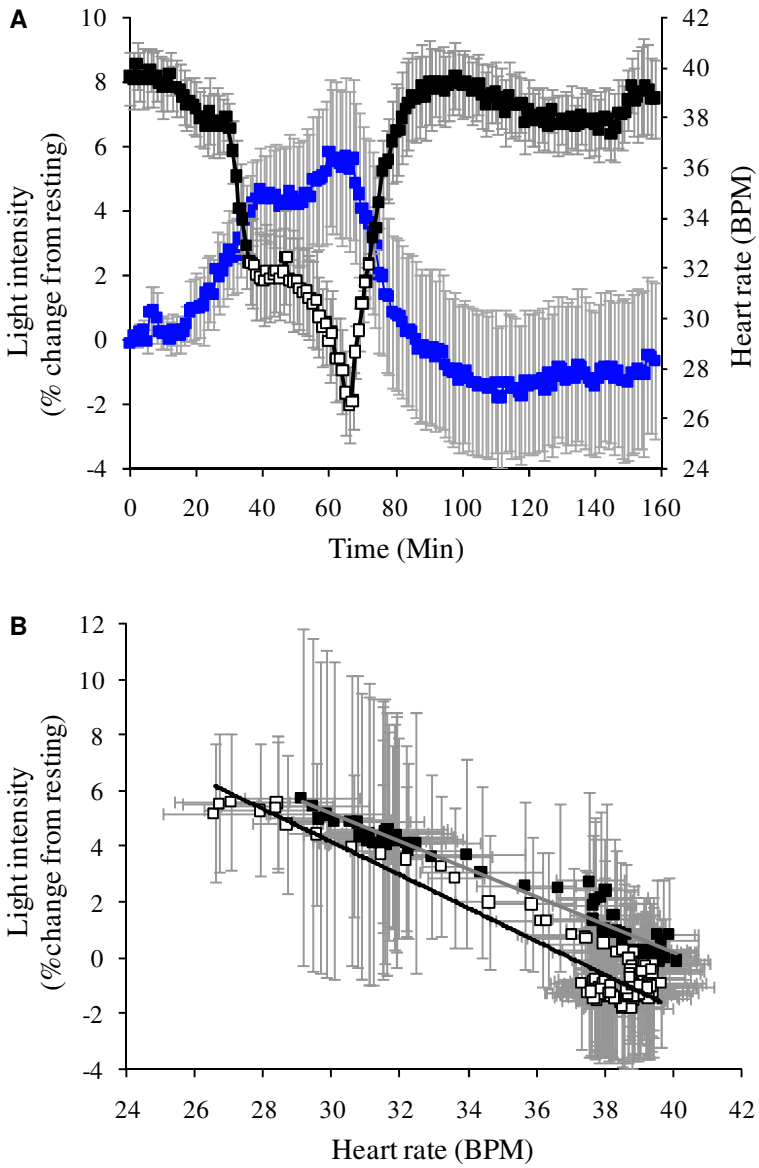


**Figure 7.9 A) Snapper heart rate (black) and light intensity from wavelength 530 nm (dark blue), recorded from the white muscle during hypoxia and re-oxygenation. A rise in light intensity indicates reduced perfusion of the muscle B) Snapper heart rate plotted against light intensity from wavelength 530 nm during hypoxia (solid) and re-oxygenation (clear).** A) Open symbols indicate a significant difference from starting values (Repeated measures ANOVA and Bonferroni's Multiple Comparison Test, $P<0.01$). $r^2$ values for linear trendlines (B) are; hypoxia (grey) 0.96, and re-oxygenation (black) 0.88. Values are mean±sem, N=7.

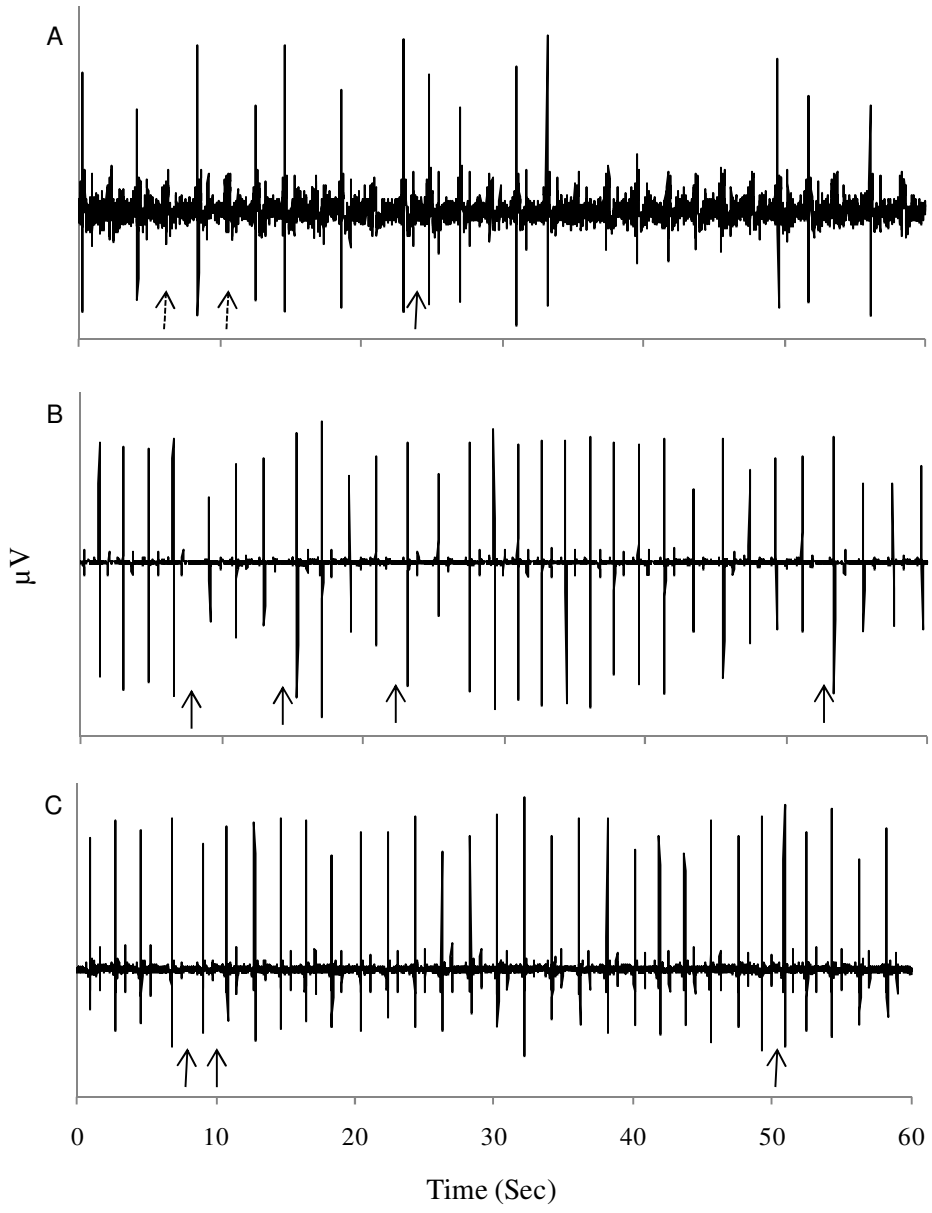


**Figure 7.10 A-C) Examples of ECG recordings from individual anaesthetised fish showing arrhythmia's during deep hypoxia (DO concentration 0.7±0.1mg.L$^{-1}$).**
Examples of missed beats (dashed black arrows) and irregular interbeat intervals (black arrows) are marked.

## 7.5 Discussion

Bradycardia is a physiological reflex where the heart rate decreases in response to hypoxia exposure (Randall 1982, Sundin et al. 1999, Vornanen and Tuomennoro 1999, Stecyk and Farrell 2002, Overgaard et al. 2004). Anaesthetised snapper showed marked bradycardia during progressive hypoxia and recovery (Figure 7.3). There was slight but, non significant fall in heart rate when the water bath DO concentration decreased below 6.1±0.1 $mg.L^{-1}$ (5 min hypoxia), with heart rate decreasing from 39.6±1.0 BPM by ~2 BPM over 20 min. When the water bath DO concentration reached 1.5±0.1 $mg.L^{-1}$ (25 min hypoxia), profound bradycardia occurred, decreasing the heart rate to ~31-32 BPM where it remained constant for aproximately 10 min before decreasing again to a low of 26.5±1.5 BPM at DO concentration 1.9 $mg.L^{-1}$ (after 4 min re-oxygenation). During re-oxygenation the heart rate increased to pre-hypoxia values within 23 min (27 min re-oxygenation, DO 6.8±0.1 $mg.L^{-1}$).

Hypoxic bradycardia in teleost fish is a reflex response involving the vagus nerve (Randall and Smith 1967). There are fish species that exhibit little or no bradycardia during hypoxia, including some “primitive species”, that lack autonomic cardiac innervation (Axelsson et al. 1990), some air-breathing fish species (Fritsche et al. 1993), some hypoxia tolerant fish species (Stecyk and Farrell 2002) and some cold water species (Fritsche 1990). However, the majority of fish species do exhibit some degree of bradycardia, the extent of which is dependent on the level of hypoxia and the water temperature. Hypoxia also has a profound effect on ventilation with increases in frequency and amplitude being recorded (Berschick et al. 1987, Sundin et al. 1999, Perry et al. 2004). However, in our research, due to the snapper being anaesthetised and artificially ventilated, we would not observe any ventilatory response.

The anaesthetised snapper heart rate during hypoxia decreased to a minimum of 31% below pre-hypoxia resting values (Figure 7.2), which is slightly less than

recorded bradycardia responses from other fish species. Sundin et al. (1999) demonstrated bradycardia greater than 40% below resting rate in the tropical fish traira (*Hoplias malabaricus*). During hypoxia, carp acclimated to 10$^{o}$C showed a minimum hypoxia heart rate ~60% and a maximum hypoxia heart rate ~35% below resting normoxia heart rate (Stecyk and Farrell 2002). Differences in the depth of hypoxia are most certainly due to interspecific differences in hypoxia tolerance. However, unlike the traira and carp, the snapper in this progressive hypoxia and recovery experiment were fully anaesthetised. Anaesthesia may influence the physiological mechanisms which induce bradycardia in fish, to the extent where all extrinsic control of cardiac function maybe lost. Burleson and Smatresk (1989) demonstrated that the bradycardia response to hypoxia was still significant in MS222 anaesthetised (but spontaneously breathing) catfish (*Ictalurus punctatus*). The heart rate in anaesthetised catfish in normoxia was elevated compared with the conscious fish, and the attenuation in heart rate when exposed to hypoxia was not as great as that in a conscious fish. They surmised that an anaesthetic preparation was still beneficial as it eliminated any adverse behavioural responses seen in conscious fish.

The recommended lower limit of DO concentration in cultured snapper is 4.0 mg.L$^{-1}$ (Partridge et al. 2003), which is lower than the DO concentration at which we saw the onset of mild bradycardia in the anaesthetised snapper (6.1±0.1 mg.L$^{-1}$,5 min hypoxia), However, it is greater than 1.5±0.1 mg.L$^{-1}$, the DO concentration at which profound bradycardia occurred. The progressive hypoxia and recovery experiments were conducted during the winter months. During summer when the temperatures are warmer and the fish have a higher metabolic rate, and therefore greater oxygen demand, we may see the onset of bradycardia at a higher ambient dissolved oxygen concentration.

Reflex experiments (Milsom and Brill 1986, Burleson and Smatresk 1990, Burleson and Milsom 1993, from Sundin and Nilsson 2002) and denervation experiments (Butler et al. 1977, Fritsche and Nilsson 1989, Sundin et al. 1999)

have shown that the branchial nerves play an important role in cardioventilatory control in teleosts. Branchial nerves relay sensory information from external (water sensing) and internal (arterial sensing) oxygen sensing receptors found on the gill arches to the central nervous system.

Butler (1977) sectioned four cranial nerves in the dogfish (*Scyliorhinus canicula*), effectively severing the neural pathways of any internal or external sensory receptors from the gill arches. When exposed to hypoxia the dogfish showed no bradycardia. More recent denervation experiments show a greater complexity of sensory receptor populations and localisation. Sundin et al. (1999) demonstrated the oxygen chemoresponse with denervated traira. Complete bilateral denervation of the first gill arch removed the hypoxic bradycardia response, however when all four gill arches were denervated the hypoxia bradycardia response, although noticeably weaker than the control treatment (no denervation), was observed.

Sundin et al. (1999) also showed a hysteresis in the relationship between the heart rate and $PO_2$ during progressive hypoxia and recovery in traira. In the control fish treatment in that study, the heart rate was greater during recovery compared with hypoxia at any given $PO_2$. This direction of hysteresis was present in all the denervation treatments except when all four gill arches were denervated (G4). With the branchial nerves to all four gill arches severed, the hysteresis between heart rate and $PO_2$ during recovery and hypoxia was reversed; heart rate was greater during hypoxia compared with recovery at any given $PO_2$. Our anaesthetised snapper demonstrated a similar pattern of hysteresis to that of the G4 traira treatment (Figure 7.4.A). Drawing from this directional similarity in hysteresis during the bradycardia response, we can suggest that the anaesthetic effects of AQUI-S$^{TM}$ may be inhibiting/slowing neural pathways, effectively "denervating" the $O_2$ chemoreceptor response in snapper. However, as bradycardia was still present in both denervated and anaesthetised fish it suggests a far greater complexity of cardioventilatory control.

Cardioventilatory research on conscious teleosts can be confounded by disturbance and stress on the experimental animal that can mask the underlying physiological response. The use of an anaesthetic produces a rested, stress-free experimental animal, but, artificial ventilation is required and the side effects of anaesthesia may also compound the physiological response. Cardiac control by the vagus nerve in an anaesthetised preparation is compromised, as shown by Burleson and Smatresk (1989). Therefore, the bradycardia response that we have shown in the anaesthetised snapper may be different to that in a conscious snapper.

Hill and Forster (2004) described the effects of anaesthetic induction and recovery on cardiac function in Chinook salmon (*Oncorhynchus tshawytscha*). They showed that induction with 60 $mg.L^{-1}$ AQUI-S$^{TM}$ on a minimally disturbed salmon caused an immediate decrease in heart rate, cardiac output (Q), stroke volume (SV) and dorsal aortic pressure (DAP). Heart rate, Q and SV all returned to pre-anaesthesia levels after 3 min, whereas DAP remained low. SV and Q continued to increase, exceeding pre-induction levels. Salmon anaesthetised with AQUI-S$^{TM}$ also showed elevated haemocrit, adrenaline and noradrenaline. Hill and Forster (2004) suggest that this initial cardiac and catecholamine response was due to the high concentration of AQUI-S$^{TM}$ used, and a nociceptor-mediated response from the salmon, rather than a true anaesthetic effect. In this present study we cannot rule out the possible anaesthetic effects which may alter the cardiac response of the snapper during progressive hypoxia and recovery. However, the snapper in the hypoxia and recovery experiments were anaesthetised with 15 $mg.L^{-1}$ AQUI-S$^{TM}$, a quarter of the concentration used by Hill and Forster (2004).

In a conscious animal, the heart is primarily slowed by a vagal reflex (Randall and Smith, 1967, Fritsche 1990). However, this is unlikely to be the case in our preparation, with AQUI-S present in the water (Hill et al. 2004). We assume inhibited neurological control of cardiac function in our anaethetised preparation, but the physiological causes of bradycardia and reduced cardiac performance are

not clear. The direct effect of hypoxia on the cardiac myocytes may be the most likely cause, but the question still remains to whether or not there may be a degree of neurological control even in an anaethetised fish?

Vornanen and Tuomennoro (1999) demonstrated that hypoxia induced depression in cardiac function in the hypoxia tolerant crucian carp (*Carassius carassius*) is primarily mediated by muscarinic cholinergic receptors on the sinoatrial pacemaker and the artial myocytes as cardiac depression is blocked with atropine. However, it is also likely that hypoxia has a direct effect on the cardiac myocytes themselves by disturbing calcium homeostasis (Allen and Orchard 1983). Hypoxia could have differential effects on the spread of the action potential and the force that the myocytes can generate. During deep hypoxia there was evidence of arrhythmias in the QRS recordings, including missed beats and variable beat intervals, suggesting severe hypoxia did have a direct effect on action potential in the cardiac myocytes (Figure 7.10).

The heart rate and amplitude of the QRS wave both decreased rapidly once the water bath DO concentration fell below 1.4-1.5 $mg.L^{-1}$ (Figure 7.4.A and B), which is suggestive of a sudden, triggered event rather than a cumulative effect of hypoxia. Although there are reasons to believe that the vagus nerve cannot influence the heart in this preparation, it is possible that catecholamines might be released at this time. The threshold for catecholamine release in rainbow trout was a $PaO_2$ of c. 20 mmHg and a $PwO_2$ of c. 55 mmHg (Fievet et al. 1990). Thus, in the live animal a fall in the concentration of oxygen in external water of 66% was sufficient to generate an internal hypoxaemia that provoked catecholamine release. Perry et al. (2004) demonstrated that the hypoxic threshold for hypoxia-mediated catecholamine release in the traira (*H. malabaricus*) and juju (*Hoplerythrinus unitaeniatus*) was blood oxygen concentrations 50-60% of normoxic values. In our preparation the rapid decline in heart rate and QRS amplitude did not occur until the DO concentration had declined to almost 15% of the starting point, though of course the snapper was inactive and anaesthetised,

with presumably a relatively lower metabolic rate. It would be interesting to measure blood catecholamine concentrations in the snapper during progressive hypoxia and recovery. Catecholamine release should be associated with an increased ventricular emptying force (Farrell and Jones 1992), which should increase cardiac output. White muscle perfusion fell at this time, which could reflect α-adrenergic activity on the vascular smooth muscle of the tail (Davie, 1981). Also, autonomic nerves are known to be involved in the afferent and efferent arms of the control of catecholamine secretion in teleosts (Perry and Bernier 1999, Perry and Reid 2002) and the nerves will be inhibited due to anaesthesia, although non-neuronal mechanisms are also known to trigger release (Reid et al. 1998).

Bradycardia during hypoxia does not necessarily mean a reduction in cardiac output as the attenuation in heart rate is often offset by an associated increase in stroke volume (Holeton and Randall 1967, Wood and Shelton 1980, Gamperl et al. 1994, Minerick et al. 2003). The physiological advantage of the bradycardia is supposed to be better synchronicity of ventilation and blood flow (Randall and Smith 1967, Fritsche 1990) and/or an increased residence time of the blood within the heart (Farrell 2007). In most teleosts, the heart is predominantly supplied with oxygen from the venous return and, therefore, is the last organ to be oxygenated. During hypoxia, when arterial oxygen concentrations are low and venous even lower, the increased dwell time of blood in the heart lumen (due to bradycardia), increases the potential delivery of oxygen to the myocardium tissues. The associated increase in stroke volume also increases myocardium oxygen uptake by stretching and thinning the walls of the cardiac chambers, decreasing oxygen diffusion distances.

The initial rise in snapper QRS amplitude exhibited during bradycardia (Figure 7.2) is similar to the increase shown by others in stroke volume (see above). From this similarity one could draw a conclusion that the the QRS amplitude may be somewhat associated with stroke volume and that the product therefore of ECG

amplitude and heart rate may approximate cardiac output. The rise in QRS amplitude at a time of falling heart rate contrasts with the parallel changes of heart rate and QRS amplitude on cold exposure (Chpt 9). To confirm that a change in the amplitude of the QRS wave correlates with an associated change in stroke volume, one would have to measure cardiac output simultaneously. To the best of our knowledge this has not been done. When a flow probe is implanted around the ventral or dorsal aorta of a fish the cardiac frequency can be derived from the flow signal, obviating the need for an ECG. At present there is no evidence relating QRS amplitude to stroke volume.

The QRS component of an ECG represents spontaneous ventricular depolarisation. One could argue that the QRS component is unaffected by hypoxia and that the ST component (repolarisation) of the ECG may be more affected due to the active transport of sodium and potassium. Rantin et al (1995) showed greater effects of hypoxia on the T wave of four teleost species than they did on the QRS complex. In this preparation the fish (and the inserted ECG electrodes) were immobile. The amplitude of the recorded ECG may have been increased with increased stroke volume due to the expanding ventricle reducing the distances to the electrode. A decrease in stroke volume (and therefore ventricular expansion), may increase the distance between the ventricle and ECG and show as an attenuated ECG signal. However as stated above the relationship between QRS amplitude and stroke volume has not been tested we cannot assume the product of the two is an approximation of cardiac output.

When Altimiras and Axelsson (2004) slowed a rainbow trout heart with zatebradine to 50% of its resting rate they found that stroke volume increased to 165% of the resting value. The concentration-dependent-increase in stroke volume was associated with increases in sinus venous pressure. If the inter-beat interval is extended (bradycardia), then filling pressures should increase, also favouring an increase in stroke volume. A reciprocal relationship between the

frequency of the heart and force development has been described (Ask et al. 1981, Farrell 2007).

In the anaesthetised snapper during deep hypoxia there was a simultaneous decrease in both heart rate and QRS amplitude (Figure 7.2). These data argue for a direct effect of hypoxia on the cardiac myocytes and pacemaker systems, the precipitous nature of the fall suggesting a rapid failure of energy supply. Stroke volume is primarily determined by venous filling pressure (Farrell and Jones 1992, Sandblom and Axelsson 2006). In our preparation the fish is anaesthetised so if we assume no changes in sympathetic tone, then it is unlikely that venous return will be influenced by factors other than cardiac output. However, venous filling pressures may have been influenced by an increase in white muscle systemic resistance due to a decrease in white muscle perfusion during hypoxia.

Axelsson and Fritsche (1991) demonstrated that hypoxia also increased visceral vascular resistance in the Atlantic cod. This would also increase the arterio-venous gradient, potentially reducing the venous filling pressures and decreasing stroke volume (and cardiac output). However, Fritsche and Nilsson (1989) showed that cardiac output was maintained at normoxia values in the hypoxia tolerant Atlantic cod (*Gadus morhua*) during hypoxic bradycardia due to the associated increase in stroke volume.

There is evidence, however, that localised hypoxia dilates arteries and reduces venous tone, decreasing vascular resistance and potentially reducing the arterio-venous pressure gradient and increasing venous filling pressures. Smith et al. (2001) showed arterial dilation and reduced venous tone in pre-contracted vessels from Rainbow trout (*O. mykiss*), subjected to hypoxia. However, as stated above, in our anaesthetised preparation we have to assume no change in sympathetic tone during hypoxia. Smith et al. (2001) showed very little response to hypoxia in vessels that were not pre-contracted and lacked tonus.

Research on perfusion in the white muscle during hypoxia is very limited, as discussed previously. Cameron (1975) showed no significant difference in the blood flow distribution to any tissues in the Arctic grayling (*T. arcticus*) during exposure to hypoxia for 60 min. By using fibre optics we were able to see sensitive changes in white muscle perfusion and haemoglobin saturation in real time during progressive hypoxia and recovery. Perfusion to the white muscle in the anaesthetised snapper decreased during progressive hypoxia when the water bath DO reached 3.3±0.1 $mg.L^{-1}$, and increased during re-oxygenation when the water bath DO reached 1.9±0.1 $mg.L^{-1}$ (Figure 7.5), however the decrease and increase were not significant (Repeated measures ANOVA and Bonferroni's Multiple Comparison Test, $P<0.05$).

Hypoxia in the white muscle can be caused environmentally by a reduction of the ambient water oxygen concentration, or physically due to anaerobic exercise within the white muscle. As the tail musculature becomes hypoxic due to anaerobic exercise there will be an in increase in glycolytic energy production. Hypoxia in the white muscle, derived from a hypoxic external environment, would also result in glycolytic energy production to maintain metabolism, but accumulation of lactate would be slower as the energy demand to maintain basal metabolism is far less than that to maintain exercise. Reducing perfusion to the white muscle during white muscle hypoxia may be a mechanism to protect other tissues and organs from a large lactate load by containing the lactate in the white muscle until favourable environmental conditions return. Dunn and Hochachka (1986) demonstrated that glycolytic activation in the white muscle produced the bulk of the lactate during environmental induced hypoxia in the hypoxia intolerant rainbow trout (*O. mykiss*). Caution needs to be taken when comparing the effects of a hypoxic external environment with the effects of exercise on the white muscle.

Oxygen consumption by the white muscle in the anaesthetised snapper in this experimental setup would have been very low as the muscle only had to maintain

basal metabolism. Presumably the white muscle was able to maintain metabolism aerobically during progressive hypoxia as the haemoglobin saturation in the white muscle remained at resting normoxia values until the ambient DO concentration reached 2.4±0.1 $mg.L^{-1}$. Below this, the white muscle might have had to rely more on anaerobic metabolism, peaking as the haemoglobin saturation reached a minimum at 0.7±0.1 $mg.L^{-1}$ DO concentration (Figure 7.6).

During hypoxia, perfusion to the white muscle had already started to decrease (3.3±0.1 $mg.L^{-1}$ DO), prior to haemoglobin saturation decreasing. During re-oxygenation, the water bath reached 2.9±0.1 $mg.L^{-1}$ DO concentration before the haemoglobin saturation in the white muscle began to increase. Perfusion, however, had already started to return to the white muscle from 1.9 ±0.1 $mg.L^{-1}$ DO. The timing of these observations suggests that the mechanism/s that reduce white muscle perfusion (in an anaesthetised fish) may be controlled by an upstream feed-forward pathway and not by localised white muscle oxygen receptors, effectively shutting the white muscle down before external environmental conditions become too hypoxic in order conserve what oxygen is left for other more vital and oxygen dependent tissues. This theory is supported by Canty and Farrell's (1985) work on the perfused Ocean pout (*M. americananus*) tail. They showed that inflow, and therefore systemic resistance, was not dependent on the $PO_2$ of the perfusate.

Canty and Farrell (1985) also demonstrated vasodilation in the tail vasculature with acidosis and vasoconstriction with alkalosis. They used a constant pressure head in a whole tail preparation, in which the vasculature in the red muscle and skin would also have influenced the inflow, whereas perfusion in this snapper experiment was determined solely from the white muscle. Their findings suggest, then, that perfusion would increase in the tail with prolonged hypoxia if the tail white muscle becomes more acidic due to increased lactate concentration. Such a mechanism might explain the increased perfusion in the snapper white muscle at a relatively lower DO when DO was rising, compared to the fall in perfusion as DO

fell. These data also contrast with the delayed recovery in HR on reoxygenation.. Given a longer hypoxia exposure duration we may have seen a return of perfusion to the white muscle as lactate accumulation (due to anaerobic metabolism) increased, acidifying the white muscle and in turn the blood.

Perfusion to the snapper white muscle increased and maintained levels above pre-hypoxia resting values during the latter stages of re-oxygenation (Figure 7.5). After hypoxia the white muscle may have had an oxygen debt and increased perfusion would be an effective way of decreasing diffusion distances, allowing rapid re-oxygenation of the myotome cells and removal of metabolic waste products.

Arterial blood pressure has been shown to decrease during hypoxia (Sundin et al. 1999, Sandblom and Axelsson 2005), which would result in capillary de-recruitment in the white muscle. Sundin et al. (1999) exposed traira (*H. malabaricus*) to hypoxia by bubbling nitrogen into the water, similar to the method used in this experiment. They showed a decrease in the ventral aortic pressure ($P_{VA}$) during hypoxia, however once the nitrogen was switched off and the tank aerated, they saw a rapid rise (<1 min) in $P_{VA}$. A rapid rise in arterial blood pressure during re-oxygenation would mediate capillary recruitment in the white muscle, increasing perfusion, as shown in the anaesthetised snapper. The delay in white muscle reperfusion in the anaesthetised snapper was 3 min (Figure 7.5), longer than the $P_{VA}$ recovery in traira, which is somewhat expected due to anaesthetic effects. Sandblom and Axelsson (2005) showed a significant decrease in dorsal aortic pressure (PDA) during severe hypoxia.

The two wavelengths recorded to estimate haemoglobin saturation mirror each other as shown in Figure 7.6. Two wavelengths, one measuring changes in oxy-haemoglobin and the other deoxy-haemoglobin, were used to confirm the methodology. The changes in intensity (relative to perfusion) are greater in the 466 nm compared than in the 516 nm recordings. This is because the difference

between the molar extinction coefficients of oxy-haemoglobin and deoxy-haemoglobin is greater at 466 nm, creating greater sensitivity gain over the saturation range (Figure 7.1). Recording the change in intensity from a wavelength between 650 nm and 700 nm would show even greater sensitivity gain as the difference between the molar extinction coefficients is greater again.

The hysteresis between haemoglobin saturations during progressive hypoxia and recovery also suggests an oxygen debt in the post hypoxia white muscle. At any given external DO below ~6 $mg.L^{-1}$ there is a greater amount of saturated haemoglobin during progressive hypoxia than during recovery (Figure 7.7.B). The lag in the recovery of haemoglobin saturation may be due to the increased oxygen demand from the white muscle to repay an anaerobic oxygen debt incurred during hypoxia.

In summary, the fibre optic methodology enabled us to visualise perfusion and haemoglobin saturation in the white muscle in real time. Combined with recorded cardiac performance we have a greater understanding of how anaesthetised snapper are affected by progressive hypoxia and re-oxygenation. The use of an anaesthetised preparation, although it removed any possible behavioural stress response and made the preparation physically possible, has made deciphering the underlying mechanisms of the hypoxia mediated cardiac response more difficult.

## 7.6 References

Allen DG, Orchard CH (1983) Intracellular calcium-concentration during hypoxia and metabolic inhibition in mammalian ventricular muscle. Journal of Physiology, London 339: 107-122

Altimiras J, Axelsson M (2004) Intrinsic autoregulation of cardiac output in rainbow trout (*Oncorhynchus mykiss*) at different heart rates. Journal of Experimental Biology 207: 195-201

Ask JA, Stene-Larsen G, Helle KB (1981) Temperature effects on the beta2-adrenoceptors of the trout atrium. Journal of Comparative Physiology B 143: 161-168

Axelsson M, Farrell AP, Nilsson S (1990) Effects of hypoxia and drugs on the cardiovascular dynamics of the Atlantic hagfish *Myxine glutinosa*. Journal of Experimental Biology 151: 297-316

Axelsson M, Fritsche R (1991) Effects of exercise, hypoxia and feeding on the gastrointestinal blood-flow in the Atlantic cod *Gadus morhua*. Journal of Experimental Biology 158: 181-198

Berschick P, Bridges CR, Grieshaber MK (1987) The influence of hyperoxia, hypoxia and temperature on the respiratory physiology of the intertidal rockpool fish *Gobius cobitis pallas*. Journal of Experimental Biology 130: 369-387

Burleson ML, Smatresk NJ (1989) The effect of decerebration and anaesthesia on the reflex responses to hypoxia in catfish. Canadian Journal of Zoology-Revue Canadienne De Zoologie 67: 630-635

Burleson ML, Smatresk NJ (1990) Effects of sectioning cranial nerve-IX and nerve X on cardiovascular and ventilatory reflex response to hypoxia and NaCl in the channel catfish. Journal of Experimental Biology 154: 407-420

Burleson ML, Wilhelm DR, Smatresk NJ (2001) The influence of fish size on the avoidance of hypoxia and oxygen selection by largemouth bass. Journal of Fish Biology 59: 1336-1349

Butler PJ, Taylor EW, Short S (1977) The effects of sectioning cranial nerves V, VII, IX and X on the cardiac response of the dogfish Scyliorhinus canicula to environmental hypoxia. Journal of Experimental Biology 69: 233-245

Cameron JN (1975) Blood flow distribution as indicated by tracer microspheres in resting and hypoxic arctic grayling (*Thymallus arcticus*). Comparative Biochemistry and Physiology 52A: 441-444

Canty AA, Farrell AP (1985) Intrinsic regulation in an isolated tail preparation of the ocean pout (*Macrozoarces americanus*). Canadian Journal of Zoology 63: 2013-2020

Davie PS, (1981) Vascular resistance responses of an eel tail preparation: alpha constriction and beta dilation. Journal of Experimental Biology 90:65-84

Dunn JF, Hochachka PW (1986) Metabolic Responses of Trout (*Salmo gairdneri*) to Acute Environmental Hypoxia. Journal of Experimental Biology 123: 229-242

Farrell AP (2007) Tribute to P. L. Lutz: a message from the heart - why hypoxic bradycardia in fishes? Journal of Experimental Biology 210: 1715-1725

Farrell AP, Clutterham SM (2003) On-line venous oxygen tensions in rainbow trout during graded exercise at two acclimation temperatures. Journal of Experimental Biology 206: 487-496

Farrell AP, Jones DR (1992) The Heart. In Hoar WS, Randall DJ, Farrell AP eds. Fish Physiology, vol. XII, Part A. Academic Press, San Diego, London, pp 1-88

Fievet B, Caroff J, Motais R (1990) Catecholamine release controlled by blood oxygen tension during deep hypoxia in trout: effect on red blood cell Na/H exchanger activity. Respiration Physiology 79: 81-90

Fritsche R (1990) Effects of hypoxia on blood-pressure and heart-rate in 3 marine teleosts. Fish Physiology and Biochemistry 8: 85-92

Fritsche R, Axelsson M, Franklin CE, Grigg GG, Holmgren S, Nilsson S (1993) Respiratory and cardiovascular-responses to hypoxia in the Australian lungfish. Respiration Physiology 94: 173-187

Fritsche R, Nilsson S (1990) Autonomic nervous control of blood pressure and heart rate during hypoxia in the cod, *Gadus morhua*. Journal of Comparative Physiology B 160: 287-292

Fritsche R, Nilsson S (1989) Cardiovascular-responses to hypoxia in the Atlantic cod *Gadus morhua*. Experimental Biology 48: 153-160

Gamperl AK, Pinder AW, Grant RR (1994) Influence of hypoxia and adrenaline administration on the coronary blood-flow and cardiac-performance in seawater rainbow trout (*Oncorhynchus mykiss*). Journal of Experimental Biology 193: 209-232

Hill JV, Davison W, Forster ME (2004) The effects of fish anaesthetics (MS222, metomidate and AQUI-S) on heart ventricle, the cardiac vagus and branchial vessels from Chinook salmon (*Oncorhynchus tshawytscha*). Fish Physiology and Biochemistry 27: 19-28

Hill JV, Forster ME (2004) Cardiovascular responses of Chinook salmon (*Oncorhynchus tshawytscha*) during rapid anaesthetic induction and recovery. Comparative Biochemistry and Physiology Part C 137: 167-177

Holeton GF, Randall DJ (1967) The Effect of Hypoxia Upon the Partial Pressure of Gases in the Blood and Water Afferent and Efferent to the Gills of Rainbow Trout. Journal of Experimental Biology 46: 317-327

Kolok AS, Spooner RM, Farrell AP (1993) The effect of exercise on the cardiac output and blood flow distribution of the largescale sucker *Catostomus macrocheilus*. Journal of Experimental Biology 183: 301-321

McKenzie DC, Wong S, Randall DJ, Egginton S, Taylor EW, Farrell AP (2004) The effects of sustained exercise and hypoxia upon oxygen tensions in the red muscle of rainbow trout. Journal of Experimental Biology 207: 3629-3637

Minerick AR, Chang HC, Hoagland TM, Olson KR (2003) Dynamic synchronization analysis of venous pressure-driven cardiac output in rainbow trout. American Journal of Physiology-Regulatory Integrative and Comparative Physiology 285: R889-R896

Neumann P, Holeton GF, Heisler N (1983) Cardiac output and regional blood flow in gills and muscles after exhaustive exercise in rainbow trout (*Salmo gairdneri*). Journal of Experimental Biology 105: 1-14

Nilsson GE, Renshaw GMC (2004) Hypoxic survival strategies in two fishes: extreme anoxia tolerance in the North European crucian carp and natural hypoxic preconditioning in a coral-reef shark. Journal of Experimental Biology 207: 3131-3139

Olson KR, Farrell, A.P (2006) The cardiovascular system. *In* Evans, DH, Claiborne JB eds, The physiology of fishers, CRC, Boca Raton, Florida, pp 119-152

Overgaard J, Stecyk JAW, Gesser H, Wang T, Farrell AP (2004) Effects of temperature and anoxia upon the performance of in situ perfused trout hearts. Journal of Experimental Biology 207: 655-665

Partridge GJ, Jenkins GI, Frankish KR (2003) Hatchery Manual for the production of Snapper (*Pagrus auratus*) and Black Bream (*Acanthopagrus butcheri*). WA Maritime Training Centre, Aquaculture Development Unit, Challenger TAFE, Fremantle, Western Australia. pp 65

Perry SF, Bernier NJ (1999) The acute humoral adrenergic stress response in fish: facts and fiction. Aquaculture 177: 285-295

Perry SF, Reid SG (2002) Cardiorespiratory adjustments during hypercarbia in rainbow trout *Oncorhynchus mykiss* are initiated by external $CO_2$ receptors on the first gill arch. Journal of Experimental Biology 205: 3357-3365

Pearce WJ (1995) Mechanisms of hypoxic cerebral vasodilation. Pharmacology and Therapeutics 65: 75-91

Perry SF, Reid SG, Gilmour KM, Boijink CL, Lopes JM, Milsom WK, Rantin FT (2004) A comparison of adrenergic stress responses in three tropical teleosts

exposed to acute hypoxia. American Journal of Physiology-Regulatory Integrative and Comparative Physiology 287: R188-R197

Prahl S (1999) Optical absorption of haemoglobin. Oregon Medical Laser Centre. http://omlc.ogi.edu/spectra/hemoglobin

Randall DJ (1982) The control of respiration and circulation in fish during exercise and hypoxia. Journal of Experimental Biology 100: 275-288

Randall DJ, Smith JC (1967) The regulation of cardiac activity in fish in a hypoxic environment. Physiological Zoology 40; 104-113

Rantin FT, Kalinin AL, Guerra CDR, Maricondi-Massari M, Verzola RMM (1995) Electrocardiographic characterization of myocardial function in normoxic and hypoxic teleosts. Brazilian Journal of Medical and Biological Research 28:1277-1289

Reid SG, Bernier N, Perry SF (1998) The adrenergic stress response in fish: control of catecholamine storage and release. Comparative Biochemistry and Physiology 120C: 1-27

Russell MJ, Dombkowski RA, Olson KR (2008) Effects of hypoxia on vertebrate blood vessels. Journal of Experimental Zoology 309A: 55-63

Sandblom E, Axelsson M (2006) Adrenergic control of venous capacitance during moderate hypoxia in the rainbow trout (*Oncorhynchus mykiss*): role of neural and circulating catecholamines. American Journal of Physiology 291: R711-R718

Schurmann H, Steffensen JF, Lomholt JP (1991) The influence of hypoxia on the preferred temperature of rainbow trout *Oncorhynchus mykiss*. Journal of Experimental Biology 157: 75-86

Smith FM, Jones DR (1981) The effect of changes in blood oxygen-carrying capacity on ventilation volume in the rainbow trout (*Salmo gairdneri*). Journal of Experimental Biology 97: 325-334

Smith MP, Russell MJ, Wincko JT, Olson KR (2001) Effects of hypoxia on isolated vessels and perfused gills of rainbow trout. Comparative Biochemistry and Physiology a-Molecular & Integrative Physiology 130: 171-181

Stecyk JAW, Farrell AP (2002) Cardiorespiratory responses of the common carp (*Cyprinus carpio*) to severe hypoxia at three acclimation temperatures. Journal of Experimental Biology 205: 759-768

Sundin LI, Reid SG, Kalinin AL, Rantin FT, Milsom WK (1999) Cardiovascular and respiratory reflexes: the tropical fish, traira (*Hoplias malabaricus*) $O_2$ chemoresponses. Respiration Physiology 116; 181-199

Sundin L, Nilsson S (2002) Branchial innervation. Journal of Experimental Zoology 293: 232-248

Vornanen M, Tuomennoro J (1999) Effects of acute anoxia an heart function in crucian carp: importance of cholinergic and purinergic control. American Journal of Physiology-Regulatory Integrative and Comparative Physiology 277: R465-R475

Wood CM, Shelton G (1980) The reflex control of heart rate and cardiac output in the rainbow trout: interactive influences of hypoxia, haemorrhage, and systemic vasomotor tone. Journal of Experimental Biology 87: 271-284

# Chapter 8 The effects of progressive hypothermia and recovery on cardiac function and white muscle perfusion in the anaesthetised snapper (*Pagrus auratus*)

## 8.1. Abstract

The effects of progressive hypothermia and re-warming on cardiac performance and white muscle perfusion and haemoglobin saturation were investigated in anaesthetised snapper (*Pagrus auratus*). Snapper were exposed to a progressive decrease in temperature from ambient (11$^{o}$C) to 6$^{o}$C and back to ambient over 315 min. During progressive hypothermia the snapper showed a marked bradycardia. The heart rate decreased and increased in a stepwise pattern following the stepwise water bath temperature profile. At 6$^{o}$C the heart rate had decreased by 44% of the pre-hypothermia resting rate. QRS amplitude and the product of QRS amplitude and heart rate also decreased during hypothermia. Perfusion in the white muscle decreased during progressive hypothermia. Changes in white muscle haemoglobin saturation were negligible. Heart rate, QRS amplitude, the product of QRS amplitude and heart rateand white muscle perfusion all increased during re-warming. The attenuation in cardiac performance and the decrease in white muscle perfusion during progressive hypothermia and recovery, with reference to metabolic rate, are discussed.

## 8.2 Introduction

Fibre optic technology and knowledge of the haemoglobin absorption spectra enabled us to observe real time perfusion and haemoglobin saturation in the white muscle of snapper during hypoxia. In the work presented in this chapter we used the same methodology to observe perfusion and haemoglobin saturation in the white muscle during progressive hypothermia and recovery.

Many teleost species experience seasonal hypothermia and have evolved physiological mechanisms to either compensate for or adjust to the lowered metabolic rate in order to survive. However, many fish species do not regularly experience hypothermia and even a slight shift in temperature has a pronounced effect on cardiac performance.

A large amount of information exists on how the cardiac performance of teleosts is affected by temperature (Barron et al. 1987, Blank et al. 2004, Overgaard et al. 2004, Gollock et al. 2006) but there is very little on how white muscle perfusion is affected by temperature. It is known that temperature and heart rate are closely related. Blank et al. (2004) examined cardiac performance in Pacific blue fin tuna (*Thunnus orientatis*) hearts over a 2-30$^{o}$C temperature range. The heart rate at 2$^{o}$C was 13 BPM and increased linearly to 105 BPM at 25$^{o}$C. Overgaard et al. (2004) showed that the heart rate of *in situ* Rainbow trout (*Salmo gairdneri*) hearts at 10$^{o}$C was 55 BPM, increased to 81.9 when exposed to 18$^{o}$C and decreased to 39.6 BPM when exposed to 5$^{o}$C. Gollock et al. (2006) showed that not only heart rate but also stroke volume and cardiac output increased with increasing temperature. Similarly, Barron et al. (1987) demonstrated that the cardiac output in free swimming rainbow trout, acclimated to varying temperatures, increased linearly with increasing temperature.

Literature describing the effects of acute temperature change on white muscle perfusion is scarce. Barron et al. (1987) described increasing blood perfusion to

the white muscle with elevated acclimation temperature (4 weeks) in rainbow trout (*S. gairdneri*). Egginton (1997) also demonstrated an increase in blood flow to the white muscle of rainbow trout acclimated to warmer autumn temperatures compared with cooler winter temperatures. No literature was found on the effects of acute temperature change on white muscle perfusion.

# 8.3 Methods

## 8.3.1 Experimental fish

### 8.3.1.1 Snapper

The same cohort of snapper was used and treated the same as in the AQUI-S$^{TM}$ uptake and recovery experiments (Section 3.3.1.1).

## 8.3.2 Experimental methodology

### 8.3.2.1 Water bath and ECG

The experimentation utilised the same methodology as that described in Section 7.3.2.1. The experimental protocol was approved by the University of Canterbury's Animal Ethics Committee.

### 8.3.2.2 Fibre optic methodology

The experimentation used the same methods as described in Section 7.3.2.2. To check for possible temperature effects on the optodes, they were placed in a haemoglobin solution (2 ml of haemolysed blood in 20ml $dH_2O$) and subjected to the same temperature cycle.

### 8.3.2.3 Hypothermia methodology

When the ECG, heart rate and white muscle perfusion and saturation levels in the anaesthetised fish had stabilised (or after a minimum period of 30 min) the temperature in the water bath was decreased to approximately half acclimated before being increased to ambient. The temperature profile is depicted in Figure 8.1. The temperature was held at 11$^{o}$C (ambient) and decreased by 1$^{o}$C over 15 min before being held at 10°C for 15 min, then again decreasing another 1$^{o}$C over

15 min, and so on. After the temperature had been held at 6°C for 15 min the inverse profile was followed until ambient temperature was regained.

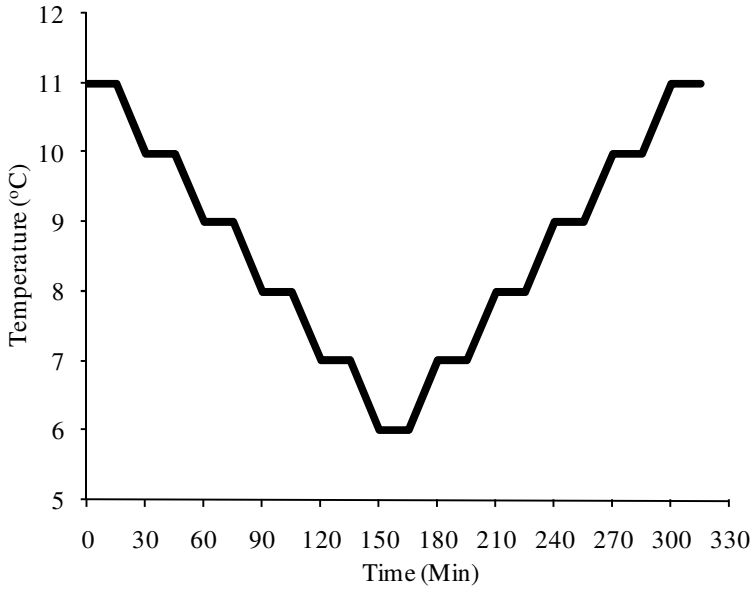


**Figure 8.1 Water bath temperature profile.**

## 8.4 Results

### 8.4.1 Progressive hypothermia and recovery

The mean fish weight was 117±2g and the mean ambient tank water temperature was 11.3±0.2$^{o}$C.

The anaesthetised snapper heart rate and QRS amplitude decreased as the water bath temperature decreased to ~6$^{o}$C. As the water bath temperature returned to ambient, both heart rate and QRS amplitude increased (Figure 8.2). During cooling heart rate fell, and it rose on rewarming (Repeated measures ANOVA and Bonferroni's Multiple Comparison Test, $P<0.05$) (Figure 8.3). There was greater variabilty in the QRS amplitude, during cooling and re-warming, but it followed the same trend as heart rate Figure 8.2).

The resting heart rate at 11.0±0.1$^{o}$C was 45.5±0.5 BPM (Figure 8.3). The heart rate decreased in a stepwise fashion to a low of 25.1±0.8 BPM at the coldest temperature recorded of 6.1±0.1$^{o}$C (165 min, 150 min cooling). QRS amplitude decreased to 53±6% of resting amplitude at 6.1±0.1$^{o}$C (165 min, 150 min hypothermia) (Figure 8.2). As the water temperature increased, snapper heart rate increased, reaching a rate similar to the pre-hypothermic resting rate of 45.5±1.4, at 10.4±0.1$^{o}$C (294 min, 129 min re-warming). The heart rate continued to increase as the water temperature increased, reaching a maximum rate of 50.0±1.0 BPM 11.0±0.1$^{o}$C (321 min, 156 min re-warming. The QRS amplitude also increased as the temperature increased, reaching and maintaining an amplitude ~5% above resting at 11.0±0.1$^{o}$C (307 min, 142 min re-warming) (Figure 8.2). Heart rate and QRS amplitude both significantly correlated (regression ANOVA, $P<0.05$) with water temperature (8.4, A and B). And were also significantly correlated with each other (regression ANOVA $P<0.001$), (Figure 8.5).

The $Q_{10}$ value for heart rate was 3.22 during cooling and 3.86 during re-warming.

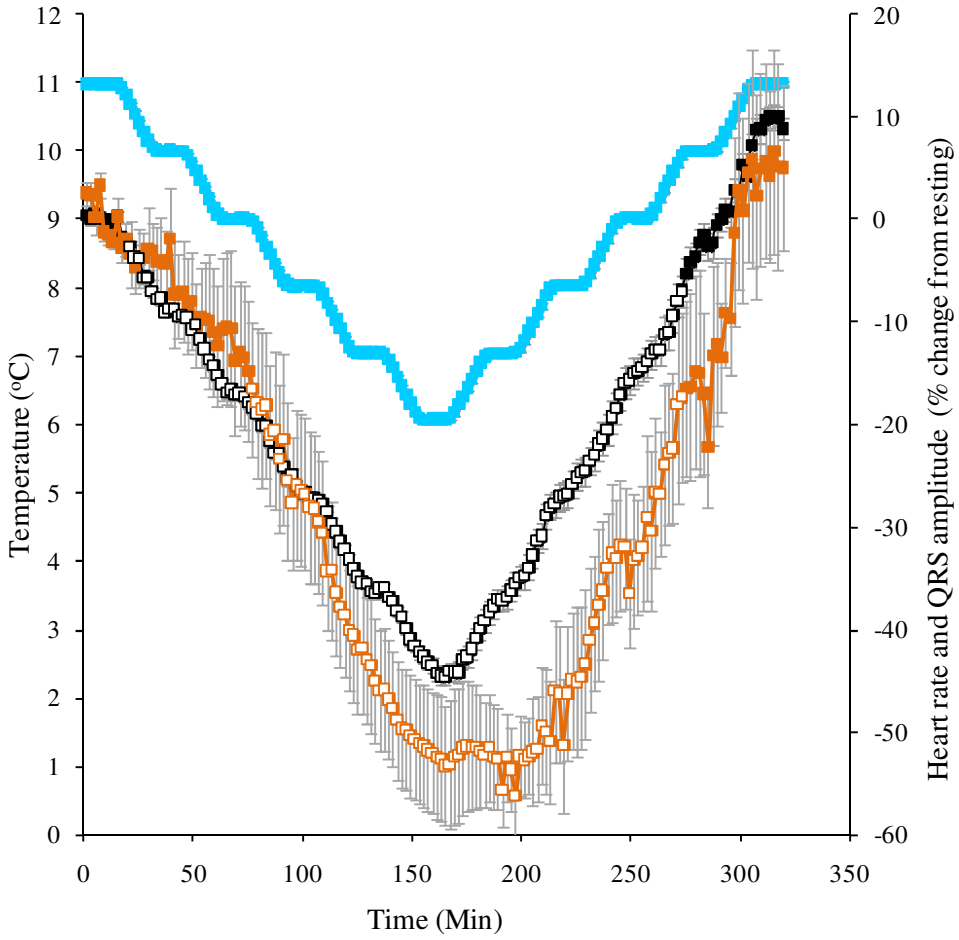


**Figure 8.2 Ambient water bath temperature (light blue), and snapper heart rate (black) and QRS amplitude (orange) during progressive hypothermia and re-warming.** Open symbols indicate a significant difference from starting values (Repeated measures ANOVA and Bonferroni's Multiple Comparison Test, $P<0.01$). Values are mean±sem, N=6.

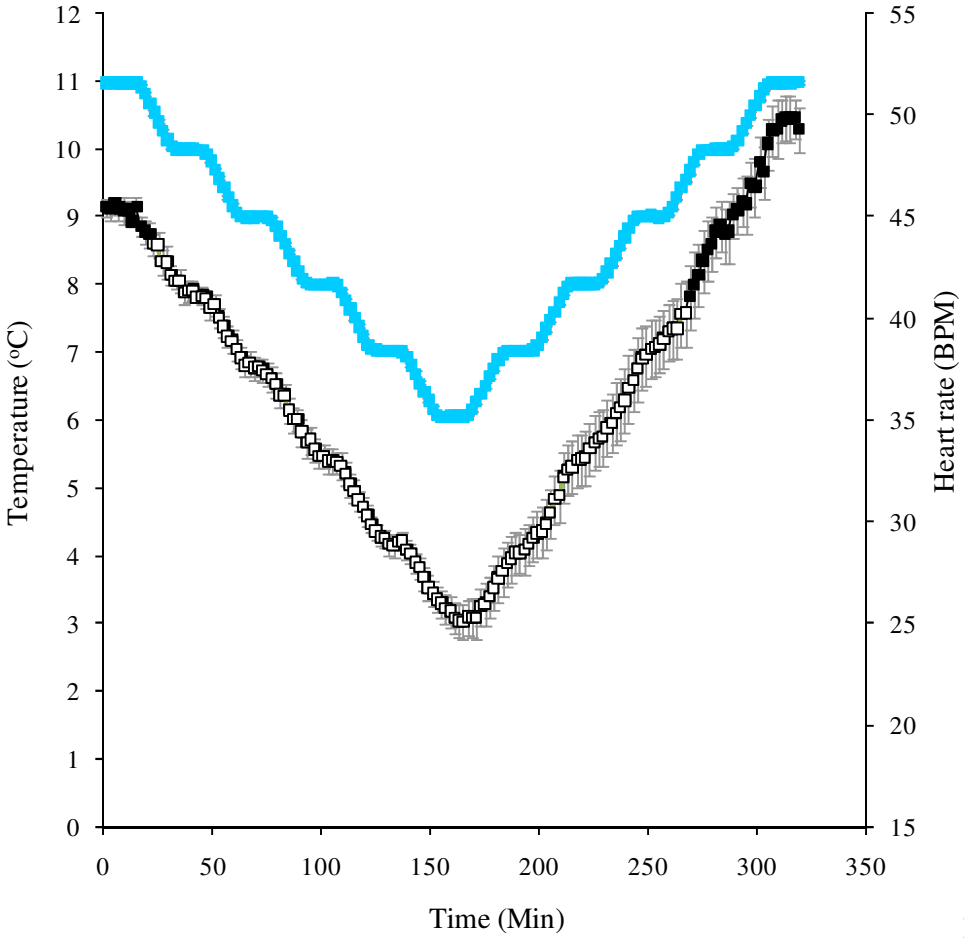


**Figure 8.3 Ambient water bath temperature (light blue), and snapper heart rate (black) during progressive hypothermia and re-warming.** Open symbols indicate a significant difference from starting values (Repeated measures ANOVA and Bonferroni's Multiple Comparison Test, P<0.01).Values are mean±sem, N=6.

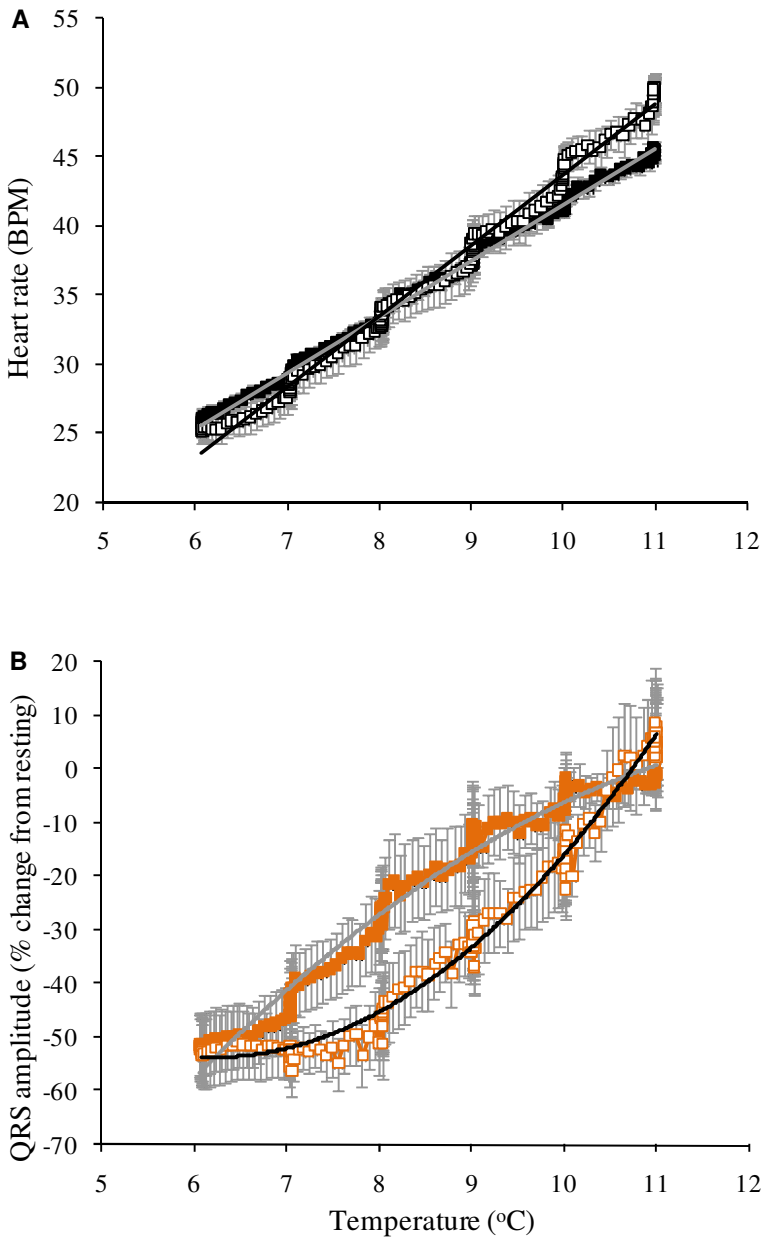


**Figure 8.4 Water bath temperature plotted with A) heart rate and B) QRS amplitude during progressive hypothermia (solid) and re-warming (clear).** A) best fit linear trendline during hypothermia; $r^2$=0.99 (grey) and re-warming; $r^2$=0.99 (black); B) best fit polynomial trendline during hypothermia $r^2$=0.98 (grey) and re-warming $r^2$=0.99 (black). Values are mean±sem, N=6.

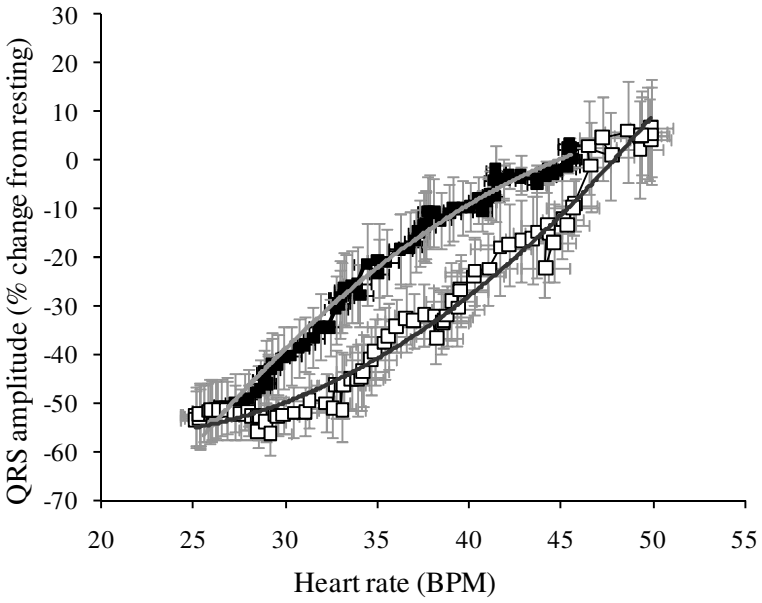


**Figure 8.5 Snapper heart rate plotted against QRS amplitude during progressive hypothermia (solid) and re-warming (clear)** Best fit polynomial trendline during hypothermia $r^2$=0.98 (grey) and re-warming $r^2$=0.99 (black). Values are mean±sem, N=6.

Caution is required interpreting the fibre optic results during the decreasing and increasing temperature because both temperature and drift can affect the recorded signal. If required, all raw data traces were individually drift corrected prior to analysis. No temperature correction has been done. The effects of temperature (including drift), when the optode was immersed in a haemoglobin solution, are included in Figure 8.7.

Although there were no significant differences (Repeated measures ANOVA and Bonferroni's Multiple Comparison Test, $P<0.05$) from resting pre-hypothermia values, the data suggest that perfusion to the white muscle increased slightly as the water bath temperature decreased, shown by a decrease in the 530nm light intensity from resting to ~3.3±6.1% below resting at water temperature of 8.8±0.1$^{o}$C (80 min, 65 min cooling) (Figure 8.6). However, some of this fall may have been be a temperature effect, as the absorbance also fell by ~2% when the optodes were subjected to a temperature change between 10 and 8.5°C in a haemoglobin solution (Figure 8.7). However, there was not a comparable rise when temperature rose through this temperature range ~250 min. The 530 nm light intensity (isobestic point representing total haemoglobin) increased to a maximum of 5.7±9.1% above resting at 6.9±0.1$^{o}$C (181 min, 16 min re-warming), indicating a decrease in perfusion to the white muscle during deep hypothermia. The haemoglobin solution did not show any change in absorbance over this range. Thus we can be confident that the change in absorbance reflects decreased perfusion at the lowest temperatures. Perfusion increased to the white muscle during re-warming, shown by a decrease in the 530 nm light intensity. The 530 nm light intensity had decreased to a value similar to resting intensity at 9.0±0.1$^{o}$C (244 min, 79 min re-warming), before continuing to decrease to 4.0±7.3% below resting intensity at 11.0±0.1$^{o}$C (327 min, 162 min re-warming). There was an increase in the 530 nm intensity in the haemoglobin solution during re-warming which may lead to an underestimation of returned perfusion to the white muscle (Figure 8.7).

Figure 8.6 also shows the light intensity changes at wavelengths 466 nm and 516 nm (representing haemoglobin saturation). However, as discussed previously (Section 7.4.1), they have an inherent perfusion element. To remove the perfusion element from the saturation element, the recorded intensity at 466 nm and 516 nm were divided by the corresponding 530 nm light intensity. There was very little change in the light intensity measured at 466 nm and 516 nm after correcting for perfusion (Figure 8.8). The 466 nm/530 nm and 516 nm/530 nm resting ratios were approximately 1.23 and 0.94, respectively. During hypothermia exposure the 466 nm/530 ratio remained fairly constant between 1.22-1.24 with the highest ratio recorded at 1.24 at 6.5±.01$^{o}$C (175 min, 10 min re-warming), from this point the 466 nm/530 nm ratio slowly decreased to reach 1.08±0.04 at 11.0±0.1 (327 min, 162 min re-warming), suggesting a slight increase in haemoglobin oxygen saturation during re-warming. The 516 nm/530 nm remained fairly constant during initial hypothermia before decreasing to the lowest recorded ratio of 0.91±0.01recorded at 6.7±0.1$^{o}$C (178 min, 13 min re-warming). During re-warming the 516 nm/530 nm ratio increased to resting values, suggesting a slight decrease in deoxy-haemoglobin. There was no significant difference (Tukey's Multiple Comparison Test, $P<0.05$) in the 466 nm/530 nm and 516 nm/530 nm ratios at any time with corrosponding resting values. However, we cannot rule out that part or all of the inferred increase and decrease in saturation may be caused by temperature effects (Figure 8.7).

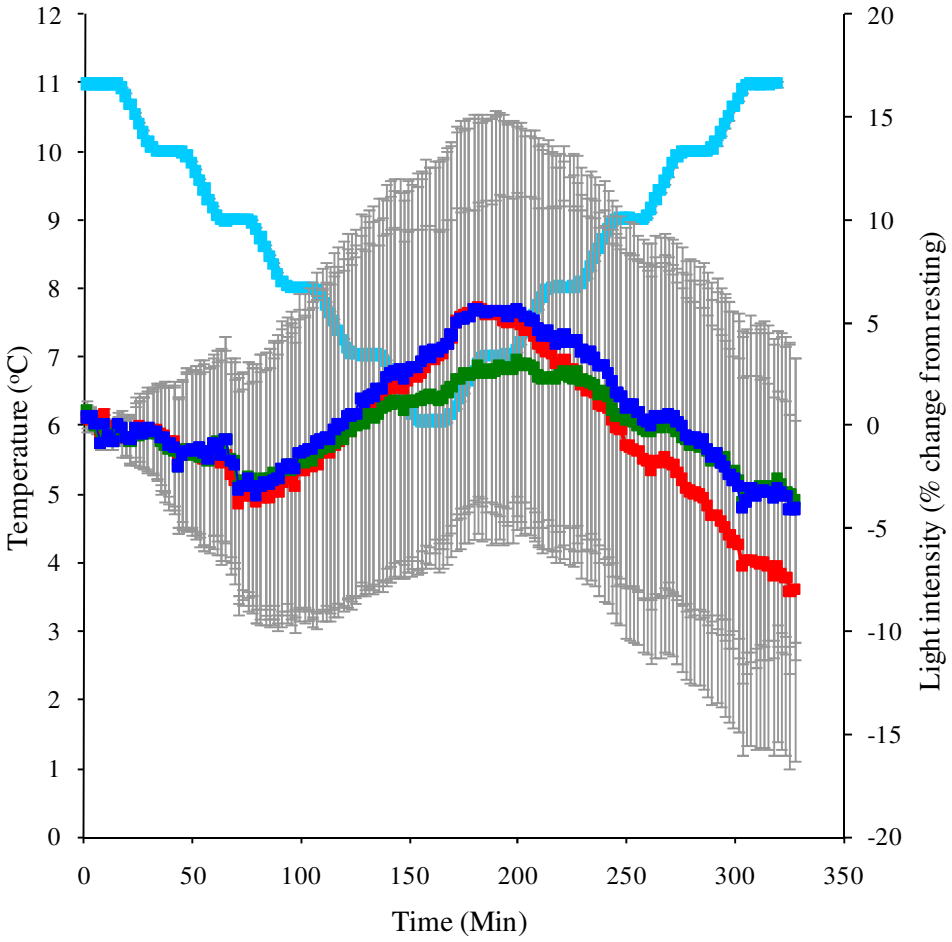


**Figure 8.6 Water bath temperature (light blue) and light intensity from wavelengths 530 nm (dark blue), 466 nm (red), and 516 nm (green) recorded from the white muscle during progressive hypothermia and re-warming.** Increases in intensity at all three wavelengths, 530 nm, 466 nm and 516 nm, indicate a decrease in total haemoglobin concentration (perfusion). There was no significant difference found at any time from initial values at any wavelength (Repeated measures ANOVA and Bonferroni's Multiple Comparison Test, $P<0.05$). Values are mean±sem, N=6.

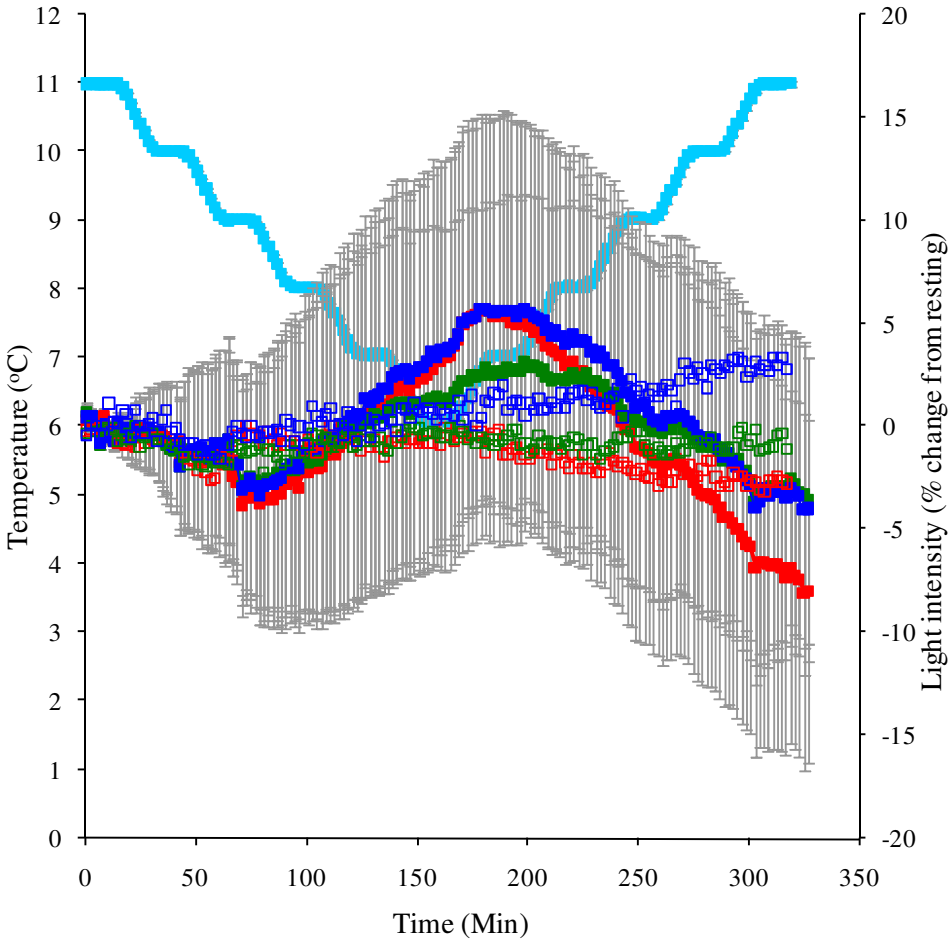


**Figure 8.7 Water bath temperature (solid light blue) and light intensity from wavelengths 530 nm (solid dark blue), 466 nm (solid red), and 516 nm (solid green) recorded from the white muscle during progressive hypothermia and re-warming.** Also plotted (corresponding clear symbols) are the temperature effects at 530 nm, 466 nm and 516 nm recorded from 10% haemoglobin solution. There was no significant difference found from initial wavelength data (Repeated measures ANOVA and Bonferroni's Multiple Comparison Test, $P<0.05$). Values are mean±sem, N=6.

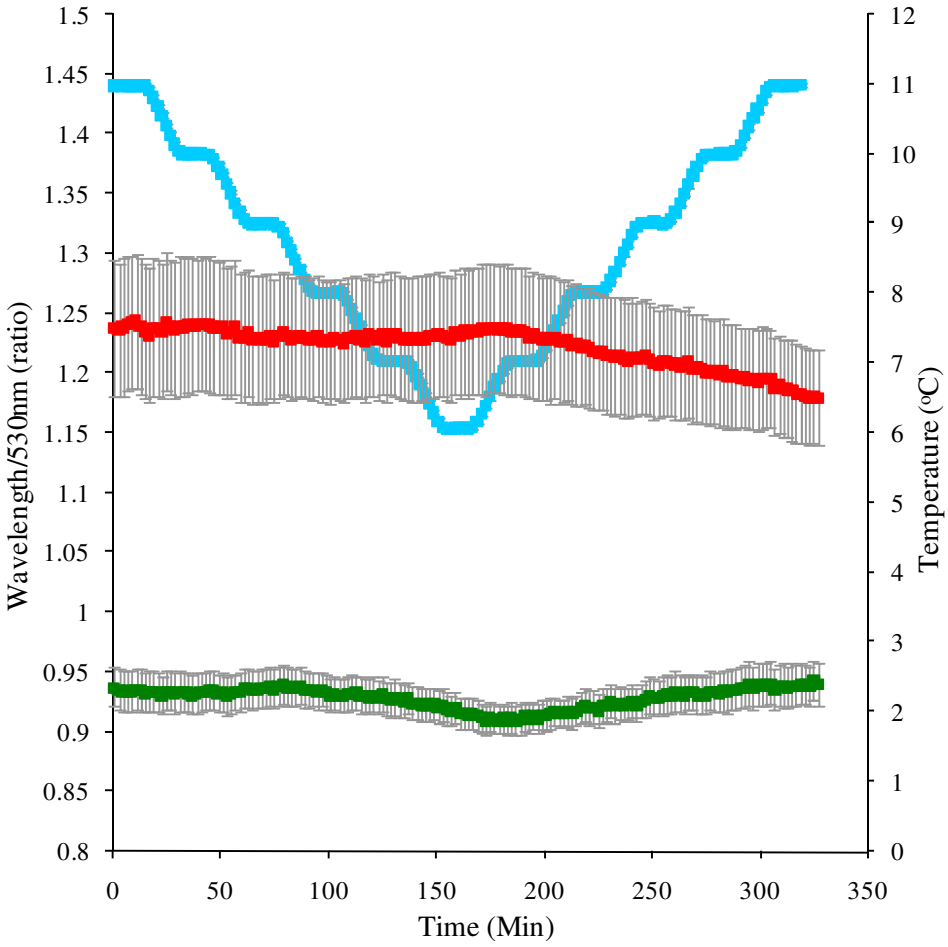


**Figure 8.8 Water bath temperature (light blue) and ratios from wavelengths 466 nm/530 nm (red) and 516 nm/530 nm (green) during progressive hypothermia and re-warming.** An increase in the 466 nm /530 nm and 516 nm/530 nm ratio indicate a decrease in the oxy-haemoglobin concentration and a decrease in the deoxy-haemoglobin concentration, respectively, and vice versa. There was no significant difference found from initial wavelength data (Repeated measures ANOVA and Bonferroni's Multiple Comparison Test, $P<0.05$). Values are mean±sem, N=6.

Figure 8.9.A and B show the relationship between white muscle perfusion and heart rate. With the onset of bradycardia, perfusion to the white muscle may have increased slightly, before decreasing as the heart rate reached its minimum rate of 25.1±0.8 BPM (530 nm light intensity increased to ~4% above resting). White muscle perfusion was at its lowest when heart rate had increased to ~27 BPM (530 nm light intensity increased to ~5.6% above resting). The heart rate continued to increase, reaching and maintaining ~50 BPM, slightly higher than the pre-hypothermic resting value. Perfusion may have also continued increasing as the 530 nm light intensity decreased to, and maintained, a level ~3.5-4% below pre-hypothermic resting levels.

Figure 8.10 A demonstrates more clearly the relationship between the water bath temperature and the recorded 530 nm light intensity (perfusion) during cooling and re-warming. The relationship between haemoglobin saturation (light intensity measured at wavelength 466 nm and 516 nm) has already been discussed, and Figure 8.10 B shows the relationship between haemoglobin saturation and temperature.

During deep hypothermia cardiac arrhythmias were observed in three of the six experimental fish. The arrhythmia observed was a variable interbeat interval (Figure 8.11). Stable cardiac rhythm returned during re-warming.

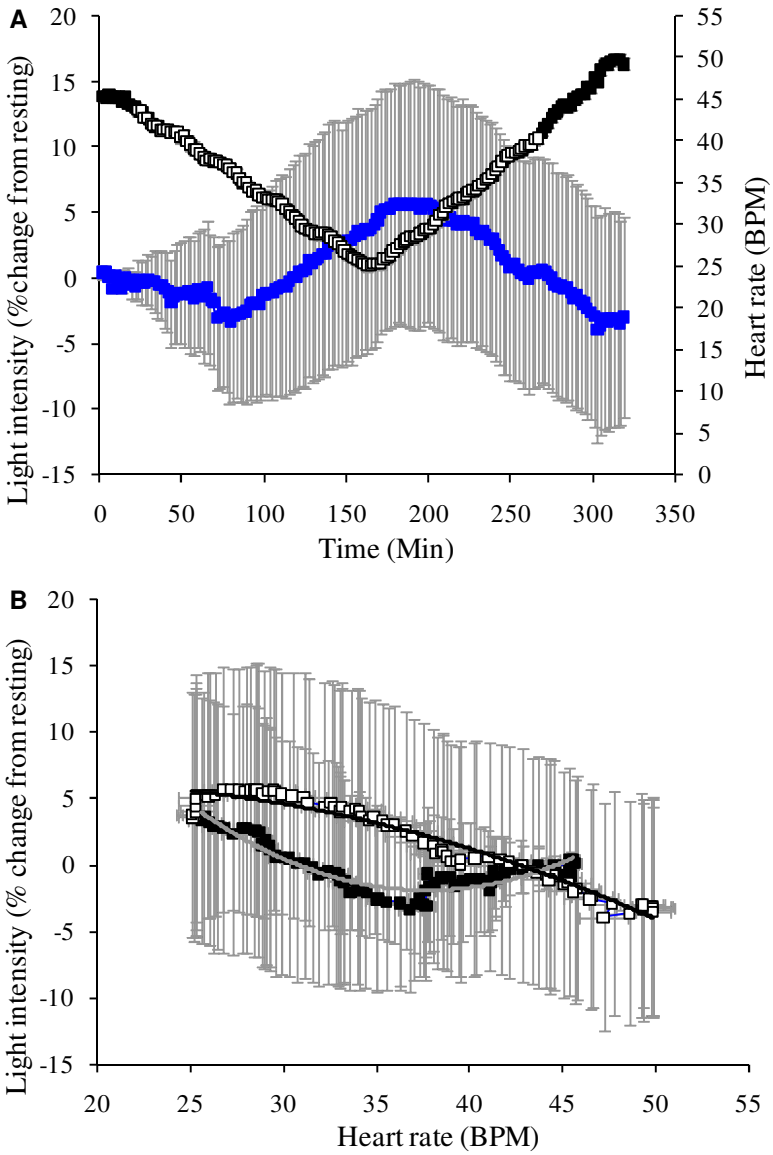


**Figure 8.9 A) Snapper heart rate (black) and light intensity from wavelengths 530 nm (dark blue), recorded from the white muscle during hypothermia and re-warming. B) Snapper heart rate plotted with light intensity from wavelength 530 nm during progressive hypothermia (solid) and re-warming (clear).** B) best fit polynomial trendline during cooling $r^2$=0.95 (grey) and re-warming $r^2$=0.86 (black). Values are mean±sem, N=6.

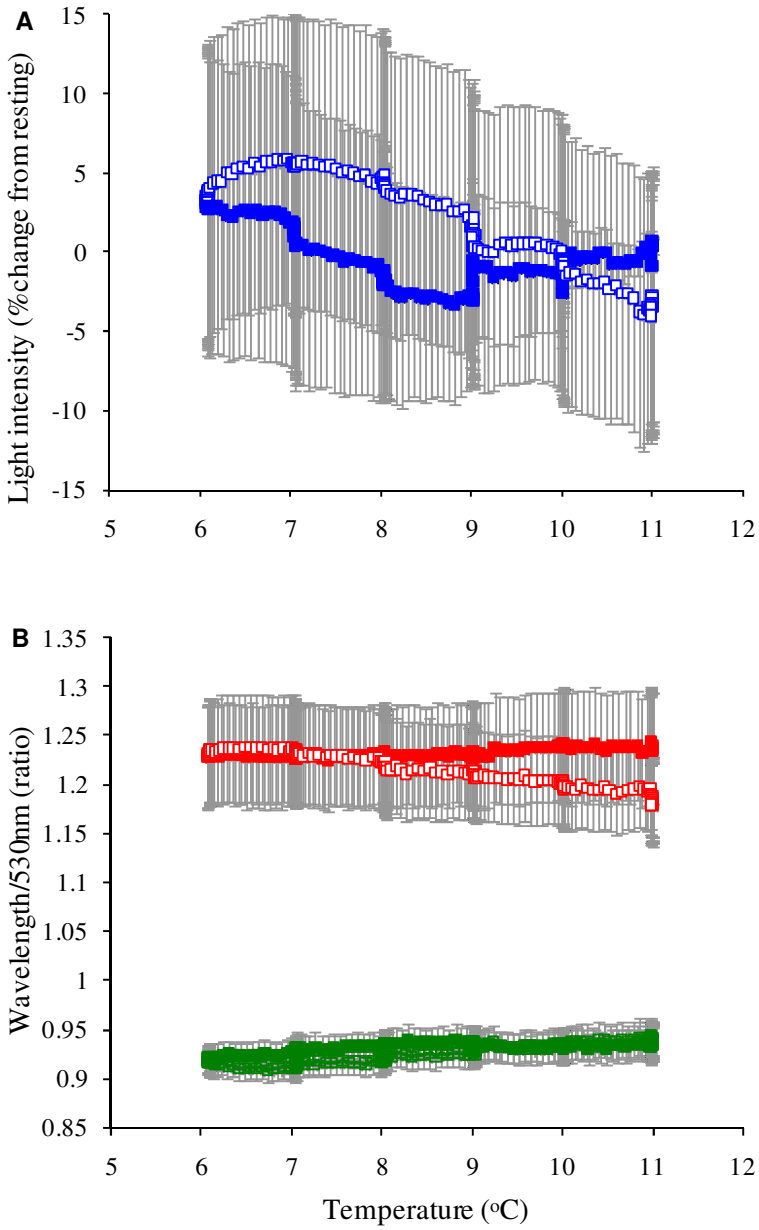


**Figure 8.10 A) Recorded change in light intensity from wavelength 530 nm and B) ratios from wavelength 466 nm/530 nm (red) and 516 nm/530 nm (green) against ambient water bath temperature during progressive hypothermia (solid) and re-warming (clear).** Values are mean±sem, N=6.

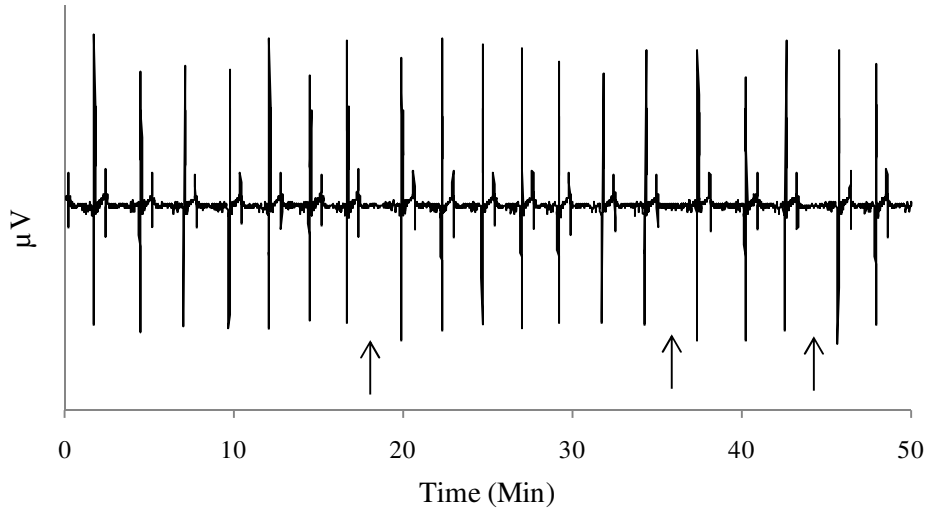


**Figure 8.11 Example of an ECG recording from an individual anaesthetised fish demonstrating arrhythmia during deep hypothermia (6.1±0.1°C).** Examples of irregular interbeat intervals (black arrows) are marked.

## 8.5 Discussion

Progressive hypothermia induced the expected cardiac response in the anaesthetised snapper, with heart rate, QRS amplitude (an approximation of stroke volume) and the product of QRS amplitude and heart rate all decreasing. There was very little delay between decreasing water bath temperature and the decrease in heart rate (Figure 8.3). Heart rate was significantly correlated (Regression ANOVA, $P<0.05$) with the ambient water bath temperature during progressive hypothermia and re-warming (Figure 8.4.A). Heart rate decreased and increased in a stepwise fashion following the water bath temperature profile. This demonstrates the high degree to which the intrinsic control of the heart rate is influenced by the external water temperature in the anaesthetised snapper. There is very little hysteresis in the heart rate changes during cooling and re-warming, except for a slightly increased heart rate at the end of recovery to 11°C (Figure 8.4.A). These changes are consistent with the loss of autonomic control of heart rate in the anaesthetised animal.

The $Q_{10}$ values for heart rate were 3.22 during cooling and 3.85 during re-warming, which implies a fairly dramatic effect of temperature in this species, compared with the heart rate $Q_{10}$ trout hearts which averaged 1.7 during acute temperature change (Overgaard et al. 2004) and Pacific blue fin tuna hearts with a $Q_{10}$ of 2.48 (Blank et al. 2004). However it is less than the sea raven (*Hemitripterus americanus*) which had a heart rate $Q_{10}$ of 5.1 during cooling from $10^{o}$C to $5^{o}$C (Bailey and Driedzic 1989).

Fish have an efficient branchial counter-current heat exchange which rapidly equilibrates their internal temperature to the surrounding ambient water temperature. The actual internal rate of cooling and re-warming in the snapper white muscle was not measured. The internal rate of cooling and re-warming in a non-anaesthetised fish may be slower than in the anaesthetised artificially ventilated preparation as ventilation rates in fish have been shown to decrease

when exposed to low temperature (Berschick et al. 1987, Szyper and Lutnesky 1991). A reduction in ventilation rate will decrease the volume of refreshed cold water flowing over the gill lamellae, potentially creating a slight lag in cooling and re-warming. In the anaesthetised snapper preparation the fish was artificially ventilated with a constant flow of cold water, potentially chilling the snapper down at a faster and more constant rate than in a non-anaesthetised fish. Our animals would not become hypoxic due to reduced ventilation as they were artificially ventilated, and thus cardiac function should be maintained, if the circulation continues.

QRS amplitude (Figure 8.4.B) was also both positively correlated with the water bath temperature during cooling and re-warming. However, there was a hysteresis between progressive cooling and re-warming. Below 10$^{o}$C, QRS amplitude (Figure 8.4.B) was greater during cooling than re-warming, at the same temperature. The relationship between the product of QRS amplitude and heart rateand temperature during cooling is almost linear, whereas it is parabolic during re-warming. During rewarming the initial rate at which the product of QRS amplitude and heart rate increases is slow, as shown by the reduced slope of the parabolic curve. The hysteresis in the QRS amplitude may be due to an effect of the low temperature on the contractile proteins of the cardiac myocytes or an excitation process that is slower to respond than the cardiac pacemaker. The hysteresis could also be due to a restricted venous return and ventricular filling once re-warming starts. Low temperature had a profound effect on the cardiac myocytes, inducing arrhythmia in half of the fish sampled (Fig 8.11). The combination of a reduced heart rate and, potentially, stroke volume should result in reduced blood volume passing through the gill lamellae, potentially reducing the initial re-warming rate until cardiac performance increases (as the temperature increases) to a point where the lag in re-warming is overcome. The elevated estimated heart rate at 11$^{o}$C, once re-warming is completed might reflect an oxygen debt incurred over the first 15 min of re-warming (Figure 8.3).

The perfusion and saturation recordings have a large degree of variability within the data, shown by large error bars, which has to be taken into account when interpreting the data.

Perfusion may have decreased during progressive hypothermia and returned during re-warming (Figure 8.6). Reduced white muscle perfusion during acute hypothermia may be beneficial, as impaired cardiovascular performance may not be able to sustain the delivery of oxygen to, and removal of waste metabolites from the white muscle. Re-direction of blood from the white muscle to other more vital organs could increase the likelihood of surviving hypothermia. Barron et al. (1987) concluded that a redistribution of blood flow to the white muscle at elevated temperatures may allow an increase in scope for burst activity in the white muscle, as clearance anaerobic waste products would be greater. The possible slight increase in white muscle perfusion during the onset of hypothermia may have an adaptive significance, similar to that surmised by Barron et al. (1987). Increased perfusion with the onset of hypothermia would allow the necessary metabolic support for burst activity for the fish to move to an area of warmer water. However, beyond a certain temperature it may become more energy efficient to reduce white muscle perfusion in order to survive the hypothermia event. In snapper at a seasonal acclimation temperature of 11$^{o}$C the transition temperature to trigger reduced perfusion to the white muscle is ~8.5$^{o}$C (Figure 8.6). This may vary by season and/or acclimation temperature. The increased blood flow at the start of perfusion could also be due to a direct effect of temperature on vascular smooth muscle. Cold induced vasodilation is a well described phenomenon in mammals (O'Brien, 2004).

There is a hysteresis between white muscle perfusion during cooling and re-warming. At any given temperature below 10$^{o}$C, perfusion during re-warming is less than during cooling (Figure 8.10.B). The lag in perfusion during re-warming may be due to the lag in cardiac function explained above, if QRS amplitude does correlate with stroke volume. Above 10$^{o}$C, perfusion during re-warming is greater

than that during cooling. Heart rate, QRS amplitude (stroke volume), and estimated cardiac output were also elevated above pre-hypothermia levels after re-warming, suggesting some compensatory effort to alleviate any residual effects of hypothermia.

As explained in the hypoxia and re-oxygenation experiments, the decrease and increase in white muscle perfusion, although closely correlated with cardiac function, might be facilitated by changes in arterial pressure, which was not measured in this experiment. Bailey and Driedzic (1989) demonstrated that pressures in the caudal artery and ventral aorta in the sea raven (*H. americanus*), decreased significantly when subjected to a change in temperature from 10$^{o}$C to 5$^{o}$C over 3 h. If a similar change occurs in our snapper, then perfusion might be expected to fall in all vascular beds.

If flow ceased for an extended period than we would expect see a reduction in haemoglobin saturation due to the metabolic demand for oxygen. During progressive hypothermia there was neglible change in haemoglobin oxygen saturation in the white muscle (Figure 8.8), at a time where perfusion and potentially flow were reduced, which suggests that the white muscle metabolic rate was highly down-regulated with hypothermia. Temperature induced changes in the affinity of haemoglobin for oxygen are also likely to result in less desaturation in this ventilated animal. With a reduced metabolic rate, a lower rate of blood perfusion should satisfy oxygen demand.

## 8.6 References

Bailey JR, Driedzic WR (1989) Effects of acute temperature-change on cardiac-performance and oxygen-consumption of a marine fish, the sea raven (*Hemitripterus americanus*). Physiological Zoology 62: 1089-1101

Barron MG, Tarr BD, Hayton WL (1987) Temperature-dependence of cardiac output and regional blood flow in rainbow trout, *Salmo gairdneri* Richardson. Journal of Fish Biology 31: 735-744

Berschick P, Bridges CR, Grieshaber MK (1987) The influence of hyperoxia, hypoxia and temperature on the respiratory physiology of the intertidal rockpool fish *Gobius cobitis pallas*. Journal of Experimental Biology 130: 369-387

Blank JM, Morrissette JM, Landeira-Fernandez AM, Blackwell SB, Williams TD, Block BA (2004) In situ cardiac performance of Pacific bluefin tuna hearts in response to acute temperature change. Journal of Experimental Biology 207: 881-890

Egginton S (1997) Control of tissue blood flow at very low temperatures. Journal of Thermal Biology 22: 403-407

Gollock MJ, Currie S, Petersen LH, Gamperl AK (2006) Cardiovascular and haematological responses of Atlantic cod (Gadus morhua) to acute temperature increase. Journal of Experimental Biology 209: 2961-2970

O'Brien C (2004) Reproducibility of the cold-induced vasodilation response in the human finger. Journal of Applied Physiology 98: 1334-1340

Overgaard J, Stecyk JAW, Gesser H, Wang T, Farrell AP (2004) Effects of temperature and anoxia upon the performance of in situ perfused trout hearts. Journal of Experimental Biology 207: 655-665

Szyper JP, Lutnesky MMF (1991) Ventilation rate and behavioural-responses of juvenile mahimahi to temperature and salinity. Progressive Fish-Culturist 53: 166-172

# Chapter 9 Summary of conclusions, their integration, and suggestions for further work

As stated in the Thesis Introduction the primary objectives of this thesis were: to explore potential delivery pathways of supportive molecules to teleost musculature, and combined with perfusion visualisation experiments, generate a greater understanding of teleost white muscle perfusion.

The blood flow distribution to the white muscle in an isolated Chinook salmon perfused tail preparation was poor compared with that in a live fish. Electrical stimulus (to mimic exercise), and the addition of SNP, a vasodilating agent, to the perfusate did not improve white muscle perfusion to a level similar to that in a live fish. Therefore, it was concluded that the perfused tail preparation, although a useful tool in fish physiology, has limitations as a method for exploring the delivery of supportive molecules to the white muscle.

Direct uptake research on teleosts to date, has focused on the negative aspects of hydrophobic molecule accumulation in fish (van de Oost et al. 2002, Belpaire and Goeman 2007). In comparison, this thesis took a novel positive approach to direct uptake, and focused on the delivery of supportive molecules.

A direct uptake delivery method was successfully evaluated with isoeugenol, the active ingredient in the aquatic anesthetic AQUI-S$^{TM}$. Isoeugenol rapidly diffused across the gills and into the blood, before being transported to the white muscle, where it accumulated to concentrations many times greater than the exposure concentration. Direct uptake of supportive molecules through the gills has many advantages over an isolated perfused tail preparation; it is non-labour intensive, non technical and potentially large numbers of fish can be treated at the same time.

Not only was direct uptake of isoeugenol useful in evaluating the direct uptake delivery methodology, but also offered the opportunity to further our understanding of the anesthetic mode of action of isoeugenol at low, medium and high concentrations. Accumulated white muscle isoeugenol concentration was highest in the low exposure treatment and lowest in the high exposure treatment, whereas plasma isoeugenol concentration was greatest in the high exposure treatment and similar in the medium and low exposure treatment. Snapper exposed to the medium and high exposures attained deep anesthesia, whereas those anaesthetised at the low exposure concentration only reached an anesthetic stage of deep sedation/partial anesthesia. These results, combined with observations of cut surface pH, ventilation rates and mobility, show that iso-eugenol plasma and white muscle concentrations do not correlate with depth of anaesthesia and suggest that hypoxia may be more of a cause than an effect of deep anesthesia. Further research into if (and how) isoeugenol effects gill oxygen diffusion efficiency is recommended to clarify the role that hypoxia plays in anesthesia.

Curcumin is found in the spice turmeric which, as discussed previously, has been shown to have numerous beneficial medicinal properties, including strong antioxidant effects (Toda et al. 1985, Jayaprakasha et al. 2006, Anand et al. 2007). Curcumin and its curcuminoid derivatives were eluted with ethanol from turmeric spice and were shown, for the first time, to be rapidly up taken into the blood, via the gills, before being delivered to the white and red muscle in a teleost. In all three exposure treatments; low, medium and high the uptake into the plasma was rapid reaching saturation levels within 10 min exposure. Maximum iso-eugenol accumulation in the plasma and red and white muscle was exposure concentration dependent. The uptake and accumulation of the curcuminoids in the red muscle was faster and greater than the white muscle. We presume this is due to the red muscle having greater vascularisation (capillarity) and smaller muscle fibres which reduces the diffusion distances, allowing faster uptake and accumulation. As the red muscle quickly became saturated, the white muscle slowly caught up

over the duration of the 60 min exposure, shown by the decreasing red muscle:white muscle blood flow distribution ratio.

Natural fluorescent markers, such as curcumin, have the potential to be used in blood flow distribution experiments without the injection and capillary blockage problems associated with radio or fluorescent labeled microspheres, which can lead to underestimates of total blood flow. The 10 min red muscle:white muscle curcuminoid staining ratio was ~1.5, indicating greater blood flow to the red muscle, similar to that found in other fish species (see Chapter 4). However, as discussed, the ratio did decrease over the duration of the exposure, which if used as a blood flow distribution indicator, would confound blood flow distribution results. Another confounding factor in using curcuminoids as blood flow distribution indicators is that they are metabolised, even in post-mortem tissue, as shown in the short term storage trial.

The potential, protecting, antioxidant activity of the curcuminoids was evaluated with a short-term storage trial. No difference in short term metabolic rundown was found between fish exposed and those not exposed to curcuminoids. However, the use of AQUI-S$^{TM}$ in this study, and its antioxidant potential, may have made it impossible to differentiate any additional antioxidant effects of the curcuminoids. Use of a different anaesthetic might resolve this issue. The characteristic yellow staining of the turmeric accumulated in the plasma and white muscle was depleted within 8 h and within 12 h in the red muscle, suggesting the curcuminoids were metabolised *in situ* into metabolites undetectable at the excitation and emission wavelengths used.

The accelerated storage trial showed that the antioxidant activity of the curcuminoids has potential as a long term storage treatment. Fish exposed to the curcuminoids prior to harvest showed reduced lipid peroxidation as measured TBARS activity was lower in the lipid rich red muscle after 4 days storage at 15$^{o}$C compared with a control treatment. There was less TBARS activity in the white

muscle in both the control and curcuminoid treatments. Accelerated storage trials, which are conducted at elevated temperatures, have potential to under estimate TBARS activity as TBARS are not stable and are metabolised. At elevated storage temperature, the rate of TBARS metabolism may be similar to that of TBARS production, resulting in reduced observed TBARS activity, especially in tissues with low lipid concentration. A reduced storage temperature might allow TBARS to accumulate and give a more accurate estimate of the rate of lipid peroxidation. Reducing the storage temperature might also reduce the confounding factors of accelerated bacterial spoilage. Aside from the limitations of an accelerated storage trial, the results suggest that a long-term frozen storage trial is warranted to further clarify the antioxidant activity of the curcuminoids and the use of the direct uptake delivery method as a potential long-term commercial storage application.

Antioxidant application in cultured fish is usually through pre-harvest dietary supplementation. Direct uptake creates and opportunity for a single pre-harvest application of a hydrophobic antioxidant which would accumulate in the fish musculature, especially the lipid rich areas (which are more susceptible to lipid peroxidation). Antioxidant application in large scale commercial wet fish processing is often topical as fish are delivered to the boat in a highly stressed state or dead. Until harvesting practices improve and return somewhat rested fish to the deck and potentially into live wells, there is little room for direct uptake of an antioxidant. However, direct uptake methodology may be applicable in current fishing practices such as aquaculture farms and fishing practices that involve live fish capture and already use live fish wells, such as the harvesting of crustacea and fish species that are trapped (crayfish, crabs, eels, cod etc.). Direct uptake methods may also be applicable to harvesting practices that corral fish with the potential of using a liner around the net to create a live well for treatment. Further research on the direct uptake delivery method in shellfish and crustacea is required.

Direct uptake at the gill is limited to small hydrophobic molecules that are readily diffused across the gill lamellae, whereas a perfused preparation offers the potential for larger and more hydrophilic molecules to be supplied to the musculature of fish. However as discussed previously, compared with a perfused preparation, direct uptake is non-invasive, non-technical and has potential for large scale application.

Delivery of beneficial molecules throughout a fish's musculature is dependent on the fish's circulatory system providing thorough perfusion. However, we know little about perfusion in teleost muscle and how it is influenced by changing external environments. As stated in Chapter 7, the effects of exercise on blood flow distribution in several species of fish have been documented (Neumann et al. 1983, Kolok et al. 1993), but nothing to date demonstrates white muscle perfusion in real time. By using fibre optic methodology and a knowledge of the haemoglobin absorption spectra we were able to observe white muscle perfusion and haemoglobin saturation in real time during progressive hypoxia and hypothermia.

During progressive hypoxia, perfusion was reduced to the white muscle and returned during re-oxygenation. The same perfusion pattern was observed during progressive hypothermia. By reducing perfusion to a large tissue mass, the blood flow is potentially able to be redirected to other tissues which are vital for survival. This adaptive advantage is only possible because of the white muscle's ability to function anaerobically as an isolated unit. However, after anaerobic metabolism there are waste products that need to be removed and an oxygen debt that needs to be repaid. During recovery from hypoxia and hypothermia, we saw that white muscle perfusion was elevated above pre-hypoxia levels. There was also less saturated haemoglobin in the white muscle during re-oxygenation than during hypoxia at any given $PO_2$. Both these observations suggested recovery from hypoxia induced anaerobic metabolism and the creation of an oxygen "debt".

The results from the hypoxia trial suggested a feed-forward control of white muscle perfusion (in the anaesthetised fish) instead of a localised white muscle oxygen sensing receptor feedback mechanism. How this could be achieved in the absence of functioning nerves is not clear. White muscle perfusion decreased before white muscle haemoglobin saturation decreased. Thus local signaling that oxygen supply was not keeping up with demand could not be responsible for vasomotion (Ellsworth 2004). Similarly, during re-oxygenation, perfusion to the white muscle increased before white muscle haemoglobin saturation increased. Cardiac function was closely correlated with white muscle perfusion. However, it is suggested that the primary factor determining white muscle perfusion in the anaesthetised snapper during hypoxia and re-oxygenation is changes in arterial pressure (not measured in this research) and its effect on capillary recruitment (and de-recruitment).

The onset of hypoxia and hypothermia elicited marked bradycardia, and reduced QRS amplitude and estimated cardiac output in anaethetised snapper. Our preparation was anaethetised and this may well have had an effect on the observed cardiovascular response. However, if we assume inhibited neurological control of cardiac function due to anaesthesia, then the effect of hypoxia or temperature is solely on the cardiac myocytes. However, the question still remains; is there still a degree of neurological control, even in an anaethetised fish?

Results from the isoeugenol uptake and recovery trials suggested that hypoxia may be either a cause or an effect of deep anaesthesia. As we have discussed already, white muscle perfusion is reduced during hypoxia, which may explain why even though we see very high plasma isoeugenol accumulation in deep anaesthetised snapper exposed to high isoeugenol concentration, we only see low isoeugenol accumulation in the white muscle. By contrast, snapper exposed to low isoeugenol concentration, which never reached deep anaesthesia, and were able to maintain mobility and ventilation, preventing hypoxia, showed the highest white muscle isoeugenol concentrations.

We have to remember that when using haemoglobin concentration to assess white muscle perfusion we are not necessarily observing changes in blood flow. Combining additional methods to measure blood flow and arterial and venous pressures and oxygen partial pressures with the fibre optic preparation, would greatly assist in further clarifying the mechanisms of perfusion in teleost white muscle.

When drawing conclusions about the direct uptake method for delivering supportive molecules to the white muscle, the effects of changing environmental parameters on perfusion and the inherent control of cardiac function, we have to remember that in all experiments conducted in this thesis were with anaesthetised fish. As discussed in Chapter 7, isoeugenol has cardiovascular effects in fish (Hill and Forster 2004, Hill et al. 2004, Rothwell and Forster 2005, Rothwell et al. 2005). As the primary neurological mode of action of isoeugenol as an anaesthetic is unknown, it is impossible to state to what degree the inherent signal systems and pathways in the fish may have been inhibited, and therefore influenced the observed responses. When weighing up the decision to use an anaesthetic during the experiments it was considered that the highly variable stress response of an un-anaesthetised fish would offer far less control than that of anaesthetised fish preparation.

## 9.1 References

Anand P, Kunnumakkara AB, Newman RA, Aggarwal BB (2007) Bioavailability of Curcumin: Problems and Promises. Molecular Pharmaceutics 4: 807-818

Belpaire C, Goemans G (2007) Eels: contaminant cocktails pinpointing environmental contamination. ICES Journal of Marine Science 64: 1423-1436

Ellsworth ML (2004) Red blood cell-derived ATP as a regulator of skeletal muscle perfusion. Medicine and Science in Sports and Exercise 36: 35-41

Hill JV, Davison W, Forster ME (2004) The effects of fish anaesthetics (MS222, metomidate and AQUI-S) on heart ventricle, the cardiac vagus and branchial vessels from Chinook salmon (*Oncorhynchus tshawytscha*). Fish Physiology and Biochemistry 27: 19-28

Hill JV, Forster ME (2004) Cardiovascular responses of Chinook salmon (*Onchorhynchus tshawytscha*) during rapid anaesthetic induction and recovery. Comparative Biochemistry and Physiology Part C 137: 167-177

Jayaprakasha GK, Jaganmohan Rao I, Sakariah KK (2006) Antioxidant activities of curcumin, demethoxycurcumin and bisemethoxycurcumin. Food Chemistry 98: 720-724

Kolok AS, Spooner RM, Farrell AP (1993) The effect of exercise on the cardiac output and blood flow distribution of the largescale sucker *Catostomus macrocheilus*. Journal of Experimental Biology 183: 301-321

Neumann P, Holeton GF, Heisler N (1983) Cardiac output and regional blood flow in gills and muscles after exhaustive exercise in rainbow trout (*Salmo gairdneri*). Journal of Experimental Biology 105: 1-14

Rothwell SE, Black SE, Jerrett AR, Forster ME (2005)a Cardiovascular changes and catecholamine release following anaesthesia in Chinook salmon (*Oncorhynchus tshawytscha*) and snapper (*Pagrus auratus*). Comparative Biochemistry and Physiology A 140: 289-298

Rothwell SE, Forster ME (2005)b. Anaesthetic effects on the hepatic portal vein and on the vascular resistance of the tail of the Chinook salmon (*Oncorhynchus tshawytscha*). Fish Physiology and Biochemistry 31: 11-21

Toda S, Miyase T, Arichi H, Tanizawa H, Takino Y (1985) Natural antioxidants III. Antioxidative components isolated from rhizome *curcua longa L.* Chemical and Pharmaceutical Bulletin 33: 1725-1728

van der Oost R, Beyer J, Vermeulen NPE (2002) Fish bioaccumulation and biomarkers in environmental risk assessment: a review. Environmental Toxicology and Pharmacology 13: 57-149

# Acknowledgements

Associate Professor Malcolm Forster, thanks not only for your academic and technical expertise as supervisor on this degree, but also for the positive influence you have had on my vocational decisions and direction over the last decade.

Alistair Jerrett, and the Higher Value Seafood Team at Crop & Food Research Ltd, thank you not only for your advice, methodologies and technical support but also for the creative and enjoyable working environment.

Mike Field-Dodgson and the harvest team at Isaac's Salmon Farm, thank you for the constant supply of salmon, and use of the farm's hatchery during the first part of this thesis.

To the staff from the School of Biological Sciences, University of Canterbury, especially the technicians, thank you for your administrative and technical support.

To my family, thank you again for your continued support in yet another chapter of postgraduate study.

To the many friends who pretend, albeit with eyes glazed, to enjoy the conversations relating to fish physiology while walking up steep hills with packs overloaded.

I saved the best for last, To Davina and the boys, thank you for everything.